Passive In Situ Treatment of Acidic and Neutral Mine Drainage: Field and Laboratory Investigations

by

Matthew Bruce James Lindsay

A thesis
presented to the University of Waterloo
in fulfillment of the
thesis requirement for the degree of
Doctor of Philosophy
in
Earth Sciences

Waterloo, Ontario, Canada, 2009

Author's Declaration

I hereby declare that I am the sole author of this thesis. This is a true copy of the thesis, including any required final revisions, as accepted by my examiners.

I understand that my thesis may be made electronically available to the public.

Abstract

Water quality degradation is the foremost environmental issue faced by the mining industry. Negative impacts on water quality are commonly associated with unmitigated drainage emanating from sulfide-bearing mine waste deposits. These impacts stem from the liberation of acidity, sulfate, metals (e.g. Fe, Ni, Cu, Zn and Pb), and trace elements (e.g. Co, As, Cd, Sb and Tl) during the oxidation of sulfide minerals. Drainage at operational mines is commonly treated using techniques such as chemical oxidation and acid neutralization, which can succeed in achieving regulatory discharge guidelines. However, active treatment techniques are commonly burdened by high capital and operating costs. The development of passive technologies for treatment of mine drainage, which promote sulfate reduction, metal-sulfide precipitation and alkalinity production, therefore present a cost-effective alternative for managing mine drainage quality. This thesis describes laboratory and field evaluations of techniques for passive in situ treatment of acidic and neutral mine waters.

Laboratory batch experiments evaluated the treatment of acid mine drainage (AMD) with mixtures of organic carbon and zero-valent iron (ZVI) for use in permeable reactive barriers (PRBs). Modest increases in sulfate-reduction rates up to 15 % were achieved by amending organic carbon mixtures with 5 to 10 % (dry wt.) ZVI. Reactive mixtures containing organic carbon supported growth of sulfate-reducing bacteria (SRB) and facilitated removal of Fe, Zn, Cd, Ni, Co and Pb. However, organic carbon was necessary to support SRB growth and sulfate reduction. Removal of Zn, Cd, Ni, Co and Pb in the absence of organic carbon is attributed to sorption and (co)precipitation reactions at the ZVI surface. Scanning electron microscopy (SEM) and X-ray absorption near-edge structure (XANES)

spectroscopy confirmed the presence of secondary Fe-sulfides in mixtures containing organic carbon. The dominant reaction product in these mixtures was identified as disordered mackinawite [$Fe_{1+x}S$]. The addition of ZVI to organic carbon enhanced AMD treatment over the duration of this experiment; however, long-term evaluation is required to identify optimal reactive mixtures.

Field-based investigations into passive management of near-neutral pH tailings pore-water were carried out at the Greens Creek mine, located near Juneau, Alaska, USA. These studies focused on delineation of mechanisms controlling tailings pore-water chemistry, and a evaluation of the effectiveness of organic carbon amendment of tailings for passive in situ management of pore-water quality.

Results demonstrate that sulfide-mineral oxidation and carbonate dissolution are the primary influences on tailings pore-water composition. Pyrite [FeS_2] accounted for < 20 to > 35 wt. % of the tailings mineral assemblage, whereas dolomite [$CaMg(CO_3)_2$] and calcite [$CaCO_3$] were present at ≤ 30 and 3 wt. %, respectively. The sulfide-mineral assemblage was dominated by pyrite; however, sphalerite [(Zn,Fe)S] and galena [PbS] were commonly observed, and tetrahedrite [$(Fe,Zn,Cu,Ag)_{12}Sb_4S_{13}$], arsenopyrite [FeAsS], and chalcopyrite [$CuFeS_2$] were present in lesser amounts. Geochemical analysis of tailings core samples generally agreed with mineralogical data. The occurrence of Cd, Cr, Co, Mo, Ni, Se, and Tl is attributed to their occurrence as impurities in primary sulfide phases. Most probable number (MPN) populations of neutrophilic sulfur-oxidizing bacteria (nSOB) and SRB were elevated at several locations within the tailings deposit. Near-neutral pH conditions dominated; however, elevated concentrations of dissolved SO_4, S_2O_3, Fe, Zn, As, Sb, and Tl were observed within and below the oxidation zone.

Field-scale experiments conducted over four years evaluated passive in situ treatment of pore-water by amending unoxidized tailings with 5 and 10 vol. % organic carbon. Field-scale cells were constructed to evaluate amendments containing differing mixtures of peat, dried spent brewing grain (SBG), and municipal biosolids (MB). Organic carbon amendment of the tailings supported the development of conditions favorable to sulfate reduction. Decreases in aqueous SO_4 concentrations were observed in three cells amended with mixtures of peat, SBG, and MB. Removal of SO_4 was generally accompanied by H_2S production, enrichment in $^{34}S\text{-}SO_4$, and increased SRB populations. Undersaturation of pore-water with respect to gypsum was observed. Sulfate reduction was sustained for the duration of the experiment in cells amended with 5 vol. % peat + SBG and 10 vol. % peat + SBG + MB. The addition of organic carbon also supported reductive dissolution of Fe(III) (oxy)hydroxides and mobilization of Fe and As. The largest increases in aqueous Fe and As concentrations were observed in cells amended with MB. Subsequent decreases in Fe and As concentrations were observed under sulfate-reducing conditions. Attenuation of Zn, Sb, and Tl accompanied SO_4 removal. Mineralogical examination by SEM revealed the presence of secondary Zn-S and Fe-S precipitates on surfaces of organic carbon particles, and carbonate and aluminosilicate grains. This study demonstrates that amendment of tailings with a small and dispersed mass of organic carbon has potential to improve the quality of tailings pore water.

Acknowledgements

First and foremost, I extend my sincerest gratitude to my (co)supervisors and mentors, Dr. David Blowes and Dr. Carol Ptacek, for their guidance and support throughout the course of this degree. Their passion for research is inspiring, and I am indebted to them for the opportunities they have provided me.

I thank Dr. Doug Gould for his guidance with microbial investigations, and for sparking my interest in the field of geomicrobiology. Thank you to Dr. Jim Barker for ensuring I stayed on track with my thesis, and for thought-provoking comments which provided a different perspective on my research. I also thank my external examiners, Dr. Briant Kimball and Dr. Josh Neufeld, for their thorough and insightful reviews of this thesis.

Thank you to Dr. Pete Condon, an unofficial member of my committee, for his unwavering support of this research, his invaluable help in the field, insightful discussions on geochemistry, and for his friendship. I am grateful to the employees of the Greens Creek Mine, especially Kerry Lear, Ted Morales, and Jennifer Saran, who were always willing to help out and graciously put up with me during five field seasons. I also thank Bruce Nelson and Jim Whitlock, who along with Pete Condon, Kerry Lear, and Mike Moncur, were instrumental to getting the field experiments up and running.

Funding for this research was provided by Greens Creek Mining Company, Hecla Mining Ltd., and Rio Tinto Ltd. Additional support was awarded through a NSERC Industrial Postgraduate Scholarship, a NSERC Canada Research Chair and Discovery Grant held by David Blowes, and a Canadian Water Network grant held by Carol Ptacek. I also

thank the Alaskan Brewing Company, City and Borough of Juneau, Alaska, and Regional Municipality of Waterloo for supplying the organic carbon sources utilized in this research.

Thank you to all of the graduate students and coop students who helped me out in the field and laboratory. This includes Mike Moncur, Corina McDonald, Laura Groza, James Tordiff, and many others. Thank you to Jeff Bain for helping me out with logistical issues surrounding field and laboratory experiments.

I want to thank the friends who have made the past years so enjoyable, especially Jen Parks, Randy Stotler, Andrea Brookfield, Mike Moncur, Paul Kremer, Marlin Rempel and Claus Haslauer.

I extend my sincere thanks to my parents, brother, parents-in-law, and everyone else who supported and encouraged me throughout this endeavor.

Finally, I am sincerely grateful to my wife, Kathryn, for her loving support, patience and understanding. You always believed in me and I would not have made it without you.

Dedication

To Kathryn and Graham.

Table of Contents

List of Tables ..... **xii**

List of Figures ..... **xiii**

List of Abbreviations ..... **xvi**

Chapter 1: *Introduction* **1**

1.1 Background 1

1.1.1 Mine Drainage Geochemistry 1

1.1.2 Passive Treatment 3

1.2 Research Objectives 6

1.3 Thesis Organization 7

Chapter 2: *Zero-Valent Iron and Organic Carbon Mixtures for Remediation of Acid Mine Drainage:Batch Experiments* **8**

2.1 Executive Summary 9

2.2 Introduction 10

2.3 Laboratory Methods 13

2.3.1 Experimental Setup 13

2.3.2 Water Sampling and Analysis 15

2.3.3 Microbiology 16

2.3.4 Mineralogical Study 18

2.3.5 Geochemical Modeling 19

2.4 Results and Discussion 20

2.4.1 Aqueous Geochemistry 20

2.4.2 Sulfate Reduction Rates 22

2.4.3 Microbial Activity 24

2.4.4 Metal Removal 27

2.4.5 In Situ Sulfur Speciation 30

2.5 Conclusions 33

Chapter 3: *Mineralogical, Geochemical, and Microbial Investigation of a Sulfide-Rich Tailings Deposit Characterized by Neutral Drainage* **44**

3.1 Executive Summary 45

3.2 Introduction 46
3.3 Study Site 47
3.4 Materials and Methods 49
3.4.1 Core-Sample Collection 49
3.4.2 Mineralogy 49
3.4.3 Particle-Size Distribution 50
3.4.4 Solid-Phase Geochemistry 50
3.4.5 Microbial Enumerations 51
3.4.6 Aqueous Geochemistry 52
3.5 Results and Discussion 53
3.5.1 Tailings Mineralogy 53
3.5.2 Particle-Size Distribution 55
3.5.3 Solid-Phase Geochemistry 56
3.5.4 Microbial Enumerations 60
3.5.5 Aqueous Geochemistry 61
3.6 Conclusions 64

Chapter 4: *Managing Pore-Water Quality in Mine Tailings by Inducing Microbial Sulfate Reduction* 75

4.1 Executive Summary 76
4.2 Introduction 76
4.3 Materials and Methods 79
4.3.1 Experimental Setup 79
4.3.2 Field Methods 79
4.3.3 Laboratory Methods 80
4.3.4 Data Interpretation 81
4.4 Results and Discussion 81
4.4.1 Hydrogeologic Setting 81
4.4.2 Initial Conditions 82
4.4.3 Sulfate Reduction 83
4.4.4 Metals and Trace Elements 86
4.4.5 Secondary Precipitates 88
4.5 Conclusions 89

Chapter 5: ***Organic Carbon Amendments for Passive In Situ Treatment of Tailings Pore Water: Field-Scale Evaluation*** **.....96**

5.1 Executive Summary 97

5.2 Introduction 98

5.3 Site Description 101

5.4 Methodology 103

5.4.1 Field Cell Construction and Instrumentation 103

5.4.2 Pore-Water Sampling and Analysis 104

5.4.3 Solid-Phase Sampling and Analysis 106

5.4.4 Hydrogeological Characterization 109

5.4.5 Data Interpretation 109

5.5 Results and Discussion 110

5.5.1 Cell Hydrogeology 110

5.5.2 Pore-Water Chemistry 111

5.5.3 Microbiology 125

5.5.4 Mineralogy 127

5.5.5 Selective Extractions 129

5.6. Conclusions 132

Chapter 6: ***Conclusions*** **.....150**

6.1 Summary of Findings 150

6.2 Scientific Contributions 154

6.3 Recommendations 154

6.3 Future Research 156

References 158

Appendices

Appendix A: ***Summary of Data Presented in Chapter 2*** **.....171**

Appendix B: ***Summary of Data Presented in Chapter 3*** **.....179**

Appendix C: ***Summary of Data Presented in Chapters 4 and 5*** **.....194**

List of Tables

Table 2.1 Target composition of simulated AMD solution. 35

Table 2.2 Composition of reactive mixtures expressed as dry weight percentages (dry wt. %). 36

Table 2.3 Mass-based sulfate reduction rates (SRRs) calculated by linear least-squares regression 37

Table 3.1 Quantitative mineralogy for tailings core samples (n = 12) determined by XRD with Rietveld refinement. Mean value and standard deviation given for each phase. 66

Table 3.2 Solid-phase concentrations of major and trace elements for borehole core samples. Number of samples (n), mean value, and standard deviation given for each parameter. 67

Table 3.3 Carbon and sulfur speciation results for tailings borehole core samples. Number of samples (n), mean value, and standard deviation given for each parameter. 68

Table 3.4 Aqueous geochemistry for saturated zone monitoring well (MW1, MW2 and MW3) and basal drain (BD1) samples. Values averaged for four annual samples collected between 2004 and 2007. Alkalinity is given in mg L^{-1} as $CaCO_3$. 69

Table 4.1 Total dissolved masses for dissolved constituents calculated by trapezoidal integration. 91

Table 5.1 Final amended composition of field cells. 135

Table 5.2 Total dissolved masses calculated by trapezoidal integration over the depth interval from 100 to 400 cm below the tailings surface 136

List of Figures

Figure 2.1 Aqueous chemistry as a function of time. Alkalinity expressed in g L^{-1} as $CaCO_3$. 38

Figure 2.2 Sulfate-reduction rates compared to percent organic carbon (OC) and zero-valent iron (ZVI) in reactive mixtures. Error bars represent 95 % confidence intervals for triplicate batch experiments. 39

Figure 2.3 Most-probable number (MPN) populations of sulfate-reducing bacteria (SRB), iron-reducing bacteria (IRB), and acid-producing (fermentative) bacteria (APB) for each reactive mixture. Esterase hydrolysis activities (FDA hydrolysis rate) expressed as nmol of FDA hydrolyzed per hour per gram of sample. 40

Figure 2.4 Dissolved metal concentrations and acid-generating potential (AGP) as a function of time. 41

Figure 2.5 Backscatter-electron micrographs of (a) hexagonal Fe hydroxyl-carbonate and (b) an Fe-O-C-S phase on zero-valent iron surfaces. Disordered Fe-S precipitate with Fe:S ratios of 0.89 and 1.18 found in (c) RM1 and (d) RM4, respectively. Scale bars represent 2 μm. 42

Figure 2.6 Sulfur K-edge XANES spectra for reactive mixture samples and reference standards. All spectra shifted by +0.5 eV to achieve consistency with reference standard S K-edge energies reported by Fleet (2005). Vertical dotted lines represent S K-edges for realgar (a; 2471.1 eV), native S (b; 2472.0 eV), and gypsum (c; 2481.9 eV) reference standards. 43

Figure 3.1 State map of Alaska with study site location (inset), and as built plan view schematic of the tailings storage facility with borehole (BH), suction lysimeter and monitoring well (MW) locations. 70

Figure 3.2 (a) Photograph of a representative tailings thin section in reflected light and (b) transmitted light with polarizers crossed. (c) Reflected light image of dolomite grain containing framboidal pyrite inclusion at the arrow. (d) Backscatter electron (BSE) image of thin section showing colloform growth of anhedral sphalerite (sp) and framboidal pyrite (py), with galena replacement at the margin of a pyrite framboid indicated by the arrow. (e) BSE image showing euhedral pyrite with galena inclusions, arsenopyrite (asp), and grains of sphalerite, framboidal pyrite and galena contained within aggregated muscovite. (f) BSE image of intergrown chalcopyrite (cp) and galena (gn) with graphite (arrow), and barite (bar). 71

Figure 3.3 Measured and calculated acid generating potential (AP) and neutralization potential (NP) values. Calculated values of AP and NP utilized Ba and C speciation data, respectively. Area enclosed by dashed line indicates range of values determined for previously analyzed samples of Greens Creek tailings. Dotted line represents net neutralization potential (NNP) of unity. 72

Figure 3.4 Most probable number (MPN) populations of neutrophilic sulfur oxidizing bacteria (nSOB), acidophilic sulfur oxidizing bacteria (aSOB), iron reducing bacteria (IRB) and sulfate reducing bacteria (SRB) as a function of elevation in meters above sea level (m.a.s.l.). Shaded area represents vertical extent of tailings at borehole location. Horizontal dashed line with inverted triangle denotes approximate location of the phreatic surface. 73

Figure 3.5 Aqueous geochemistry of tailings for pore-water samples as a function of depth below the tailings surface. Circles and triangles represent samples collected in 2005 and 2007, respectively. Alkalinity (Alk) is given as mg L^{-1} as $CaCO_3$. 74

Figure 4.1 Depth profile of pore-water chemistry for control (top row) and amended (bottom row) cells. Horizontal dashed lines represent the lower extent of the organic carbon amended zone. The vertical dotted line indicates the average $\delta^{13}C$ value of the organic carbon amendments. 92

Figure 4.2 Depth profiles of pore-water sulfur species, $\delta^{34}S$ in sulfate, and most probable number populations of sulfate reducing bacteria (SRB) for control (top row) and amended (bottom row) cells. Horizontal dashed lines represent lower extent of organic carbon amended zone. Data points located on y-axis indicate values below analytical detection limits. 93

Figure 4.3 Depth profiles of pore-water metal and trace-element concentrations for control (top row) and amended (bottom row) cells. Horizontal dashed lines represent the lower extent of the organic carbon amended zone. Data points located on y-axis indicate values below analytical detection limits. 94

Figure 4.4 Backscatter electron (BSE) micrographs of solid-phase samples collected from the organic carbon amended cell (TC4) showing (a) Zn-Fe-S and (b) Fe-S precipitates on organic carbon particles. Scale bars represent 1 μm. 95

Figure 5.1 Location of the Greens Creek Mine. 137

Figure 5.2 Schematic diagrams of field cell design in cross section (left) and plan view (right). 138

Figure 5.3 Depth profiles of in situ moisture content and pressure head values measured in 2006 and 2007. 139

Figure 5.4 Depth profiles of pH, Eh, alkalinity (Alk), dissolved organic carbon (DOC), and $\delta^{13}C$ in dissolved inorganic carbon ($\delta^{13}C$-DIC) for pore-water samples collected from tension lysimeters in 2004, 2006, and 2008. Dotted lines represent $\delta^{13}C$ values of organic carbon. 140

Figure 5.5 Depth profiles of magnesium (Mg), calcium (Ca), calculated Ca:Mg ratios (mol/mol), total ammonia as N (NH_3-N), and orthophosphate (o-PO_4) for pore-water samples collected from tension lysimeters in 2004, 2006, and 2008. 141

Figure 5.6 Depth profiles of sulfate (SO_4), thiosulfate (S_2O_3), hydrogen sulfide (H_2S), ^{34}S in sulfate ($\delta^{34}S$-SO_4), and gypsum [$CaSO_4 \cdot 2H_2O$] saturation indices (SI) for pore-water samples collected from tension lysimeters in 2004, 2006, and 2008. 142

Figure 5.7 Pore-water $\delta^{13}C$-DIC plotted against $\delta^{34}S$-SO_4 for 2008 lysimeter samples. 143

Figure 5.8 Depth profiles of total iron (Fe_T), zinc (Zn), arsenic (As), antimony (Sb), and thallium (Tl) for pore-water samples collected from tension-lysimeters in 2004, 2006, and 2008. 144

Figure 5.9 Mean acid-generating potentials (AGP) and standard deviations calculated for pore-water samples collected in 2004, 2006, and 2008. 145

Figure 5.10 Depth profiles of MPN populations of APB, SRB, and IRB for core samples collected in 2004, 2006, and 2008. Depth profiles of saturation indices (SI) for ferrihydrite and siderite calculated for pore-water samples collected in 2004, 2006, and 2008. 146

Figure 5.11 Backscatter electron (BSE) images of (a) spheroidal Zn-S phase, (b) aggregated Fe-S precipitates, (c) spheroidal Zn-S and cubic Fe-S phases, and (d) disordered Fe-S precipitate on surfaces of organic carbon particles and dolomite grains. Scale bars represent 1 μm. 147

Figure 5.12 Water soluble SO_4 extracted from 2008 core samples using $Ar_{(g)}$-purged deionized water. 148

Figure 5.13 Solid-phase iron (Fe), zinc (Zn), arsenic (As), antimony (Sb), and thallium (Tl) concentrations for 2008 cores samples determined by selective extractions. Dotted line on Fe plots represents Fe(II) measured in filtrate. 149

List of Abbreviations

ABA	acid-base accounting
AMD	acid mine draiange
AGP	acid-generating potential
APB	acid producing (fermentative) bacteria
aSOB	acidophilic sulfur-oxidizing bacteria
BD	basal drain
BH	borehole
BSE	backscatter electron
CBE	charge balance error
DI	deionized
DIC	dissolved inorganic carbon
DOC	dissolved organic carbon
DSR	dissimilatory sulfate reduction
EDTA	ethylenediaminetetraacetic acid
EDX	energy dispersive X-ray
FDA	fluorescein diacetate
FE-SEM	field emission-scanning electron microscopy
IC	ion chromatography
ICP-AES	inductively coupled plasma-atomic emission spectroscopy
ICP-MS	inductively coupled plasma-mass spectrometry
ICP-OES	inductively coupled plasma-optical emission spectroscopy
IRB	iron-reducing bacteria
MB	municipal biosolids
MPN	most-probable number
MW	monitoring well
NMD	neutral mine drainage
NNP	net neutralization potential
NP	neutralization potential

nSOB	neutrophilic sulfur-oxidizing bacteria
OC	organic carbon
PRB	permeable reactive barrier
RM	reactive mixture
RSD	relative standard deviation
SAI	sulfide alteration index
SBG	spent brewing grain
SEM	scanning electron microscopy
SFCA	surfactant-free cellulose acetate
SI	saturation index
SOB	sulfur-oxidizing bacteria
SRB	sulfate-reducing bacteria
SRR	sulfate-reduction rate
TC	test cell
VOC	volatile organic carbon
VPDB	Vienna Pee Dee Belemnite
XANES	X-ray absorption near edge structure
XAS	X-ray absorption spectroscopy
XRD	X-ray diffraction
ZVI	zero-valent iron

Chapter 1:

Introduction

1.1 Background

1.1.1 Mine Drainage Geochemistry

Drainage from mine waste deposits can have widespread negative impacts on the quality of water resources (Moncur et al., 2005). These impacts are generally associated with the oxidation of sulfide minerals in the unsaturated zone of tailings and waste rock deposits. Sulfide-mineral oxidation is controlled both by abiotic and microbially-mediated processes, and oxidation mechansisms generally are described either as direct or indirect where O_2 or Fe(III) are the oxidant, respectively. Rates of sulfide-mineral oxidation are therefore dependent on pore-water pH and O_2 availability (Nordstrom and Alpers, 1999). Under near-neutral pH conditions, direct oxidation of sulfide minerals, such as pyrite [FeS_2], generates acidity and contributes SO_4 and Fe(II) to pore water (Blowes et al., 2003):

$$(1.1) \qquad FeS_{2(s)} + 7/2O_2 + H_2O \rightarrow 2SO_4^{2-} + Fe^{2+} + 2H^+$$

Additional metal(loid)s occurring as impurities in primary sulfide minerals will also be liberated during oxidation. Nordstrom and Alpers (1999) reported similar reaction rates for both chemical and microbially-mediated direct oxidation mechanisms. Microbially-mediated

direct oxidation is catalyzed by neutrophilic sulfur oxidizing bacteria (nSOB) such as *Thiobacillus thioparus* under near-neutral pH (Nordstrom and Southam, 1997; Gould and Kapoor, 2003). Under these conditions, the oxidation of liberated Fe(II) to Fe(III) and precipitation of Fe(III) (oxy)hydroxides generates additional acidity:

$$(1.2) \qquad Fe^{2+} + 1/4O_2 + 5/2H_2O \rightarrow Fe(OH)_{3(s)} + 2H^+$$

Acidity generated by sulfide-mineral oxidation and Fe(III) (oxy)hydroxide precipitation is neutralized by a series of mineral dissolution reactions. Neutral mine drainage (NMD) conditions will persist due to the dissolution of calcite [$CaCO_3$], dolomite [$CaMg(CO_3)_2$] and other carbonate phases (Jurjovec et al., 2002):

$$(1.3) \qquad CaMg(CO_3)_{2(s)} + 2H^+ \rightarrow Ca^{2+} + Mg^{2+} + 2HCO_3^-$$

Depletion of carbonate minerals as a result of ongoing neutralization may lead to subsequent decreases in pore-water pH and the development of acid mine drainage (AMD) conditions. The solubility of Fe(III) increases with decreasing pH, and indirect oxidation becomes the dominant pathway of sulfide-mineral oxidation at pH < 3.5 (Nordstrom, 2003). Indirect chemical oxidation of pyrite by Fe(III) also generates acidity and liberates Fe(II), SO_4 and associated metal(loid)s:

$$(1.4) \qquad FeS_{2(s)} + 14Fe^{3+} + 8H_2O \rightarrow 15Fe^{2+} + 2SO_4^{2-} + 16H^+$$

Rapid oxidation of Fe(II) to Fe(III) by acidophilic iron oxidizing bacteria (IOB), such as *Acidithiobacillus ferrooxidans* and *Leptospirillum ferrooxidans*, propagates the chemical oxidation mechanism. Direct abiotic sulfide oxidation can occur under acidic conditions; however, reaction rates are typically one to two orders of magnitude less than those reported for indirect oxidation rates (Nordstrom and Alpers, 1999).

Intermediate sulfoxyanion species, such as thiosulfate (S_2O_3), sulfite (SO_3) and polythionates (S_nO_6), may form via sulfide oxidation by atmospheric oxygen or during the sulfide mineral flotation process (Moses et al., 1987; Luther, 1987; Lotens and Wesker, 1987; Moses and Herman, 1991; Nordstrom and Southam, 1997; Schippers and Sand, 1999). The oxidation of thiosulfate in the presence of O_2 produces SO_4 and generates acid:

$$(1.5) \qquad S_2O_3^{2-} + 2O_2 + H_2O \rightarrow 2SO_4^{2-} + 2H^+$$

This reaction is catalyzed by *Thiobacillus sp.*; however, abiotic thiosulfate oxidation may also occur in the presence of Fe(III), Mn(IV) and NO_3 (Jorgensen, 1990; Suzuki, 1999).

Extended periods of sulfide-mineral oxidation can result in the development of large plumes of mine drainage impacted groundwater. Regardless of pH, the transport and subsequent discharge of these plumes to surface water bodies may facilitate the oxidation of Fe(II), Mn(II), NH_3 and S_2O_3, and acid generation (e.g. Equations 1.2 and 1.5). The oxidation of sulfur-bearing compounds in mine wastes may therefore have significant negative impacts on water resource quality.

1.1.2 Passive Treatment

The primary approaches to treatment of mine drainage may be described either as active or passive (Johnson and Hallberg, 2005). Active treatment systems generally involve pumping drainage into treatment plants where chemical reagents are added to promote oxidation, acid neutralization and floculation. This process removes acidity, metal(loid)s, and SO_4 prior to discharge; however, active treatment systems are generally burdened by high capital investment and long-term operating costs (Blowes, 2002). In contrast, passive systems utilize intrinsic (bio)geochemical reactions and hydraulic gradients to promote treatment. Passive

treatment systems are inherently cost-effective due to lower operating and capital costs (Johnson and Hallberg, 2005). However, enhancing the performance of passive treatment systems is essential for ensuring their acceptance among regulators and decision makers.

Passive systems which promote dissimilatory sulfate reduction (DSR), such as anaerobic bioreactors, anaerobic wetlands, and permeable reactive barriers (PRBs), have proven effective for treatment of mine drainage (Dvorak et al., 1992; Machemer and Wildeman, 1992; Benner et al., 1997). These treatment systems commonly utilize organic carbon-bearing materials to support DSR. Under strict anaerobic conditions, sulfate reduction is mediated by a diverse group of prokaryotes generally known as sulfate reducing bacteria (SRB). The majority of SRB are heterotrophic bacteria; however examples of archaea and autotrophic bacteria that mediate DSR have also been identified (Ehrlich, 2002). Heterotrophic SRB utilize low molecular weight (i.e. labile) organic carbon molecules (CH_2O) as electron donors and SO_4 as the terminal electron acceptor:

$$(1.6) \qquad SO_4^{2-} + 2CH_2O \rightarrow H_2S + 2HCO_3^-$$

Contribution of carbonate alkalinity neutralizes acidity and generates acid neutralizing potential. Production of H_2S promotes the precipitation of low-solubility metal-sulfide minerals, thereby reducing aqueos concentrations of Fe(III) and other metals:

$$(1.7) \qquad Fe^{2+} + H_2S \rightarrow FeS_{(s)} + 2H^+$$

Furthermore, (co)precipitation and sorption reactions with these metal-sulfide phases may contribute to the removal of additional metal(loid)s (Labrenz et al., 2000; Farquhar et al., 2002; Chen et al., 2003; Laforte et al., 2005).

Treatment of AMD was demonstrated by Tuttle et al. (1969) using wood dust to support growth of *Desulfovibrio desulficurans*. Additional organic carbon sources, including wood chips, livestock manure, crop residues, municipal compost, pulp mill waste, organic soil, sewage sludge and wine waste have been utilized for passive treatment of mine drainage (Dvorak et al., 1992; Christensen et al, 1996; Waybrant et al., 1998; Chang et al., 2000; Cocos et al., 2002; Hulshof et al., 2003; Gibert et al., 2004; Costa et al., 2009). Rates of DSR within these passive treatment systems depend on the availability of labile organic carbon compounds such as lactate and acetate. These low molecular weight organic carbon molecules are generated by the degradation of cellulose and lignin, followed by fermentation of the degradation products (Gould and Kapoor, 2003; Logan et al., 2005). Initial rates of sulfate reduction within passive systems are controlled by the original pool of organic acids present in solid-phase carbon sources. However, these rates generally decline with time and long-term sulfate-reduction rates become dependent on in situ production of labile organic carbon (Benner et al., 1999; Hemsi et al., 2005; Logan et al., 2005; Pruden et al., 2007).

Zero-valent iron (ZVI) also has proven effective for the remediation of AMD contaminated by metal(loid)s such as As, Cd, Co, Cr, Hg, Ni, Se, U and Zn (Blowes et al., 1997; Gu et al., 1998; Shokes and Moller, 1999; Herbert, 2003; Wilkin and McNeil, 2003; Weisener et al., 2005). Abiotic treatment is controlled by reduction and secondary sorption and (co)precipitation reactions (Shokes and Moller, 1999). In addition, ZVI corrosion may contribute to SO_4 reduction by generating H_2, in addition to Fe(II) and OH^-, under anaerobic conditions:

$$(1.8) \qquad Fe_{(s)} + 2H_2O \rightarrow Fe^{2+} + 2OH^- + H_2$$

Molecular hydrogen is utilized by some SRB species as an electron donor for SO_4 reduction (Karri et al., 2005):

$$(1.9) \qquad SO_4^{2-} + 4H_2 + 2H^+ \rightarrow H_2S + 4H_2O$$

Autotrophic species of SRB, such as *Desulfobacter hydrogenophilus*, are capable of growth in the presence of H_2 and CO_2, whereas heterotrophic species, for example *Desulfovibrio desulfuricans*, may oxidize H_2 but require OC as a growth substrate (Ehrlich, 2002).

1.2 Research Objectives

The primary objective of the research described in this thesis was to evaluate novel techniques for passive in situ treatment of acidic and neutral mine drainage. Passive treatment of mine water provides a cost-effective alternative to traditional active treatment systems. The goal of research into passive treatment is to improve the performance of existing technologies and develop new techniques for managing water quality in mining environments. Specific objectives of this research included:

- Evaluate the potential for enhancing passive AMD treatment using PRBs containing mixtures of ZVI and organic carbon.
- Investigate mineralogical, geochemical, and microbiological controls on pore-water and drainage chemistry under near-neutral pH conditions.
- Assess the potential for managing pore-water quality by amending tailings with a small and dispersed mass of organic carbon.
- Examine the influence of different organic carbon sources and amendment rates on sulfate reduction and pore-water chemistry.

1.3 Thesis Organization

This thesis is presented as a series of four research papers related to the objectives outlined in the previous section. The first research paper, which is presented as Chapter 2, describes laboratory batch experiments conducted to evaluate varied mixtures of ZVI and organic carbon for enhancing AMD treatment. The following three chapters describe a field-scale experiment designed to evaluate the potential for organic carbon amendment of tailings as a passive technique for managing pore-water quality. Chapter 3 presents a detailed study of mineralogical, geochemical and microbial mechanisms controlling the pore-water chemistry at the field site. Chapter 4 presents data from two of six experimental field cells (TC2 and TC4) as proof of principle for passive in situ treatment of pore-water by amending tailings with a small and dispersed mass of organic carbon. Chapter 5 presents a field-scale comparison of pore-water chemistry associated with varied organic carbon amendments from six field cells (TC2–TC7). The final chapter, Chapter 6, presents a general summary of findings from the individual research papers.

Chapter 2:

Zero-Valent Iron and Organic Carbon Mixtures for Remediation of Acid Mine Drainage:Batch Experiments

2.1 Executive Summary

A series of laboratory batch experiments was conducted to evaluate the potential for treatment of acid mine drainage (AMD) using organic carbon (OC) mixtures amended by zero-valent iron (ZVI). Modest increases in sulfate reduction rates (SRRs) of up to 15 % were achieved by augmenting OC materials with 5 and 10 dry wt. % ZVI. However, OC was essential for supporting sulfate reducing bacteria (SRB) and therefore sulfate reduction. This observation suggests a general absence of autotrophic SRB which can utilize H_2 as an electron donor. Sulfate reduction rates (SRRs), calculated using a mass-based approach, ranged from -12.9 to -14.9 nmol L^{-1} d^{-1} g^{-1} OC. Elevated populations of SRB, iron reducing bacteria (IRB), and acid producing (fermentative) bacteria (APB) were present in all mixtures containing OC. Effective removal of Fe (91.6–97.6 %), Zn (> 99.9 %), Cd (> 99.9 %), Ni (> 99.9 %), Co (> 99.9 %), and Pb (> 95 %) was observed in all reactive mixtures containing OC. Abiotic metal removal was achieved with ZVI only, however Fe, Co and Mn removal was less effective in the absence of OC. Secondary disordered mackinawite [$Fe_{1+x}S$] was observed in field-emission scanning electron microscopy (FE-SEM) backscatter electron micrographs of mixtures that generated sulfate reduction. Energy dispersive X-ray (EDX) spectroscopy revealed that Fe-S precipitates were Fe-rich for mixtures containing OC and ZVI, and S-rich in the absence of ZVI amendment. Sulfur K-edge spectra collected by synchrotron-radiation based bulk X-ray adsorption near edge structure (XANES) spectroscopy indicate solid-phase S is in a reduced form in all mixtures that contained OC. Pre-edge peaks on XANES spectra suggest tetragonal S coordination, which is consistent with the presence of a Fe-S phase such as mackinawite. The addition of

ZVI enhanced AMD remediation over the duration of these experiments, however long-term evaluation is required to identify optimal ZVI and OC mixtures.

2.2 Introduction

Drainage emanating from mine waste deposits is a serious threat to the quality of groundwater and surface water resources. Deposition of mill tailings and waste rock in surface impoundments exposes residual sulfide minerals to atmospheric oxygen. Under near-neutral pH conditions, oxidation of sulfide minerals is catalyzed by bacteria such as *Thiobacillus thioparus* in the unsaturated zone of mine wastes (Suzuki, 1999; Blowes et al., 2003). The oxidation of pyrite [FeS_2] and other sulfide minerals generates acidity and releases SO_4, Fe(II), metals and trace elements to pore-water:

$$(2.1) \qquad FeS_{2(s)} + 7/2O_2 + H_2O \rightarrow 2SO_4^{2-} + Fe^{2+} + 2H^+$$

Additional acidity is subsequently produced *via* the oxidation of Fe(II) to Fe(III) and precipitation of hydrous ferric oxides. Over extended periods of sulfide oxidation, acid production consumes the neutralizing potential of the mine wastes and decreases in pore-water pH often are observed (Blowes and Jambor, 1990; Jurjovec et al., 2002; Blowes et al., 2003; Moncur et al., 2005; Gunsinger et al., 2006). Continual sulfide oxidation combined with a loss of acid neutralization potential can eventually result in the formation of large plumes of AMD impacted groundwater. Transport and subsequent discharge of AMD impacted groundwater to receiving surface water bodies is followed by further acidification:

$$(2.2) \qquad Fe^{2+} + 1/4O_2 + 5/2H_2O \rightarrow Fe(OH)_{3(s)} + 2H^+$$

Therefore, remediation generally focuses either on treating or preventing AMD discharge.

Microbially mediated sulfate reduction has been successfully utilized in AMD treatment systems. Passive AMD remediation systems, including constructed wetlands (Hedin et al., 1989; Machemer and Wildeman, 1992), anaerobic bioreactors (Dvorak et al., 1992; Christensen et al., 1996) and permeable reactive barriers (PRBs; Benner et al., 1999; Blowes et al., 2000; Ludwig et al., 2002; Hulshof et al., 2006), have provided varied levels of success in treating SO_4, metals and trace elements, buffering pH, and generating carbonate alkalinity. These methods are similar in that organic carbon (OC) is utilized to promote microbially mediated sulfate reduction. However, only PRBs are designed to treat AMD prior to discharge. Under strict anaerobic conditions, SRB gain energy by catalyzing the oxidation of low molecular weight OC compounds (e.g. CH_2O) coupled with sulfate reduction (Postgate, 1984):

$$(2.3) \qquad SO_4^{2-} + 2CH_2O \rightarrow H_2S + 2HCO_3^-$$

The ensuing increase in the concentration of dissolved H_2S promotes the precipitation of low-solubility metal-sulfides. Consequently, decreases in dissolved concentrations of metals, such as Fe, Zn, Cd, Ni, and Pb, are generally coupled with H_2S production. Adsorption onto OC, precipitation of metal hydroxides and carbonates, and (co)precipitation with these hydroxides may also contribute to metal removal (Machemer and Wildeman, 1992; Gibert et al., 2005). These processes minimize the discharge of metals and trace elements to surface water bodies, and prevent extensive acidification.

Zero-valent iron (ZVI) also has proven effective in the remediation of AMD contaminated by metals and trace elements such as As, Cd, Co, Cr, Hg, Ni, Se, U and Zn (Blowes et al., 1997; Gu et al., 1998; Shokes and Moller, 1999; Herbert, 2003; Wilkin and

McNeil, 2003; Weisener et al., 2005). Abiotic removal is controlled by several processes including adsorption onto ZVI surfaces and precipitation reactions (Shokes and Moller, 1999). However, ZVI corrosion may contribute to SO_4 reduction by generating H_2, in addition to Fe(II) and OH^-, under anaerobic conditions:

$$(2.4) \qquad Fe_{(s)} + 2H_2O \rightarrow Fe^{2+} + 2OH^- + H_2$$

Molecular hydrogen is utilized by some SRB species as an electron donor for SO_4 reduction (Karri et al., 2005):

$$(2.5) \qquad SO_4^{2-} + 4H_2 + 2H^+ \rightarrow H_2S + 4H_2O$$

Autotrophic SRB, such as *Desulfobacter hydrogenophilus*, are capable of growth in the presence of H_2 and CO_2, while heterotrophic species, for example *Desulfovibrio desulfuricans*, may oxidize H_2 but require OC for growth (Ehrlich, 2002).

The addition of ZVI to PRBs containing OC therefore has potential to enhance sulfate reduction, pH buffering, and the removal of metals and trace elements. Guo (2008), Geets et al. (2005) and Gibert et al. (2003) demonstrated that such mixtures can support enhanced sulfate reduction but the effect of the proportion of ZVI has not been evaluated. Karri et al. (2005) suggested that ZVI may be utilized as an inexpensive material for donating electrons; however, ZVI can cost in excess of 20 times more per m^3 than OC. Minimizing the mass of ZVI required to achieve desired enhancements in PRB performance would therefore be required to maximize the cost-effectiveness of this technique. This study evaluates the geochemical effects of the addition of varying proportions of ZVI to OC mixtures for AMD remediation.

2.3 Laboratory Methods

2.3.1 Experimental Setup

Laboratory batch experiments were conducted using simulated mine drainage water to evaluate sulfate reduction, metal removal, and acid neutralization associated with five reactive mixtures. Experiments were conducted in a Coy Laboratory Products Inc. anaerobic chamber using 1000 mL glass reaction flasks, each fitted with two sampling ports and one access port. Sampling ports were sealed with Teflon®-lined septa to permit repeated sample collection using syringes. Access ports were sealed with vacuum grease and ground glass stoppers held in place with Keck clamps. Evolved gases were vented into a beaker of deionized (DI) water using a needle attached to Tygon® tubing inserted into one of the two sampling ports. Anaerobic conditions were monitored using GasPak™ methylene blue anaerobic indicator strips.

The simulated AMD solution chemistry (Table 2.1) was based on data collected from the Nickel Rim mine site near Sudbury, ON, and additional mines located in northern Ontario and Manitoba. A stock solution, excluding Fe(II), was prepared by dissolving metal-sulfate and metal-chloride salts in $CaCO_3$ saturated deionized water. This solution was transferred to the anaerobic chamber and purged with anaerobic grade $Ar_{(g)}$ for at least 2 hours. The Fe(II) solution was prepared by dissolving $FeSO_4 \cdot 7H_2O$ in 0.1 N H_2SO_4 and bubbling 5 % $H_{2(g)}$ for 24 hours in the presence of a Pd catalyst. This solution was then transferred into the anaerobic chamber and added to the stock solution. The final pH was adjusted to between 4.5 and 4.8. The solution was vacuum filtered inside the anaerobic chamber using 0.45 μm surfactant-free cellulose acetate (SFCA) filters.

Five reactive mixtures, consisting of four primary components, were prepared. Each mixture contained 50 dry wt. % reactive materials, 32 dry wt. % porous support, 16 dry wt. % neutralizing agent, and 2 dry wt. % inoculum. The component of reactive materials in each mixture (Table 2.2) consisted of a 4:3:3 ratio of composted leaf mulch to chipped wood to hardwood sawdust. This mixture was augmented by an increasing proportion of ZVI (Connelly-GPM Inc., Chicago, IL, USA). The two end-member mixtures contained only OC or ZVI as the reactive component. Acid-washed silica sand (ASTM 20–30 mesh) was added for porous support, and pulverized agricultural limestone was utilized as a pH-neutralizing agent. These components were washed with DI water and allowed to air-dry prior to being added to the reactive mixtures. Sediment collected from the anaerobic zone of a local creek (Laurel Creek, Waterloo, ON) bed was utilized as SRB inoculum. The gravimetric water content of each component was determined by weighing samples before and after drying at 105°C for 24 hours. These values were used to calculate equivalent dry weights. Two reactive mixtures were evaluated in triplicate to facilitate statistical analysis.

The reactive mixtures were prepared to a total dry mass of 150 g and placed in the reaction flasks. The flasks were transferred, unsealed, into the anaerobic chamber and allowed to equilibrate with the anaerobic atmosphere. After 24 hours, 850 mL aliquots of the input solution were dispensed into each flask. The access and sampling ports were sealed, and the flasks wrapped with aluminum foil to limit exposure to light and inhibit the growth of phototrophic bacteria. Flasks were agitated at least twice per week to ensure that reaction rates were not diffusion limited.

2.3.2 Water Sampling and Analysis

Aqueous samples were collected with time using 60 mL syringes. Glass syringes were used for collection of $H_2S_{(aq)}$ samples and disposable polyethylene syringes were used to collect all other samples. Anaerobic grade $Ar_{(g)}$ was injected into the flasks during sample collection to prevent introduction of $H_{2(g)}$ from the glove box atmosphere. All measurements and sample collection took place within the anaerobic chamber. Measurements of pH and Eh were made in sealed cells on unfiltered samples immediately following sample collection. The pH electrode (Orion ROSS 81–56) was calibrated with standard pH 4 and 7 buffers, and then checked against pH 10 buffer. The redox electrode (Orion 96–78) was regularly checked against ZoBell's (Nordstrom, 1977) and Light's (Light, 1972) solutions. All additional samples were filtered using 0.45 μm SFCA filters. Alkalinity was determined by adding bromocresol green-methyl red indicator and titrating to pH 4.5 with H_2SO_4. Samples for cation analysis (Al, Ba, Ca, Cd, Cr, Co, Cu, Fe, K, Li, Mg, Mn, Mo, Na, Ni, Pb, Si, Sr, and Zn) were preserved with trace-metal grade HNO_3 and analyzed by inductively-coupled plasma atomic emission spectroscopy (ICP-AES). Concentrations of SO_4 and NO_3 were determined on unacidified samples using ion-chromatography (IC). Samples for H_2S, NH_3 and ortho-phosphate (o-PO_4) analysis were collected at alternating sample collection times to minimize mass removal. The methylene blue spectrophotometric method (Lindsay and Baedecker, 1988) was used to determine aqueous H_2S concentrations. Samples collected for NH_3 and o-PO_4 analysis were preserved with trace-metal grade H_2SO_4 and analyzed using the phenate and ascorbic acid spectrophotometric methods, respectively (SMEWW, 2005). Dissolved organic carbon (DOC) concentrations were determined by combustion and infrared detection.

Replicate, filter blanks, acid blanks, and DI water samples were submitted for quality control evaluation. A total of four sets of duplicates and one triplicate were submitted for IC and ICP-AES analysis. Percent relative standard deviations were consistently < 1 % for SO_4 and < 5 %, for ICP-AES analyses, with the exception of one duplicate analyses for both Fe (10.6 %) and Pb (8.6 %). Standard deviation bars are not displayed on figures as the symbol size for individual data points is generally larger than the standard deviation of the measurement. Trace concentrations of major cations (Ca, Mg, Fe, Na, K) were detected in blank samples, however SO_4 and all other metals were consistently below analytical detection limits.

2.3.3 Microbiology

Microbial populations associated with the remediation of AMD were enumerated following completion of the batch experiments. Samples of each reactive mixture were collected under anaerobic conditions and sealed in sterile 40 mL amber glass volatile organic compound (VOC) vials with Teflon-lined septa. The vials were placed in a GasPak™ anaerobic jar and refrigerated for 7 days. Relative populations of SRB, iron reducing bacteria (IRB) and acid-producing (fermentative) bacteria (APB) were determined. Esterase activity was measured as an indication of general microbial activity.

The most probable number (MPN) technique (Cochran, 1950) was use to determine populations of SRB, IRB and APB. Modified Postgate (1984) medium C and a Fe(III)-EDTA growth medium were used to promote SRB and IRB growth, respectively (Benner et al., 2000; Gould et al., 2003). The SRB media was prepared by dissolving 0.5 g L^{-1} KH_2PO_4, 1.0 g L^{-1} NH_4Cl, 4.5 g L^{-1} Na_2SO_4, 0.04 g L^{-1} $CaCl_2 \cdot 2H_2O$, 0.06 g L^{-1} $MgSO_4 \cdot 7H_2O$,

0.004 g L^{-1} $FeSO_4 \cdot 7H_2O$, 2.92 g L^{-1} 60 % Na-lactate, 1.28 g L^{-1} Na-acetate, 1.0 g L^{-1} yeast extract and 0.3 g L^{-1} Na-citrate dihydrate in DI water. The solution pH was buffered to 7.5 and 2.0 mL L^{-1} of 0.1 % Na-resazurin solution was added as an O_2 indicator. Growth media for IRB consisted of 2.5 g L^{-1} $NaHCO_3$, 1.5 g L^{-1} NH_4Cl, 0.6 g L^{-1} $NaH_2PO_4 \cdot H_2O$, 0.1 g L^{-1} $CaCl_2 \cdot 2H_2O$, 0.1 g L^{-1} KCl, 0.1 g L^{-1} $MgCl_2 \cdot 6H_2O$, 0.005 g L^{-1} $MnCl_2 \cdot 4H_2O$, 0.001 g L^{-1} $Na_2MoO_4 \cdot 2H_2O$, 1.84 g L^{-1} Fe(III) EDTA and 1.5 g L^{-1} protease peptone dissolved in DI water and buffered to a final pH of 7.0. The SRB and IRB media was boiled and bubbled with $N_{2(g)}$ for 1 hr to reduce dissolved O_2 concentrations. The solutions were transferred to the anaerobic chamber, and 9.0 mL aliquots were dispensed into 20 mL serum bottles which were then sealed with butyl rubber stoppers and Al crimp seals. Fermenters (APB) were grown in media that was prepared by adding 5.0 g L^{-1} dextrose, 1.0 g L^{-1} beef extract, 10.0 g L^{-1} protease peptone, 5.0 g L^{-1} NaCl and 0.1 g L^{-1} bromothymol blue to DI water and adjusting the pH to 7.2 (Hulshof et al., 2003). The APB media was dispensed in 9.0 mL aliquots into glass culture tubes. All media was sterilized at 121°C for 30 minutes, allowed to cool, and inoculated by adding 1.0 ± 0.05 g of sample to each of five serum bottles or culture tubes. A series of nine serial dilutions was performed such that a 10 order of magnitude range in concentration was achieved. Incubation occurred at ambient temperature (22 ± 2°C) over a period of four weeks for SRB and IRB, and 96 hours for APB. Positive results for SRB were identified by the presence of black Fe-sulfide precipitates. A change in media color to purple following the addition of 0.1 mL of ferrozine solution (Gibbs, 1979) indicated the presence of IRB. A change in media color from green to yellow signified the presence of APB. The number of positive results at each dilution level was recorded and an MPN table (Alexander, 1965) was used to enumerate the population as cells g^{-1} sample.

Fluorescein diacetate (FDA) hydrolysis rates were determined as a measure of esterase activity and therefore overall microbial biomass (Schnurer and Rosswall, 1982). A pH buffer solution was prepared by dissolving 8.16 g L^{-1} of KH_2PO_4 in DI water and adjusting the final pH to 7.7 using 0.1 N NaOH. A 20 mg mL^{-1} solution of FDA was prepared in reagent-grade acetone. The hydrolysis reaction was initiated by combining 5.0 g of sample, 50 mL of buffer solution and 0.5 mL of FDA solution in Erlenmeyer flasks. Hydrolysis was stopped after 60 minutes by adding 50 mL of acetone to each flask. Solutions were funnel filtered using Whatman No. 1 qualitative filters and hydrolyzed FDA was measured at a wavelength of 480 nm using a Hach DR2400 spectrophotometer. The blank for the spectrophometric analysis contained 50 mL each of DI water and reagent-grade acetone. The rate of FDA hyrolysis was calculated using the method described by Schnurer and Rosswall (1982).

2.3.4 Mineralogical Study

Solid-phase samples of each reactive mixture were collected after approximately 60 days. Samples were homogenized and dried, under anaerobic conditions, in a vacuum desiccator. Dried samples were stored in 20 mL amber glass VOC vials with Teflon-lined septa and frozen until analysis.

Field emission-scanning electron microscopy (FE-SEM) with energy dispersive X-ray (EDX) spectroscopy was utilized for examination of reaction products. Samples were fixed to Al stubs using double sided conductive C adhesive and the surface was coated with Au approximately 8 nm thick. A LEO 1530 FE-SEM fitted with a Robinson backscatter detector and an EDAX Pegasus 1200 EDX system was utilized for electron micrograph

collection and semi-quantitative chemical analysis, respectively. Electrons were emitted at an accelerating potential of 20 kV for both techniques, and EDX spectra were collected for a minimum of 120 s prior to standardless quantification.

Synchrotron-radiation based bulk X-ray Adsorption Spectroscopy (XAS) was utilized to examine solid-phase sulfur speciation in the reactive mixtures. Sulfur K-edge spectra were collected for reference standards and samples. Bulk X-ray Adsorption Near-Edge Structure (XANES) spectroscopy was carried out on beam-line X15b at the National Synchrotron Light Source located at Brookhaven National Laboratory in Upton, New York. Samples were placed into 0.12 mil Mylar X-ray film pouches and mounted within the experimental chamber, which was then sealed and purged with $He_{(g)}$ for at least 30 min. Scans were performed over an energy range of 2420 to 2520 eV with absorbance being measured for a 1 mm^2 area. Gypsum [$CaSO_4 \cdot 2H_2O$], native sulfur [S_8], and realgar [α-As_4S_4] were analyzed as reference standards. A minimum of two locations were analyzed on each sample and standard, and at least two replicate scans were performed at each location. Spectral data were averaged for replicate scans and edge step normalization was performed using Athena XAS data analysis software (Ravel and Newville, 2005).

2.3.5 Geochemical Modeling

The geochemical equilibrium/mass-transfer code MINTEQA2 (Allison et al., 1990) was used to assist with interpretation of aqueous geochemistry data. The MINTEQA2 database was modified for consistency with that of WATEQ4F (Ball and Nordstrom, 1991). Additional solubility data for Co (Papelis et al., 1988), PO_4 (Baker et al., 1998) and siderite (Ptacek, 1992) was also incorporated into the database. Saturation indices (SI) calculated by

MINTEQA2 were used to identify mineral phases potentially controlling the composition of the aqueous phase. Concentrations of H_2S, NO_3, NH_3, and o-PO_4 were estimated by linear interpolation for times when sample analyses were not performed for these parameters.

2.4 Results and Discussion

2.4.1 Aqueous Geochemistry

Conditions favorable for sulfate reduction developed rapidly in all reactive mixtures with near-neutral pH conditions observed within the first 6 to 13 days (Figure 2.1). Decreases in Eh from initial values between 50 and 100 mV to < -200 mV were observed over this period, with the lowest value of -273 mV measured in the mixture with no OC (RM5). Increases in pH from initial values of 4.50 and 4.80 to between 6.38 and 6.87 were observed in mixtures containing OC (RM1–RM4). Carbonate alkalinity increased from < 50 mg L^{-1} to between 1600 and 2000 mg L^{-1} (as $CaCO_3$) in the OC containing mixtures (RM1–RM4), indicating that bicarbonate contributed by OC degradation influenced the pH in these reactive mixtures. Gibert et al. (2003) reported pH buffering by a mixture of ZVI and OC to between 6 and 8 after approximately 10 days in a column experiment and Waybrant et al. (1998) observed similar trends in pH and alkalinity in batch experiments containing only OC. Larger increases in pH, from 4.80 to 7.32 within the first 11 days (maximum 7.61), were observed in RM5 (0 dry wt. % OC) however carbonate alkalinity remained below 55 mg L^{-1} (as $CaCO_3$). This alkalinity was likely contributed by calcite and creek sediment included in the reactive mixture. The larger pH increase in RM5 presumably resulted from ZVI corrosion and less buffering by carbonate alkalinity.

Increases in DOC at early times in RM1 through RM4 were coupled with decreases in NO_3-N and increases in NH_3-N and o-PO_4 concentrations. Complete reduction of NO_3 occurred in all mixtures during the initial 7 to 14 days of the experiment. Observed contributions of dissolved NH_3 and o-PO_4 likely resulted from OC degradation in RM1–RM4, which is consistent with observations of Waybrant et al. (2002). Decreases in NO_3-N were not reflected by a 1:1 increase in NH_3-N concentrations in the absence of OC (RM5). This observation suggests that denitrification, or a removal mechanism such as sorption onto ZVI surfaces, controlled NH_3 availability in RM5 (Westerhoff and James, 2003). Dissolved o-PO_4 concentrations increased to maximum values ranging from 6.5 to 33 mg L^{-1} for mixtures containing OC, but for RM5 remained < 1 mg L^{-1} throughout the experiment.

Development of conditions favorable for sulfate reduction occurred prior to decreases in dissolved SO_4 concentrations in all reactive OC bearing mixtures. The time for removal of 10 % of initial aqueous mass of SO_4 ranged from 12 to 15 days in these batches. Aqueous H_2S concentrations and carbonate alkalinity increased between days 12 and 32, while decreases in both SO_4 and DOC were observed over this period. These results suggest that DOC oxidation was coupled with sulfate reduction, leading to production of H_2S and carbonate alkalinity. The largest increase in aqueous H_2S concentrations of 0.2 mg L^{-1} was observed for RM1. These concentrations were much lower than those observed in similar experiments by Waybrant et al. (1998) who reported H_2S concentrations in excess of 60 mg L^{-1} following complete removal of Fe and Zn. In the current study; however, Fe was contributed by the input solution, and by ZVI corrosion for RM2 through RM4. Therefore, the precipitation of Fe(II) and other metal sulfides likely limited aqueous H_2S concentrations.

2.4.2 Sulfate Reduction Rates

Sulfate reduction rates (SRRs) were calculated using a mass-based rather than the concentration-based approach used in previous studies (Waybrant et al. 1998; Cocos et al., 2002, Gibert et al., 2004). Waybrant et al. (1998) suggested this approach as more accurate for determining SRRs because the mass of SO_4 removed during sampling is excluded from rate calculations. The SRRs calculated using this mass-based approach were lower than those calculated using only aqueous concentrations. However, this approach is still an approximation as precipitation-dissolution reactions, adsorption/desorption, and aqueous concentrations of SO_4 and H_2S are not accounted for in the rate calculations (MacPherson and Miller, 1963; Brock et al., 1984).

Linear least-squares regression was applied to the mass-differentiated data following methods described by Waybrant et al. (1998) and Cocos et al. (2002), which exclude early-time and late-time data. Excluding the early time data removes potential influences of the acclimation period, and sulfur inputs, from soluble phases, such as gypsum, or organic sulfur dissolution. Initial increases in aqueous SO_4 concentrations were generally observed over the first 5 days for all reactive mixtures containing OC (RM1–RM4). Data reported in previous studies shows similar initial increases in dissolved SO_4 concentrations for some reactive mixtures (Waybrant et al., 1998; Cocos et al., 2002; Gibert et al., 2004). The acclimation period, determined using these early-time SO_4 concentrations, combined with pH, Eh and alkalinity measurements, was excluded from the rate calculations. Late-time data were also excluded from the regression analysis as reduction rates may be limited at low dissolved SO_4 concentrations (Boudreau and Westrich, 1984). This approach resulted in sample sizes (n) of 6 or 7 and coefficients of determination (r^2) based on linear least-squares regression ranged

from 0.92 to 0.95 (Table 2.3). Rates are reported as negative values, to indicate SO_4 removal, and are normalized to the dry mass of OC. The total mass of reactive components (OC and ZVI) remained a constant 50 dry wt. % in all batches. However, expressing the SRRs on a per gram of OC basis demonstrates the contribution of ZVI to SO_4 reduction.

Statistical evaluation of RM1 and RM4 triplicates was used to calculate 95 % confidence intervals for these mixtures. These results indicate that data points for each batch are from the same population and therefore calculated SRRs are representative of those populations. Furthermore, 95 % t-test confidence intervals calculated for triplicate batches indicate that 95 % of the time, the mean SO_4 reduction rates fall within ± 0.26 (RM1) and ± 0.43 (RM4) nmol L^{-1} d^{-1} g^{-1} of the actual rate.

Results indicate that the addition of ZVI to OC mixtures can enhance SO_4 reduction rates (Figure 2.2). Sulfate reduction rates for reactive mixtures RM1–RM4 ranged from -12.9 to -14.9 nmol L^{-1} d^{-1} g^{-1}. Greater than 94 % of the decrease in total mass of SO_4 for RM5 was due to sample collection therefore calculation of a sulfate reduction rate was not warranted. The highest SRR, -14.9 nmol L^{-1} d^{-1} g^{-1}, was observed in RM3 (5 dry wt. % ZVI), however this rate is not statistically different from a mean rate of -14.6 nmol L^{-1} day^{-1} g^{-1} observed in RM4 (10 dry wt. % ZVI). Reactive mixtures RM2 (2 dry wt. % ZVI) and RM1 (0 dry wt. % ZVI) supported lower SRRs of -13.8 and -12.9 nmol L^{-1} d^{-1} g^{-1}, respectively. These results represent a modest increase of 15 % associated with RM3 (5 dry wt. % ZVI) and RM4 (10 dry wt. % ZVI) as compared to RM1 (0 dry wt. % ZVI). These results suggest that incorporation of > 5 dry wt. % ZVI into OC mixtures does not further enhance SRRs and is therefore not cost-effective. However, a 15 % increase in SRR equates to a large increase in the mass of SO_4 reduced over the life-span of a PRB, which may be several years (Benner et

al., 2002). Furthermore, consumption of OC is known to result in decreases in SO_4 reduction rates over extended periods of time (Benner et al., 2002; Hemsi et al., 2005). Therefore, the incorporation of ZVI may also sustain higher long-term SRRs; however this aspect was not the focus of this study.

Sulfate reduction rates measured in this study are similar to values reported for previous laboratory batch experiments. Waybrant et al. (1998) and Cocos et al. (2002) reported SRRs ranging from -0.15 to -4.4 nmol L^{-1} d^{-1} g^{-1}. These rates were likely overestimated as mass removal during sample collection was not considered. In the present study, SRRs calculated on the basis of aqueous concentration were 19.2 % (± 1.5 %) higher than those determined using the mass-based approach. However, the total mass removed by sample collection for RM1–RM4 was 29.4 % (± 1.1 %) of initial aqueous mass of SO_4. The 10.2 % difference in these values arises because mass removed per unit volume of sample collected decreases proportionally with dissolved SO_4 concentrations. Therefore the percent mass of SO_4 removed during sample collection cannot be directly applied as a correction factor for concentration-based SRRs.

2.4.3 Microbial Activity

Populations of SRB, IRB, and APB were elevated in samples collected from RM1–RM4 compared to RM5 (Figure 2.3). Reactive mixtures RM1 - RM4 supported comparable SRB populations ranging from $7.0 \cdot 10^6$ to $1.7 \cdot 10^7$ cells g^{-1}, while no evidence of SRB growth was observed in samples collected from RM5. Populations of IRB ranged from $4.6 \cdot 10^4$ to $1.7 \cdot 10^6$ cells g^{-1} in mixtures containing OC, and the MPN value was approximately 2 orders of magnitude lower for RM5. The abundance of APB was reasonably uniform in RM1 to

RM4 as populations were between $1.3 \cdot 10^3$ and $4.3 \cdot 10^3$ cells g^{-1}, while a slight decrease in the APB population to $2.4 \cdot 10^2$ cells g^{-1} was observed in RM5. Esterase activity, determined by FDA hydrolysis rate, also showed little variability between the mixtures containing OC, with values ranging from 2.6 to 3.5 nmol h^{-1} g^{-1}. Microbial biomass was lower for RM5 as indicated by a FDA hydrolysis rate of 0.2 nmol h^{-1} g^{-1}.

The SRB populations are consistent with calculated SRRs (Figure 2.2), while the absence of SRB in RM5 suggests a physiological constraint imposed by limited OC or PO_4 availability (Harder and Dijkhuizen, 1983; Chapelle, 1993). Although $H_{2(aq)}$ concentrations were not measured, increases in pH and decreases in Eh are indicative of anaerobic ZVI corrosion which produces H_2. Studies performed by Guo (2008), Geets et al. (2005), Karri et al. (2005) and Gu et al. (1999) demonstrate that SRRs can be enhanced with the addition of H_2 as an electron donor. However, each of these studies included an OC source, which would promote the growth of heterotrophic SRB (Ehrlich, 2002). Geets et al. (2005) also demonstrated that variation of the OC source and electron donor promotes time-dependent adaptive changes in phylogenic composition of SRB populations. Increases in SRRs in the presence of ZVI may therefore correspond to higher relative populations of H_2 oxidizing SRB. Additional increases in SRRs may have been observed if additional time, and SO_4, were provided to allow the SRB communities to adapt to H_2 as an electron donor. The absence of SRB, and sulfate reduction, observed in RM5 may result from a lack of autotrophic SRB species in the inoculum (Pruden et al., 2007). This interpretation would explain the absence of SRB in RM5 (0 dry wt. % OC); however, sequencing techniques were not employed in this study.

The abundance of IRB was generally 1 to 2 orders of magnitude lower than that of SRB, with the exception of RM5. Although SRB were not detected in RM5, an IRB population of $2.4 \cdot 10^2$ cells g^{-1} was enumerated. This observation initially suggests that the system is not limiting for IRB which may be heterotrophic or autotrophic, and either strict or facultative anaerobes (Ehrlich, 2002). However, inoculation of IRB media with RM5 samples contributed ZVI and solution containing elevated dissolved concentrations of Fe(II). Corrosion of ZVI during inoculation and transfer of aqueous Fe(II) during serial dilutions likely produced false positive results for RM5. This interpretation is supported by FDA hydrolysis rates approximately 1 order of magnitude lower than those observed for RM1–RM4. Populations of IRB were consistently > 10^4 cells g^{-1} in mixtures containing OC. These samples contained less ZVI and exhibited low dissolved Fe(II) concentrations, therefore false positive results are not likely for RM1–RM4.

All reactive mixtures containing OC supported elevated APB, SRB and IRB populations as compared to RM5. The presence of APB is important in OC PRB systems because heterotrophic SRB and IRB utilize low molecular weight OC molecules produced by APB during fermentation (Gould and Kapoor, 2003; Pruden et al., 2007). Microbial biomass, determined by esterase activity, also showed little variation between mixtures containing OC. Once again, RM5 was the exception with a measured FDA hydrolysis rate approximately one order of magnitude lower than mixtures RM1–RM4.

These results suggest that the inclusion of OC in reactive mixtures for AMD remediation is important for SRB growth and overall microbial activity. The impact of not including OC as a reactive component may be twofold. First of all, the lack of substrate will limit the activity of heterotrotrophs, and autotrophs that require CO_2 only as a substrate for

growth. Secondly, the system may be nutrient limited as OC is the primary source of available P and N. Both of these constraints may impose physiological limitations on microbial growth and activity within PRB systems.

2.4.4 Metal Removal

Substantial decreases in dissolved concentrations of all metals were observed for RM1–RM5 (Figure 2.4). Decreases in dissolved Fe ranged from 97.6 to 95.4 % for RM1–RM4, respectively, and 31.3 % for RM5. Greater than 99 % removal of Al, Cd, Co, Ni, and Zn, was consistently observed for mixtures containing OC (RM1–RM4). Removal of Co and Zn with RM5 was less effective with 76.7 and 98.2 % declines, respectively. Although > 99 % of Ni and Cd was removed with RM5, removal was not as rapid as observed in mixtures containing OC. Calculation of metal removal efficiencies utilized half of the value of the analytical detection limit for non-detectable concentrations. This likely resulted in lower calculated Pb removal percentages, which ranged from 94.6 to 96.9 %, as dissolved concentrations decreased to below the 0.07 mg L^{-1} detection limit within 1 day in all reactive mixtures. Removal of Mn, with mixtures RM1–RM4, ranged from 89.9 and 90.6 %, however, an increase in Mn of 28.3 % was observed in RM5. Acid generating potential (AGP), which was calculated as described by Waybrant et al. (1998), decreased from an average of 24.5 meq L^{-1} to < -31 meq L^{-1} in all batches containing OC. A decrease in AGP from 24.2 to 16.2 meq L^{-1} observed for RM5 indicates the sustained potential for this solution to produce acid via Fe(II) oxidation and $Fe(OH)_3$ precipitation.

Metal-sulfide mineral precipitation dominates metal removal under sulfate-reducing conditions in passive OC-based remediation systems (Machemer and Wildeman, 1992).

However, other mechanisms such as (oxy)hydroxide precipitation, (co)precipitation and surface complexation may be important under less reducing conditions. Rapid decreases in metal concentrations observed during day one of the experiment were accompanied by a pH increase to between 6.2 and 6.3. Results from MINTEQA2 calculations indicate supersaturation with respect to both Fe and Al (oxy)hydroxide phases at early times. Precipitation of Mn, Cd, Ni, Co and Pb hydroxides is not favoured at pH < 8, therefore another mechanism likely contributed to large decreases in aqueous concentrations. Backscatter-electron micrographs combined with EDAX analysis confirmed the common presence of a hexagonal Fe-O-C phase (Figure 2.5a) and a Fe-O-C-S phase (Figure 2.5b) both of which contained minor amounts of Al and Zn. These precipitates are consistent in appearance with those commonly observed in studies utilizing ZVI as reactive media in PRBs (Gu et al., 1999; Herbert, 2003; Wilkin and McNeil, 2003). The Fe-O-C precipitate is likely a Fe hydroxycarbonate phase which consists of positively charged layered Fe (oxy)hydroxide sheets with CO_3 anions occupying the interlayer space. The Fe-O-C-S precipitate was less abundant on ZVI surfaces and similar in appearance to Fe hydroxysulfate precipitates (Gu et al., 1999). Spherical Fe-O precipitates characteristic of amorphous Fe (oxy)hydroxide containing trace Al were also observed on ZVI surfaces.

Complexation or (co)precipitation with Fe hydroxycarbonate, Fe hydroxysulfate or Fe (oxy)hydroxides may have contributed to the rapid decrease in Zn concentrations in RM2 - RM5 prior to development of sulfate-reducing conditions. Herbert (2003) and Wilkin and McNeil (2003) reported an association of Zn and Ni with Fe indicating that these precipitates may contribute to metal removal. Gibert et al. (2005) found that (co)precipitation with Fe and Al (oxy)hydroxides, as well as adsorption onto these phases and organic matter, contributed

to metal retention. Differences were observed between early time removal rates of Cd, Ni and Co with RM5 and mixtures containing OC. This observation suggests that adsorption onto organic matter may contribute to removal of some metals. However, metal-sulfide precipitation is expected to dominate under sulfate-reducing conditions, which developed within the first 14 days in mixtures containing OC (RM1–RM4).

Dissolved Mn concentrations decreased by 89 to 91 % in reactive mixtures containing OC; however a 23 % increase in Mn was observed in the absence of organic carbon (RM5). Precipitation of Mn-hydroxides is not favoured at pH < 8 and MINTEQA2 SI values indicate constant undersaturation with respect to MnS. Slight supersaturation (0.1–0.5) with respect to rhodochrosite [$MnCO_3$] was observed in all batches after 7 to 12 days. An inverse relationship ($r^2 = 0.90$) between Mn and alkalinity for RM1–RM4 suggests that $MnCO_3$ precipitation controlled dissolved Mn concentrations. However, precipitation of $MnCO_3$ was not effective in reducing dissolved Mn concentrations in RM5. Wilkin and McNeil (2003) reported similar increases in aqueous Mn at pH < 8, resulting from ZVI corrosion.

A portion of decreases in Fe concentrations may be attributed to (oxy)hydroxide or hydroxycarbonate precipitation, however 56.8 % (+/- 5.6 %) of Fe removal in RM1–RM4 occurred under SO_4 reducing conditions. Results of the MINTEQA2 modeling suggest that precipitation of mackinawite [FeS], greigite [Fe_3S_4], or an amorphous FeS phase contributed to Fe removal. Backscatter-electron micrographs revealed the common presence of a disordered Fe-sulfide phase (Figure 2.5c; Figure 2.5d) similar in appearance to that identified by Benner et al. (1999) as disordered mackinawite. Semi-quantitative EDX analysis indicated mean Fe:S ratios averaged 0.89 for RM1 and 1.18 for RM2–RM4. These non-

stoichiometrically ideal ratios are consistent with Fe-S phases such as disordered mackinawite [$Fe_{1+x}S$]. These data also agree with the general order of Fe-S precipitation, where $Fe_{1+x}S$ is the first phase to precipitate in the presence of dissolved Fe(II) and H_2S (Wolthers et al., 2003). Incorporation of metallic cations into octahedral vacancies between the tetrahedral Fe-S layers is commonly observed with $Fe_{1+x}S$ (Mullet et al., 2002). Non-stoichiometric Fe:S ratios do not generally exceed 1.08, however incorporation of Fe into these octahedral vacancies could account for higher ratios observed in this study. In addition, the presence of minor amounts of Zn in some of these precipitates indicates that Zn may also be removed by this mechanism. The presence of Ni, Cd, Co, or Pb was not detected in association with the $Fe_{1+x}S$ phase, however solid-phase concentrations of these metals were expected to be below EDX detection limits. Therefore, removal of Zn, Ni, and Co under SO_4 reducing conditions may be due to precipitation of low-solubility metal-sulfides or association with Fe-S phases such as $Fe_{1+x}S$.

2.4.5 In Situ Sulfur Speciation

Synchrotron-radiation based bulk XANES spectra (Figure 2.6) confirm that reduced forms of S predominate in the reactive mixtures containing OC. Sulfur K-edge energies obtained for realgar (S_4^{2-}), native S (S_8^0), and gypsum (S^{6+}), reference standards were found to be 2470.6 eV, 2471.5 eV, and 2481.4 eV, respectively. Energy shifts between S_8 and $CaSO_4 \cdot 2H_2O$ (9.9 eV), and S_8 and As_4S_4 (0.9 eV), match previously reported values for reference standards (Li et al., 1995; Fleet, 2005). However, the observed S K-edge energy for the S_8 reference standard exhibited a -0.5 eV shift from the commonly accepted energy of 2472.0 eV (Fleet, 2005). Consequently, all spectra were normalized to these previously

reported values by applying an energy shift of +0.5 eV. Discussions of all subsequent S K-edge values refer to the normalized energies.

Sulfur K-edge energies ranged from to 2470.1 to 2470.9 eV for samples containing OC. These S K-edge energies fall between reported S K-edge energies of 2470.0 eV, for pyrrhotite [$Fe_{1-x}S$] and troilite [$Fe_{0.923}S$], and 2471.5 eV for pyrite [FeS_2], indicating that solid-phase sulfur is present in a reduced form, most likely as a covalently bonded metal sulfide phase (Fleet, 2005). This result is consistent with aqueous geochemical, microbiological and mineralogical observations, which indicate that bacterially mediated sulfate reduction and metal-sulfide precipitation controlled the aqueous chemistry.

Pre-edge peaks were observed in S K-edge XANES spectra for all mixtures that contained both OC and ZVI (RM2–RM4). These pre-edge peaks were located 2 eV (± 0.2 eV) below the associated S K-edges. The presence of a pre-edge peak suggests that sulfur may be present in tetragonal coordination with a 3d transition metal, such as Fe (Bunker and Stern, 1984; Watson et al., 2000). Disordered mackinawite is commonly stoichiometrically deficient in sulfur, and exhibits tetragonal coordination of Fe with four S atoms in layered sheets (Mullet et al., 2002; Wolthers et al., 2003). These properties are consistent with a mineral structure that would produce a pre-edge peak similar to that observed for RM2–RM4. The differences in S K-edge energies between these samples may be attributable to differences in Fe:S ratios. Although a reference standard was not available for this study, the results suggest that S is present in $Fe_{1+x}S$ or a similar phase. This interpretation is consistent with results reported by Watson et al. (2000), FE-SEM-EDX analysis, and geochemical modeling results.

The S K-edge was located at 2470.9 eV for RM1, indicating that S may be covalently bonded with a metallic element (Fleet, 2005). However, in contrast to S K-edge spectra collected for RM2–RM5, a pre-edge peak was not observed for RM1. The absence of a pre-edge peak suggests that the dominant Fe-S phase is not in tetrahedral coordination and indicates the presence of a Fe-S phase other than $Fe_{1+x}S$. Hydrogen sulfide production within RM1 was observed to continue following removal of > 97% of aqueous Fe (Figure 2.1; Figure 2.2). This excess of dissolved H_2S, as compared to Fe, could lead to the sulfurization of mackinawite, with Fe_3S_4 and pyrrhotite [$Fe_{1-x}S$] as possible reaction products (Posfai et al., 1998; Neretin et al., 2004; Jambor et al., 2005). Greigite occurs as a mixed tetrahedral-octahedral structure whereas $Fe_{1-x}S$ exhibits octahedral coordination of Fe with S. The occurrence of Fe_3S_4 and $Fe_{1-x}S$ has previously been observed in PRBs for AMD remediation, and was thought to be preceded by $Fe_{1+x}S$ precipitation (Herbert et al., 2000; Jambor et al., 2005). In addition to Fe and S removal, precipitation of Fe-S phases, such as mackinawite, has been shown to contribute to the removal of divalent metals and trace elements (Arakaki and Morse, 1993; Gallegos et al., 2007; Jeong et al., 2007).

Incorporation of a secondary S K-edge peak into the spectrum for RM1 is also a possibility. The presence of an S_8 grain was observed in a FE-SEM electron backscatter micrograph of RM1. Standardless quantitative EDX data indicated that the atomic S content of this grain was 91 %. The S K-edge peak for RM1 spans approximately 3 eV and a change in the slope of the spectrum at 2472.5 eV may be associated with a S_8 peak. The presence of S_8^0 and S_X^{2-} species in RM1 is possible; however, separation of these S K-edges could not be achieved without additional reference standard spectra.

The S K-edge for RM5 is located at 2480.3 eV, indicating that solid-phase sulfur is dominated by an elevated oxidation state. The XANES spectrum for RM5 is consistent with FE-SEM-EDX data which shows the common presence of an iron hydroxy-sulfate phase (Figure 2.4b). A shift of -1.6 eV between S K-edges for the gypsum reference standard and RM5 suggests that S is most likely present as SO_4; however, in different coordination to SO_4 in gypsum. The absence of a secondary S K-edge peak for RM5 indicates that sulfate reduction and metal-sulfide precipitation were limited in the absence of OC.

2.5 Conclusions

Sulfate reduction, metal removal and acid neutralization were observed in all reactive mixtures containing OC (RM1–RM4). The addition of ZVI promoted modest increases in SRRs; however, OC was essential for SRB activity and therefore sulfate reduction. An increase of 15 % in SRRs, as compared to the OC control, was observed for a reactive mixture containing 5 dry wt. % ZVI (RM3), while the addition of 10 dry wt. % ZVI (RM4) produced a statistically similar rate. The ZVI control batch (RM5) did not support sulfate reduction and a SRR was therefore not calculated. Although conditions favorable to sulfate reduction were generated in all mixtures, OC was essential for SRB growth. Elevated populations of IRB and APB, in addition to elevated FDA hydrolysis rates, generally accompanied SRB activity. Conversely, microbial activity was limited in the absence of OC. Greater than 99 % removal of dissolved Zn, Ni, Co, Cd, and Pb, was observed in batches containing OC (RM1–RM4). Some metal removal may be attributed to adsorption, precipitation or (co)precipitation with (oxy)hydroxides, Fe-hydroxycarbonate or Fe-hydroxysulfate phases. These mechanisms most likely dominated in RM5 which did not

support SO_4 reduction. However, in RM1–RM4, > 50 % removal of Fe occurred under sulfate-reducing conditions. Effective removal of Al, Zn, Cd, Ni and Pb was achieved with ZVI in the absence of OC. Amorphous Fe-S precipitates were abundant in backscatter electron micrographs. The appearance of these phases, Fe:S ratios of 0.89 to 1.18, and general order of precipitation indicate that the dominant Fe-S phases are $Fe_{1+x}S$, Fe_3S_4 or $Fe_{1-x}S$. Solid phase bulk XANES spectra confirm that reduced S dominates in all samples containing OC (RM1–RM4). The S K-edge spectra suggest that $Fe_{1+x}S$ dominates in mixtures containing OC and ZVI, while Fe_3S_4 or $Fe_{1-x}S$ may be present in the mixture containing only OC. These Fe-S phases are known sinks for metals and therefore the precipitation of such phases should contribute to overall improvements in water quality.

The addition of ZVI to OC mixtures modestly enhanced sulfate reduction over the duration of these experiments. However, these modest rate increases correspond to a substantial increase in the total mass of SO_4 that could be reduced over the life-span of a PRB. Furthermore, consumption of OC over time generally corresponds to decreases in SRRs and therefore remediation efficiency. The contribution of an alternate electron donor by ZVI may provide potential for enhanced long-term performance. Furthermore, ZVI supports effective abiotic removal of metals, such as Al, Zn, Cd, Ni and Pb, thereby providing another potential remedial advantage. This study demonstrates that improvements to PRB performance may be achieved with minimal ZVI addition, and that larger ZVI proportions may not be cost-effective in the short-term. However, evaluation of long-term trends in AMD remediation is necessary for identification of optimal OC and ZVI mixtures.

Table 2.1
Target composition of simulated AMD solution.

Parameter	Value
pH	4.5
Alk (mg L^{-1} as $CaCO_3$)	50
SO_4 (mg L^{-1})	3600
Fe (mg L^{-1})	750
Zn (mg L^{-1})	100
Mn (mg L^{-1})	20
Ni (mg L^{-1})	15
Cd (mg L^{-1})	10
Co (mg L^{-1})	5
Pb (mg L^{-1})	1
NO_3 (mg L^{-1} as N)	5
PO_4 (mg L^{-1})	0
DOC (mg L^{-1})	0

Table 2.2

Composition of reactive mixtures expressed as dry weight percentages (dry wt. %).

Reactive Mixture	Reactive mixture composition (dry wt. %)				
	OC	ZVI	Sand	Limestone	Inoculum
RM1	50	0	32	16	2
RM2	48	2	32	16	2
RM3	45	5	32	16	2
RM4	40	10	32	16	2
RM5	0	50	32	16	2

Table 2.3

Mass-based sulfate reduction rates (SRRs) calculated by linear least-squares regression.

Reactive Mixture	*n*	SRR (nmol L^{-1} d^{-1} g^{-1})	95% C.I.	r^2
RM1	3	-12.9	± 0.26	0.95
RM2	1	-13.8		0.92
RM3	1	-14.9		0.93
RM4	3	-14.6	± 0.43	0.93
RM5	1			

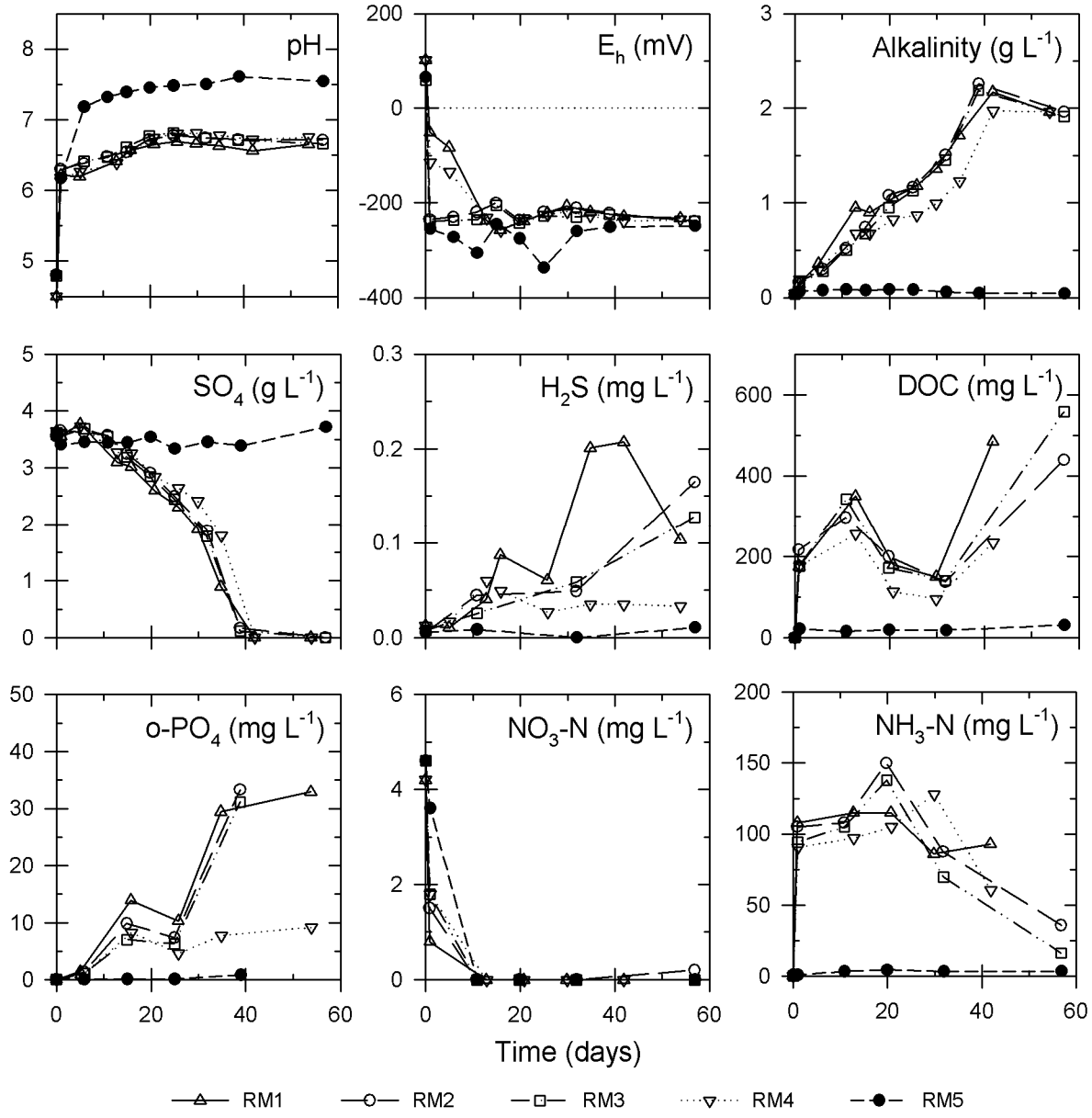

Figure 2.1 Aqueous chemistry as a function of time. Alkalinity expressed in g L^{-1} as $CaCO_3$.

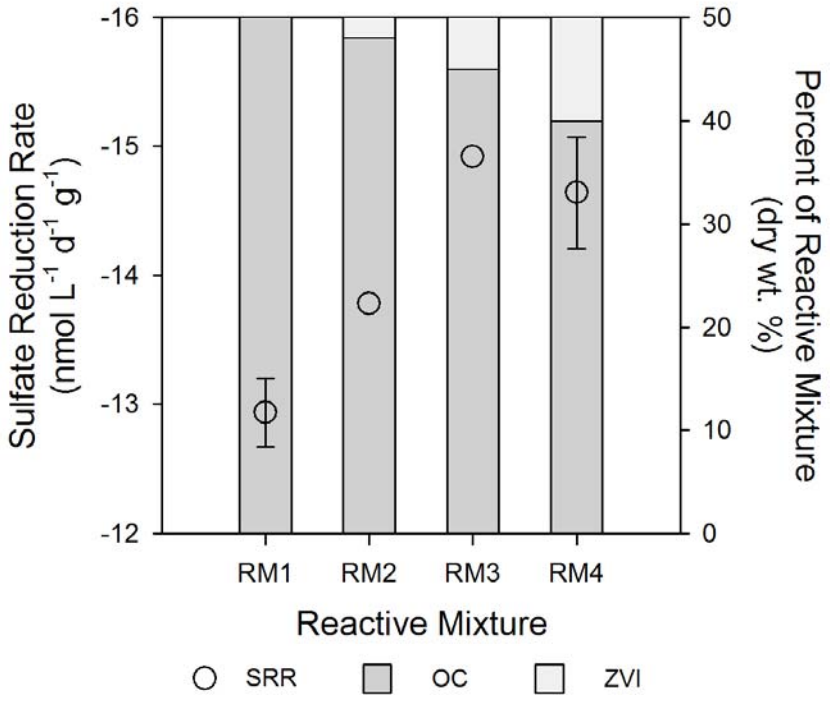

Figure 2.2 Sulfate reduction rates compared to percent organic carbon (OC) and ZVI in reactive mixtures. Error bars represent 95% confidence intervals for triplicate batch experiments.

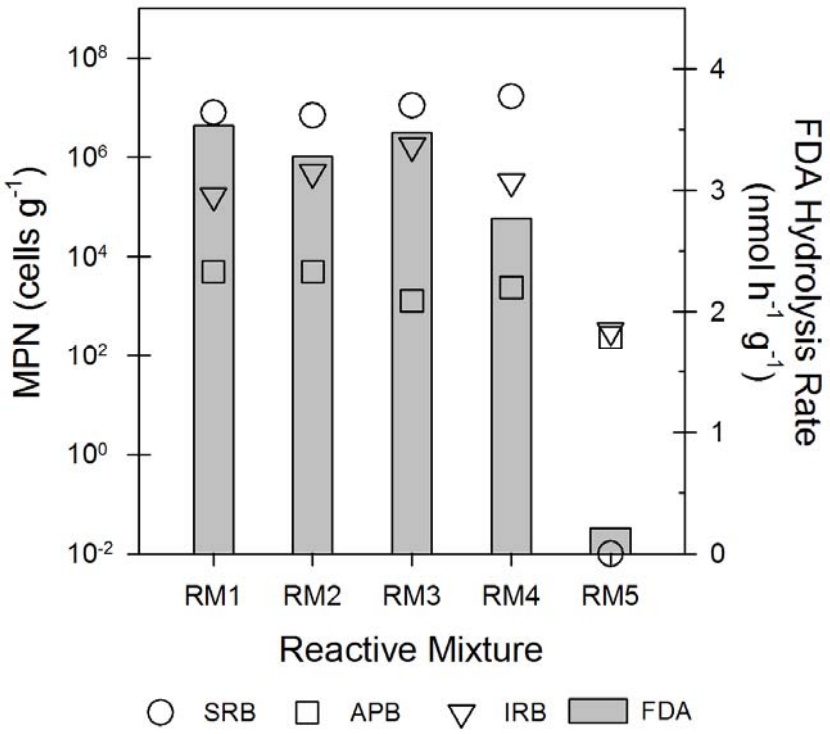

Figure 2.3 Most probable number populations of sulfate reducing bacteria (SRB), iron reducing bacteria (IRB), and acid producing (fermentative) bacteria (APB) for each reactive mixture. Esterase activities (FDA hydrolysis rate) expressed as nmol of FDA hydrolyzed per hour per gram of sample.

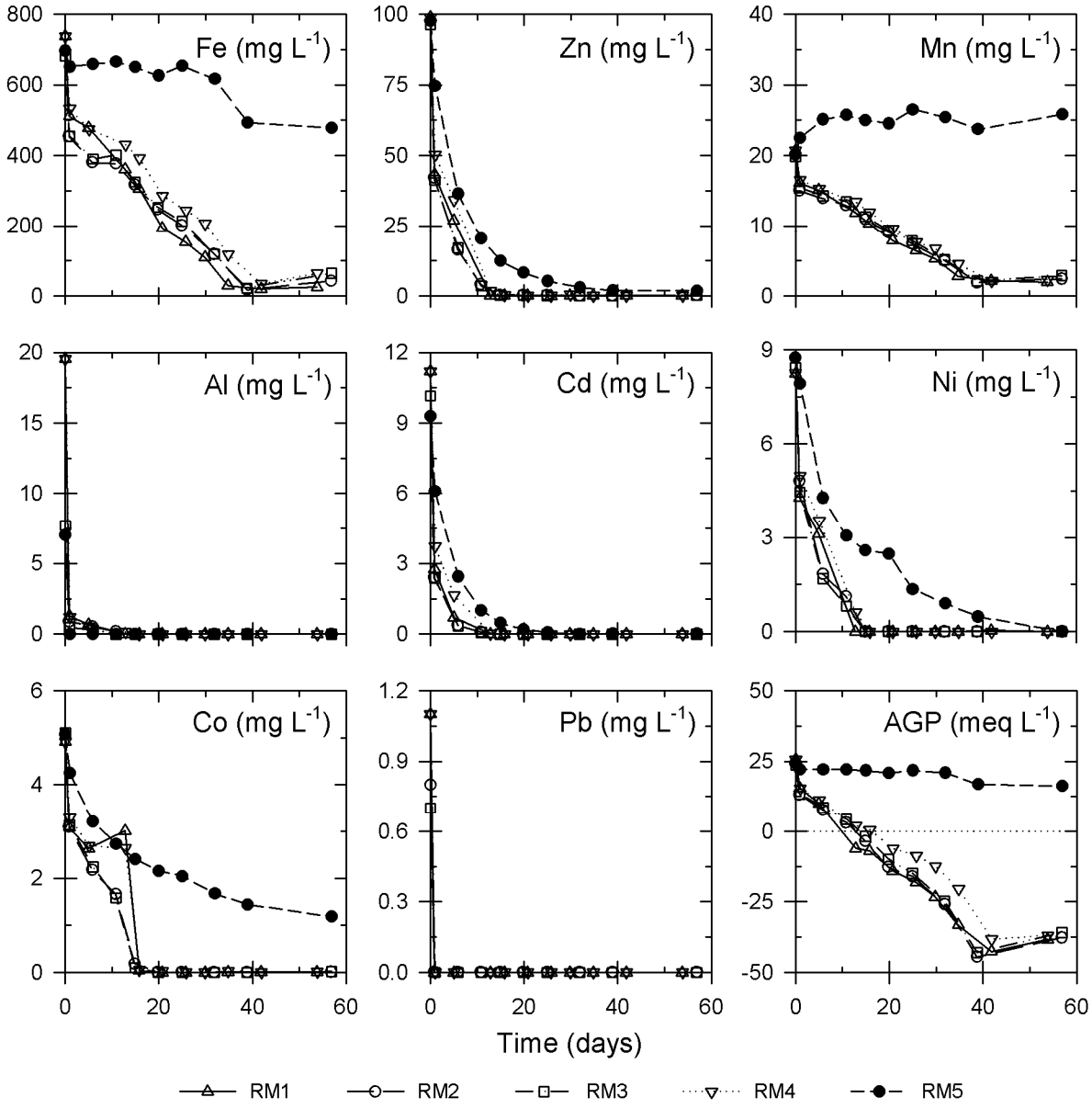

Figure 2.4 Dissolved metal concentrations and acid generating potential (AGP) as a function of time.

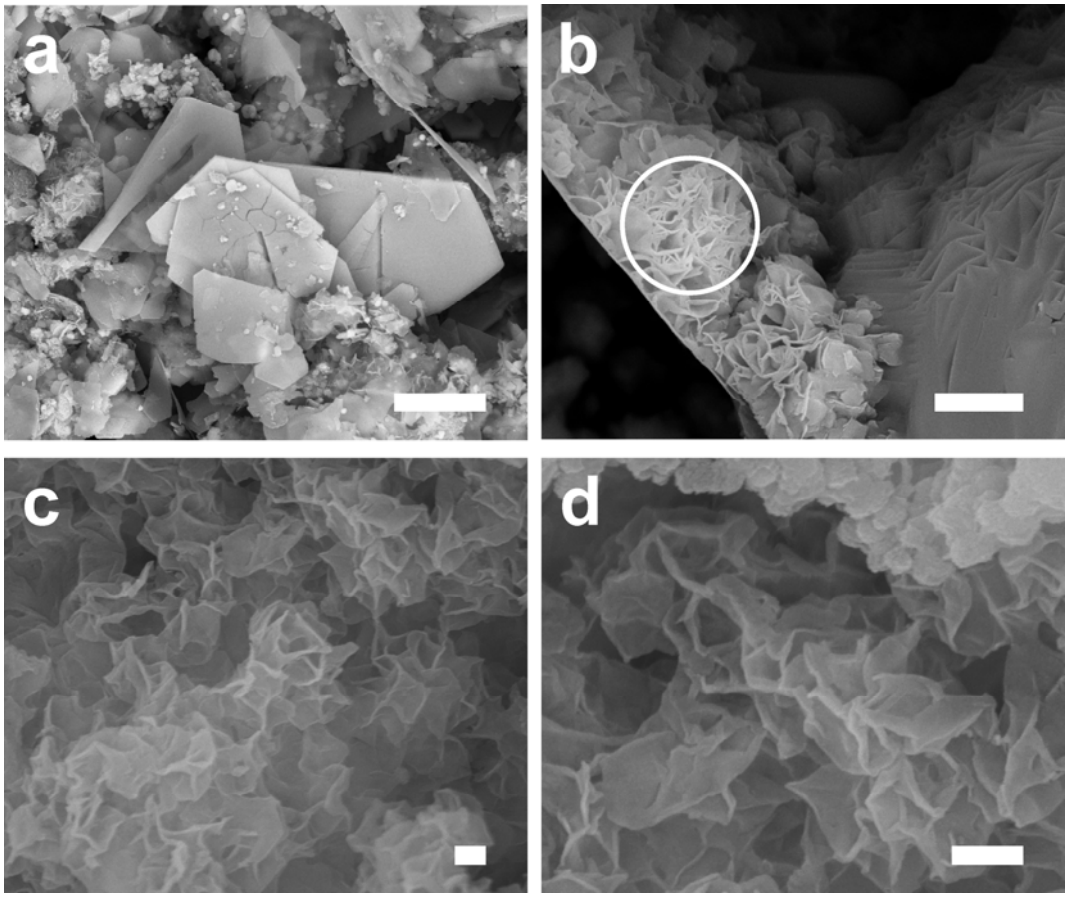

Figure 2.5 Backscatter-electron micrographs of hexagonal Fe hydroxycarbonate (a) and an Fe-O-C-S phase (b) on zero-valent iron surfaces. Disordered FeS precipitate with Fe:S ratios of 0.89 and 1.18 found in RM1 (c) and RM4 (d), respectively. Scale bars represent 2 μm.

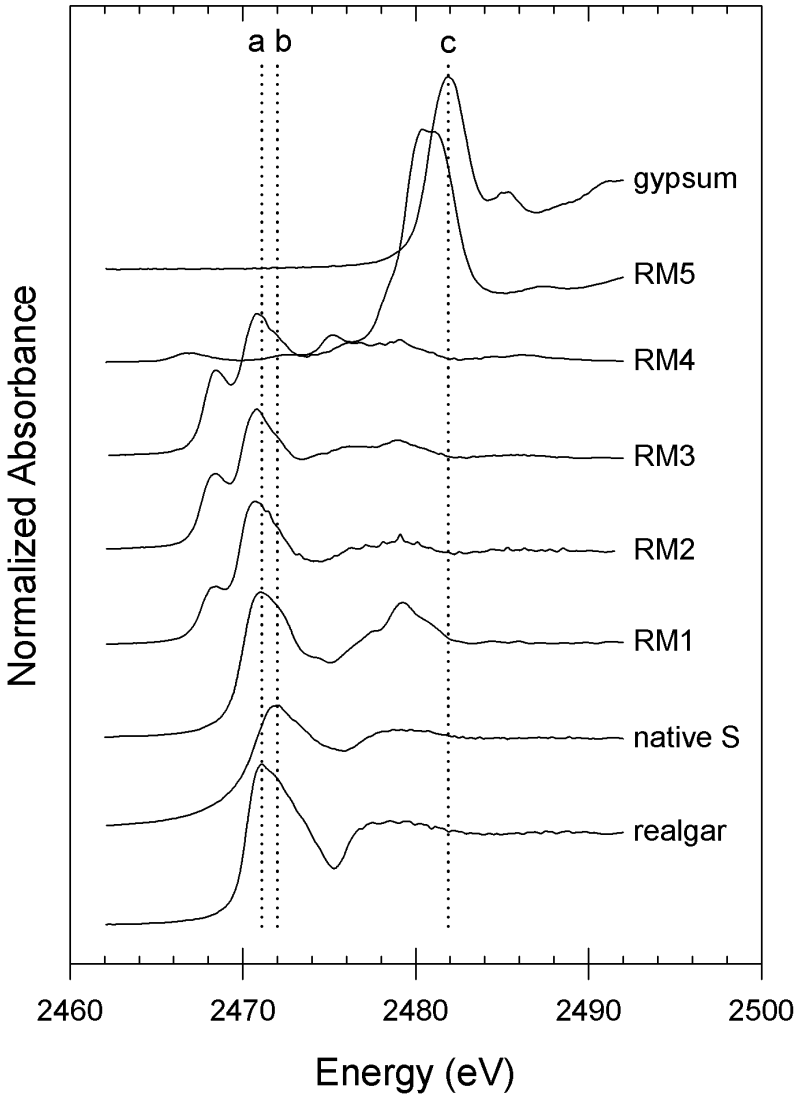

Figure 2.6 Sulfur K-edge XANES spectra for reactive mixture samples and reference standards. All spectra shifted by +0.5 eV to achieve consistency with reference standard S K-edge energies reported by Fleet (2005). Vertical dotted lines represent S K-edges for realgar (a; 2471.1 eV), native S (b; 2472.0 eV), and gypsum (c; 2481.9 eV) reference standards.

Chapter 3:

Mineralogical, Geochemical, and Microbial Investigation of a Sulfide-Rich Tailings Deposit Characterized by Neutral Drainage

Reproduced with permission from: Lindsay, M.B.J., Condon, D.W., Jambor, J.L., Lear, K.G., Blowes, D.W., Ptacek, C.J., 2009. Mineralogical, geochemical, and microbial investigation of a sulfide-rich tailings deposit characterized by neutral drainage. Appl. Geochem. 24, 2212–2221. Copyright 2009 Elsevier Ltd., License Number 2275381203492. Editorial and formatting changes have been made to accommodate reproduction in this thesis.

3.1 Executive Summary

Mineralogical, geochemical, and microbial characterization of tailings solids from the Greens Creek Mine, Juneau, Alaska, was performed to evaluate mechanisms controlling aqueous geochemistry of neutral-pH pore water and drainage. Core samples of the tailings were collected from five boreholes ranging from 7 to 26 m in depth. The majority of the 51 samples (77 %) were collected from the vadose zone, which can extend > 18 m below the tailings surface. Mineralogical investigation indicates that the occurrence of sulfide minerals follows the general order: pyrite [FeS_2] >> sphalerite [(Zn,Fe)S] > galena [PbS], tetrahedrite [$(Fe,Zn,Cu,Ag)_{12}Sb_4S_{13}$] > arsenopyrite [FeAsS] and chalcopyrite [$CuFeS_2$]. Pyrite constitutes < 20 to > 35 wt. % of the tailings mineral assemblage, whereas dolomite [$CaMg(CO_3)_2$] and calcite [$CaCO_3$] are present at ≤ 30 and 3 wt. %, respectively. The solid-phase geochemistry generally reflects the mineral assemblage. The presence of additional trace elements, including Cd, Cr, Co, Mo, Ni, Se and Tl, is attributed to substitution into sulfide phases. Results of acid-base accounting (ABA) underestimated both acid generating potential (AP) and neutralization potential (NP). Recalculation of AP and NP based on solid-phase geochemistry and quantitative mineralogy yielded more representative results. Most probable number (MPN) populations of neutrophilic sulfur-oxidizing bacteria (nSOB) and sulfate-reducing bacteria (SRB) reached 10^7 and 10^5 cells g^{-1}, respectively. Acidophilic sulfur-oxidizing bacteria (aSOB) and iron-reducing bacteria (IRB) were generally less abundant. Primary influences on aqueous geochemistry are sulfide oxidation and carbonate dissolution at the tailings surface, gypsum precipitation-dissolution reactions, as well as Fe reduction below the zone of sulfide oxidation. Pore-water pH values generally ranged from

6.5 to 7.5 near the tailings surface, and from approximately 7 to 8 below the oxidation zone. Elevated concentrations of dissolved SO_4, S_2O_3, Fe, Zn, As, Sb and Tl persisted under these conditions.

3.2 Introduction

Sulfide deposits are an important source of base- and precious-metal bearing minerals. Mining and concentration of sulfidic ore generates waste rock and tailings which are inherently sulfide bearing. Deposition of these materials in subaerial storage facilities subjects residual sulfide phases to atmospheric oxygen, thereby facilitating sulfide oxidation. Mechanisms of sulfide oxidation are generally described as either direct or indirect where the oxidant is O_2 or Fe(III), respectively (Nordstrom and Alpers, 1999). Under near-neutral pH conditions, direct oxidation of sulfide phases, such as pyrite [FeS_2], generates acid and liberates metals and associated trace elements (Blowes et al., 2003):

$$(3.1) \qquad FeS_2 + 7/2O_2 + H_2O \rightarrow Fe^{2+} + 2SO_4^{2-} + 2H^+$$

This reaction is catalyzed by sulfur oxidizing bacteria (SOB) such as *Thiobacillus thioparus* (Nordstrom and Southam, 1997; Gould and Kapoor, 2003). Subsequent dissolution of dolomite [$CaMg(CO_3)_2$] and other carbonate phases neutralizes acidity and can effectively maintain near-neutral pH conditions (Jurjovec et al., 2002):

$$(3.2) \qquad CaMg(CO_3)_2 + 2H^+ \rightarrow Ca^{2+} + Mg^{2+} + 2HCO_3^-$$

Carbonate dissolution consumes protons and generates alkalinity, which in turn decreases the net acidity of pore water. Depletion of the neutralization capacity of tailings may be followed by development of acid mine drainage (AMD) conditions. However, aqueous geochemistry

associated with neutral mine drainage (NMD) is also of interest in the context of water quality (Heikkinen et al., 2009).

Aqueous geochemistry of tailings pore water and drainage is intrinsically linked to tailings mineralogy, geochemistry, microbiology, and hydrology. Rates of sulfide oxidation and the mobility of associated reaction products depend on multiple (bio)geochemical processes, including precipitation-dissolution, redox, and sorption reactions. Under near-neutral pH conditions, several metals and trace elements, such as Fe, Zn, Sb, As, Cr, Co, Cu, Mn, Mo, Ni, Se, and Tl, may remain soluble under appropriate redox conditions (Masscheleyn et al., 1991; Balistrieri et al., 1994; Filella et al., 2002; Laforte et al., 2005). These elements can be released to pore water by sulfide-mineral oxidation at the tailings surface or contributed by residual mill process water during tailings deposition (Holmström and Öhlander, 1999). Therefore, development of low-quality pore water does not necessarily require extended periods of sulfide oxidation or the generation of acidic conditions.

Characterization of the Greens Creek tailings deposit, which exhibits near-neutral pH pore water and drainage, was performed between 2004 and 2007. Tailings pore water and drainage samples were collected at various times, while solid-phase core samples were collected in February and March of 2005. This study examines the mineralogy, geochemistry, and microbiology of this sulfide- and carbonate-rich tailings deposit, and evaluates controls on near-neutral pH pore water and drainage.

3.3 Study Site

The Greens Creek Mine is located approximately 30 km southwest of Juneau, Alaska, USA (58° 05’ 03” N, 134° 38’ 05” W), on Admiralty Island in the Tongass National Forest (Figure

3.1). This underground Zn-Ag-Au-Pb mine extracts ore from a volcanogenic massive sulfide-sedimentary exhalative (VMS-SEDEX) hybrid deposit which is hosted in Triassic calcareous argillite and siliceous phyllite (Taylor et al., 1999). Development of the Greens Creek mine began in 1987 and full-scale production commenced in 1989. The mill uses a flotation process to produce concentrates containing sphalerite [(Zn,Fe)S], tetrahedrite [$(Cu,Fe,Zn,Ag)_{12}Sb_4S_{13}$], galena [PbS], pyrargyrite [Ag_3SbS_3], and electrum [AuAg]. The gangue mineral assemblage is dominated by pyrite [FeS_2], dolomite [$CaMg(CO_3)_2$], and quartz [SiO_2], although barite [$BaSO_4$] and calcite [$CaCO_3$] are also common. Mill tailings are thickened to between 60 and 70 % solids, and filter-pressed to roughly 12 wt. % moisture. Approximately one-half of the tailings are returned underground as structural backfill, and the remainder are dry-stacked and roller-compacted in a 25 ha tailings storage facility. This method of tailings placement is utilized to enhance the geotechnical stability of the tailings deposit while minimizing the footprint of the storage facility. At the time of this study, approximately $4 \cdot 10^6$ tonnes of tailings had been deposited in the storage facility. The maximum vertical extent of the tailings was 25 m, and the vadose zone extended > 18 m below the tailings surface at some locations.

The mine site is located in a coastal temperate rainforest and mean annual precipitation at the tailings facility was 1380 mm between 1997 and 2007. Average annual air temperature was +6.0°C over this period. Near-surface tailings temperatures fluctuated from approximately -1°C to +21°C and a median value of +7.8°C was observed in the upper 400 cm.

Drainage emanating from the tailings facility is collected *via* basal under-drains and, prior to discharge, treated using a high-density sludge process. Nonetheless, tailings

deposited at the Greens Creek mine provide the opportunity to examine geochemistry, mineralogy and microbiology of a tailings facility characterized by circumneutral pH drainage.

3.4 Materials and Methods

3.4.1 Core-Sample Collection

Solid-phase samples were collected for mineralogical investigation, geochemical analysis, microbial enumerations, and determination of physical properties. Core samples were collected at regular depth intervals from four boreholes located along a west to east transect (A–A') and one additional location at the southwest corner of the tailings facility (Figure 3.1). Boreholes were drilled using a track-mounted rig fitted with a 10.2 cm hollow-stem auger and a 45.7 cm long split-spoon sampler. Core samples were collected into 15.5 cm brass and plastic liner tubes using standard penetration tests. Upon retrieval, all core samples were immediately sealed with low-density polyethylene (LDPE) caps and vinyl tape, and were refrigerated until analysis. Additional material was transferred to polypropylene (PP) bags and frozen until analysis. Refrigerated and frozen samples were packaged and shipped to the University of Waterloo for analysis.

3.4.2 Mineralogy

Mineralogical investigation was performed on sub-samples collected from refrigerated core samples. These samples were collected into 20 mL polypropylene (PP) vials under anaerobic conditions and allowed to dry under ambient conditions. Polished thin sections were prepared by Vancouver Petrographics in Langley, British Columbia in the absence of water to prevent

the dissolution of soluble phases or oxidation of sulfide minerals. Optical microscopy was performed using both transmitted- and reflected-light modes. Selected thin sections were then coated with carbon and examined by scanning electron microscopy (SEM) and energy-dispersive X-ray (EDX) spectroscopy on a Philips XL-30 fitted with a Princeton Gamma IMIX-4 system, respectively. Quantitative mineralogical analysis was performed using X-ray diffractometry (XRD) and Rietveld refinement. This technique utilized a Siemens D5000 powder diffractometer at the University of British Columbia in Vancouver, BC.

3.4.3 Particle-Size Distribution

Particle-size distribution was determined using a Malvern Instruments Mastersizer S laser diffraction particle-size analyzer. This method provides distribution in terms of vol. % and eliminates the need to assume an average particle density for a given sample.

3.4.4 Solid-Phase Geochemistry

Frozen samples were submitted to an external laboratory for carbon and sulfur speciation, whole-rock digestion, aqua regia extraction, acid-base accounting, and particle size distribution analysis. Carbon and sulfur speciation was performed using an ELTRA CS 2000 induction and resistance furnace. Samples were combusted at 1350°C, and evolved $CO_{2(g)}$ and $SO_{2(g)}$ was measured by infrared (IR) detection. Sulfate-S contents were determined as the difference between total-S measured before and after pyrolysis at 800°C, which was performed to remove sulfide-S. Whole-rock digestions were performed using a Li-metaborate/Li-tetraborate fusion, HNO_3 dissolution, and inductively coupled plasma-optical emission spectroscopy (ICP-OES) detection. Trace-element analyses were performed by inductively coupled plasma-mass spectrometry (ICP-MS) on samples digested at 95°C with

aqua regia. Static acid-base accounting (ABA) was performed using a modified Sobek method, which determined acid-generating potential (AGP) using the sulfide-S content.

3.4.5 Microbial Enumerations

Enumeration of neutrophilic sulfur-oxidizing bacteria (nSOB), acidophilic sulfur-oxidizing bacteria (aSOB), iron-oxidizing bacteria (IOB), iron-reducing bacteria (IRB), and sulfate-reducing bacteria (SRB) was performed using the most probable number (MPN) technique (Cochran, 1950). Growth media for nSOB and aSOB consisted of 0.1 g L^{-1} NH_4Cl, 3.0 g L^{-1} KH_2PO_4, 0.2 g L^{-1} $MgCl_2 \cdot 6H_2O$, 5.0 g L^{-1} $Na_2S_2O_3 \cdot 5H_2O$ and 0.1 g L^{-1} $CaCl_2$ dissolved in DI water. The final pH of these solutions was adjusted to 7.0 and 4.2 for nSOB and aSOB, respectively. Media for promoting IOB growth was prepared by dissolving 0.5 g L^{-1} KH_2PO_4, 0.5 g L^{-1} $(NH_4)_2SO_4$, 0.5 g L^{-1} $MgSO_4 \cdot 7H_2O$ and 33.4 g L^{-1} $FeSO_4 \cdot 7H_2O$ into DI water which was adjusted to pH 2.0. The final pH of the solution was then readjusted to 2.2. Preparation of media for SRB, IRB and APB enumerations is described in Chapter 2.

Bacterial growth was promoted in sterile culture tubes (nSOB, aSOB and IOB) or serum bottles (SRB and IRB) containing 9 mL of selective growth media. Innoculation was performed by adding 1.0 ± 0.05 g of tailings to each of five bottles or tubes. A series of nine 1:10 serial dilutions was carried out and samples were incubated at room temperature (22 ± 1ºC) for four weeks. Recognition of positive results for nSOB and aSOB was indicated by a 0.2 unit decrease in pH, whereas Fe(III) (oxy)hydroxide precipitation indicated IOB growth. A description of techniques used to identify positive results for SRB and IRB is presented in Chapter 2. An MPN table was used to estimate microbial populations as cells g^{-1} sample (Alexander, 1965).

3.4.6 Aqueous Geochemistry

Tension lysimeters (Campbell Monoflex) were installed to monitor the chemical composition of pore water in the vadose zone. Lysimeters were installed at 25 to 50 cm depth intervals in recently placed tailings located at the west side of the tailings facility (Figure 3–1). Pore water was collected into lysimeters under a $N_{2(g)}$ atmosphere, by applying a vacuum of approximately 70 kPa. Lysimeters were purged twice before samples were collected into disposable 60 mL polyethylene (PE) syringes. Additional samples were collected from previously installed monitoring wells (MW1, MW2 and MW3) as well as a basal drain (BD1) located at the base of the tailings deposit. At the time of installation, these wells were screened from 17.7 to 19.8 m below the tailings surface. Ongoing tailings deposition has gradually raised the elevation of the tailings surface at these wells. Monitoring wells were sampled with PE bailers while samples from the basal drain were collected into sterile low-density polyethylene (LDPE) bottles.

Measurements of pH and Eh were made on unfiltered samples using previously reported methods (Lindsay et al., 2008). Remaining sample was passed through 0.45 µm surfactant-free cellulose acetate (SFCA) syringe filters. Carbonate alkalinity was determined by titration with normalized H_2SO_4 using bromocresol green-methyl red indicator. Samples for determination of anions, major cations, trace elements, ortho-phosphate (o-PO_4), and NH_3 were stored in PE bottles and preserved according to standard methods (SMEWW, 2005). Dissolved organic carbon (DOC) samples were stored in 40 mL amber glass volatile organic compound (VOC) vials fitted with Teflon (PTFE) lined septa. Ion chromatography was used to measure inorganic anion concentrations, including S_2O_3. Determination of major cations and trace elements was performed by inductively coupled plasma-optical emission

spectroscopy (ICP-OES) and inductively coupled plasma-mass spectrometry (ICP-MS), respectively. Geochemical speciation modeling was performed to assist with interpretation of aqueous geochemistry. Mineral saturation indices (SIs) were calculated using the geochemical speciation-mass transfer code MINTEQA2 and the WATEQ4F thermodynamic database (Allison et al., 1990; Ball and Nordstrom, 1991).

3.5 Results and Discussion

3.5.1 Tailings Mineralogy

Optical investigation revealed that samples are megascopically sulfide- and carbonate-rich (Figure 3.2a; Figure 3.2b). Pyrite is overwhelmingly the predominant sulfide mineral in the tailings assemblage (Table 3.1). Sphalerite was consistently the next most abundant sulfide phase, while lesser amounts of galena and tetrahedrite were present. Minor amounts of chalcopyrite and arsenopyrite were also observed. The non-opaque assemblage consists largely of quartz and dolomite, however minor amounts of calcite, muscovite [$KAl_2AlSi_3O_{10}(OH)_2$] and clinochlore chlorite [$(Mg,Fe)_5Al(Si_3Al)O_{10}(OH)_8$] also were observed. Examination by SEM-EDX further revealed the presence of barite [$BaSO_4$], hydroxylapatite [$Ca_5(PO_4)_3(OH)$], and numerous grains of a Ba-Al silicate phase identified by XRD as cymrite [$BaAl_2Si_2(O,OH)_8 \cdot H_2O$]. Goethite [αFeOOH] pseudomorphs after pyrite were observed, in addition to minor amounts of graphite [C].

Pyrite grains generally range from > 10 to < 100 μm in cross-section, with maximum grain sizes reaching approximately 150 μm. Framboidal pyrite was observed as occlusions within non-opaque phases (Figure 3.2c) or in association with other sulfides

(Figure 3.2d); however, the framboids are interpreted as originating from the primary assemblage. Sulfide textures were highly variable and included common intergrowth of pyrite with sphalerite. Multi-mineral colloform intergrowths of framboidal pyrite with sphalerite and galena inclusions were also observed (Figure 3.2e). Replacement of pyrite by galena occurred in both euhedral (Figure 3.2d) and framboidal (Figure 3.2e) grains. This association of sulfide phases could facilitate galvanic interaction during oxidation, and therefore preferential dissolution of sphalerite or galena relative to pyrite (Abraitis et al., 2004a). The occurrence of pyrite as framboids could potentially increase total surface area, thereby facilitating enhanced oxidation (Pugh et al., 1984; Moses and Herman, 1991; Liu et al., 2008). Most framboids were occluded within non-opaque phases or occur as intergrowths with other sulfide phases, potentially limiting exposure of the framboid surfaces. Surfaces of sulfide phases generally appeared pristine and little to no indication of oxidation was observed. A sulfide alteration index (SAI) of 0 to 1 on a scale of 1 to 10 would therefore apply to all samples examined in this study (Blowes and Jambor, 1990).

Particles of non-opaque phases were generally larger than sulfide grains (Figure 3.2b). Lithic fragments of polycrystalline dolomite as large as 3 by 5 mm were observed, however the majority of grains were < 1 mm across. Dolomite particles were occasionally found to contain inclusions of framboidal pyrite and trace concentrations of Fe and Mn were detected by SEM-EDX. Quartz was observed both as individual grains in association with dolomite, chlorite, chlorite-muscovite, and in lithic fragments. Principal non-fragmental phases include dolomite and quartz, which are commonly accompanied by muscovite, chlorite and barite. Aggregated muscovite was found to contain enclosed anhedral sphalerite, framboidal pyrite and galena, which has replaced framboidal pyrite (Figure 3.2d). Dolomite

is overwhelmingly the primary source of acid neutralization potential (NP) within the tailings assemblage. Acid neutralization *via* dolomite dissolution will result in a stoichiometric excess of SO_4 in pore water, relative to Ca.

Quantitative XRD analysis generally agreed with the optical assessment (Table 3.1), however some minor phases observed in thin sections were not detected in the diffractograms. Retrospective examination of thin sections reconfirmed the presence of minor phases, such as tetrahedrite, chalcopyrite and arsenopyrite, not identified by XRD. Average pyrite and dolomite contents were 34 and 27 wt. %, respectively. Quartz and barite exhibited similar abundance of approximately 12 wt. %, while the proportion of calcite, muscovite, sphalerite and cymrite ranged from 2 to 4 wt. %. Pyrite and dolomite are likely the primary mineralogical controls on aqueous geochemistry, whereas calcite and these additional sulfide phases are also expected to influence water quality.

3.5.2 Particle-Size Distribution

Tailings particles were consistently fine-grained, and ranged in classification from fine sand to clay (Friedman and Sanders, 1978). The proportion of individual samples categorized by cumulative vol. % finer as sand- and silt-sized particles averaged 51 and 44 %, respectively. The clay-sized fraction was consistently the smallest proportion of the particle-size distribution, and accounted for 2 to 11 % (average 5 %) of samples. Textural classification following the ternary diagram method described by Shepard (1954) gives: 4 % sand, 34 % silty sand, 58 % sandy silt and 4 % silt.

A distribution of particle sizes ranging from < 0.1 to > 500 μm was commonly observed. However, samples were generally characterized by 1 or 2 dominant particle sizes.

Approximately 62 % of samples exhibited unimodal distribution, while 28 % of samples can be characterized as bimodal. The remaining 10 % of samples exhibited a broad distribution of particle sizes. Although these samples range in classification from sand to silt, the actual range in particle size is approximately 3 orders of magnitude. Calculated uniformity coefficients (C_u), which is the ratio of d_{60} to d_{10}, classify all samples as poorly sorted (Fetter, 2000). Based solely upon particle size distribution data, the saturated hydraulic conductivity (K) of the tailings is expected to range from 10^{-9} to 10^{-5} m s^{-1} (Freeze and Cherry, 1979; Fetter, 2000). Field measured K values for various locations within the tailings deposit typically vary from 10^{-9} to 10^{-7} m s^{-1}. However, hydraulic conductivity in the vadose zone will decline with decreasing moisture content and increasing tension. Secondary mineral precipitation and consolidation of tailings at depth may have a similar influence on K.

3.5.3 Solid-Phase Geochemistry

3.5.3.1 Major and Trace Elements

Gangue and residual ore minerals present in the tailings assemblage may contain a variety of metals and trace elements. The occurrence of Fe, Zn, Pb, Sb, Ag, As, and Cu are expected based on ideal stoichiometry of the sulfide assemblage (Table 3.1). However, additional trace elements, such as Ni, Co, Cr, Cd, Mo, Se and Tl, may occur as impurities in primary sulfide minerals, and are therefore important in the context of pore-water and drainage quality. Elements contributed by weathering of non-sulfide phases may also influence pore-water geochemistry and quality.

The occurrence of major elements from the whole-rock analysis was found to follow the order: Si > Ca > Fe > Mg > Al > K > Na > P > Ti, Mn > Ba (Table 3.2). This order

generally agrees with the tailings mineralogy, for which quartz, dolomite and pyrite are the dominant phases. Depth and borehole dependent trends were not evident, and observed variations in concentrations are attributed to ore mineralogy and milling efficiencies. The presence of Al, K and Na is attributed to muscovite, chlorite, K-feldspar and cymrite, while P is presumably contributed by hydroxylapatite. Strong correlation between Ti and Al ($r^2 = 0.91$) suggests that Ti is substituting for Al in tetrahedral layers of aluminosilicate phases.

The relative abundance of metals and trace elements in core-samples after aqua regia digestion generally follows the order: Zn, Pb > Mn> As, Cu > Sb > Ag > Cd, Ni, Mo, Tl, Cr > Se. These elements are indicative of the sulfide minerals commonly present in the Greens Creek deposit. Average solid-phase Zn and Pb concentrations were > 1000 mg kg^{-1} and reflect the occurrence of sphalerite and galena as the most abundant sulfide phases after pyrite. Manganese concentrations ranged from 910 to 3560 mg kg^{-1} and exhibited an average solid-phase concentration of 2330 mg kg^{-1}. The solid-phase Mn suggests that it is contributed by a relatively abundant phase. Substitution of Mn for Zn in sphalerite is the most probable source among the sulfide assemblage (Abraitis et al., 2004b; Vaughan and Rosso, 2006). Solid-phase As and Cu concentrations averaged 1360 and 1310 mg kg^{-1}, respectively. Arsenopyrite and chalcopyrite are obvious As and Cu sources, while tetrahedrite may also contain both of these elements. Pyrite may also be a major source of As and several other trace elements, such as Cr, Co, Mo, Ni, Se, Sn and Tl, in tailings samples (Abraitis et al., 2004b).

The oxidation of pyrite, sphalerite and other sulfide phases will release these metals and trace elements to pore water. The observed aqueous concentrations will depend on the

trace element content of primary sulfides, the mass of sulfides within the tailings deposit, and the extent of secondary reactions occurring following dissolution. Near-neutral pH conditions are expected to limit the aqueous concentrations of Fe(III), Al, and Pb. However, concentrations of several elements may remain elevated under near-neutral pH and reducing conditions.

3.5.3.2 Carbon and Sulfur Speciation

Minor variations in C and S speciation were observed among boreholes; however, depth dependent trends were not observed (Table 3.3). Total carbon contents ranged from 1.9 to 5.7 dry wt. % and, on average, carbonates accounted for 87 % of total C. Graphitic and organic carbon were detected in all samples and exhibited average contents of 0.2 and 0.3 wt %, respectively. These results are consistent with mineralogy which shows that dolomite and calcite can account for > 30 wt. % of the bulk mineralogy. Graphitic carbon was observed in mineralogical analysis and organic carbon may be contributed from residual process water. Sulfide-S and SO_4-S were generally present in similar proportions. The reported total S content ranged from 8.2 to 24.2 wt. % and exhibited an average value of 16.8 wt. %. Total S values generally agree with quantitative mineralogical analysis, however, discrepancies were observed for speciated S data. Sulfur contributed by SO_4 accounted for 28.6 to 58.6 wt. % (average 45.5 %) of total sulfur. These values suggest an average barite content of 57.0 wt. %, whereas quantitative mineralogy and solid-phase Ba concentrations indicate values of 12.0 and 10.7 wt. %, respectively. Contribution of Ba by cymrite may result in overestimation of barite from whole-rock data; however, this contribution would likely account for < 10 % of total Ba in tailings samples. The large overestimation of SO_4 likely results from incomplete removal of sulfide-S by pyrolysis.

3.5.3.3 Acid-Base Accounting

Laboratory ABA data suggests that all samples were potentially net-acid generating (NAG). Paste pH values for these borehole core samples were consistently near neutral, exhibiting minimum and maximum values of 7.02 and 8.06, respectively. Ratios of AP to NP ranged from 0.26 to 0.80, while net neutralization potential (NNP) averaged -184 kg $CaCO_3$ t^{-1} of tailings. Average measured values of NP and AP were 102 and 284 kg $CaCO_3$ t^{-1}, respectively (Figure 3.3). However, these values differ substantially from previous analyses of Greens Creek tailings which reported average AP and NP values (n = 31) of 465 and 258 kg $CaCO_3$ t^{-1}, respectively. The discrepancy between AP values is attributed to the calculation of AP from sulfide-S values, which were clearly underestimated. Recalculation of SO_4 contents, and therefore AP values, based on Ba concentrations gives an average value of 470 kg $CaCO_3$ t^{-1} if all Ba is assumed to be contributed by barite (Figure 3.3). This calculated AP value agrees well with previous ABA and mineralogy data. The reported NP values also are consistently lower than those calculated based on C speciation data and generally differ from quantitative mineralogy results. Calculation of NP from C speciation data gives a range from 120 to 419 kg $CaCO_3$ t^{-1} (average 284 kg $CaCO_3$ t^{-1}), which generally corresponds to mineralogical data and previous ABA results. The relatively narrow range in current NP values, from 58 to 171 kg $CaCO_3$ t^{-1}, may result from insufficient acid addition, and therefore incomplete carbonate dissolution, during analysis. Correlation between current NP values and the volume of acid added (r^2 = 0.72) supports this interpretation. Recalculation of NNP using AP and NP values based on Ba concentrations and C speciation gives an average value of -195 kg $CaCO_3$ t^{-1}, and NP:AP ratios consistently < 1 suggest that these tailings are likely to generate acid (Jambor and Blowes, 1998; Jambor, 2003). Acid-base accounting is

commonly used to predict the potential for tailings and waste rock to generate acidic drainage. However, these results illustrate possible discrepancies between methods and demonstrate that mineralogical data should be considered when selecting methods for AP and NP determination.

3.5.4 Microbial Enumerations

Autotrophic SOB, both neutrophilic and acidophilic, were observed throughout the tailings facility (Figure 3.4). Neutrophilic SOB dominated sulfur oxidizers relative to aSOB populations which were generally lower by > 2 orders of magnitude. The largest populations of nSOB, which exceeded 10^7 cells g^{-1}, were observed near the tailings surface in BH3 and BH5 (Figure 3.4). Elevated populations > 10^6 cells g^{-1} were also observed at greater depth within the tailings facility. These enumerations are not a direct measure of microbial activity, but the presence of viable bacteria. Therefore, elevated populations of nSOB observed at greater depth may have developed at exposed impoundment elevations that subsequently were buried. Iron oxidizing bacteria (IOB) were not detected under near-neutral pH conditions.

Populations of IRB and SRB were variable both between boreholes and with depth within individual boreholes. The presence of SRB was observed in 31 of 32 core samples for which MPN enumerations were performed. Populations of SRB ranged from below detection to > 10^6 cells g^{-1} of tailings and were not clearly influenced by the depth of the water table. Large variation in the magnitude of SRB populations was observed over relatively small depth intervals (i.e. < 2 m). These variations indicate that SRB populations were highly dependent on local hydrogeochemical conditions. Populations of IRB ranged from below the

detection limit to > 10^4 cells g^{-1}, and their occurrence was also highly variable over small depth intervals. Elevated MPN populations of SRB and IRB at some sample locations, indicate that SO_4 and Fe reduction could occur in the presence of available organic carbon.

3.5.5 Aqueous Geochemistry

Vadose zone pore-water samples were collected from suction lysimeters installed in the upper 400 cm of the tailings deposit. Pore water exhibited near-neutral pH and elevated concentrations of SO_4, Fe, Zn, Mn and trace elements (Figure 3.5). Sulfide oxidation at the tailings surface resulted in a 1.5 unit decrease in pH from 200 to 25 cm below the tailings surface. An increase in average alkalinity from 120 to 350 mg L^{-1} (as $CaCO_3$), between 2005 and 2007, is indicative of sulfide oxidation and subsequent acid neutralization via carbonate dissolution. Modeled saturation indices (SIs) confirm that pore water is generally at saturation or supersaturated with respect to dolomite and calcite. Sulfide oxidation also resulted in near-surface increases in SO_4 between 2005 and 2007. Average SO_4 concentrations increased from approximately 2200 to 4000 mg L^{-1} within 200 cm of the tailings surface. Concomitant increases in Mg concentrations were observed, however, average Ca concentrations decreased by approximately 80 mg L^{-1} over this period. The increase in dissolved Mg concentrations indicates that dolomite dissolution is the primary acid neutralization mechanism. Pore water was saturated with respect to gypsum and undersaturated with respect to epsomite [$MgSO_4 \cdot 7H_2O$], which is consistent with the differences in the relative solubilities of secondary Ca- and Mg-sulfate phases. Dissolution of dolomite followed by the precipitation of gypsum likely accounts for the differences between trends in dissolved Ca and Mg concentrations (Blowes et al., 1998).

Decreases in DOC and S_2O_3 concentrations were observed from 2005 to 2007. Maximum S_2O_3 and DOC concentrations were approximately 1900 and 80 mg L^{-1}, respectively. Low concentrations of S_2O_3 and DOC within 150 cm of the tailings surface are attributed to pore-water migration and disproportionation (Jorgensen and Bak, 1991). Near-surface decreases in DOC and S_2O_3 with time suggest that these pore-water constituents were contributed *via* tailings placement. The milling process utilizes Na-isopropyl xanthate [$(CH_3)_2CHOCSSNa$] which may contribute DOC and S_2O_3 to residual process water retained in the tailings (Hao et al., 2000). Strong correlations between DOC and S_2O_3 ($r^2 = 0.81$) and DOC and Na ($r^2 = 0.91$) suggests that these constituents may be contributed by xanthate.

A maximum Fe concentration of 27 mg L^{-1} was observed at approximately 50 cm below the tailings surface, and elevated Fe concentrations persisted in the upper 200 cm and remained below minimum quantification limits (MQL) at depths > 200 cm. Modeling results suggest that the precipitation of secondary Fe (oxy)hydroxides is occurring between 50 and 100 cm below the tailings surface. A subsequent increase in Fe concentrations between 100 and 200 cm below the tailings surface may result from the development of reducing conditions and undersaturation of pore-water with respect to Fe (oxy)hydroxides. Similar trends in Fe concentrations below the oxidation zone have been reported for other sulfide-rich tailings deposits (Moncur et al., 2005; Gunsinger et al., 2006a).

Zinc, Mn and Ni exhibited maximum concentrations 25 cm below the tailings surface, and decreased rapidly with depth. Average concentrations of 27, 4.7 and 0.15 mg L^{-1} were observed in 2007 for Zn, Mn and Ni, respectively. Low concentrations of these metals were observed at depths greater than 100 cm. Modeled SIs suggest that precipitation of rhodochrosite [$MnCO_3$] may limit Mn concentrations. Attenuation of Zn and Ni *via* sorption

and (co)precipitation with secondary Fe (oxy)hydroxide precipitates has been observed for other tailings deposits (Moncur et al., 2005; Sidenko and Sherriff, 2005; Gunsinger et al., 2006b). These mechanisms may contribute to decreases in aqueous concentrations of Zn and Ni below the sulfide oxidation zone.

Several trace elements, including Cu, Se, As, Sb, Tl and Mo were observed in pore-water samples, however, Cd, Cr, Co, and Pb concentrations were generally below analytical detection limits. Copper and Se were present in pore-water samples collected in 2005, but average concentrations subsequently decreased to < 5 $\mu g\ L^{-1}$ by 2007. Arsenic concentrations averaged 12 $\mu g\ L^{-1}$ in 2007, and elevated concentrations generally corresponded to the presence of dissolved Fe. Average pore-water Sb concentrations decreased from 34 $\mu g\ L^{-1}$ in 2005 to 14 $\mu g\ L^{-1}$ in 2007. The lowest Sb concentrations were consistently observed at pH $\leq$ 7.0, suggesting that sorption onto Fe (oxy)hydroxides is limiting Sb mobility within 100 cm of the tailings surface (Filella et al., 2002). The mean Tl concentration was approximately 75 $\mu g\ L^{-1}$, during both sampling periods, and depth dependent trends in concentration were not evident. However, the highest Tl concentration of 315 $\mu g\ L^{-1}$ was observed 25 cm below the tailings surface. Molybdenum was present at concentrations up to 17 $\mu g\ L^{-1}$ with maximum concentrations observed from 50 to 100 cm below the tailings surface.

Water collected from the saturated zone wells and basal drain exhibited similar geochemistry to pore water collected from 200 to 400 cm below the tailings surface (Table 3.4). Measured pH and alkalinity values among wells averaged 7.66 to 8.22 and 282 to 484 $mg\ L^{-1}$ (as $CaCO_3$), respectively. Relatively low Mg concentrations observed within these samples suggest that sulfide oxidation and acid neutralization have had limited

influence on aqueous geochemistry at depth. Elevated concentrations of SO_4 were observed in monitoring wells, however, higher near-surface SO_4 concentrations were consistently observed. The presence of DOC in these wells, and the common occurrence of SRB within the tailings deposit, suggests a potential for sulfate reduction. Nonetheless, SO_4, S_2O_3, Fe, Mn, Zn, As, Cu, Ni, Se and Sb persist in saturated zone pore water and drainage.

3.6 Conclusions

Sulfide oxidation at the tailings surface has generated elevated concentrations of SO_4, Mg, Fe, Zn, Mn, Ni, Se and Tl near the tailings surface. Acidity generated by the oxidation of pyrite and other sulfides is neutralized by subsequent dissolution of carbonate minerals, and near-neutral pH conditions were maintained throughout the tailings facility. Gypsum precipitation was initially an effective control on SO_4 concentrations. However, neutralization of acidity generated by sulfide oxidation is dominated by dolomite dissolution. The resulting stoichiometric excess of SO_4 to Ca and, subsequent precipitation of gypsum, resulted in relatively constant Ca concentrations and relative increases in aqueous Mg and SO_4. Precipitation of secondary Fe (oxy)hydroxides may limit the mobility of Fe, Zn and Ni immediately below the oxidation zone. Development of Fe reducing conditions below this zone resulted in the transport of As, Sb and Tl in the vadose zone. Elevated concentrations of S_2O_3, DOC, and Na observed within the vadose zone are attributed to the presence of xanthate in residual mill process water. Pore water geochemistry within the saturated zone was generally consistent with conditions observed 200 to 400 cm below the tailings surface. However, lower concentrations of SO_4 and Mg indicate that sulfide oxidation has had less influence on water quality within the saturated zone.

Mineralogical analysis and geochemical investigation of tailings borehole core samples revealed complex sulfide mineralogy and the presence of a host of metals and trace elements. Methodologies used for AP and NP determination in this study were ineffective for the mineralogy of the Greens Creek tailings, and resulted in underestimation of both values. Recalculation using solid-phase geochemical and quantitative mineralogical yielded much higher AP and NP values which were consistent with previous results for Greens Creek tailings. The occurrence of nSOB and SRB varied with depth and among boreholes. The activity of both groups of bacteria is likely limited by localized availability of electron donors and acceptors. Static testing of NP and AP indicates that the tailings exhibit potential to generate acid. Solid-phase and aqueous geochemistry data suggest that near-neutral pH conditions may be maintained for many years. Nonetheless, elevated concentrations of SO_4, Fe, Zn and other metals and trace elements may persist under near-neutral pH conditions.

Table 3.1

Quantitative mineralogy for tailings core samples (n = 12) determined by XRD with Rietveld refinement. Mean value and standard deviation given for each phase.

Phase	Ideal Formula	wt. %
pyrite	FeS_2	34.3 ± 4.3
dolomite	$CaMg(CO_3)_2$	27.2 ± 3.0
quartz	SiO_2	12.1 ± 3.6
barite	$BaSO_4$	12.0 ± 3.8
muscovite	$KAl_2AlSi_3O_{10}(OH)_2$	3.8 ± 2.5
calcite	$CaCO_3$	3.4 ± 0.8
sphalerite	(Fe,Zn)S	2.5 ± 1.0
cymrite	$BaAl_2Si_2(O,OH)_8?H_2O$	2.1 ± 0.6
K-feldspar	$KAlSi_3O_8$	1.5 ± 0.6
chlinochlore	$(Mg,Fe)_5Al(Si_3Al)O_{10}(OH)_8$	1.5 ± 0.4
hydroxylapatite	$Ca_5(PO_4)_3(OH)$	1.2 ± 0.3
galena	PbS	0.7 ± 0.2

Table 3.2

Solid-phase concentrations of major and trace elements for borehole core samples. Number of samples (n), mean value, and standard deviation given for each parameter. All reported values for means > 1000 mg kg^{-1} were greater than the upper limit of quantification.

Parameter	Unit	BH1	BH2	BH3	BH4	BH5
n		3	9	13	7	11
Whole-rock						
SiO_2	wt. %	19.9 ± 1.6	22.1 ± 6.8	26.8 ± 8.2	20.4 ± 3.4	33.6 ± 6.3
Fe_2O_3	wt. %	16.1 ± 2.9	12.6 ± 2.6	11.3 ± 2.2	13.7 ± 1.1	10.8 ± 2.3
CaO	wt. %	11.1 ± 1.8	9.7 ± 1.4	8.1 ± 1.7	11.6 ± 2.4	9.1 ± 1.6
MgO	wt. %	6.2 ± 0.6	5.6 ± 1.0	4.6 ± 0.9	6.8 ± 1.5	5.7 ± 0.9
Al_2O_3	wt. %	3.5 ± 0.4	3.5 ± 4.5	4.5 ± 1.4	3.1 ± 0.6	4.5 ± 0.7
K_2O	wt. %	0.7 ± 0.1	0.6 ± 0.2	0.8 ± 0.3	0.5 ± 0.1	0.9 ± 0.1
MnO	wt. %	0.3 ± 0.1	0.3 ± 0.1	0.2 ± 0.1	0.3 ± 0.1	0.4 ± 0.1
P_2O_5	wt. %	0.3 ± 0.1	0.4 ± 0.2	0.6 ± 0.2	0.3 ± 0.1	0.4 ± 0.1
Na_2O	wt. %	0.3 ± 0.0	0.2 ± 0.0	0.2 ± 0.1	0.2 ± 0.0	0.3 ± 0.3
TiO_2	wt. %	0.2 ± 0.0	0.2 ± 0.1	0.3 ± 0.1	0.2 ± 0.0	0.2 ± 0.0
Ba	g kg^{-1}	49.2 ± 16.7	74.1 ± 25.7	89.4 ± 44.4	52.0 ± 28.3	36.6 ± 19.6
Aqua regia						
Zn	mg kg^{-1}	>1000	>1000	>1000	>1000	>1000
Pb	mg kg^{-1}	>1000	>1000	>1000	>1000	>1000
Mn	mg kg^{-1}	2330 ± 277	2200 ± 676	1570 ± 439	2560± 403	2760 ± 523
As	mg kg^{-1}	2260 ± 90	1540 ± 934	686 ± 437	1590 ± 105	1590 ± 526
Cu	mg kg^{-1}	1460 ± 159	1510 ± 259	1320 ± 555	1450 ± 262	1060 ± 264
Sb	mg kg^{-1}	378 ± 27	377 ± 70	376 ± 243	318 ± 91	374 ± 119
Ag	mg kg^{-1}	247 ± 22	221 ± 44	168 ± 58	222 ± 58	232 ± 53
Cd	mg kg^{-1}	130 ± 27	111 ± 27	99.1 ± 38.4	120 ± 22	90.9 ± 26.7
Tl	mg kg^{-1}	114 ± 10	79.8 ± 39.4	43.0 ± 29.1	94.2 ± 9.6	72.7 ± 26.0
Ni	mg kg^{-1}	93.2 ± 7.5	92.9 ± 27.2	71.8 ± 22.7	91.5 ± 9.9	95.8 ± 24.6
Mo	mg kg^{-1}	75.8 ± 9.6	69.1 ± 17.7	49.5 ± 17.0	76.3 ± 14.2	75.1 ± 18.4
Cr	mg kg^{-1}	37.4 ± 16.2	59.8 ± 11.1	44.5 ± 13.5	63.9 ± 12.5	57.5 ± 10.7
Se	mg kg^{-1}	21.8 ± 2.6	21.2 ± 2.8	20.4 ± 4.4	20.4 ± 4.4	25.5 ± 4.9

Table 3.3

Carbon and sulfur speciation results for tailings borehole core samples. Number of samples (n), mean value, and standard deviation given for each parameter.

Parameter	Units	BH1	BH2	BH3	BH4	BH5
n		3	12	14	8	13
Carbon (as C)						
total	wt. %	4.2 ± 0.5	4.0 ± 0.6	3.4 ± 0.7	4.7 ± 0.9	3.9 ± 0.7
carbonate	wt. %	3.5 ± 0.4	3.5 ± 0.6	2.9 ± 0.6	4.1 ± 0.8	3.5 ± 0.6
graphitic	wt. %	0.2 ± 0.1	0.2 ± 0.1	0.2 ± 0.1	0.2 ± 0.1	0.3 ± 0.2
organic	wt. %	0.5 ± 0.0	0.3 ± 0.2	0.3 ± 0.2	0.4 ± 0.1	0.4 ± 0.2
Sulfur (as S)						
total	wt. %	20.5 ± 2.2	19.5 ± 3.6	15.8 ± 3.3	18.3 ± 0.9	13.7 ± 3.0
sulfide	wt. %	12.4 ± 2.5	11.6 ± 3.2	7.0 ± 1.8	10.7 ± 1.4	7.1 ± 2.1
sulfate	wt. %	8.1 ± 0.8	7.9 ± 1.4	7.8 ± 1.9	7.7 ± 1.5	6.5 ± 1.1

Table 3.4

Aqueous geochemistry for saturated zone monitoring well (MW1, MW2 and MW3) and basal drain (BD1) samples. Values averaged for four annual samples collected between 2004 and 2007. Alkalinity is given in mg L^{-1} as $CaCO_3$.

Sample Location	pH	[1]Eh mV	Alk. mg L^{-1}	DOC mg L^{-1}	[1]H_2S mg L^{-1}	Ca mg L^{-1}	Mg mg L^{-1}	SO_4 mg L^{-1}	S_2O_3 mg L^{-1}
MW1	7.66	-100	484	5.5	> 1	146	200	971	78
MW2	8.22	-30	414	16.6	> 1	52	287	1413	0.7
MW3	8.05	-60	282	6.4	> 1	165	468	2673	8.1
BD1	6.82	-160	309	5.2	< 1	389	173	1488	0.4

Sample Location	Fe mg L^{-1}	Mn mg L^{-1}	Zn µg L^{-1}	As µg L^{-1}	Sb µg L^{-1}	Se µg L^{-1}	Cu µg L^{-1}	Cd µg L^{-1}	Ni µg L^{-1}
MW1	< 0.1	0.2	9	21	2.9	270	4.1	< 0.4	4.4
MW2	< 0.1	0.1	3.6	9.9	28	78	3.2	< 0.4	2.3
MW3	< 0.1	0.2	16	6.2	21	122	3.4	< 0.4	6.6
BD1	17	4.1	1908	33	0.7	1.9	1.9	3.4	69

[1]Single Eh and H_2S measurements made in January 2003.

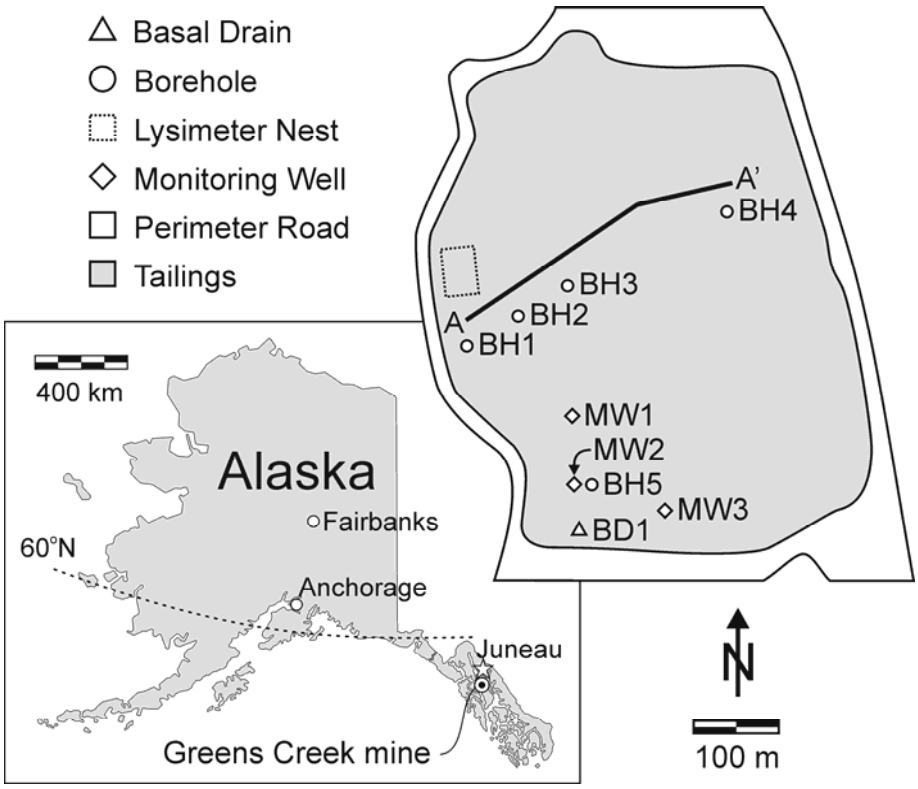

Figure 3.1 State map of Alaska with study site location (inset), and as built plan view schematic of the tailings storage facility with borehole (BH), suction lysimeter and monitoring well (MW) locations.

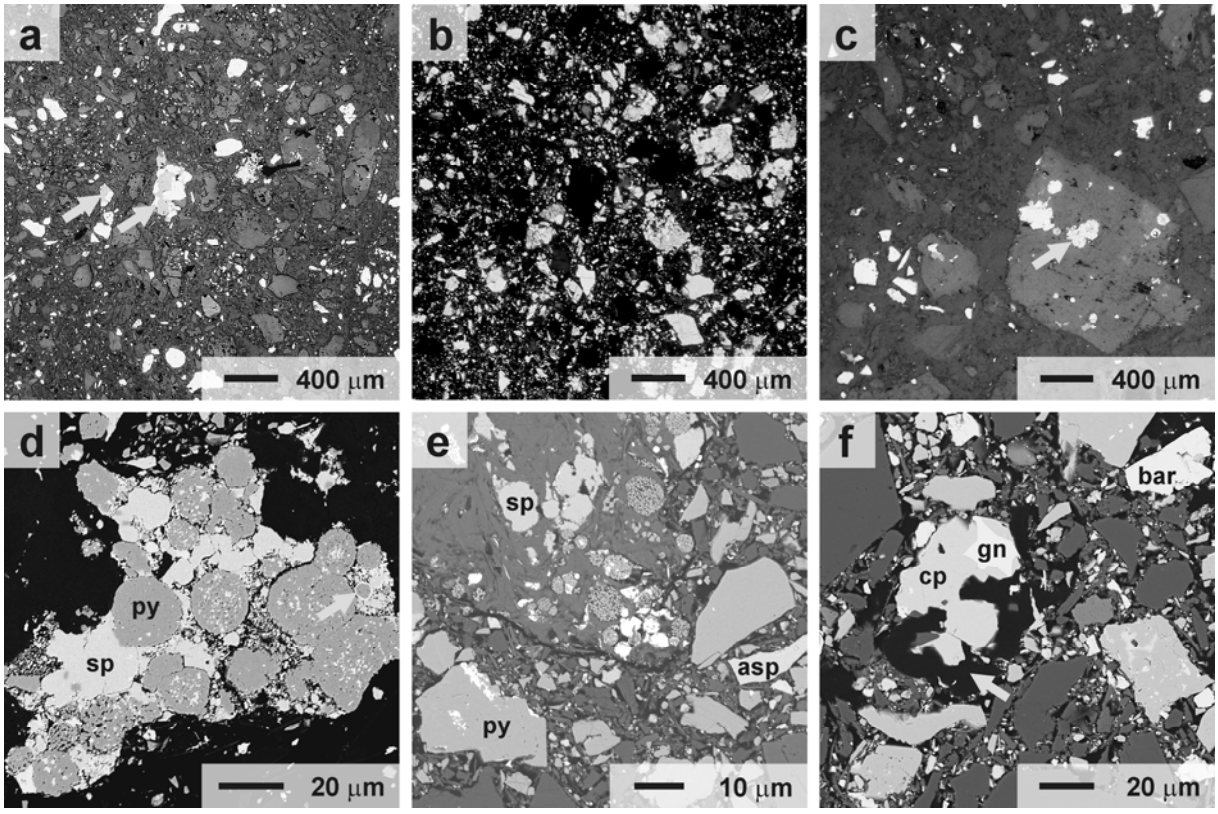

Figure 3.2 (a) Photograph of a representative tailings thin section in reflected light and (b) transmitted light with polarizers crossed. (c) Reflected light image of dolomite grain containing framboidal pyrite inclusion at the arrow. (d) Backscatter electron (BSE) image of thin section showing colloform growth of anhedral sphalerite (sp) and framboidal pyrite (py), with galena replacement at the margin of a pyrite framboid indicated by the arrow. (e) BSE image showing euhedral pyrite with galena inclusions, arsenopyrite (asp), and grains of sphalerite, framboidal pyrite and galena contained within aggregated muscovite. (f) BSE image of intergrown chalcopyrite (cp) and galena (gn) with graphite (arrow), and barite (bar).

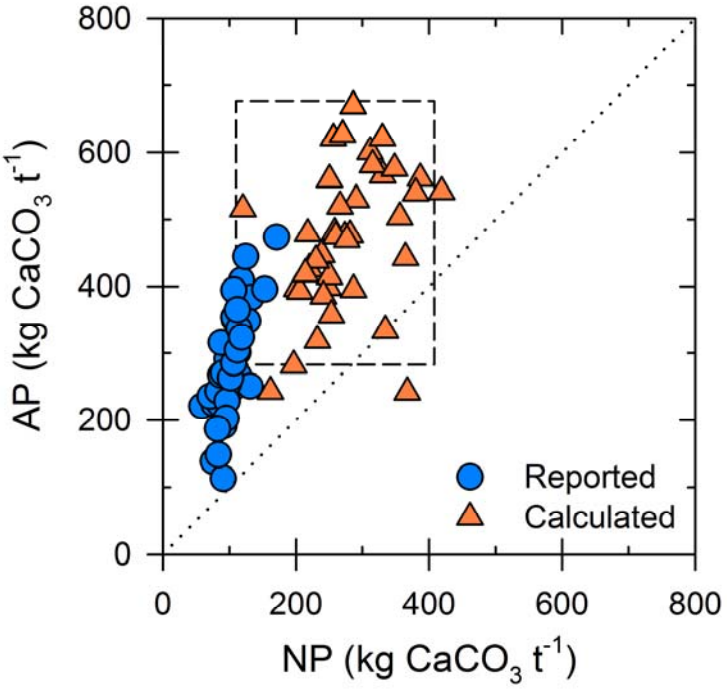

Figure 3.3 Measured and calculated acid generating potential (AP) and neutralization potential (NP) values. Calculated values of AP and NP utilized Ba and C speciation data, respectively. Area enclosed by dashed line indicates range of values determined for previously analyzed samples of Greens Creek tailings. Dotted line represents net neutralization potential (NNP) of unity.

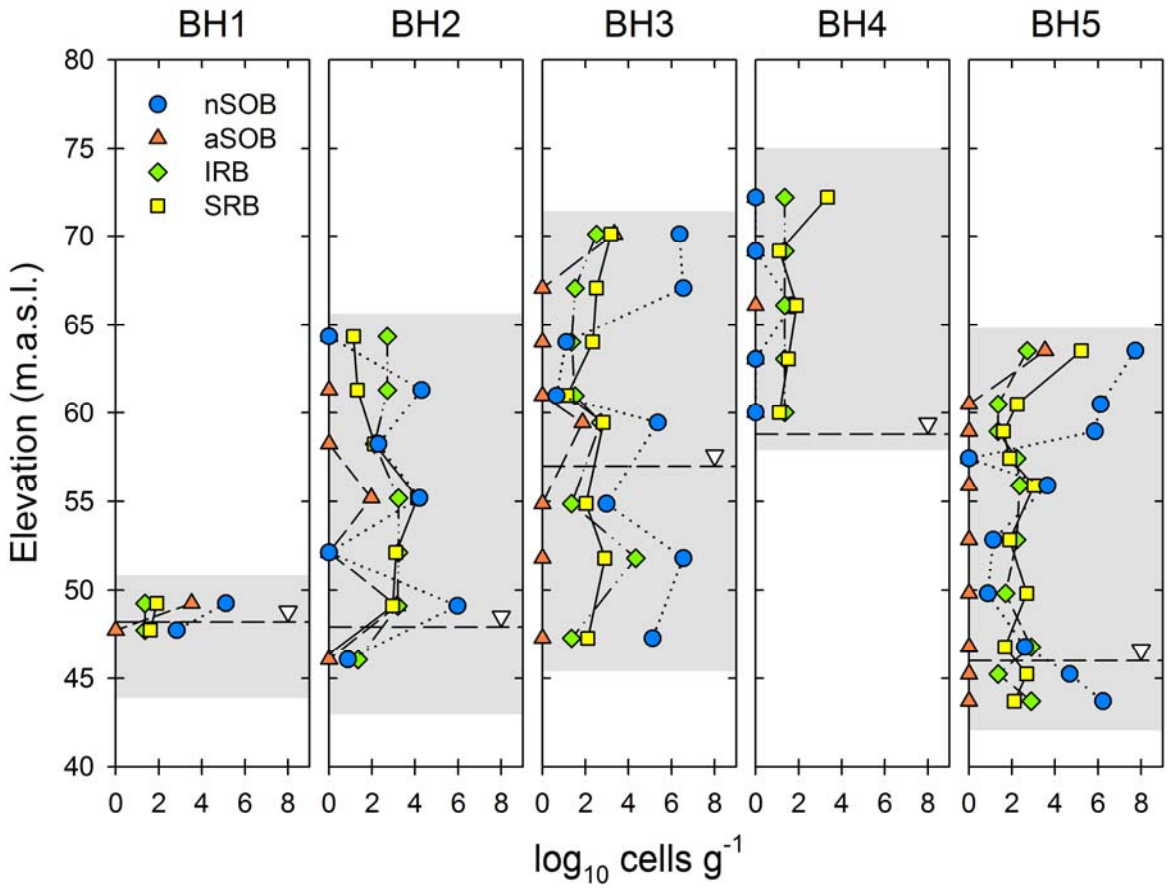

Figure 3.4 Most probable number (MPN) populations of neutrophilic sulfur oxidizing bacteria (nSOB), acidophilic sulfur oxidizing bacteria (aSOB), iron reducing bacteria (IRB) and sulfate reducing bacteria (SRB) as a function of elevation in meters above sea level (m.a.s.l.). Shaded area represents vertical extent of tailings at borehole location. Horizontal dashed line with inverted triangle denotes approximate location of the phreatic surface.

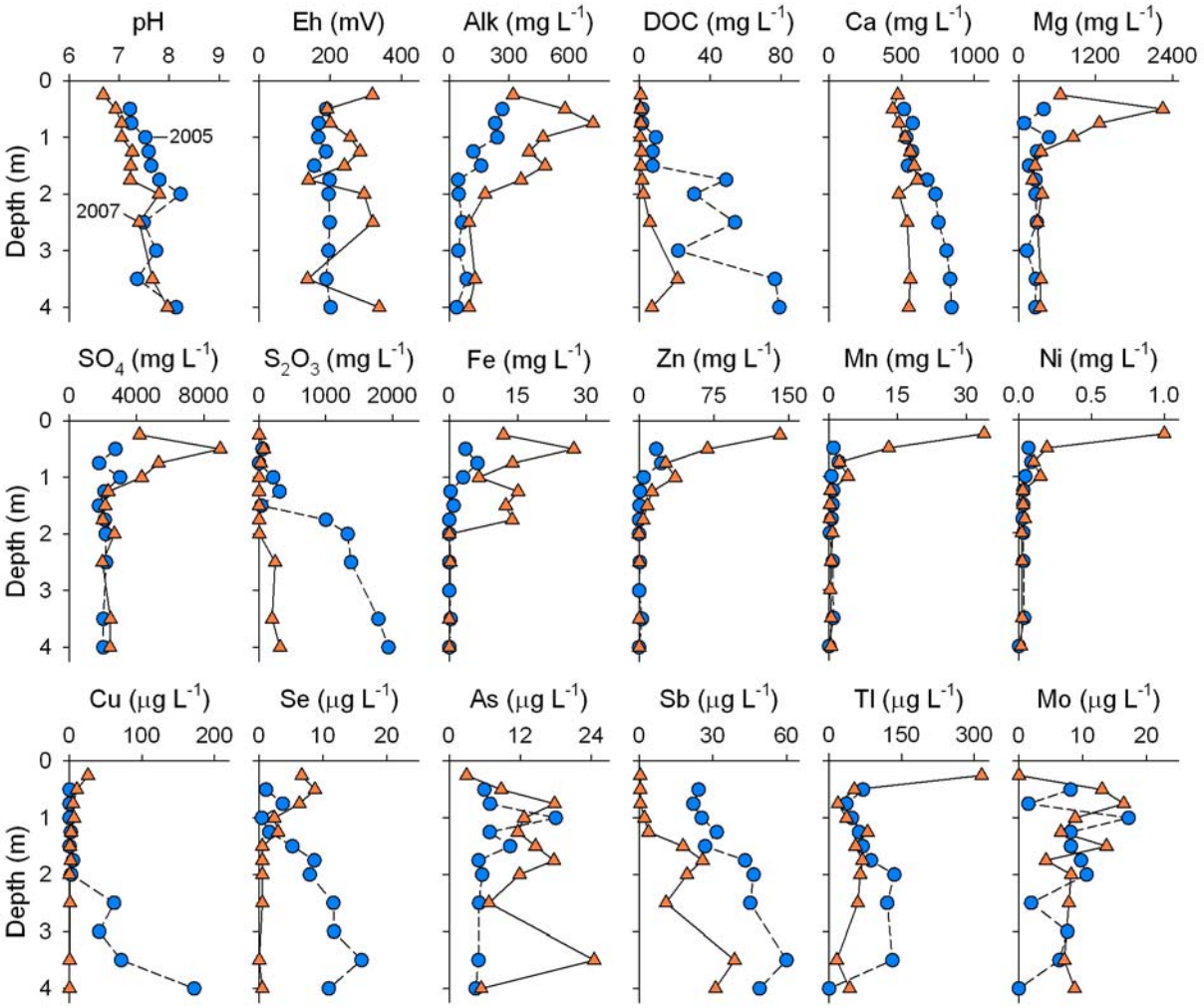

Figure 3.5 Aqueous geochemistry of tailings for pore-water samples as a function of depth below the tailings surface. Circles and triangles represent samples collected in 2005 and 2007, respectively. Alkalinity (Alk) is given as mg L^{-1} as $CaCO_3$.

Chapter 4:

Managing Pore-Water Quality in Mine Tailings by Inducing Microbial Sulfate Reduction

4.1 Executive Summary

A field-scale experiment was conducted to evaluate the potential for inducing microbial sulfate reduction as a passive in situ technique for managing water quality in mine tailings deposits. Sulfide- and carbonate-rich mine tailings, characterized by near-neutral pH pore water, were amended with < 1 dry wt. % (5 vol. %) organic carbon. The geochemical evolution of pore water was monitored for four years. The results demonstrate that organic carbon supported dissimilatory sulfate reduction (DSR) in the vadose zone. Decreases in dissolved SO_4 and S_2O_3 were accompanied by $H_2S_{(aq)}$ production, increased populations of sulfate-reducing bacteria (SRB), $^{34}S\text{-}SO_4$ enrichment, and undersaturation of pore water with respect to gypsum [$CaSO_4 \cdot 2H_2O$]. The mass of dissolved S decreased by > 45 % during the monitoring period, and coincided with the removal of Zn, Sb and Tl. Mobilization of Fe and As occurred initially; however, subsequent decreases in aqueous concentrations were observed. Mineralogical investigation confirmed the presence of secondary Fe-S and Zn-Fe-S phases. Amendment of tailings with a small and dispersed mass of organic carbon resulted in a general decrease in mass transport of sulfide oxidation products.

4.2 Introduction

Mining is central to economic growth and development; however, mining activities often have negative impacts on water resource quality. Metals, trace elements and minerals of economic importance are commonly hosted in sulfide-ore deposits, or rocks containing sulfide minerals. Extraction and concentration of these materials produces tailings and waste rock which are inherently sulfide bearing. These materials are regularly deposited in

subaerial storage facilities where residual sulfide minerals are exposed to atmospheric oxygen. The oxidation of pyrite [FeS_2] and other sulfides generates acidity, and releases SO_4 and associated metals and trace elements to pore water (Nordstrom et al. 2000; Blowes et al., 2003). Unmitigated acid mine drainage (AMD) can have widespread impacts on water quality and ecosystem health (Moncur et al., 2006, Van Damme et al., 2008). Water quality may also be impacted by neutral mine drainage (NMD) as several metals and metalloids, including Fe(II), Zn, As, Sb, and Tl, may remain soluble at near-neutral pH given appropriate redox conditions (Balistrieri et al., 1994; Filella et al., 2002; Laforte et al., 2005). Management of drainage quality is therefore essential during tailings placement and following closure.

Conventional active treatment methods often require substantial long-term energy, reagent, labor, and consequently, financial inputs (Blowes, 2002). In contrast, passive methods, which minimize the transport and subsequent discharge of sulfide oxidation products, may reduce environmental and financial liabilities associated with mineral extraction. Strategies for passive management of tailings drainage water quality are generally categorized as either source control or migration control (Johnson and Hallberg, 2005). Source control techniques, such as subaqueous disposal, inhibit oxidation by minimizing exposure of sulfide minerals to oxygen. These techniques can, however, be impractical to implement during active tailings deposition. Furthermore, source control generally disregards dissolved S, metals and trace elements contributed by residual process water (Hölmstrom and Öhlander, 1999). Migration control may therefore be a more pragmatic approach for active mining operations. A decrease in the mass flux of sulfide oxidation products would improve drainage quality and reduce reliance on active water treatment systems.

Dissimilatory sulfate reduction (DSR) provides potential for minimizing the discharge of sulfide oxidation products from mine wastes. This biogeochemical process is mediated by sulfate-reducing bacteria (SRB) which catalyze DSR in the presence of organic carbon. This reaction generates H_2S and promotes the removal of metals, such as Fe and Zn, *via* metal-sulfide precipitation (Dvorak et al., 1992; Machemer and Wildeman, 1992). Sorption or (co)precipitation of metals and metalloids with secondary sulfide phases may also contribute to treatment (Labrenz et al., 2000). This process has been utilized for treatment of AMD by anaerobic bioreactors (Dvorak et al., 1992), constructed wetlands (Machemer and Wildeman, 1992), and permeable reactive barriers (Benner et al., 1999). Alternatively, Hulshof et al. (2006) demonstrated remediation of slightly acidic tailings pore water using in situ organic-carbon layers added to the saturated zone of a mine sulfide-bearing tailings deposit. Amendment of tailings with a small and dispersed mass of organic carbon has potential to support DSR below the oxidation zone. This approach to water quality management could reduce mass transport of sulfide oxidation products, minimize associated mass loading to receiving waters, and decrease post-mining requirements for remediation. The current study evaluates the potential for passive in situ treatment of pore water within the vadose zone of a sulfide- and carbonate-rich tailings deposit. A detailed description of the study site is provided in Chapter 3.

4.3 Materials and Methods

4.3.1 Experimental Setup

Field-scale experimental cells, measuring 3 by 3 m in area and extending to a depth of 4 m, were installed in freshly placed tailings. Excavation of tailings was followed by installation of an impermeable reinforced polypropylene liner along the vertical cell boundaries to constrain pore-water migration. The lower 50 cm was backfilled with unamended tailings and compacted. Remaining tailings were amended with organic carbon at a rate of roughly 0.6 wt. % (5 vol. %), with peat and dried spent brewing grain (SBG) each accounting for 0.3 % of the final mass. Approximately 4 kg (dry wt.) of peat, collected from the anaerobic zone of a tailings drainage retention pond, was added to TC4 as SRB inoculum. The cell was backfilled with amended tailings, which were compacted at approximately 50 cm intervals. Construction of a control cell followed the same method; however, excavated tailings were not amended with organic carbon. Tension lysimeters, tensiometers and thermistors were installed at 25 and 50 cm intervals, to a maximum depth of 400 cm. Approximately 80 % of lysimeter installations were duplicated within each cell and average values are presented.

4.3.2 Field Methods

Pore-water was collected into lysimeters under an initial vacuum of 60 to 70 kPa. Lysimeters were purged twice before samples were retrieved into sterile polyethylene (PE) syringes by displacement with $N_{2(g)}$. Field determinations of pH and Eh were performed on unfiltered samples according to standard methods. Remaining sample was passed through sterile 0.45 μm surfactant-free cellulose-acetate (SFCA) syringe filters. Carbonate alkalinity and

H_2S were measured immediately by titration with normalized H_2SO_4 and by the methylene blue spectrophotometric method, respectively. Samples for inorganic anions, major cations, trace elements, and $^{34}S\text{-}SO_4$ were stored in PE bottles at 4°C until analysis. Major cation and trace element samples were acidified to $pH < 2$ with trace-metal grade HNO_3. Additionalsamples for ^{13}C in dissolved inorganic carbon (^{13}C-DIC) and dissolved organic carbon (DOC), were stored in amber glass volatile organic compound (VOC) vials fitted with rubber or Teflon®-lined septa. Tailings core samples were collected using a direct-push method (Gunsinger et al., 2006), sectioned into 30 to 45 cm segments, and refrigerated or frozen until analysis. Tensiometer and tension-infiltrometer measurements were performed to evaluate cell hydrology.

4.3.3 Laboratory Methods

Unacidified samples were analyzed for inorganic anions, including S_2O_3, by ion chromatography (IC) within 48 hours of sample collection. Major cations and trace elements were analyzed by inductively coupled plasma-optical emission spectrometry (ICP-OES) and inductively coupled plasma-mass spectrometry (ICP-MS), respectively. Dissolved organic carbon was measured by combustion and infrared detection. Values of $\delta^{34}S\text{-}SO_4$ and $\delta^{13}C$-DIC were determined using previously described methods (Giesemann et al., 1994; St-Jean, 2003), and reported relative to NBS 127 $BaSO_4$ and VPDB standards for ^{34}S and ^{13}C, respectively.

Enumerations of SRB and iron-reducing bacteria (IRB) were performed using a five-tube most-probable number (MPN) method (Chapter 2; Lindsay et al., 2008). Selective extraction of water-soluble SO_4 phases was carried out using a 1:25 mass ratio of tailings to

$Ar_{(g)}$-purged double-deionized water (Gunsinger et al., 2006). Mineralogical examination was performed on a LEO 1530 field-emission scanning electron microscope (FE-SEM) fitted with an EDAX Pegasus 1200 energy-dispersion spectroscopy (EDS) system. Moisture content and bulk density were determined gravimetrically, and particle densities were measured using a Beckman model 930 air compression pycnometer.

4.3.4 Data Interpretation

The geochemical equilibrium/mass-transfer code MINTEQA2 was used to calculate mineral saturation indices (SIs) for each sample location (Allison et al., 1990). The database was modified for consistency with that of WATEQ4F (Ball and Nordstrom, 1991), and additional solubility data was added for PO_4 (Baker et al., 1998) and siderite [$FeCO_3$] (Ptacek, 1992). Total dissolved masses of pore-water constituents in each cell were calculated by trapezoidal integration (Haas, 1996).

4.4 Results and Discussion

4.4.1 Hydrogeologic Setting

The base of the experimental cells was located > 5 m above the water table. The tailings were consistently fine grained and porosities ranged from 30 to 36 vol. %. Moisture contents were high, with values consistently > 75 % (v/v). Negative pore pressures dominated; however, positive pressures and saturated conditions developed near the tailings surface following rainfall events. Hydraulic conductivities ranged from $< 10^{-8}$ to 10^{-6} cm s^{-1} for pressures observed. Mean annual precipitation was 1380 mm during this study. The downward pore-water flux is estimated at 70 to 80 cm a^{-1} for both cells, which corresponds to a residence

time of roughly five years. The mean annual air and tailings temperatures were 6.0 and 7.6°C, respectively. Tailings temperatures ranged from approximately -1 to +21°C and +5 to +11°C at depths of 25 and 400 cm, respectively.

4.4.2 Initial Conditions

Pore water was characterized by near-neutral pH conditions, with initial average values of 8.2 ± 0.5 and 7.9 ± 0.4 observed for the control cell (TC2) and amended cell (TC4), respectively (Figure 4.1). Initial Eh values were consistently > 200 mV, reflecting the introduction of $O_{2(g)}$ during cell installation performed two weeks earlier. Carbonate alkalinity ranged from 20 to 70 mg L^{-1} (as $CaCO_3$) and pore water was consistently at saturation with respect to dolomite and calcite [$CaCO_3$], suggesting that carbonate mineral dissolution was the primary pore-water pH control within TC2. Initial elevated DOC concentrations, which averaged 82 ± 14 mg L^{-1}, probably were contributed by residual milling flotation reagents. Relative increases in alkalinity and DOC observed in TC4 are attributed to the organic carbon amendment.

Aqueous SO_4 and S_2O_3 concentrations were generally consistent at the onset of the experiment (Figure 4.2). Initial pore-water SO_4 concentrations averaged 1880 ± 95 mg L^{-1} in TC2 and 2030 ± 32 mg L^{-1} in TC4. Pore water initially exhibited saturation with respect to gypsum [$CaSO_4 \cdot 2H_2O$]. The presence of S_2O_3 at concentrations up to 2080 mg L^{-1} (average 1590 ± 290 mg L^{-1}) was also observed at this time. These high concentrations are attributed to metastability of S_2O_3 under near-neutral pH and low temperature conditions (Xu and Schoonen, 1995). Sulfur contributed by S_2O_3 accounted for approximately 60 % of initial dissolved S of 18.5 and 19.5 kg for TC2 and TC4, respectively (Table 4.1). Initial SRB

populations were consistently $< 10^2$ cells g^{-1}, suggesting their growth was limited by the presence of O_2 or the availability of nutrients, growth substrate or electron donors (Pallud and Van Cappellen, 2006).

Introduction of $O_{2(g)}$ during cell installation likely promoted Fe(III) (oxy)hydroxide precipitation and therefore low initial concentrations of Fe and As in TC2 (Figure 4.3). Dissolved Fe and Zn were observed in TC4, however As remained below the analytical detection limit of 10 μg L^{-1}. Pore water in TC2 also contained Sb and Tl at average concentrations of 58 and 37 μg L^{-1}, respectively.

4.4.3 Sulfate Reduction

The geochemical evolution of the pore water differed substantially between the control (TC2) and the organic carbon amended cell (TC4). The addition of organic carbon supported the development of conditions favorable to DSR, including decreased Eh and increased DOC concentrations. Average Year 2 S_2O_3 concentrations decreased to 210 and 4 mg L^{-1} for TC2 and TC4, respectively. Sulfate reducers have been reported to mediate S_2O_3 disproportionation and reduction (Jørgensen and Bak, 1991); however, reduction is presumably the dominant pathway under DSR observed in TC4. Average S_2O_3 concentrations within TC2 decreased to 230 mg L^{-1} after two years, whereas > 99 % of S_2O_3 was removed from TC4. Decreases in dissolved SO_4 concentrations were observed between depths of 25 and 100 cm in both cells. Initial SIs suggest that gypsum precipitation contributes to SO_4 removal within this zone. Year 4 SO_4 concentrations in TC2 ranged from 1350 to 10,800 mg L^{-1} and pore water remained saturated with respect to gypsum. In contrast, after four years, SO_4 concentrations in TC4 were consistently < 1000 mg L^{-1}

between depths of 250 and 400 cm, decreasing to a minimum of < 10 mg L^{-1} within this zone. Modeled SIs indicate that pore water in the most active DSR zone was consistently undersaturated with respect to gypsum. Selective extractions indicated a large decrease in the mass water-soluble sulfates in this zone.

Decreases in aqueous SO_4 concentrations in TC4 corresponded to H_2S production, enriched $\delta^{34}S\text{-}SO_4$ values and elevated SRB populations. Production of H_2S within TC4 resulted in aqueous H_2S concentrations > 1 mg L^{-1}, and the largest concentrations were observed from 125 to 200 cm below the tailings surface. The accumulation of H_2S within this zone suggests that SO_4 removal may be limited by the precipitation of metal-sulfide phases. Both cells exhibited initial $\delta^{34}S\text{-}SO_4$ values of approximately -14 ‰ at a depth of 25 cm. Slight enrichment in $\delta^{34}S\text{-}SO_4$ observed with depth in TC2 may be attributed to S_2O_3 disproportionation (Habicht and Canfield, 1998). In contrast, organic-carbon induced DSR supported increases in $\delta^{34}S\text{-}SO_4$ values up to +23.5 ‰. After four years, a shift in $\delta^{34}S\text{-}SO_4$ of +34.6 ‰ corresponded to an 8000 mg L^{-1} decrease in SO_4 concentrations from 25 to 175 cm below the tailings surface. A $^{34}S\text{-}SO_4$ enrichment factor (ε) of -20.8 ‰ was calculated for TC4 using the method described by Strebel et al. (1990). However, underestimation of ε may arise given that gypsum dissolution is expected to contribute relatively depleted $^{34}S\text{-}SO_4$ to pore water under DSR conditions. Enriched $\delta^{34}S\text{-}SO_4$ values in TC4 generally correspond to elevated SRB populations, which averaged $5 \cdot 10^6$ and $2 \cdot 10^6$ cells g^{-1} after two and four years, respectively. In contrast, SRB populations within the control cell averaged < 10^2 cells g^{-1} throughout the experiment. A correlation ($r^2 = 0.78$) between $\delta^{34}S\text{-}SO_4$ values and aqueous SO_4 concentrations was observed for TC4.

Carbonate alkalinity generated within TC4 produced increases in aqueous concentrations to > 2000 mg L^{-1} (as $CaCO_3$). Increased alkalinity generally corresponded to depleted δ^{13}C-DIC values, which shifted toward δ^{13}C values for peat (-27.2 ‰) and SBG (-26.9 ‰). This shift in δ^{13}C-DIC to < -20 ‰ within TC4 is indicative of organic carbon mineralization. These general trends in δ^{13}C and alkalinity in TC4 are consistent with δ^{34}S data and indicate that SRB are utilizing organic carbon during DSR (Londry and Des Marais, 2003). Elevated SRB populations within TC4 suggest that organic carbon availability did not limit SRB growth during this experiment. Limited SRB growth and relatively enriched δ^{13}C-DIC values in TC2 indicate alkalinity production from carbonate mineral dissolution *via* acid neutralization.

The reduction and subsequent removal of aqueous SO_4 and S_2O_3 from TC4 resulted in a 46 % relative decrease in the total dissolved mass of S in TC4. However, after four years the difference in the total dissolved S mass was only 2 % in the upper 100 cm. This slight difference in dissolved S is attributed to consistent rates of sulfide mineral oxidation and saturation of pore-water with respect to gypsum. In contrast, organic carbon amendment supported a 65 % relative decline in the dissolved mass of S from 100 to 400 cm below the tailings surface. This large decline in aqueous S under DSR conditions suggests that extensive precipitation of metal-sulfide phases has occurred. Furthermore, these results demonstrate that amendment of tailings with small fractions of organic carbon can support DSR and effective S removal within the vadose zone.

4.4.4 Metals and Trace Elements

Elevated Fe and Zn concentrations developed near the tailings surface due to sulfide mineral oxidation (Figure 4.3). Maximum aqueous concentrations of 16 and 105 mg L^{-1} were observed for Fe and Zn, respectively. Decreasing concentrations of these elements with depth in TC2 is attributed to the precipitation of secondary mineral phases below the sulfide-oxidation zone. Geochemical modeling results suggest that precipitation of Fe and Zn in Fe(III) (oxy)hydroxide phases may reduce their mobility within the upper 50 cm of the control cell. Coprecipitation of Zn in Fe(III) (oxy)hydroxides has been reported for other tailings impoundments (Gunsinger et al., 2006), and this mechanism could explain low Fe and Zn concentrations at depths > 200 cm in TC2.

The addition of organic carbon supported increased populations of iron-reducing bacteria (IRB) and enhanced Fe mobilization within TC4. The dissolved mass of Fe in TC4 exhibited a 230 % relative increase after two years, however, subsequent Fe removal was observed under DSR conditions. Removal of Fe occurred at depths > 75 cm below the tailings surface in TC4, and resulted in 26 % decrease in the total dissolved mass relative to the control (TC2). Modeled SIs indicate that conditions favorable to the precipitation of Fe-sulfides developed in TC4.

Elevated initial Zn concentrations in TC4 may result from reductive dissolution of Fe(III) (oxy)hydroxides. Subsequent removal of Zn was observed to correspond to S and Fe removal, and Year 4 concentrations were consistently < 0.7 mg L^{-1} at depths > 75 cm in TC4. A relative decrease of 50 % in the dissolved mass of Zn was observed by Year 2, and this value increased to 60 % after four years. Removal of Zn under DSR conditions is attributed

to the precipitation of low solubility Zn-sulfide phases such as sphalerite [(Zn,Fe)S] (Hulshof et al., 2006).

Concomitant increases in aqueous As and Fe were observed in TC4, and the dissolved mass of As exhibited a relative increase of 550 % after two years. Reduction of As(V) to As(III), which generally exhibits greater mobility in groundwater, was likely favored under conditions observed in TC4 (Kocar and Fendorf, 2009). However, similar average Year 4 As concentrations of 20 and 30 $\mu g\ L^{-1}$ were observed for TC2 and TC4, respectively. Removal of As by (co)precipitation or sorption reactions with secondary sulfides may control decreases in aqueous concentrations observed from year two to four (Labrenz et al., 2000; Farquhar et al., 2002). The lowest As concentrations in TC4, which were $< 10\ \mu g\ L^{-1}$, were observed between 100 and 250 cm below the tailings surface. Modeling results indicate that formation of Fe(III) (oxy)hydroxides was not favored within this zone. The precipitation of discrete As-sulfide phases, such as realgar [As_4S_4] and orpiment [As_2S_3], was not favored; therefore, (co)precipitation and sorption reactions with Fe and Zn sulfides likely contribute to As removal.

Removal of Sb and Tl was observed in the organic carbon amended cell (TC4) relative to the control (TC2). Average Year 4 concentrations of Sb and Tl were 27 and 50 $\mu g\ L^{-1}$ for TC2 compared to 7 and 10 $\mu g\ L^{-1}$ for TC4. Less effective sorption of Sb(V) onto Fe(III) (oxy)hydroxides at pH > 6.5 may explain the persistence of aqueous Sb in TC2 (Leuz et al., 2006). In contrast, conditions in TC4 were favorable for the reduction of Sb(V) to Sb(III), which is readily sorbed to Fe(III) (oxy)hydroxides under pH conditions observed in this experiment. However, reductive Fe mobilization was observed in this cell, suggesting that sorption may not be an effective control on Sb mobility. In contrast, Tl is expected to be

mobile under reducing conditions and a wide range in pH (Vink, 1993). Removal of Sb and Tl in TC4 generally corresponded to H_2S production and S removal, with the lowest concentrations observed from 100 to 300 cm below the tailings surface. Modeled SIs indicate that pore water was supersaturated with respect to stibnite [Sb_2S_3] and undersaturated with respect to $Tl_2S_{(s)}$. Mechanisms for Sb and Tl removal under SO_4 reducing conditions also may include (co)precipitation or sorption with secondary metal sulfides (Chen et al., 2003; Laforte et al., 2005).

4.4.5 Secondary Precipitates

Examination of core samples by FE-SEM and EDS revealed the presence of secondary Zn-S and Fe-S phases in TC4 (Figure 4.4). A general absence of similar phases was noted for samples collected from TC2. These sulfide phases were observed on surfaces of organic carbon particles, as well as carbonate and aluminosilicate phases. Precipitates observed on the surface of organic carbon particles commonly contained S, Zn and Fe (Figure 4.4a). A Zn-S phase occurring as clusters of spherules was similar in appearance to that previously identified as sphalerite by Labrenz et al. (2000). These precipitates varied in composition, but were generally S rich and consistently contained < 10 % Fe. The formation of Fe-S precipitates also was observed on the surface of organic carbon particles (Figure 4.4b). These precipitates varied in appearance from cubic to spheroidal, contained up to 10 % Zn, and exhibited S:(Fe + Zn) ratios of approximately 2:1 which is consistent with the stoichiometry of pyrite.

The occurrence of these Zn-S and Fe-S phases on SBG surfaces is consistent with in situ formation as a result of DSR and metal-sulfide precipitation. Unlike primary pyrite, the

cubic Fe-S precipitates were consistently < 1 μm in cross-section, exhibited unaltered surfaces, and displayed little to no intergrowth with other phases. The formation of pyrite under DSR conditions is generally thought to be preceded by the precipitation of mackinawite [FeS_{1+x}] and greigite [Fe_3S_4] (Rickard and Luther, 2007). A phase resembling that previously reported as disordered mackinawite by Benner et al. (1999) was observed on organic carbon particles. However, this phase was far less abundant than secondary Fe-S and Zn-S precipitates. The common occurrence of these secondary sulfide precipitates suggests that metal-sulfide precipitation is a major removal mechanism for aqueous Fe and Zn. Individual As, Sb and Tl sulfides were not observed, however, the low abundances of these elements relative to Fe and Zn would likely make locating these phases difficult. Removal of As, Sb and Tl also may result from (co)precipitation or sorption reactions with secondary Fe- and Zn-sulfides.

4.5 Conclusions

Amendment of tailings with organic carbon supported dissimilatory sulfate reduction and metal removal within the vadose zone. Removal of SO_4 was accompanied by H_2S production, enrichment of ^{34}S-SO_4, increased SRB populations, and undersaturation of pore water with respect to gypsum. The addition of organic carbon also supported increased IRB populations, the reductive dissolution of Fe(III) (oxy)hydroxides, and initial increases in Fe and As concentrations in pore water. Removal of Zn, Sb, and Tl were observed, and subsequent decreases in Fe and As concentrations form maximum values was observed under sulfate-reducing conditions. Metal removal is attributed to the precipitation of secondary Zn and Fe sulfides, and (co)precipitation or sorption of As, Sb, and Tl with these phases. This

technique for managing the quality of tailings pore-water has potential to limit mass transport of sulfide-oxidation products and reduce reliance on traditional active drainage treatment systems.

Table 4.1

Total dissolved masses for dissolved constituents calculated by trapezoidal integration.

sample period	field cell	S (kg)	Fe (g)	Zn (g)	As (mg)	Sb (mg)	Tl (mg)
initial	TC2	19	1	1	6	640	550
	TC4	20	3	21	6	813	410
Year 2	TC2	13	39	140	75	300	510
	TC4	9	120	72	500	57	180
Year 4	TC2	16	66	220	210	500	620
	TC4	8	49	91	460	99	150

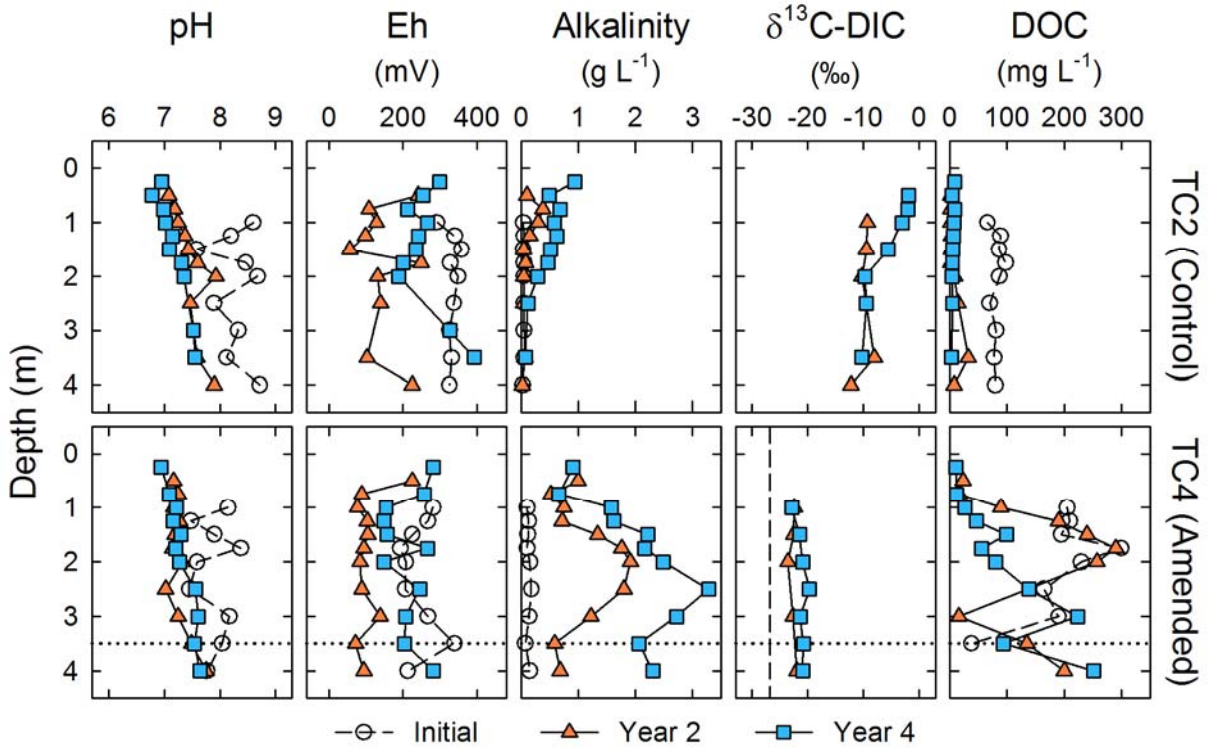

Figure 4.1 Depth profile of pore-water chemistry for control (top row) and amended (bottom row) cells. Horizontal dashed lines represent the lower extent of the organic carbon amended zone. The vertical dotted line indicates the average $\delta^{13}C$ value of the organic carbon amendments.

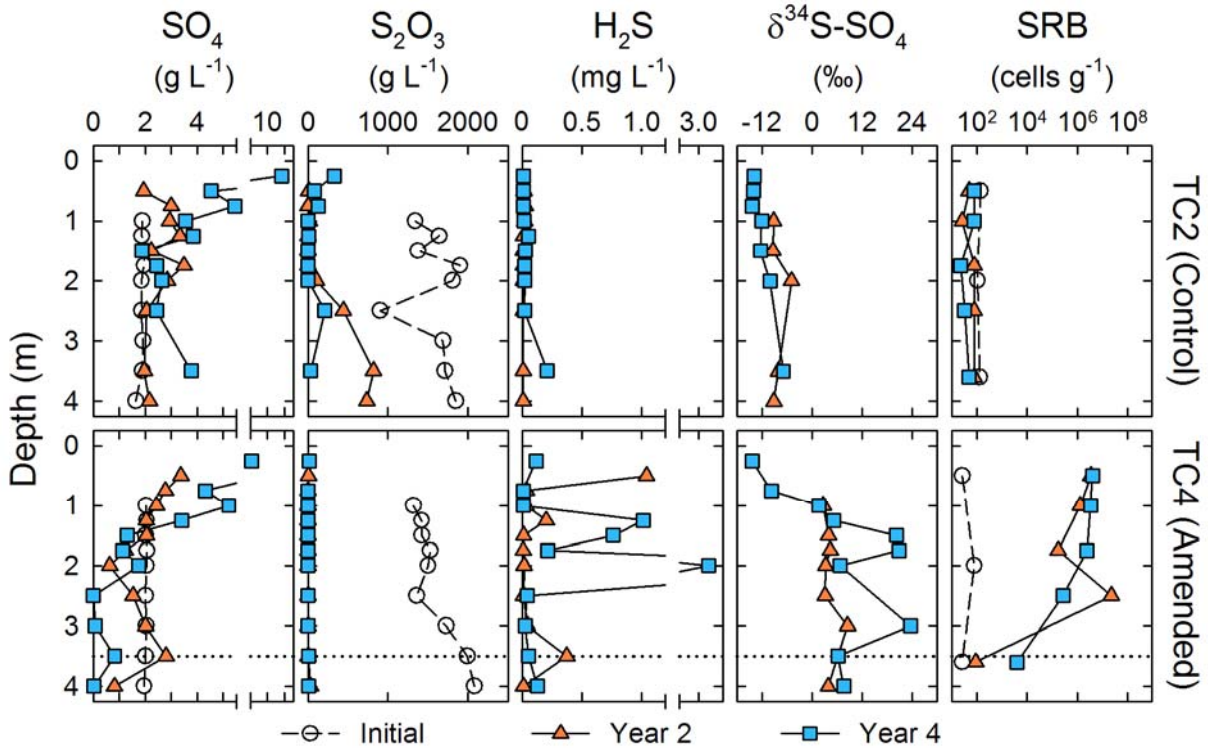

Figure 4.2 Depth profiles of pore-water sulfur species, $\delta^{34}S$ in sulfate, and most probable number populations of sulfate reducing bacteria (SRB) for control (top row) and amended (bottom row) cells. Horizontal dashed lines represent lower extent of organic carbon amended zone. Data points located on y-axis indicate values below analytical detection limits.

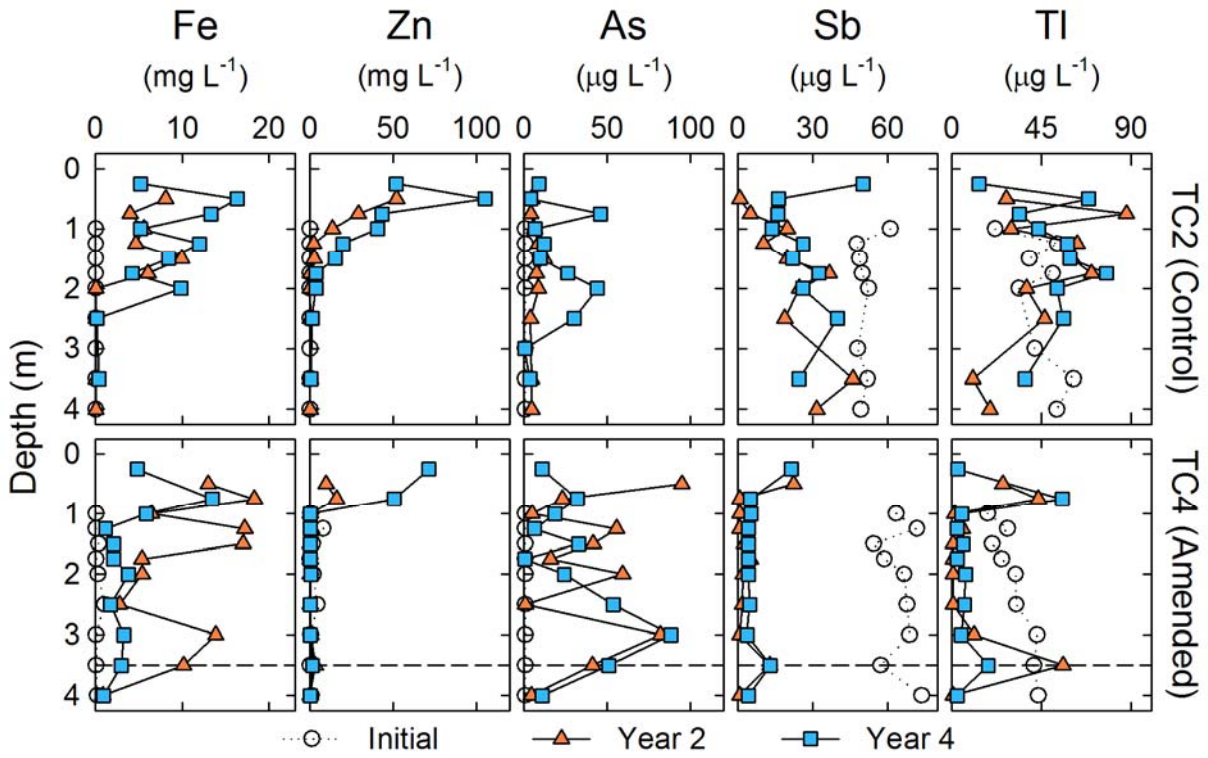

Figure 4.3 Depth profiles of pore-water metal and trace-element concentrations for control (top row) and amended (bottom row) cells. Horizontal dashed lines represent the lower extent of the organic carbon amended zone. Data points located on y-axis indicate values below analytical detection limits.

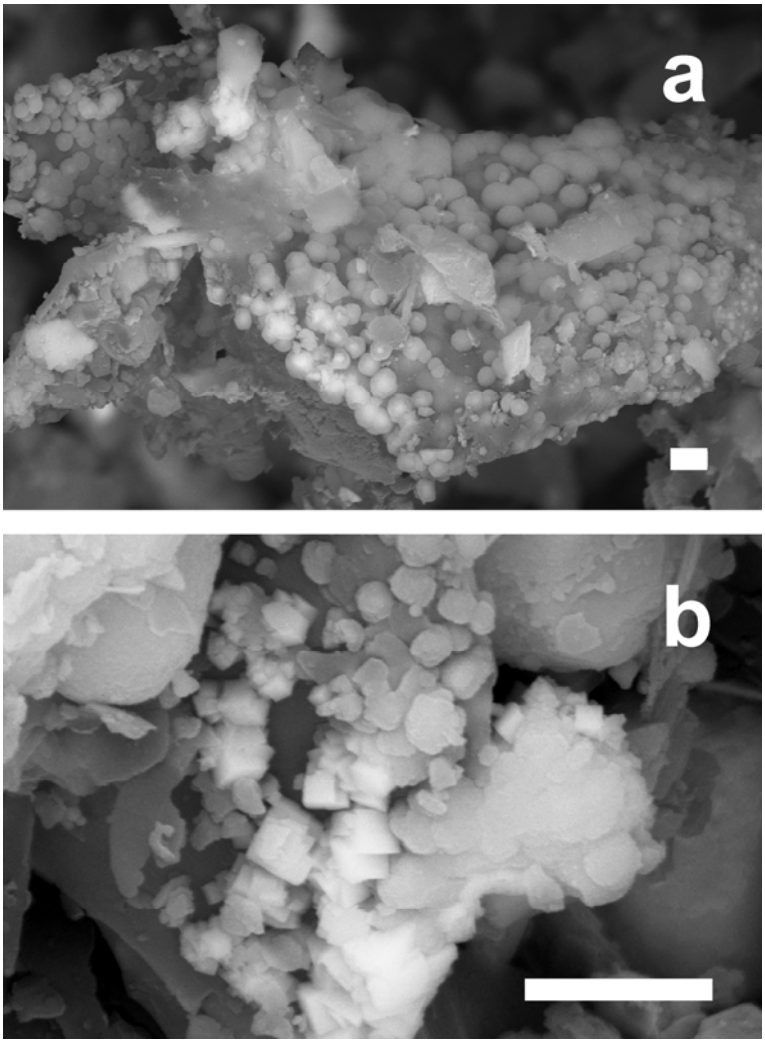

Figure 4.4 Backscatter electron (BSE) micrographs of solid-phase samples collected from the organic carbon amended cell (TC4) showing (a) Zn-Fe-S and (b) Fe-S precipitates on organic carbon particles. Scale bars represent 1 μm.

Chapter 5:

Organic Carbon Amendments for Passive In Situ Treatment of Tailings Pore Water: Field-Scale Evaluation

5.1 Executive Summary

A field experiment was conducted to evaluate tailings pore-water treatment using organic carbon amendments to support sulfate reduction. Field-scale cells were constructed in the vadose zone of a sulfide- and carbonate-rich tailings deposit characterized by neutral drainage. Amendments containing peat, plus varied mixtures of spent-brewing grain (SBG) and municipal biosolids (MB), were blended with unoxidized tailings. The geochemistry, microbiology, and mineralogy of the cells was monitored for four years. Organic carbon amendments containing SBG and SBG + MB supported increases in DOC concentrations to > 200 mg L^{-1} and decreases in pore-water SO_4 from > 3000 to < 500 mg L^{-1}. Removal of SO_4 was accompanied by H_2S production, increases in $\delta^{34}S$-SO_4 values by > +30 ‰, undersaturation of pore-water with respect to gypsum [$CaSO_4 \cdot 2H_2O$], and most-probable number (MPN) populations of sulfate reducing bacteria (SRB) > 10^6 cells g^{-1}. Solid-phase masses of soluble SO_4 decreased by 55 to 90 %, relative to the control, in cells which supported sulfate reduction. Effective removal of Zn and Tl generally accompanied SO_4 removal; however, the addition of organic carbon also supported reductive dissolution of Fe(III) (oxy)hydroxides. Although increases in Fe and As concentrations were observed in all cells, maximum concentrations were observed in cells amended with MB. Subsequent decreases in Fe and As concentrations from maximum values were observed under sulfate-reducing conditions. Examination of core samples from cells that supported sulfate-reduction by field emission-scanning electron microscopy (FE-SEM) and energy dispersive X-ray (EDS) spectroscopy revealed the common presence of spheroidal Zn-S and disordered to cubic Fe-S precipitates. These precipitates were observed on surfaces of organic carbon

particles and primary mineral grains, and exhibited Zn-S and Fe-S stoichiometry consistent with sphalerite [(Zn,Fe)S] and pyrite [FeS_2]. Discrete As, Sb, and Tl phases were not observed; however, (co)precipitation or sorption reactions with secondary Zn-S and Fe-S precipitates may contribute to removal of these elements under sulfate-reducing conditions. Amendment of tailings with a small and dispersed mass of organic carbon has potential to minimize the transport of sulfide-mineral oxidation products below the oxidation zone. However, organic carbon sources which support sustained DOC production were required to support sulfate reduction and metal-sulfide precipitation over the duration of this experiment.

5.2 Introduction

Water quality degradation is the foremost environmental issue faced by the mining industry. Unmitigated drainage emanating from mine waste deposits can have extensive impacts on the quality of water resources (Moncur et al., 2005). These impacts are often associated with sulfide-bearing mill tailings and waste rock generated from the mining of sulfidic ore bodies (Blowes et al., 2003). The oxidation of sulfide minerals, such as pyrite [FeS_2], generates acidity and contributes SO_4 and Fe(II) to pore water:

$$(5.1) \qquad FeS_2 + 7/2O_2 + H_2O \rightarrow Fe^{2+} + 2SO_4^{2-} + 2H^+$$

Associated metal and trace element impurities also are liberated during sulfide oxidation. Acidity generated by this process is neutralized by a series of mineral dissolution reactions (Jurjovec et al., 2002). The dissolution of carbonate phases, for example dolomite [$CaMg(CO_3)_2$], can effectively maintain near-neutral pH conditions:

$$(5.2) \qquad CaMg(CO_3)_2 + 2H^+ \rightarrow Ca^{2+} + Mg^{2+} + 2HCO_3^-$$

However, depletion of carbonate minerals due to acid neutralization may support the generation of acid mine drainage (AMD). Extensive acidification promotes increased solubility of several metals (e.g. Fe(III), Al, Cu) and subsequent increases in rates of sulfide-mineral oxidation (Stumm and Morgan, 1994; Nordstrom and Alpers, 1999). Furthermore, neutral mine drainage (NMD) also may have negative influences on water quality (Heikkinen et al., 2009). Metals and trace elements, including Fe(II), Zn, Ni, Mn, As, Sb, Se, Mo and Tl, may remain mobile under near-neutral pH conditions (Balistrieri et al., 1994; Fillela et al., 2002; Laforte et al., 2005). Management of water quality is therefore critical from the onset of mining activities through post closure.

Passive treatment of AMD using organic carbon to support microbially-mediated sulfate reduction was demonstrated by Tuttle et al. (1969). Under strict anaerobic conditions, sulfate-reducing bacteria (SRB) catalyze the reduction of SO_4 coupled with organic carbon oxidation (e.g. CH_2O):

$$(5.3) \qquad SO_4^{2-} + 2CH_2O \rightarrow H_2S + 2HCO_3^-$$

The generation of carbonate alkalinity supports acid neutralization and associated decreases in the acid-generating potential (AGP) of pore-water (Waybrant et al., 1998; Hulshof et al., 2006). Production of H_2S promotes the removal of metals, such as Fe(II), which exhibit low-solubility as metal-sulfide phases:

$$(5.4) \qquad Fe^{2+} + H_2S \rightarrow FeS + 2H^+$$

Decreases in aqueous concentrations of Fe, Zn, Ni, Pb, and Cu due to metal-sulfide precipitation are well documented (White et al., 1997; Waybrant et al., 1998; Benner et al., 1999). Removal of additional metals and trace elements, including As, Sb, Se, and Tl, also

may result from (co)precipitation or sorption reactions with secondary metal sulfides (Huerta-Diaz et al., 1998; Labrenz et al., 2000; Laforte et al., 2005).

Various organic carbon sources, such as wood dust, wood chips, livestock manure, crop residues, wine waste, municipal compost, pulp mill waste, organic soil, and sewage sludge, have been utilized for passive AMD treatment (Tuttle et al., 1969; Dvorak et al., 1992; Christensen et al, 1996; Waybrant et al., 1998; Chang et al., 2000; Cocos et al., 2002; Hulshof et al., 2003; Gibert et al., 2004; Costa et al., 2009). Sulfate reduction is supported by low molecular weight organic carbon molecules (i.e. organic acids) which are utilized as electron donors by SRB. These labile forms of organic carbon are generated by the degradation of cellulose and lignin, and subsequent fermentation of these degradation products (Gould and Kapoor, 2003; Logan et al., 2005). Initial rates of sulfate reduction within passive systems are controlled by the original pool of organic acids present in solid-phase carbon sources. However, these rates generally decline with time and long-term sulfate-reduction rates become dependent on in situ production of labile organic carbon (Benner et al., 1999; Hemsi et al., 2005; Logan et al., 2005; Pruden et al., 2007).

Passive treatment systems which utilize microbially-mediated sulfate reduction for AMD remediation include anaerobic wetlands (Hedin et al., 1989; Machemer and Wildeman, 1992;), anaerobic bioreactors (Dvorak et al., 1992; Christensen et al., 1996), and permeable reactive barriers (Benner et al., 1997; Jarvis et al., 2006). These technologies commonly have been employed for AMD treatment at sites impacted by extended periods of sulfide oxidation. However, passive treatment systems also provide potential as tools for managing the quality of tailings pore-water and drainage. Hulshof et al. (2006) effectively utilized layers of organic carbon to promote sulfate reduction and minimize mass transport of sulfide

oxidation products within a sulfide-rich tailings impoundment. Removal of SO_4, metals, and trace elements via sulfate reduction has potential to improve tailings pore-water and drainage quality, thereby reducing reliance on traditional active treatment systems. Decreased mass discharge of sulfide-mineral oxidation products may also improve the performance of active treatment systems by reducing reagent requirements and the mass of sludge generated during treatment.

Sulfate reducing bacteria are commonly observed in sulfidic tailings deposits; however rates of sulfate reduction may be limited by organic carbon or nutrient availability (Benner et al., 2000; Praharaj and Fortin, 2008). Amendment of tailings with a small and dispersed mass of organic carbon bearing materials has the potential enhance or induce sulfate reduction, thereby promoting in situ metal-sulfide precipitation and minimizing transport of sulfide-oxidation products. This chapter describes a four-year field-based evaluation of different organic carbon amendments for supporting microbially-mediated sulfate reduction in a sulfide- and carbonate-rich tailings deposit. This research builds upon the previous chapter, which presented the proof of principle for this pore-water quality management technique (Lindsay et al., 2009).

5.3 Site Description

The Greens Creek Mine is located at Hawk Inlet on Admiralty Island, approximately 30 km southwest of Juneau, Alaska, USA (Figure 5.1). The mine exploits a volcanogenic massive sulfide-sedimentary exhalative (VMS-SEDEX) hybrid deposit, where ore is hosted in calcareous argillite and siliceous metavolcanic rocks (Taylor et al., 1999). Ore is processed to silt- to fine sand-sized particles, with > 80 vol. % generally ranging from 0.1 to 500 μm. A

series of gravity and alkaline flotation circuits are used to concentrate sphalerite [(Zn,Fe)S], galena [PbS], tetrahedrite [$(Fe,Zn,Cu,Ag)_{12}Sb_4S_{13}$], electrum [AuAg], and pyrargyrite [Ag_3SbS_3]. Mill tailings are filter pressed to approximately 12–14 wt. % moisture, deposited by dry-stacking, and roller compacted in a 25 ha storage facility. This method of tailings placement is employed to enhance geotechnical stability and minimize the footprint of the tailings storage facility.

The tailings mineral assemblage is dominated by pyrite, exhibiting framboidal and euhedral textures, and dolomite which may account for up to 40 and 35 wt. %, respectively (Chapter 3). Quartz [SiO_2] and barite [$BaSO_4$] each represent > 10 wt. % of tailings solids, whereas calcite [$CaCO_3$], sphalerite, galena, hydroxylapatite [$Ca_5(PO_4)_3(OH)$] generally account for < 4 wt. % each. Tetrahedrite, chalchopyrite [$CuFeS_2$], and arsenopyrite [FeAsS] are observed in lesser amounts. Static acid-base accounting analysis indicates that the tailings are generally net acid generating (NAG). However, tailings pore water and drainage are characterized by near-neutral pH conditions, and can contain elevated aqueous concentrations of SO_4, S_2O_3, Zn, Fe, As, Sb, and Tl. Drainage from the tailings facility is collected via basal underdrains and treated using a ferric chloride high-density sludge process.

Mean annual precipitation at the tailings facility was 1380 mm from 1997 to 2007, and the corresponding mean annual temperature was 6.0°C. Tailings temperatures were monitored from 2006 and 2008, and ranged from -0.9 to +19.4°C in the upper 50 cm of the tailings surface. The magnitude in seasonal fluctuation in temperature decreased with depth and a mean annual temperature of 7.8ºC (± 2.0ºC) was observed at a depth of 400 cm.

5.4 Methodology

5.4.1 Field Cell Construction and Instrumentation

Six field-scale experimental cells (TC2–TC7) were constructed and instrumented from October to November of 2004 (Figure 5.2). The cells were installed along a 60 m transect of unoxidized tailings that had been deposited during the previous four months. Cells were constructed by excavating a 3 by 3 m area of tailings to a depth of 4 m, and temporarily storing this material on the surface of the tailings deposit. Impermeable liners constructed of 0.7 mm thick reinforced polypropylene were installed along the vertical extent of the excavated cells to constrain pore-water migration. The lower 0.5 m was backfilled with unamended tailings, and the remaining material was amended with varied mixtures of locally available organic carbon sources, at rates of 5 and 10 vol. %. (Table 5.1). Amendments containing peat, spent-brewing grain (SBG), and municipal biosolids (MB) were blended into the tailings by spreading and mixing the materials on the tailings surface. Tailings from an unamended control cell (TC2) were also handled in this manner. Approximately 4 kg (dry wt.) of peat collected from the anaerobic zone of an on-site tailings drainage retention pond was added to organic carbon amended cells (TC3–TC7) to ensure SRB were present in these cells. The amended material was then backfilled into the upper 3.5 m of the cells, and compacted at approximately 0.5 m intervals. Following construction, the liner was trimmed flush with the tailings surface, and the area was passed over with a vibratory roller compactor.

Each cell was instrumented with a series of tension lysimeters (Campbell Monoflex), tensiometers (Soil Measurement Systems), and moisture probe access tubes (Figure 5.2).

Tension lysimeters were installed at depth intervals of 25 and 50 cm, from 25–200 and 200–400 cm below the tailings surface, respectively. However, installation of lysimeters at depths < 100 cm was postponed to prevent freezing during the winter. The lysimeters were 4.8 cm in diameter and fitted with 10 cm long porous ceramic cups, which had a bubbling pressure of 1 bar. Each lysimeter was saturated and flushed with deionized (DI) water prior to installation. Holes were drilled into test cells using a gas-powered auger fitted with a 5 cm diameter continuously flighted bit. Drill cuttings were collected and mixed with DI water to form a thick slurry. To ensure hydraulic contact between lysimeters and tailings, the slurry was poured into the drill holes before the lysimeters were installed. A vacuum of 70 kPa was applied immediately following installation to remove added DI water and ensure hydraulic contact with tailings was achieved. Purging was repeated two additional times prior to sampling. Tensiometers were installed in May 2005 at 50 cm depth intervals using the same technique. Approximately 80 % of lysimeters were duplicated at discrete depths within opposing sections of each test cell. Averaged concentrations of pore-water constituents are presented for depths where duplicate samples were collected. Thermistors were installed at 25 and 50 cm depth intervals in undisturbed tailings adjacent to the test cells. Moisture-probe access tubes were installed concurrently with core-sample collection in 2006. Access tubes were constructed of 5 cm diameter Al tubing, and extended from the tailings surface to the base of each cell.

5.4.2 Pore-Water Sampling and Analysis

Pore-water samples were collected annually between November 2004 and August 2008. A vacuum of 60–70 kPa was applied to the lysimeters and pore water was collected over a

period of 18–24 hours. Samples were retrieved into 60 mL disposable polyethylene (PE) syringes by pressurizing the sample chamber with $N_{2(g)}$ at approximately 50 kPa.

Measurements of pH (Orion Ross 8156BNU; Oakton 35811–71) and Eh (Orion 9678BNWP), conductivity and temperature (Oakton CON 6) were made on unfiltered samples immediately following collection. Electrodes were regularly calibrated to NIST traceable pH and conductivity buffers, and performance of the redox electrode was checked against ZoBell (Nordstrom, 1977) and Light's (Light, 1972) solutions. Remaining pore-water was passed through sterile 0.45 μm surfactant-free cellulose-acetate (SFCA) syringe filters. Alkalinity was determined by titration with normalized H_2SO_4 using bromocresol green/methyl red as the end-point indicator. Anion, major cation, trace element, ortho-phosphate (o-PO_4), NH_3-total and ^{34}S-SO_4 samples were stored in 30 mL PE bottles. Samples for analysis of dissolved organic carbon (DOC) and ^{13}C in dissolved inorganic carbon (^{13}C-DIC) were collected into 40 mL amber borosilicate glass vials and sealed with no headspace. Major cation and trace element samples were acidified to pH < 2 with ultra trace-metal grade HNO_3. Acidification of NH_3 and o-PO_4 samples to pH < 2 was performed using trace metal grade H_2SO_4. All samples were refrigerated at approximately 4°C until analysis.

Anion samples were analyzed by ion chromatography (IC) for Br, Cl, F, NO_3, NO_2, SO_4, and S_2O_3 within 48 hours of collection. Major cations were analyzed for Al, B, Ca, Fe, Li, Mg, K, Si, Ag, Na, Sr, Ti, and Zn by inductively-coupled plasma-optical emission spectrometry (ICP-OES). Trace element analysis by inductively-coupled plasma-mass spectrometry (ICP-MS) included Sb, As, Ba, Cd, Cr, Co, Cu, Pb, Mn, Mo, Ni, Se, Ag, Tl, V, and Zn as analytes. The ascorbic acid spectrophometric method was used for determination of o-PO_4, while combustion with infrared detection was employed for DOC analysis. Total

ammonia was measured using an ion-specific electrode (2004, 2006) or salicylate spectrophotometric method (2008). Isotope ratios of ^{13}C-DIC and ^{34}S-SO_4 were measured on unacidified samples according to methods described by St-Jean (2003) and Giesemann et al. (1994). Values of $\delta^{13}C$ and $\delta^{34}S$ are reported relative to Vienna Pee Dee Belemnite (VPDB) and NBS $BaSO_4$ standards, respectively.

Replicate pore-water samples, including duplicates and triplicates, were collected at a rate of approximately 10 %, and average values of replicate analyses are presented. Syringe-filtered reverse osmosis purified blank samples were submitted with approximately 50 % of submissions, and all parameters were consistently below analytical detection limits. Speciated and unspeciated charge-balance errors (CBEs), and percent relative standard deviations (RSDs) were calculated as a check of data quality. Samples with speciated CBEs > 10 % were reanalyzed for major cations and anions when possible.

5.4.3 Solid-Phase Sampling and Analysis

Tailings core samples were collected annually using a direct-push piston coring technique described by Starr and Ingleton (1992). Three sequential 1.5 m core samples were collected into 5 cm diameter aluminum tubing and sectioned into 30–40 cm lengths. Core samples were then sealed with PE caps and vinyl tape, and refrigerated until analysis.

5.4.3.1 Microbial Enumerations

Enumerations of SRB, iron-reducing bacteria (IRB), and acid-producing (fermentative) bacteria (APB) were performed using a five-tube most probable number (MPN) method (Chapter 2; Cochran, 1950). Growth of SRB and IRB was promoted under anaerobic conditions in 20 mL serum bottles. Growth of SRB was supported using a modified version

of Postgate medium C (Postgate, 1984) described by Benner et al. (1999), and IRB were grown in a Fe(III)-EDTA medium developed by Gould et al. (2003). Fermenters were grown in culture tubes under ambient atmospheric conditions using a saccharide- and peptide-rich medium (Hulshof et al., 2003). Inoculation was performed by weighing 1 ± 0.05 g of sample into serum bottles or culture tubes containing 9 mL of sterilized growth media. A series of nine 1:10 serial dilutions was performed immediately following inoculation. Samples were incubated at approximately 22ºC over a period of 4 weeks for SRB and IRB, and 96 hours for APB. The formation of black precipitates was used to verify SRB growth, while the presence of Fe(II) confirmed IRB growth. A change in medium color from green to yellow indicated a decrease in pH from 7.2 to < 6.0 and the presence of APB. Control samples were prepared and a consistent lack of false positive results was noted.

5.4.3.2 Mineralogy

Field emission-scanning electron microscopy (FE-SEM) and energy dispersive X-ray (EDX) spectroscopy was employed for examination of secondary precipitates. Sub-samples of microbiology core samples were collected under anaerobic conditions and dried by vacuum desiccation. Dried samples were mounted on Al sample holders using C tape, and Au coating was applied to a thickness of approximately 10 nm. Samples from amended cells and the control were examined on a LEO 1530 FE-SEM fitted with an EDAX Pegasus 1200 EDX system. An accelerating potential of 20 kV was used for acquisition of backscatter micrographs and EDS spectra.

5.4.3.3 Selective Extractions

Selective extractions were performed on sub-samples of core samples collected in August 2008. Extractant solutions were prepared by dissolving reagents in Milli-Q® water and

purging with anaerobic-grade Ar(g) for at least two hours. Samples and solutions were combined in amber glass vials, which were sealed with screw-top caps and Teflon®-lined septa in a glove box containing an inert (i.e. N_2) atmosphere. Vials were then mixed on an orbital shaker, located in the glove box, at 60 rpm for the duration of the extraction. Gravimetric moisture contents were measured for each sample, and equivalent dry weights were used for calculation of solid to solution ratios. Water-soluble phases were extracted with $Ar_{(g)}$-purged Milli-Q® water, using a solid-to-solution ratio of 1:25 (Ribet et al., 1995). A neutral-pH weak reductant, containing 0.12 M Na-ascorbate, 0.6 M Na-bicarbonate, and 0.17 M Na-citrate, was used to target amorphous Fe(III) (oxy)hydroxides (Amirbahman et al., 1998). This extraction utilized a 1:20 solid to solution ratio, and samples were reacted for 24 hours. Poorly crystalline phases, carbonates, and sorbed metal(loid)s were extracted with 0.5 N HCl (Heron et al., 1994). Samples were digested in HCl for 24 hours using a solid to solution ratio of 1:20 to prevent complete acid neutralization.

Extractants were vacuum filtered through 0.45 μm SFCA membranes. Sulfate concentrations were measured by IC on unpreserved samples from the DI extraction. Samples for major cation and trace element analysis were acidified to $pH < 2$ with trace-metal grade HNO_3. Concentrations of Fe, Zn, As, Sb, and Tl were determined by ICP-MS. The ferrozine spectrophometric method was used for determination of Fe(II) and total Fe for the HCl extraction (Gibbs, 1979). The masses of dissolved constituents contributed with residual pore water were calculated and subtracted from the final extracted masses.

5.4.4 Hydrogeological Characterization

The elevation of the phreatic surface was monitored using a vibrating wire piezometer (Slope Indicator) installed adjacent to the field cells. In situ moisture contents were measured using a neutron probe (CPN 503DR Hydroprobe) which was calibrated to the tailings matrix. Replicate 30 s counts were collected at 15 cm depth intervals and averaged values were used to calculate volumetric moisture contents. Pressure head measurements were made in tensiometerss by inserting a needle attached to a pressure transducer, through septa and into the headspace above the water column. Pressure head values were corrected to the installed depth by subtracting the head imposed by the height of the water column from the measured tension. Gravimetric moisture content, particle density, and porosity were measured in the laboratory. Hydraulic conductivity was measured at the tailings surface using a tension infiltrometer (Soil Measurement Systems). Measurements were performed under tensions ranging from -20 to -5 cm and the method of Reynolds and Elrick (1991) was used to calculate hydraulic conductivity. Application of a KBr tracer was unsuccessful due to low infiltration rates and the high mass of Br required for achieving appropriate pore-water concentrations.

5.4.5 Data Interpretation

Mineral saturation indices (SIs) were calculated using the geochemical equilibrium/mass-transfer code MINTEQA2 (Allison et al., 1990). The thermodynamic database was modified to ensure consistency with WATEQ4F (Ball and Nordstrom, 1991). Thiosulfate was incorporated as an aqueous component, and additional thermodynamic data was added for

PO_4 (Baker et al., 1998) and siderite [$FeCO_3$] (Ptacek, 1992). Non-detectable concentrations of relevant parameters were input as one half of the analytical detection limit.

Trapezoidal integration of aqueous chemistry data was performed to estimate dissolved masses within each cell. Masses were calculated for the depth interval from 100 to 400 cm below the tailings surface. This interval facilitated mass comparisons among all cells and years, as not all lysimeters were initially installed at depths < 100 cm. These calculations were made with the assumption that porosity and saturation were consistently 33 and 90 %, respectively.

The acid generating potential of the dissolved constituents in the tailings pore water was calculated following the method of Waybrant et al. (1998). In addition to Fe(II), ammonia, which was assumed to be in the form of NH_4^+, and thiosulfate were added as acid-generating species:

$$(5.5) \qquad NH_4^+ + 2O_2 \rightarrow NO_3^- + 2H^+ + H_2O$$

$$(5.6) \qquad S_2O_3^{2-} + 2O_2 + H_2O \rightarrow 2SO_4^{2-} + 2H^+$$

Calculated AGP values > 0 and < 0 are indicative of net potential for acid generation and acid neutralization, respectively.

5.5 Results and Discussion

5.5.1 Cell Hydrogeology

The water table was > 5 m below the base of the field cells for the duration of the monitoring period. Nonetheless, pressure head values measured in October of 2006 and 2007 indicate that moisture content values approached the porosity within 200 cm of the tailings surface

(Figure 5.3). Decreases in pressure head were generally observed with depth, suggesting that saturated conditions are discontinuous over the depth of the cells. Average in situ moisture content values for individual cells ranged from 27 to 32 % and 27 to 30 % in October of 2006 and 2007, respectively. The lowest and highest average moisture content values for both years were observed in TC4 and TC7, respectively. Porosity measurements for 2008 core samples ranged from 27 to 36 % (average 33 %; $n = 18$) and values were variable within and among cells. Near-saturated conditions likely dominate from September through March, during which 80 % of annual precipitation is received. In contrast, decreases in pressure head within the upper 200 cm of each cell were observed in May 2007. These decreases in pressure head were generally accompanied by slight decreases in moisture content near the tailings surface. This reversal in pressure head gradient within 200 cm of the tailings surface is due to evaporation at the tailings surface, and these conditions are likely limited to April through July. Hydraulic conductivity measurements made at the tailings surface ranged from $< 10^{-8}$ to 10^{-6} cm s^{-1} for pressure head conditions observed in the field cells. Elevated moisture content, and therefore saturation, would result in higher effective porosity and hydraulic conductivity values toward the upper end of this range. Residence times within the test cells are estimated at approximately 4 to 5 years and assumed to be equal among cells.

5.5.2 Pore-Water Chemistry

5.5.2.1 General Conditions

Pore-water was initially slightly alkaline in pH, with an average value of 8.0 ± 0.5 observed for TC2–TC7 (Figure 5.4). These elevated initial pH values are an artifact of residual mill process water from the alkaline flotation circuit. Initial Eh values averaged +310 ± 60 mV for

all cells, and reflect the introduction of O_2 during cell implementation. Declining Eh values over the first two years of the experiment indicate the development of reducing conditions. Pore-water pH generally decreased during the experiment, and by 2008 average pH values for individual cells fell within a narrow range of 7.2 to 7.3. Minimum pH values within each cell, which ranged from 6.7 to 6.9, were generally observed within 50 cm of the tailings surface. Decreasing trends in pH towards the tailings surface are indicative of acid generation via sulfide-mineral oxidation (Equation 5.1). However, near-neutral pH conditions were maintained by carbonate mineral dissolution (Jurjovec et al., 2002). Increases in aqueous Mg concentrations and saturation of pore-water with respect to dolomite also were observed near the tailings surface. These observations suggest that acid neutralization and near-neutral pH conditions were controlled by dolomite dissolution.

5.5.2.2 Carbon and Nutrients

Initial variations in carbonate alkalinity among cells are attributed to the organic carbon amendment of the tailings (Figure 5.4). Alkalinity samples collected in 2004 exceeded 200 mg L^{-1} (as $CaCO_3$) at many locations in cells amended with MB (TC5–TC7), whereas alkalinity averaged 45 ± 13 mg L^{-1} (as $CaCO_3$) in the control cell (TC2). Initial DOC concentrations generally corresponded to these trends in alkalinity. The highest average DOC concentration of 380 mg L^{-1} (as $CaCO_3$) was observed in the cell amended with 10 wt. % organic carbon (TC7). Rapid contribution of DOC to pore water was also apparent in TC4, TC5, and TC6 which exhibited average DOC concentrations of 190, 210, and 180 mg L^{-1}, respectively. These cells were amended with 5 vol. % organic carbon, and initial DOC concentrations were approximately one half of those observed for TC7. Elevated initial DOC concentrations were observed for TC2 (average 74 mg L^{-1}) and TC3 (average 110 mg L^{-1}). A

correlation ($r^2 = 0.76$) between initial TC2 concentrations of DOC and Na suggests that DOC may be contributed by the flotation reagent Na-isopropyl xanthate [$(CH_3)_2CHOCSSNa$]. Initial $\delta^{13}C$ values of peat and SBG were -27.2 and -26.8 ‰, respectively. The $\delta^{13}C$ signature of MB was not determined; however, this value is expected to be similar to that of peat (Gerzabek et al., 2001).

Increases in carbonate alkalinity were observed in all organic carbon amended cells (TC3–TC7) and the control (TC2). Despite relatively low DOC concentrations observed in TC2, alkalinity increased to 900 mg L^{-1} (as $CaCO_3$) near the tailings surface. Alkalinity exhibited similar trends for the cell amended with 5 vol. % peat (TC3); however, slightly lower $\delta^{13}C$-DIC values indicate a DIC contribution from the oxidation of the organic carbon contained in the peat. Increases in DOC concentrations occurred rapidly in TC4–TC7, which were amended with varied mixtures of peat, SBG, and MB. The largest increases in DOC concentration were observed in TC7, which was amended with 10 vol. % organic carbon compared to 5 vol. % for TC3 through TC6. Nonetheless, average DOC concentrations in TC5–TC7 had decreased to < 40 mg L^{-1} by 2006 and < 15 mg L^{-1} by 2008. These trends in DOC concentrations within TC5–TC7 indicate that MB contributed a large initial pool of labile organic carbon which was rapidly depleted. Conversely, elevated DOC concentrations were sustained in TC4 and average values of 150 and 90 mg L^{-1} were observed in 2006 and 2008, respectively. Ongoing DOC production observed in TC4 corresponded to increases in alkalinity from 1100 to 2000 mg L^{-1} between 2006 and 2008. The other amended cells exhibited differences in average alkalinity concentrations of +40 % (TC5), -17 % (TC6) and 0 % (TC7) during the last two years of monitoring. The increase in alkalinity in TC5 indicates that organic carbon oxidation continued from 2006–2008. Alkalinity production

within TC4–TC7 was generally accompanied by depleted δ^{13}C-DIC values, which shifted towards δ^{13}C values of the solid-phase organic carbon sources. Values of δ^{13}C-DIC < -20 ‰ were observed in TC4–TC7, and the lowest values were generally associated with the highest alkalinity values. Alkalinity production was likely associated with organic carbon oxidation by heterotrophic bacteria such as SRB (Londry and Des Marais, 2003).

Initial NH_3-N concentrations averaged 6.3, 7.0, and 6.0 mg L^{-1} for TC2, TC3 and TC4, respectively (Figure 5.5). The occurrence of elevated NH_3 concentrations in these cells is primarily attributed to residual blasting agents (Koren et al., 2000). Higher average NH_3-N concentrations, which ranged from 48 to 67 mg L^{-1}, were observed in MB amended cells (TC5–TC7). Initial NO_3-N concentrations ranged from 0 to 5 mg L^{-1} in TC2, whereas values were consistently below detection for organic carbon amended cells. Large increases in NH_3-N concentrations were observed in cells amended with MB and SBG. Maximum average pore-water NH_3-N concentrations for TC5–TC7 ranged from 120 to 140 mg L^{-1} in 2006 and from 50 to 80 mg L^{-1} in 2008. These decreases in aqueous NH_3-N, combined with declining DOC concentrations, suggest that rates of solid-phase organic carbon degradation in these cells declined with time. Conversely, the average pore-water NH_3-N concentration in TC4 increased from 40 to 70 mg L^{-1} between 2006 and 2008. This ongoing contribution of NH_3-N corresponds to sustained DOC concentrations in TC4. Limited contribution of NH_3-N by peat was observed in TC3, and decreased NH_3-N concentrations in TC2 and TC3 are primarily attributed to advective transport.

Pore-water o-PO_4 concentrations were generally < 0.05 mg L^{-1} in 2004. Orthophosphate concentrations generally remained < 20 μg L^{-1} in the control cell (TC2); however, the small contribution of PO_4 to pore water is attributed to hydroxylapatite

dissolution. Cells amended with peat and MB supported the smallest increases o-PO_4 concentrations among carbon-amended cells. Degradation of SBG supported average 2008 o-PO_4 concentrations of 180, 70 and 650 mg L^{-1} in TC4, TC6 and TC7, respectively.

5.5.2.3 Sulfur

Dissolved SO_4 concentrations were initially similar both among and within cells (Figure 5.6). The average initial pore-water SO_4 concentration was 2000 ± 220 mg L^{-1} for TC2–TC7. This limited variation is attributed to consistent saturation of pore water with respect to gypsum. Elevated S_2O_3 concentrations among all cells averaged 1600 ± 240 mg L^{-1} in 2004. The presence of elevated S_2O_3 concentrations may result from the oxidation of xanthate in residual flotation process water (Hao et al., 2000). Near-neutral pH conditions and the presence of pyrite may support S_2O_3 metastability within the field cells (Goldhaber, 1983; Xu and Schoonen, 1995). Although variations in S_2O_3 values were observed, amendment and depth dependent trends were not apparent. Dissolved H_2S and $\delta^{34}S$-SO_4 were not measured in 2004, and initial values are therefore not presented.

Sulfide-mineral oxidation generated large increases in SO_4 concentrations near the tailings surface. Increases in pore-water SO_4 from 2006 to 2008 were accompanied by slight decreases in pore-water pH and increased Mg concentrations resulting from dolomite dissolution. After four years, maximum SO_4 concentrations exceeded 8,000 mg L^{-1} in TC2–TC7, and similar depth profiles were observed in the upper 100 cm in the majority of cells. Pore-water within this zone was generally saturated with respect to gypsum and undersaturated with respect to epsomite [$MgSO_4 \cdot 7H_2O$]. These increases in near-surface SO_4 concentrations between 2006 and 2008 are attributed to declining Ca concentrations associated with gypsum precipitation, and consistent undersaturation of pore water with

respect to Mg sulfates. These differences in the solubility of Ca and Mg sulfates are reflected in decreasing ratios of Ca:Mg observed with time in the upper 100 cm of each cell.

Sulfate reduction resulted in decreases in aqueous SO_4 concentrations in TC4, TC6, and TC7 relative to the control cell. These cells included SBG as a proportion of the organic carbon amendment. Cells TC6 and TC7 also contained MB as a source of organic carbon. Samples collected in 2006 from TC6 and TC7 exhibited large decreases in dissolved SO_4 concentrations at depths > 100 cm below the tailings surface. Pore-water SO_4 concentrations for 2006 samples were commonly < 1000 mg L^{-1} in these cells. A minimum SO_4 concentration of 60 mg L^{-1} was observed in TC7, which was amended with 10 vol. % organic carbon. Observed decreases in pore-water SO_4 concentrations account for approximately 40 % (TC6) and 70 % (TC7) removal of the mass of S relative to the control cell (Table 5.2). Extensive removal of SO_4 between 2004 and 2006 is attributed to large initial contributions of DOC within these cells. Effective removal of SO_4 was also observed in TC4; however, minimum concentrations were observed in 2008 as compared to 2006 for TC6 and TC7. This lag in minimum SO_4 concentrations indicates that MB promoted more rapid development of sulfate-reducing conditions than SBG. After four years, SO_4 concentrations in TC4 were consistently < 1000 mg L^{-1} at depths > 200 cm below the tailings surface, and a minimum concentration of 10 mg L^{-1} was observed within this zone. This cell exhibited relative decreases in the aqueous S mass of 40 and 60 % in 2006 and 2008, respectively. Pore-water within TC4, TC6, and TC7 was undersaturated with respect to gypsum in zones where extensive SO_4 removal was observed. Decreased aqueous SO_4 concentrations within these cells therefore are attributed to sulfate reduction and sulfide-mineral precipitation. Sulfate removal in TC4, TC6, and TC7 was accompanied by H_2S production and enrichment of ^{34}S

in aqueous SO_4. Values of $\delta^{34}S\text{-}SO_4$ increased from approximately -14 ‰ within 25 cm of the tailings surface, to maximum values of +23.5, +18.7, and +27.8 ‰ in TC4, TC6, and TC7, respectively. Enrichment in dissolved $^{34}S\text{-}SO_4$ in these cells accompanied carbonate alkalinity production and depleted $\delta^{13}C$-DIC values (Figure 5.7). This trend between $^{34}S\text{-}SO_4$ and ^{13}C-DIC is indicative of microbially mediated sulfate reduction coupled with organic carbon oxidation (Londry and Des Marais, 2003). Modeled SI values indicate that the conditions within these tests cells favour the precipitation of secondary Fe or Zn sulfide phases, including pyrite and sphalerite, which may contribute to SO_4 removal.

Removal of SO_4 due to sulfate reduction was not observed in the cell amended with 5 vol. % peat (TC3) or the control (TC2). Saturation of pore-water with respect to gypsum was maintained throughout the experiment and pore-water SO_4 concentrations generally did not decrease below the average initial value. Dissolved masses of S in TC2 and TC3 were relatively consistent over the duration of the experiment. These cells exhibited low DOC concentrations compared to TC4–TC7, and alkalinity production was primarily attributed to carbonate-mineral dissolution. These results indicate that initial DOC contributed with residual process water was not sufficient to support sustained sulfate reduction. Furthermore, low DOC concentrations and a general lack of sulfate reduction in TC3 indicate that peat is a refractory source of organic carbon. Conversely, the cell amended with 2.5 vol. % MB and 2.5 vol. % peat (TC5) exhibited a 40 % increase in the dissolved mass of DOC relative to the control. Nonetheless, $\delta^{34}S\text{-}SO_4$ values for 2006 samples were generally > 0 ‰, suggesting that SO_4 reduction did occur in TC5. Increases in aqueous SO_4 concentrations also were observed in TC6 and TC7 from 2006 to 2008. Over this period, the total dissolved S mass in TC6 increased from -40 to +20 % relative to TC2. Modest increases in aqueous SO_4

concentrations were observed for TC7; however, the 2008 dissolved mass of S remained 60 % below that of the control cell. This difference in treatment performance between TC6 and TC7 indicates that an increase in the organic carbon amendment rate from 5 to 10 vol. % supported sulfate reduction over a longer period of time. The observed increases in dissolved SO_4 in TC5–TC7 are attributed to Ca removal and the subsequent dissolution of gypsum. Alkalinity generation within these cells promoted slight supersaturation of pore-water with respect to calcite and aragonite, and corresponded to decreases in aqueous Ca concentrations. The observed increases in SO_4 concentrations are therefore attributed to declining rates of sulfate removal and the dissolution of gypsum to maintain saturation of pore-water with respect to this phase. Large decreases in Ca concentrations were also observed in TC4; however, low SO_4 concentrations persisted as sulfate-reducing conditions were maintained through 2008.

Complete removal of S_2O_3 was observed by 2006 in cells amended with organic carbon (i.e. TC3–TC7), whereas slightly elevated concentrations persisted in the control cell (TC2). The removal of S_2O_3 under anaerobic conditions can result from reduction (Equation 5.7) or disproportionation (Equation 5.8) reactions (Jørgensen and Bak, 1991):

$$(5.7) \qquad S_2O_3^{2-} + 2CH_2O + H_2O \rightarrow 2H_2S + 2HCO_3^-$$

$$(5.8) \qquad S_2O_3^{2-} + H_2O \rightarrow H_2S + SO_4^{2-}$$

Removal of S_2O_3 over the first two years was generally accompanied by decreased Ca concentrations. These decreases in Ca concentrations indicate that gypsum precipitation resulted from SO_4 production via S_2O_3 oxidation (Equation 5.6) or disproportionation (Equation 5.8). Furthermore, production of SO_4 corresponding to decreases in S_2O_3

concentrations suggests that reduction was not the primary mechanism of removal. Slight enrichments in $^{34}S\text{-}SO_4$ observed with depth in TC2 and TC3 are indicative of S_2O_3 disproportionation, which may be mediated by some SRB species (Jørgensen and Bak,1991; Habicht et al., 1998). Production of H_2S associated with S_2O_3 disproportionation may have promoted metal-sulfide precipitation prior to 2006; however, the proportion of S_2O_3 removal attributed to disproportionation versus oxidation could not be elucidated.

5.5.2.4 Iron and Zinc

Initial total Fe concentrations were generally below analytical detection limits (Figure 5.8). The introduction of O_2 during cell construction, and near-neutral pH conditions, likely promoted the precipitation of Fe(III) (oxy)hydroxides, thereby limiting initial aqueous Fe concentrations. However, modeled SI values indicate that pore-water was generally slightly undersaturated with respect to ferrihydrite [$Fe(OH)_3$], goethite [α-FeO(OH)], and lepidocrocite [γ-FeO(OH)] in 2004. Pore-water Zn concentrations exhibited an initial average value of 1.2 mg L^{-1} (TC2–TC7) and a maximum Zn concentration of 11 mg L^{-1} was observed in TC5. Contributions derived from the organic carbon amendments, or changes in geochemical conditions associated with amendments, may have resulted in the slight increases in pore-water Zn concentrations observed in TC3–TC7.

The development of reducing conditions resulted in the reductive dissolution of iron (oxy)hydroxides and mobilization of dissolved Fe; however, the organic carbon amended cells exhibited the largest increases in Fe concentrations. Organic carbon is utilized as an electron donor for dissimilatory Fe reduction (Lovley and Phillips, 1988). Rapid mobilization of Fe was observed in cells which exhibited elevated initial DOC concentrations. The highest Fe concentrations were observed in cells amended with MB or SBG, in addition to peat

(TC4–TC7). These cells exhibited the highest initial DOC concentrations, and the magnitude of aqueous Fe concentrations likely was dependent on rates of mass transfer between the solid and aqueous phases. Average Fe concentrations within TC4–TC7 ranged from 9 to 12 mg L^{-1} in 2006, whereas values of 4 and 7 mg L^{-1} were observed for TC2 and TC3, respectively. Sulfide mineral oxidation at the tailings surface also contributed to increased Fe concentrations. Relatively low concentrations of Fe were observed near the tailings surface in 2008. However, the highest Fe concentrations consistently exceeded 20 mg L^{-1} in 2008, and were generally observed from 50 to 100 cm below the tailings surface. These peaks in dissolved Fe concentrations are attributed to a zone of Fe mobilization below the sulfide-mineral oxidation zone (Moncur et al., 2005).

Removal of Fe also was observed under sulfate-reducing conditions. In 2006, decreases in Fe concentrations with depth in TC7 generally accompanied SO_4 removal under sulfate-reducing conditions. Similar trends in Fe and SO_4 concentrations were observed in TC4 and TC6, which also exhibited H_2S production, enriched $\delta^{34}S$-SO_4 values, and undersaturation of pore-water with respect to gypsum. Total dissolved masses of Fe within TC4 and TC7 were 52 and 14 % lower than the control by 2008, whereas TC6 exhibited a 46 % higher dissolved mass of Fe as compared to TC2. Removal of SO_4 and Fe under these conditions is attributed to the precipitation of low-solubility metal-sulfides and siderite. Modeled SI values indicate that pore-water in these cells approached saturation with respect to mackinawite and siderite [$FeCO_3$], whereas supersaturation with respect to pyrite, sphalerite, and greigite was observed in all cells (i.e. TC2–TC7). Removal of Fe, however, was not apparent in cells which did not exhibit decreases in SO_4 concentrations (i.e. TC2, TC3, and TC5). The total dissolved mass of Fe was highest in TC5 (2.5 vol. % peat and

2.5 vol. % MB), during the 2006 and 2008 sampling periods. This result is consistent with trends in DOC and alkalinity, which suggest that MB contributed a large initial mass of labile organic carbon, but did not support prolonged SO_4 reduction and metal-sulfide precipitation. Alkalinity production and subsequent precipitation of siderite likely contributed to Fe attenuation below the sulfide oxidation zone.

Pore-water Zn concentrations generally remained low at depths > 200 cm, while elevated concentrations were observed near the tailings surface. The oxidation of sphalerite released Zn concentrations > 50 mg L^{-1} in TC2–TC4 and > 100 mg L^{-1} in TC5–TC7. However, sharp decreases in aqueous Zn concentrations were observed with depth, and 2008 values for TC4 and TC7 were < 1 mg L^{-1} from 100 to 400 cm below the tailings surface. These cells exhibited large decreases in aqueous SO_4 concentrations, and SI values calculated with MINTEQA2 indicate that sphalerite, wurtzite, and amorphous ZnS precipitation was favoured in these locations. Furthermore, alkalinity production in all cells promoted conditions favorable to smithsonite [$ZnCO_3$] precipitation. Mass removal of Zn, relative to the control, had exceeded 90 % for TC4 and TC7 by 2008. Extensive removal of S was observed in these cells, and the precipitation of Zn-sulfides is likely a major sink for reduced S. Conversely, increases in Zn and SO_4 concentrations in TC5 and TC6 were observed over this period. These increases suggest that rates of metal-sulfide precipitation were insufficient to remove Zn contributed by reductive Fe(III) (oxy)hydroxide dissolution and sphalerite oxidation. Decreasing Zn concentrations with depth in the control cell may result from smithsonite precipitation, and absorption or (co)precipitation reactions with secondary Fe (oxy)hydroxides or carbonates (Al et al., 2000; Moncur et al., 2005; Gunsinger et al., 2006).

5.5.2.5 Arsenic, Antimony, and Thallium

Initial aqueous As concentrations were consistently below analytical detection limits. The precipitation of Fe(III) (oxy)hydroxide phases following cell construction likely limited As mobility (Dixit and Herring, 2003). Elevated Sb concentrations, ranging from 37–102 μg L^{-1}, observed at the onset of the experiment are indicative of less effective sorption of Sb(VI) to Fe(III) (oxy)hydroxides at pH > 7 (Leuz et al., 2006). The average initial pore-water Tl concentration was 39 ±13 μg L^{-1}(TC2–TC7) and a maximum concentration of 82 μg L^{-1} was observed in the control cell (TC2). The Tl(I) oxidation state is thermodynamically favored in most natural waters, and elevated concentrations are therefore attributed to high solubility of $TlOH_{(s)}$ at pH < 9 (Cheam, 2000).

Increases in aqueous As concentrations were observed in locations where the reductive dissolution of Fe(III) (oxy)hydroxides is inferred. The reduction of As(V) to As(III), which exhibits greater mobility in groundwater systems, is thermodynamically favoured under iron-reducing conditions (Kocar and Fendorf, 2009). The largest increases in As concentrations were observed in cells amended with MB, which also exhibited the highest Fe concentrations. Average 2006 pore-water As concentrations for TC5–TC7 ranged from 81 to 120 μg L^{-1}, which represented increases in the total dissolved As mass of greater than one order of magnitude. Relative increases in As concentrations were also observed in TC3 and TC4, compared to the control cell. However, average and maximum 2006 aqueous As concentrations were consistently lower in TC3 (14 μg L^{-1}) and TC4 (39 μg L^{-1}) relative to cells amended with MB. Enhanced As mobilization in the presence of MB is attributed to greater availability of electron donors (i.e. labile organic carbon) near the onset of the experiment. Maximum pore-water As concentrations in organic carbon amended cells were

generally observed in 2006, whereas As mobilization in the control continued throughout the experiment. Decreases in aqueous As concentrations in TC4–TC7 were associated with SO_4 removal and enriched $\delta^{34}S\text{-}SO_4$ values. Total dissolved masses of As in TC5–TC7 decreased by 20 to 50 % over this period, whereas values for TC3 and TC4 remained constant. Saturation indices calculated with MINTEQA2 indicate that geochemical conditions did not favor the precipitation of discrete As-sulfide phases. Sorption and (co)precipitation reactions with secondary sulfides, such as mackinawite, pyrite, and sphalerite, may contribute to As removal in these cells (Labrenz et al., 2000; Farquhar et al., 2002).

Antimony exhibited markedly different mobility in pore water relative to As. Maximum aqueous concentrations of Sb were generally observed at the onset of the experiment. Speciation of Sb was not performed; however, Chen et al. (2003) found that Sb(III) dominated under Fe and SO_4 reducing conditions in anaerobic lake sediments. Sorption of Sb(III) to Fe(III) (oxy)hydroxides, which occurs over a broad range in pH (3 to 12), may have contributed to Sb attenuation in the organic carbon amended cells (Leuz et al., 2006). However, (co)precipitation or sorption reactions with secondary Fe-sulfide phases may contribute to Sb removal under sulfate-reducing conditions (Chen et al., 2003). Sorption of Sb(V) to Fe(III) (oxy)hydroxides is most effective at pH < 7, and the persistence of Sb in the control cell suggests that Sb(V) was the dominant species. Reductive dissolution of Fe(III) (oxy)hydroxides was limited in TC2 and sorption reactions may have limited Sb mobility. Gradual decreases in Sb concentrations in TC2 are attributed to decreasing pH or the reduction of Sb(V) to Sb(III) with time.

In contrast to Sb, effective removal of Tl was only observed in organic carbon amended cells that exhibited decreases in aqueous SO_4 concentrations due to sulfate

reduction (i.e. TC4, TC6, and TC7). Total dissolved masses of Tl in these cells had decreased by 65 to 97 % relative to the control cell. Modeled SIs indicate that pore-water was generally undersaturated with respect to $Tl_2S_{(s)}$. Removal of Tl under sulfate-reducing conditions may be attributed to (co)precipitation or sorption reactions with secondary sulfide phases (Laforte et al., 2005). Consistently elevated Tl concentrations in TC2, TC3, and TC5 indicate that sorption of Tl to organic carbon and Fe(III) (oxy)hydroxides did not effectively limit Tl mobility.

5.5.2.6 Acid-Generating Potential

Calculated values of AGP were between +16 and +43 meq L^{-1} at the onset of the experiment (Figure 5.9). The potential for acid generation within these cells results from the high concentrations of $S_2O_3^{2-}$ in pore water in 2004. Decreases in AGP were consistently observed from 2004 to 2006; however, pore-water in TC2, TC5, and TC6 retained potential for acid generation upon oxidation. Smaller decreases in AGP in TC5 and TC6 are attributed to NH_3 and Fe mobilization, and less effective alkalinity production compared to TC4 and TC7. Subsequent decreases in AGP were observed in TC5 and TC6; however, pore-water in TC5 maintained the potential for acid generation upon oxidation. Decreases in AGP values were observed with time in all remaining cells. Carbonate alkalinity production associated with SRB activity in TC4 and TC7 supported average decreases to < -20 meq L^{-1}, which indicates that more than 20 times the acid generated by Fe(II), NH_3, and S_2O_3 oxidation could be neutralized by associated carbonate alkalinity. Increases in carbonate alkalinity observed in TC2 and TC3 were also sufficient to support net acid consumption.

5.5.3 Microbiology

Fermentative bacteria (APB) were absent in initial samples collected from TC2 and TC3 (Figure 5.10). The addition of SBG and MB supported increased APB populations, which exceed 10^6 cells g^{-1} at some locations in TC4–TC7. However, samples were collected approximately two weeks after initiating the experiment, and elevated APB populations are attributed to the organic carbon amendments rather than in situ growth. Populations of APB in TC2 and TC3 remained < 10^1 cells g^{-1} over the duration of the experiment. This apparent lack of APB in TC2 and TC3 is consistent with low DOC and o-PO_4 concentrations, which may impose physiological constraints on the growth of heterotrophic bacteria (Harder and Dijkhuizen, 1983). Furthermore, these results indicate that peat is refractory and most likely an ineffective source of labile organic carbon. In contrast, 2006 core samples collected from TC4 and TC7 exhibited APB populations > 10^4 MPN g^{-1}. These cells contained 2.5 vol. % SBG, which is presumably an effective source of fermentative bacteria. Subsequent APB numbers were < 10^4 MPN g^{-1} for samples collected from TC4 and TC7, whereas APB populations in TC5 and TC6 were consistently < 10^3 cells g^{-1} in 2006 and 2008. These decreases in APB populations may be indicative of declining availability of labile organic carbon within these cells. Conversely, a zone of elevated APB population was observed in TC4 from 100 to 300 cm below the tailings surface. This zone generally corresponds to increased alkalinity and DOC and depleted SO_4 and Fe concentrations, suggesting that increased DOC availability supported enhanced treatment.

Populations of SRB were generally < 10^2 cells g^{-1} at the onset of the experiment, with the exception of one sample location in each of TC5 and TC6. Elevated populations of SRB (> 10^7 cells g^{-1}) observed at these locations may arise from the localized presence of

inoculum in core samples. Organic carbon amendments containing SBG supported SRB growth over the first two years of the experiment. Average SRB populations within TC4, TC6, and TC7 increased to > 10^6 cells g^{-1} by 2006, and remained above this value through 2008. The cell amended with 2.5 vol. % peat and 2.5 vol % MB supported average SRB populations of 10^5 and 10^6 cells g^{-1} in 2006 and 2008, respectively. This slight increase in SRB numbers, combined with alkalinity production and some APB activity, indicates that sulfate reduction may be occurring within this cell. Nonetheless, rates of sulfate reduction within TC5 are likely limited by organic carbon availability. Elevated SRB populations for TC4–TC7 were observed within 50 cm of the tailings. Sulfate reducers are obligate anaerobes, and the presence of elevated SRB populations near the tailings surface reflects the limited $O_{2(g)}$ ingress below the tailings surface. Low populations of SRB were consistently observed in the control. Slight increases in SRB numbers at some locations in TC3 indicate that peat may have supported limited sulfate reduction. However, low DOC concentrations and APB numbers within TC2 and TC3 suggest a constraint on SRB activity imposed by limited organic carbon availability.

Iron reducers exhibited low initial numbers in TC2–TC4 compared to TC5–TC7. Populations of IRB were consistently < 10^3 cells g^{-1} in TC2–TC4, whereas amendments containing MB supported populations > 10^5 cells g^{-1} in the upper 200 cm of TC5–TC7. During the first two years of the experiment, average IRB populations increased to 5×10^4 cells g^{-1} in TC3 and 7×10^5 cells $^{-1}$ in TC4. Conversely, average IRB populations in TC5–TC7 generally decreased over this period, with the largest decreases observed in the upper 250 cm of each cell. These decreases in IRB populations may be associated with declining DOC concentrations or competition for electron donors (i.e. labile organic carbon)

with other heterotrophs. Depletion of poorly crystalline Fe(III) (oxy)hydroxides, which are preferred electron acceptors, may have had a similar effect on IRB activity (Nevin and Lovley, 2002). Declining trends in IRB activity continued to 2008, and populations $< 10^2$ were consistently observed in TC2–TC4. Cells amended with MB (TC5–TC7) supported average 2008 populations ranging from 4×10^2 to 2×10^3 cells $^{-1}$. Nonetheless, the influence of dissimilatory Fe reduction on pore-water chemistry diminished with time.

5.5.4 Mineralogy

The removal of SO_4, Zn, and Fe under sulfate-reducing conditions is attributed to metal-sulfide precipitation. Secondary Fe- and Zn-S phases were observed on surfaces of organic carbon particles, primary carbonate grains, and aluminosilicate margins in core samples collected from cells that supported sulfate reduction (Figure 5.11). Similar phases were not observed in samples collected form the control cell (TC2). The secondary precipitates were generally consistent among TC4, TC6, and TC7. The most commonly observed reaction product was a spheroidal Zn-S precipitate which resembled a phase previously identified by Labrenz et al. (2000) as sphalerite (Figure 5.11a). Standardless EDX analysis revealed that this phase generally exhibited a composition (by atomic wt.) of (Zn + Fe) : S < 1 by atomic weight. Pore-water commonly exhibits molar S : (Zn + Fe) ratios > 100, and excess S observed in these precipitates may be attributed to incorporation of excess S during formation. However, the precipitation of Ca or Mg sulfates during sample desiccation may also contribute to this apparent S excess. Iron generally accounted for < 10 % (atomic wt.) of these precipitates, and trace element contents were generally below quantification.

Incorporation of As into biogenic sphalerite has been reported (Labrenz et al., 2000), and this mechanism may influence As mobility under sulfate-reducing conditions.

Precipitates composed primarily of Fe and S also were observed on organic carbon and mineral surfaces (Figure 5.11b). These precipitates ranged in texture from disordered to cubic and commonly exhibited S:Fe ratios > 2. Cubic grains were commonly associated with non-cubic aggregates of Fe-S (Figure 5.11b) and Zn-S (Figure 5.11c). The cubic Fe-S grains differed in appearance from primary pyrite present in the tailings assemblage. Primary pyrite exhibits framboidal and euhedral textures, intergrowth with sphalerite, and replacement by galena, whereas cubic Fe-S precipitates are generally characterized by unaltered surfaces (Lindsay et al., In Press). Furthermore, primary pyrite grains generally range from 10 to 100 μm in cross-section, whereas secondary Fe-S precipiates were consistently < 1 μm across. Modeled SIs indicate that pore-water was generally undersaturated with respect to mackinawite and supersaturated with respect to pyrite. Rapid precipitation of pyrite has been reported under similar conditions (Howarth, 1978), and reaction of precursor Fe-S phases with aqueous thiosulfate and H_2S may promote pyrite formation (Wilkin and Barnes, 1996). An Fe-S phase was observed on organic carbon particles resembling that identified by Benner et al. (1999) as disordered mackinawite (Figure 5.11d). This phase was not commonly observed; however, the presence of mackinawite may indicate that conditions were favorable to pyrite formation (Rickard and Luther, 2007).

Saturation indices calculated by MINTEQA2 indicate that pore-water was near saturation with respect to stibnite [Sb_2S_3] and undersaturated with respect to orpiment [As_2S_3], realgar [As_4S_4], and $Tl_2S_{(s)}$. Discrete As, Sb, and Tl sulfides were not observed; however, the presence of these phases cannot be excluded. Sorption and (co)precipitation

reactions with Zn and Fe sulfides likely contribute to the attenuation of metals and trace elements (White et al., 1997; Labrenz et al., 2000; Farquhar et al, 2002; Laforte et al., 2005).

5.5.5 Selective Extractions

5.5.5.1 Sulfate

Variations in solid-phase masses of water-soluble SO_4 were observed among and within cells (Figure 5.12). However, average values for individual cells reflect trends in aqueous SO_4 concentrations. The largest average SO_4 contents of 1900 and 1600 mg L^{-1} were observed for samples collected from TC3 and TC2, respectively. Sulfate reduction was limited in these cells and gypsum accumulation contributed to increases in soluble SO_4 contents to > 2500 mg kg^{-1} within 100 cm of the tailings surface. Gypsum accumulation also resulted in a soluble SO_4 content of 4100 mg L^{-1} at a depth of 175 cm in TC5. Declining SRB activity with depth in TC5 may have resulted in this deeper zone of gypsum accumulation. Cells amended with mixtures containing SBG exhibited the lowest average soluble SO_4 contents of 713 mg kg^{-1} (TC4), 136 mg kg^{-1} (TC6), and 79 mg kg^{-1} (TC7). Water-soluble SO_4 contents were < 50 mg kg^{-1} at several locations within these cells, which also exhibited large decreases in aqueous SO_4 concentrations and undersaturation of pore water with respect to gypsum. Dissolution of gypsum under sulfate-reducing conditions presumably preceded reprecipitation of S as metals sulfides. These phases exhibit low solubility and are generally stable under anaerobic conditions.

5.5.5.1 Metals and Trace Elements

Extractions performed with DI water demonstrate that Fe and Zn mobility is limited under neutral pH conditions, and in the absence of electron donors (Figure 5.13). However, these

elements were mobilized by the neutral-pH weak reductant (ascorbate) and 0.5 M HCl. Pore-water in all cells was consistently supersaturated with respect to goethite and lepidocrocite, and conditions favorable to ferrihydrite and siderite precipitation were observed (Figure 5.9). The presence of Fe in the ascorbate-reducible fraction is attributed to the reductive dissolution of amorphous Fe(III) (oxy)hydroxides. Cells containing SBG (i.e. TC4, TC6, and TC7) exhibited average Fe contents of 1.4 mg g^{-1} in the ascorbate-reducible fraction, which were 15 to 22 % lower than values observed in TC3, TC4, and the control cell. These results indicate that the reducible mass of Fe(III) (oxy)hydroxides decreased in TC4, TC6, and TC7 as a result of DOC contribution and IRB activity. The acid-soluble fraction exhibited average Fe concentrations ranging from 4.4 mg kg^{-1} (TC6) to 5.5 mg kg^{-1} (TC3). Speciation of Fe in the 0.5 M HCl filtrate revealed that Fe(II) accounted for 89 to 97 % of total Fe. These results indicate that the majority of Fe present in the acid-soluble fraction was associated with carbonate phases. Alkalinity production in organic carbon amended cells promoted conditions favorable to the precipitation of siderite and Ca carbonates. Al et al. (1999) demonstrated that incongruent dissolution of dolomite during acid-neutralization resulted in the formation of siderite. Furthermore, unaltered grains of primary dolomite were found to contain Fe in trace amounts (Lindsay et al., In Press). Therefore, consistently high proportions of Fe(II) observed in the acid-soluble fraction indicates that the majority of Fe was contributed by carbonate dissolution. Slightly larger discrepancies between Fe(II) and total Fe observed in TC2 and TC3 are attributed to dissolution of Fe(III) (oxy)hydroxide phases. Partial dissolution of pyrite in 0.5 N HCl may also liberate Fe (Rickard and Morse, 2005); however, the Fe contribution from this reaction is expected to be relatively small.

Average Zn contents in the ascorbate-reducible and acid-soluble fractions ranged from 0.8 to 1.2 mg g^{-1} and 1.8 to 2.4 mg $^{-1}$, respectively. The reducible fraction represented 23 to 61 % of Zn extracted with 0.5 M HCl, which indicates that Zn may be mobilized by acid generation or an increase in the availability of electron donors. The presence of Zn in the ascorbate-reducible fraction suggests that adsorption or (co)precipitation of Zn with amorphous Fe(III) (oxy)hydroxides likely contribute to Zn attenuation below the oxidation zone. The dissolution of primary dolomite, and secondary Ca and Zn carbonates, may have contributed to differences in Zn concentrations between the ascorbate-reducible and acid-soluble fractions.

Arsenic and Sb were not present in filtrates from the DI water extraction, and exhibited similar concentrations in the reducible and acid-extractable fractions. Approximately 70 % of As and 95 % of Sb extracted by 0.5 M HCl was accounted for in the ascorbate-reducible fraction. These results indicate that amorphous Fe(III) (oxy)hydroxides are important control on As and Sb mobility. Observed discrepancies between Fe(II) and total Fe in TC2 and TC3 were attributed to Fe(III) (oxy)hydroxides. Liberation of As during dissolution of Fe(III) (oxy)hydroxides may account for differences between As in the ascorbate-reducible and acid-soluble fractions observed for these cells. Dissolution of acid volatile sulfide (AVS) phases, such as mackinawite, is expected with the 0.5 M HCl extraction (Rickard and Morse, 2005). The release of As associated with AVS phases may have contributed to differences in As between the ascorbate-reducible and acid-soluble fractions in TC4 and TC7. Slight differences in Sb extracted by the weak reductant and 0.5 M HCl. These results confirm that amorphous Fe(III) (oxy)hydroxides are important

controls on As and Sb mobility, and reductive dissolution of Fe(III) (oxy)hydroxides will likely release these elements to pore water.

Thallium mobility generally differed from that of Fe, Zn, As and Sb. The majority of Tl was associated with the acid-soluble fraction; however, Tl also was observed in the water-soluble fraction, but not the ascorbate-reducible fraction. The presence of Tl in the water soluble fraction was limited to cells amended with organic carbon. These results are attributed to complexation of Tl(III) with DOC, which has been shown to enhance Tl mobility within aqueous systems (Lin and Nriagu, 1999). A general lack of Tl in the ascorbate-reducible fraction suggests that amorphous Fe(III) (oxy)hydroxides do not effectively limit Tl mobility. However, the ascorbate solution was buffered to a pH of 8, and precipitation of $TlOH_{(s)}$ may have limited Tl solubility in these extractions (Cheam, 2000). The highest Tl contents in the acid-soluble fraction were observed in TC2 and TC3, which suggests that an acid-soluble phase influenced aqueous Tl mobility. Vaněk et al. (2009) reported that sorption of Tl to Mn (oxy)hydroxides was the dominant control on Tl mobility in soils. This process could explain higher Tl contents observed in the acid-soluble fraction for TC2 and TC3, which exhibited less extensive reductive dissolution. Moreover, Tl also may be liberated by AVS or pyrite dissolution in 0.5 M HCl.

5.6. Conclusions

Amendment of tailings with a small and dispersed mass of organic carbon provides potential as a technique for managing pore-water and drainage quality. However, organic carbon amendments which support and sustain sulfate reduction were essential for long-term treatment. Rapid increases in DOC concentrations were observed in cells that contained

municipal biosolids (MB) and/or spent brewing grain (SBG). Contribution of DOC from MB was short lived, whereas SBG supported a sustained DOC contribution. Peat did not support increases in DOC concentrations relative to the control and was therefore a poor source of organic carbon. Removal of S_2O_3 via disproportionation was observed in all organic carbon amended cells (TC3–TC7) and the control (TC2). Sulfate liberated by this process enhanced gypsum precipitation and subsequent decreases in aqueous Ca concentrations in all cells. Amendments containing SBG supported decreases in SO_4 concentrations, H_2S production, enrichment of $^{34}S\text{-}SO_4$, undersaturation of pore water with respect to gypsum, and large decreases in the solid-phase mass of soluble SO_4. The addition of MB resulted in rapid development of conditions favorable to sulfate reduction; however, declining DOC concentrations likely resulted in less effective treatment with time. Enhanced SO_4 removal was achieved by doubling the organic carbon amendment rate from 5 (TC3–TC6) to 10 vol. % (TC7). Organic carbon amendment of tailings also supported reductive dissolution of Fe(III) (oxy)hydroxides, and subsequent increases in Fe and As concentrations. The highest Fe and As concentrations were associated with amendments that contained MB, although elevated concentrations developed in all cells with time. Decreases in Fe and As from maximum values were observed under sulfate-reducing conditions. Increases in carbonate alkalinity due to organic carbon oxidation promoted conditions favorable to calcite or aragonite precipitation. Precipitation of these carbonate phases was most evident in cells amended with SBG or SBG + MB. Subsequent decreases in Ca concentrations promoted gypsum dissolution in these cells, and increased SO_4 concentrations in cells which did not effectively support effective sulfate reduction.

Elevated populations of fermentative bacteria (APB) were observed in cells amended with SBG (i.e. TC4, TC6, and TC7). These cells generally supported the largest SRB and IRB populations; however, similar MPN numbers were observed in a cell amended with MB and peat (TC5). Peat supported SRB and IRB populations that were moderately higher than the control and consistently lower than the other organic carbon amended cells. Examination of core samples by FE-SEM revealed the presence of spheroidal Zn-S and disordered to cubic Fe-S precipitates. These precipitates were observed in cells which supported increased SRB activity and decreases in SO_4 concentrations. Calculated saturation indices and selective extraction measurements suggest that precipitation of siderite and smithsonite may also contribute to Fe and Zn attenuation. Discrete As, Sb, and Tl sulfide phases were not observed, and their removal in cells amended with SBG and/or MB is attributed to (co)precipitation and sorption reactions with secondary metal-sulfides. However, sorption reactions with Fe(III) (oxy)hydroxide phases also may have contributed to As and Sb attenuation. Carbonate alkalinity production combined with decreases in Fe concentrations generated pore-water which was net acid consuming.

This technique for tailings pore-water treatment may be an effective management strategy for active mines. Organic carbon amendment of tailings during deposition limits mass transport of sulfide-mineral oxidation products and could improve drainage quality and reduce mass loading to receiving waters. These decreases in mass discharge also could reduce inputs associated with active treatment and minimize sludge generation. Combining alternate reclamation strategies, such as cover systems, with this technique for pore-water treatment has potential to improve drainage quality and reduce demand on active treatment systems.

Table 5.1
Final amended composition of field cells.

Field	Volume Percent (vol. %)			
Cell	Peat	SBG	MB	Tailings
TC2				100
TC3	5.0			95
TC4	2.5	2.5		95
TC5	2.5		2.5	95
TC6	2.5	1.25	1.25	95
TC7	5.0	2.5	2.5	90

Table 5.2

Total dissolved masses calculated by trapezoidal integration over the depth interval from 100 to 400 cm below the tailings surface.

Field Cell	Sampling Period	S (g)	Ca (g)	Mg (g)	Fe (g)	Zn (g)	As (mg)	Sb (mg)	Tl (mg)
TC2	2004	9400	8500	2100	0	0	0	440	390
	2006	8100	4300	2900	17	9	54	250	330
	2008	8600	4500	5400	66	46	130	130	480
TC3	2004	10300	7300	2800	3	31	0	480	440
	2006	7900	4200	3400	56	58	110	72	290
	2008	8500	4100	6000	97	110	110	40	410
TC4	2004	10100	8000	2700	2	17	0	570	300
	2006	5200	3500	4000	77	6	340	33	100
	2008	3600	1100	6500	32	1	350	24	32
TC5	2004	9900	7500	2800	0	14	0	480	340
	2006	9200	3600	3400	90	35	670	26	430
	2008	11800	3800	8400	140	130	530	20	450
TC6	2004	10000	7800	2700	0	2	0	560	340
	2006	4700	1900	3200	65	2	920	38	43
	2008	10300	2300	8800	97	73	760	41	170
TC7	2004	10600	8000	2800	1	6	0	640	350
	2006	2300	1400	3100	62	23	830	27	11
	2008	3800	1800	5100	57	2	390	18	15

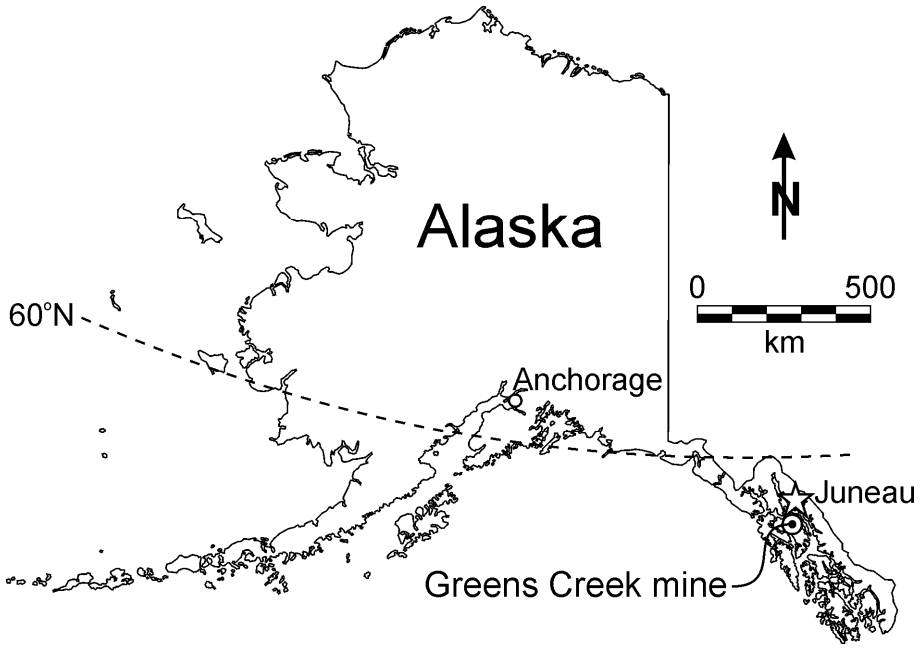

Figure 5.1 Location of the Greens Creek Mine.

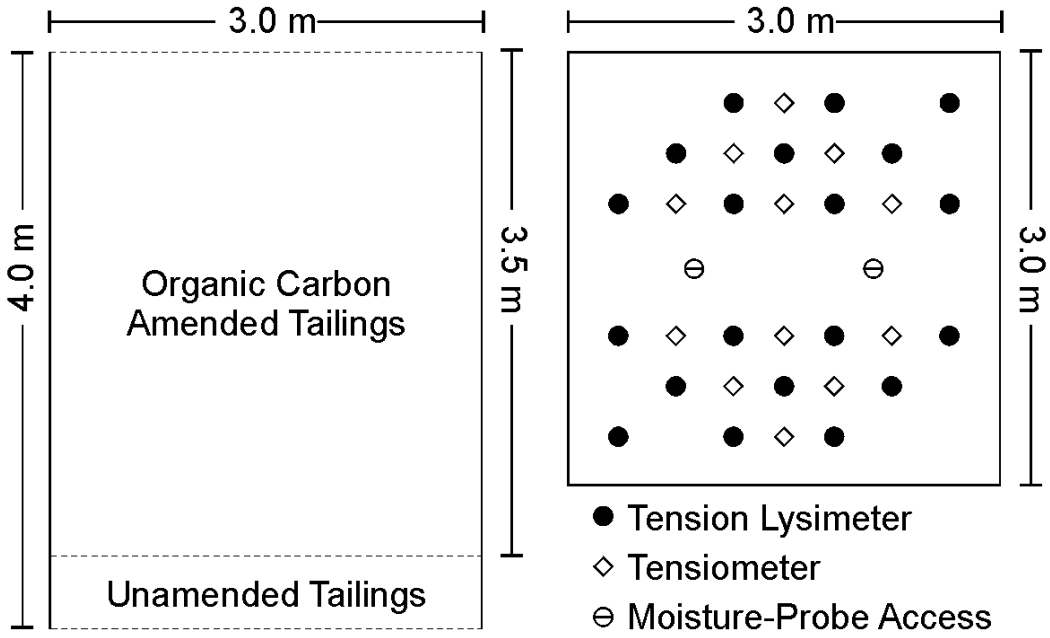

Figure 5.2 Schematic diagrams of test cell design in cross section (left) and plan view (right).

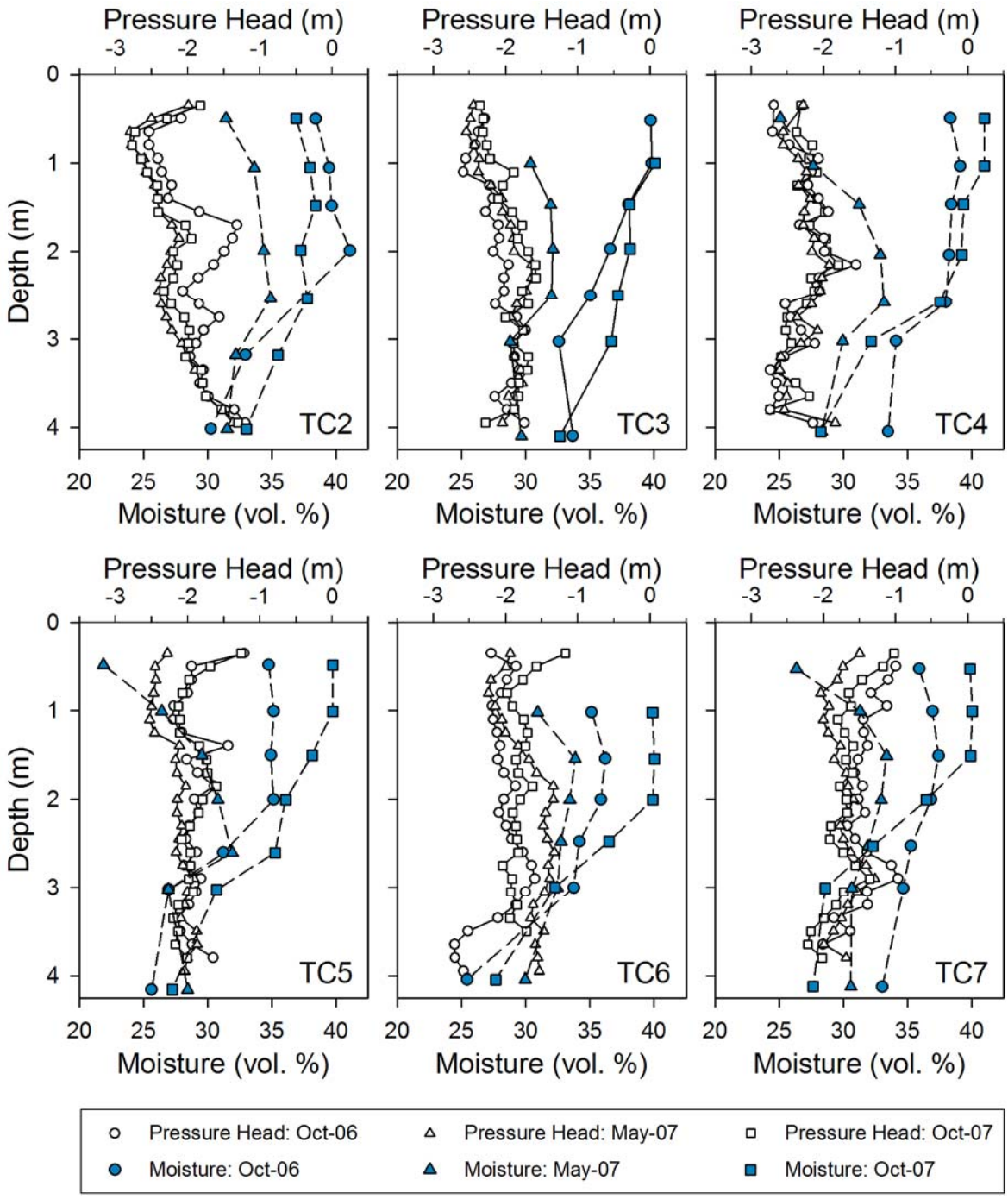

Figure 5.3 Depth profiles of in situ moisture content and pressure head values measured in 2006 and 2007.

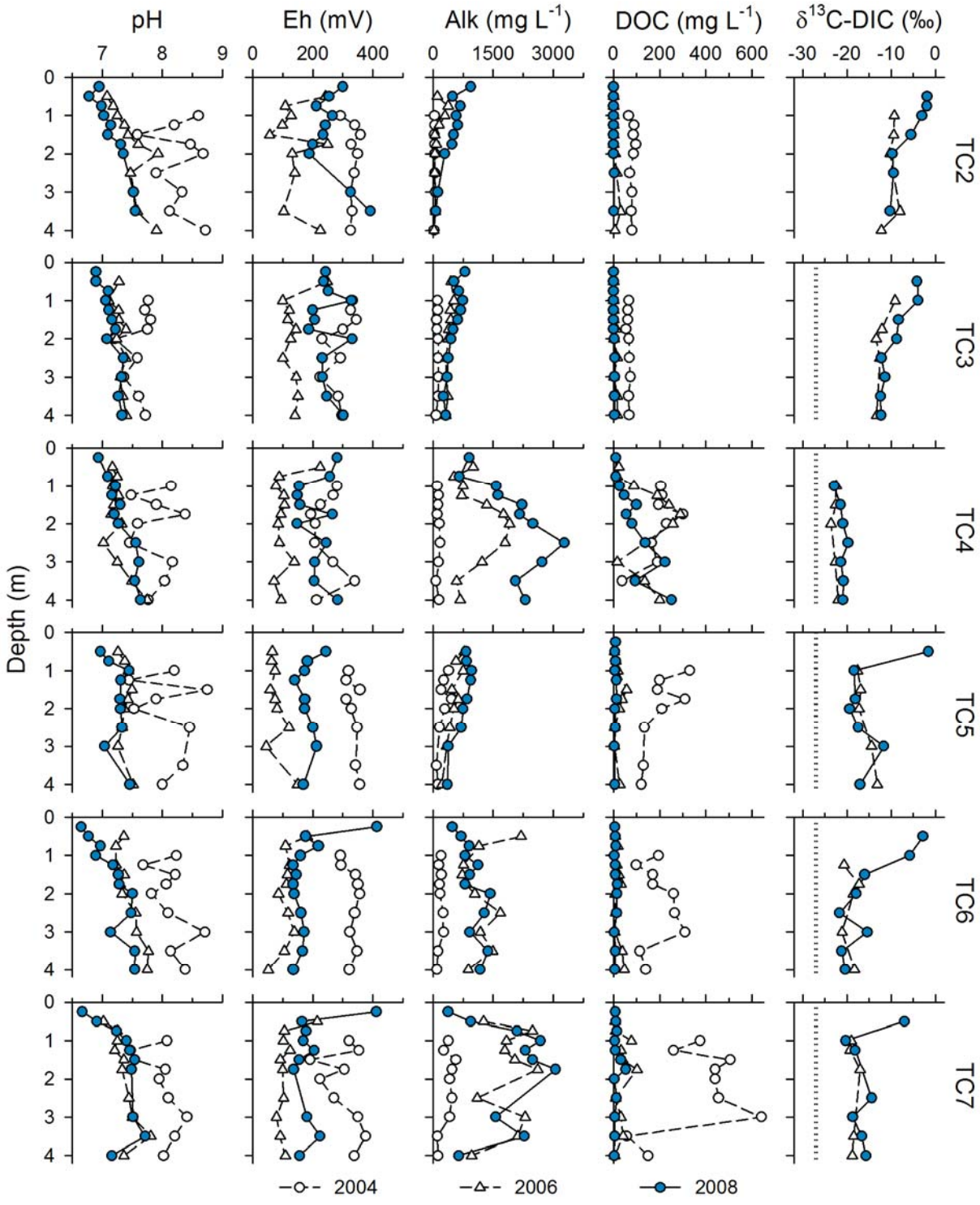

Figure 5.4 Depth profiles of pH, Eh, alkalinity (Alk), dissolved organic carbon (DOC), and $\delta^{13}C$ in dissolved inorganic carbon ($\delta^{13}C$-DIC) for pore-water samples collected from tension-lysimeters in 2004, 2006, and 2008. Dotted lines represent $\delta^{13}C$ values of organic carbon.

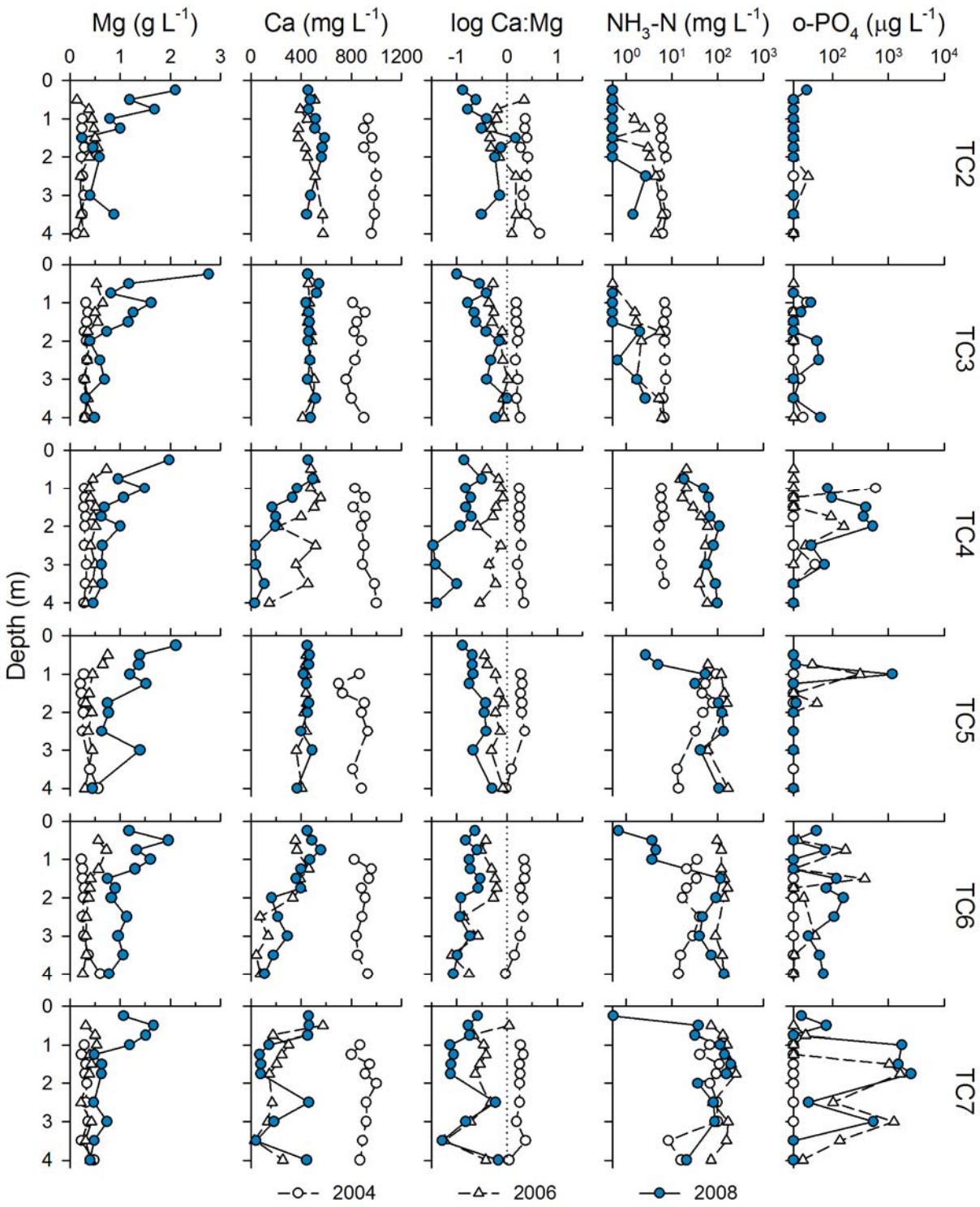

Figure 5.5 Depth profiles of magnesium (Mg), calcium (Ca), calculated Ca:Mg ratios (mol/mol), total ammonia as N (NH_3-N), and orthophosphate (o-PO_4) for pore-water samples collected from tension-lysimeters in 2004, 2006, and 2008.

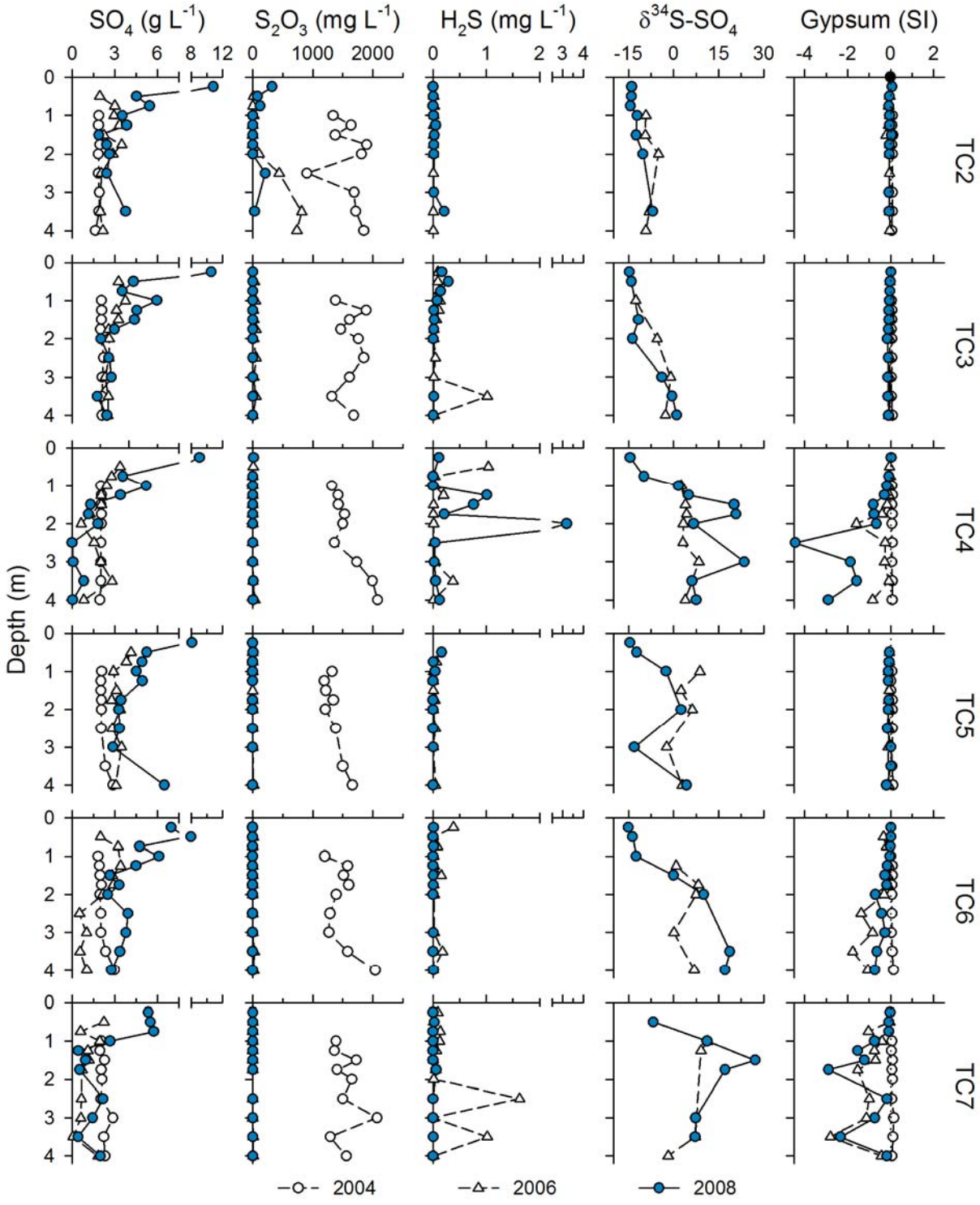

Figure 5.6 Depth profiles of sulfate (SO_4), thiosulfate (S_2O_3), hydrogen sulfide (H_2S), ^{34}S in sulfate ($\delta^{34}S$-SO_4), and gypsum [$CaSO_4 \cdot 2H_2O$] saturation indices (SI) for pore-water samples collected from tension-lysimeters in 2004, 2006, and 2008.

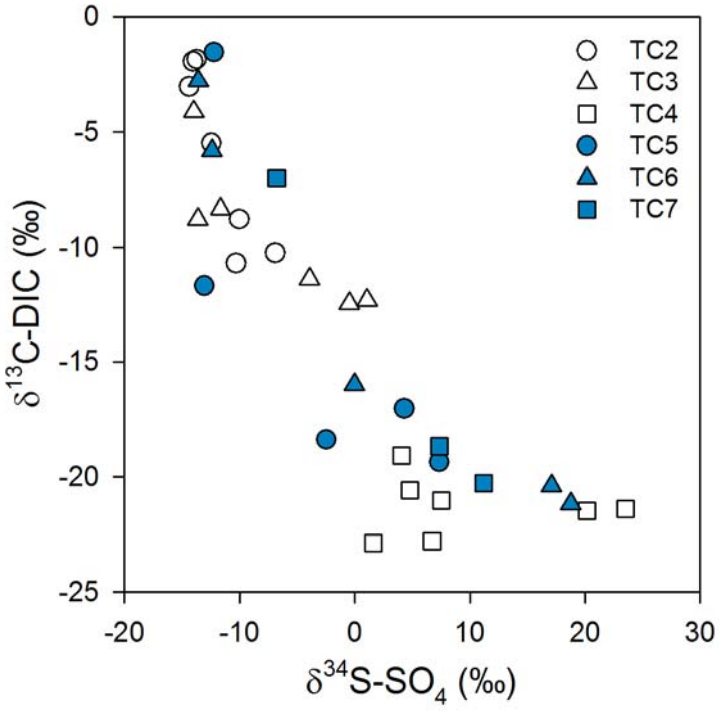

Figure 5.7 Pore-water δ^{13}C-DIC plotted against δ^{34}S-SO_4 for 2008 lysimeter samples.

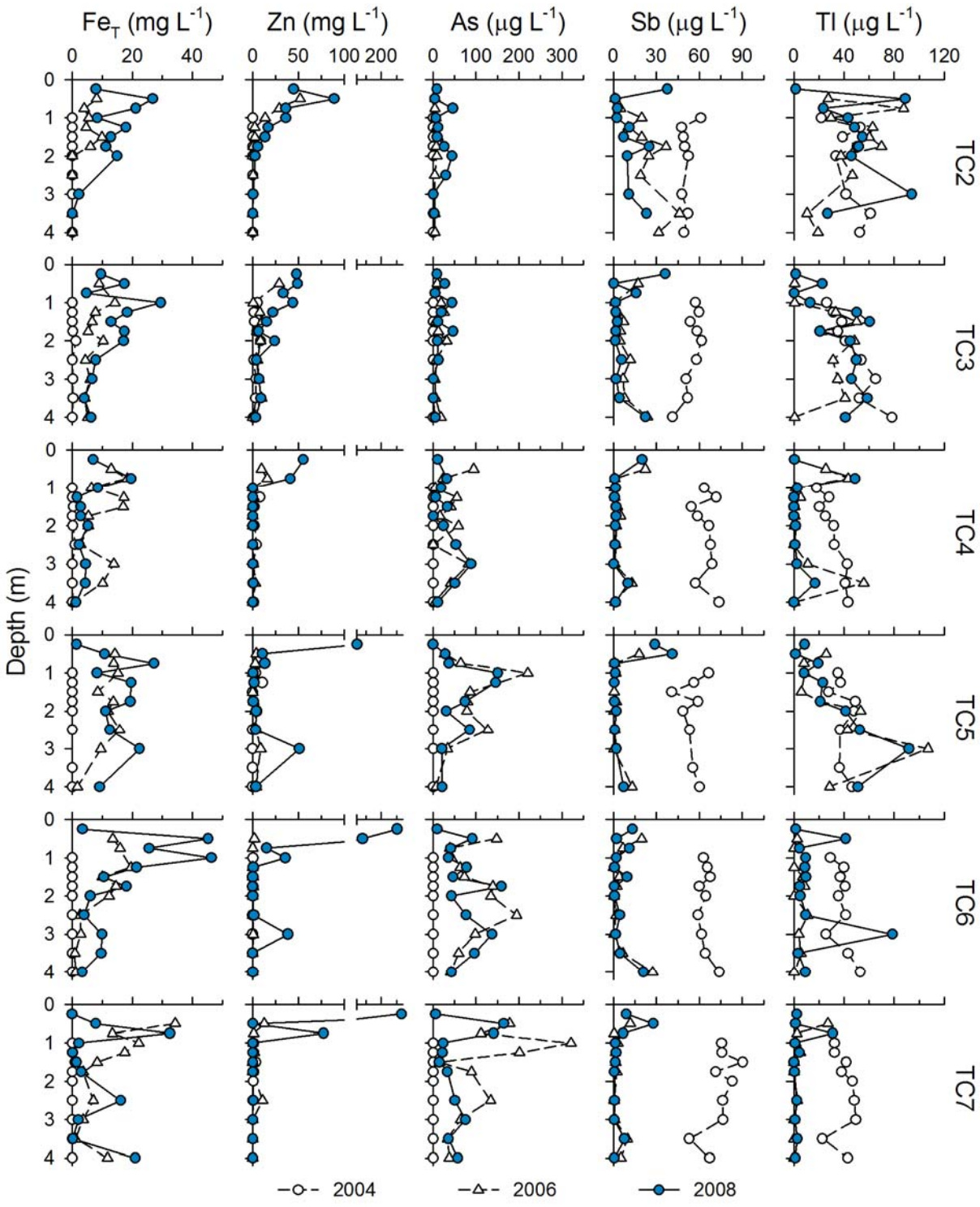

Figure 5.8 Depth profiles of total iron (Fe_T), zinc (Zn), arsenic (As), antimony (Sb), and thallium (Tl) for pore-water samples collected from tension-lysimeters in 2004, 2006, and 2008.

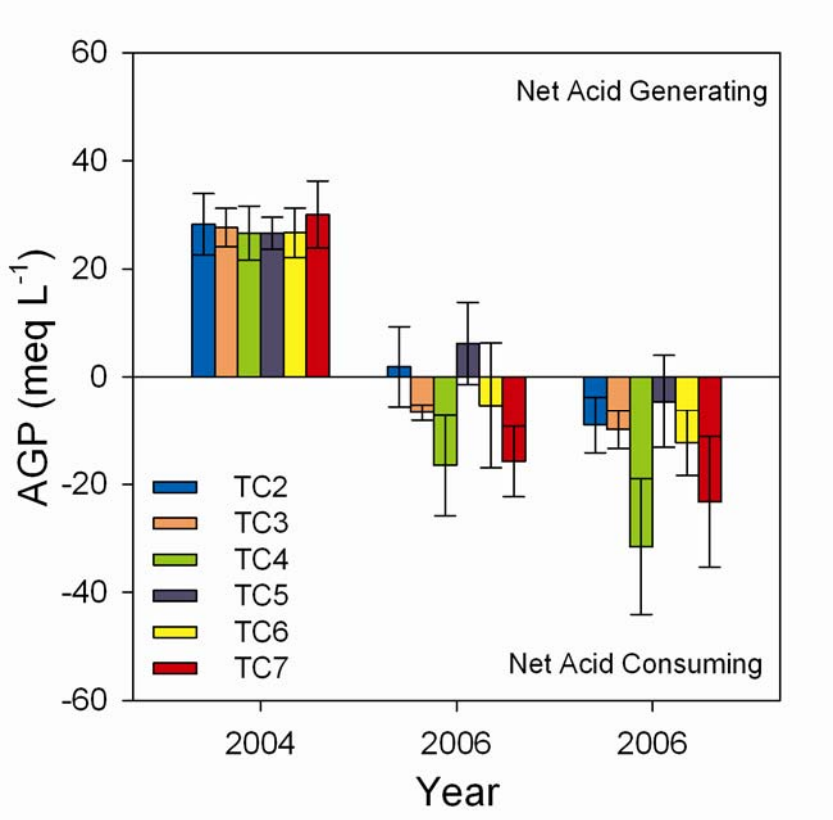

Figure 5.9 Mean acid-generating potentials (AGP) and standard deviations calculated for pore-water samples collected in 2004, 2006, and 2008.

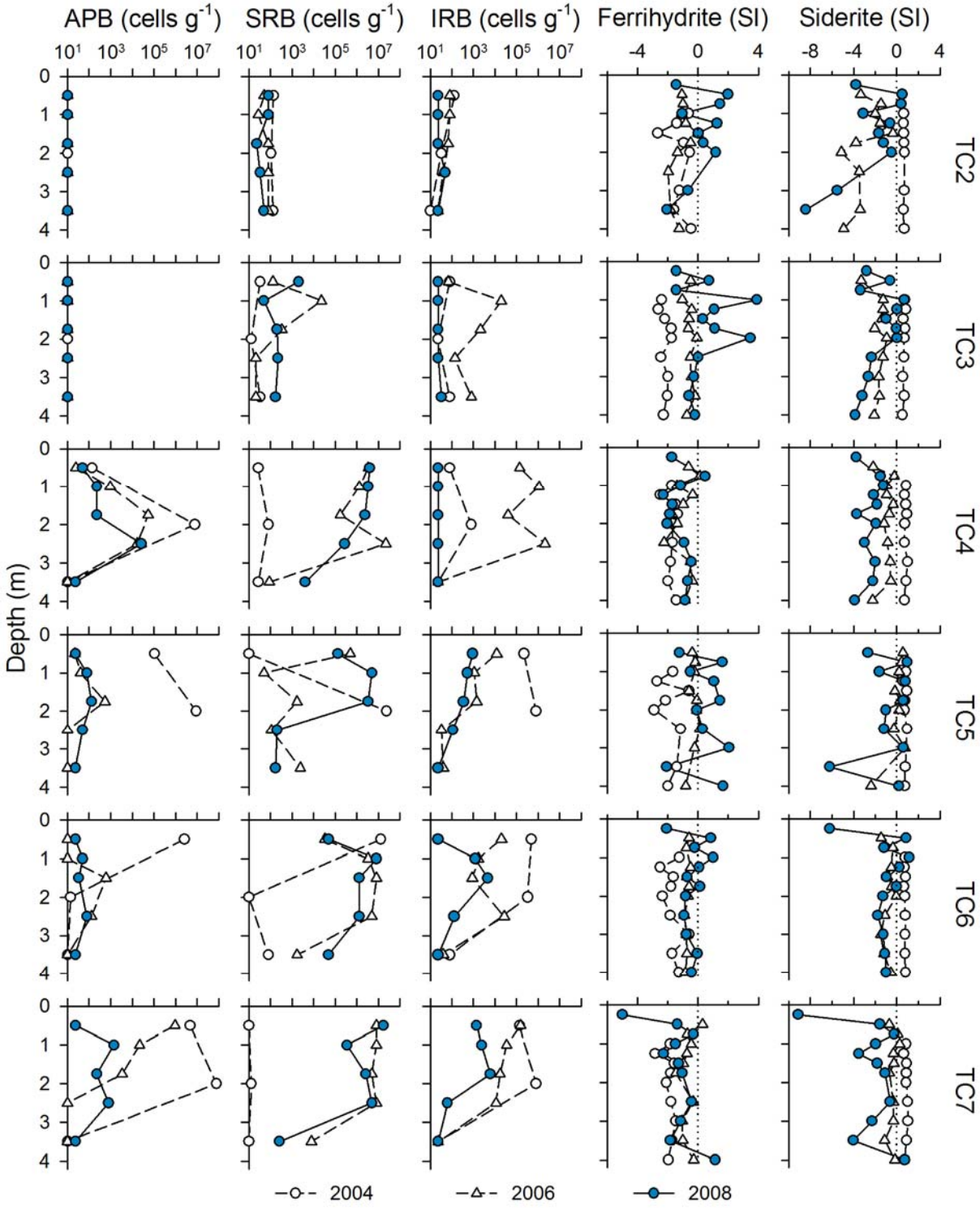

Figure 5.10 Depth profiles of MPN populations of APB, SRB, and IRB for core samples collected in 2004, 2006, and 2008. Depth profiles of saturation indices (SI) for ferrihydrite and siderite calculated for pore-water samples collected in 2004, 2006, and 2008.

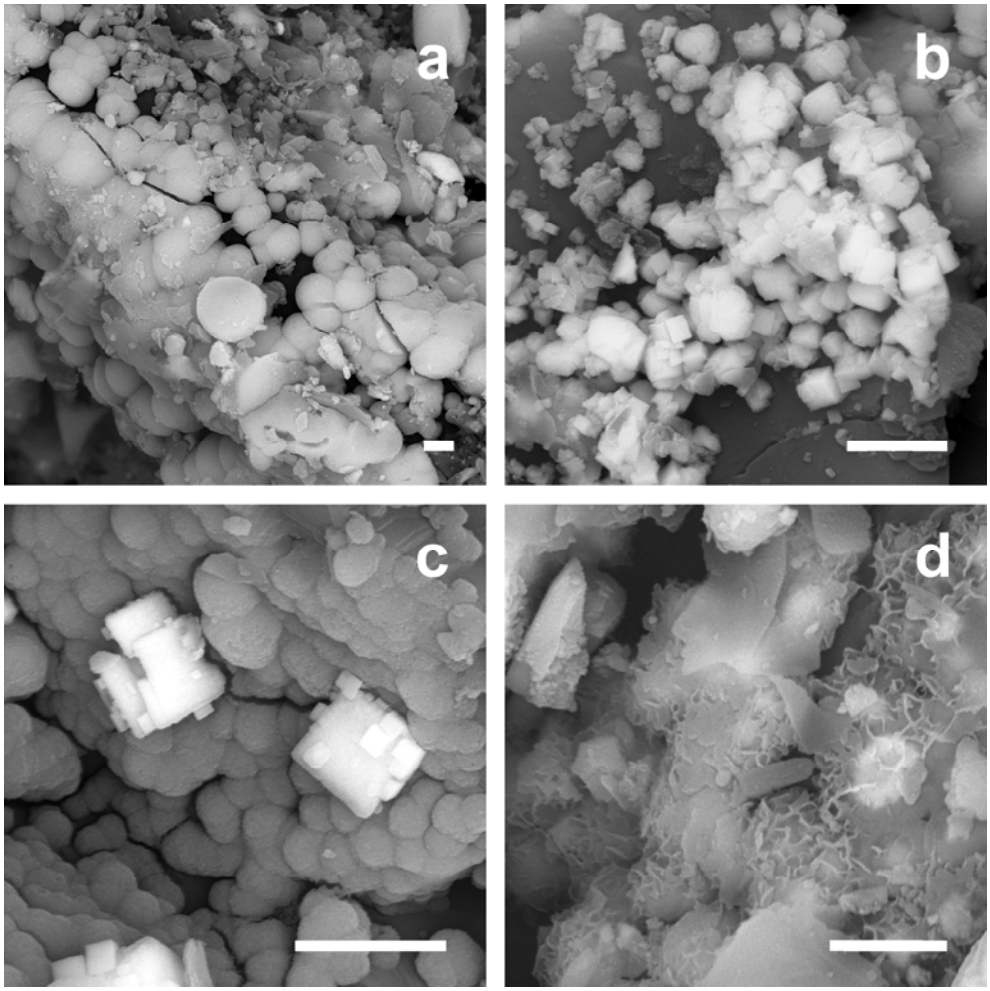

Figure 5.11 Backscatter electron (BSE) images of (a) spheroidal Zn-S phase, (b) aggregated Fe-S precipitates, (c) spheroidal Zn-S and cubic Fe-S phases, and (d) disordered Fe-S precipitate on surfaces of organic carbon particles and dolomite grains. Scale bars represent 1 μm.

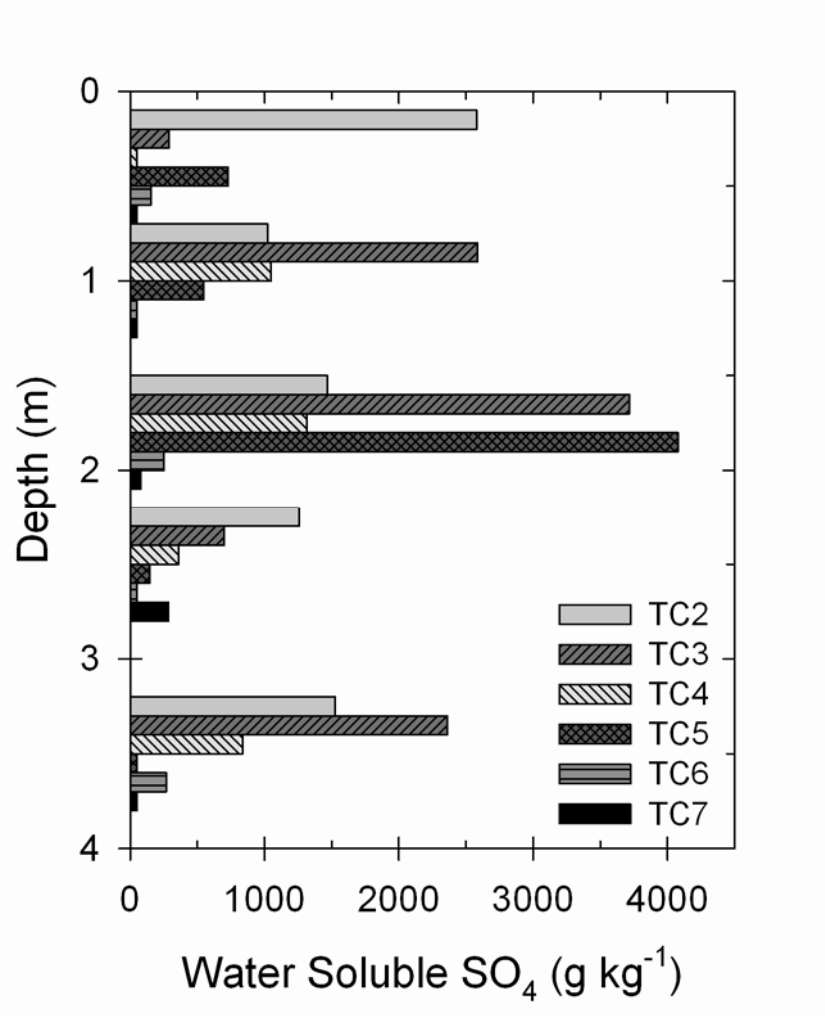

Figure 5.12 Water soluble SO_4 extracted from 2008 core samples using $Ar_{(g)}$-purged deionized water.

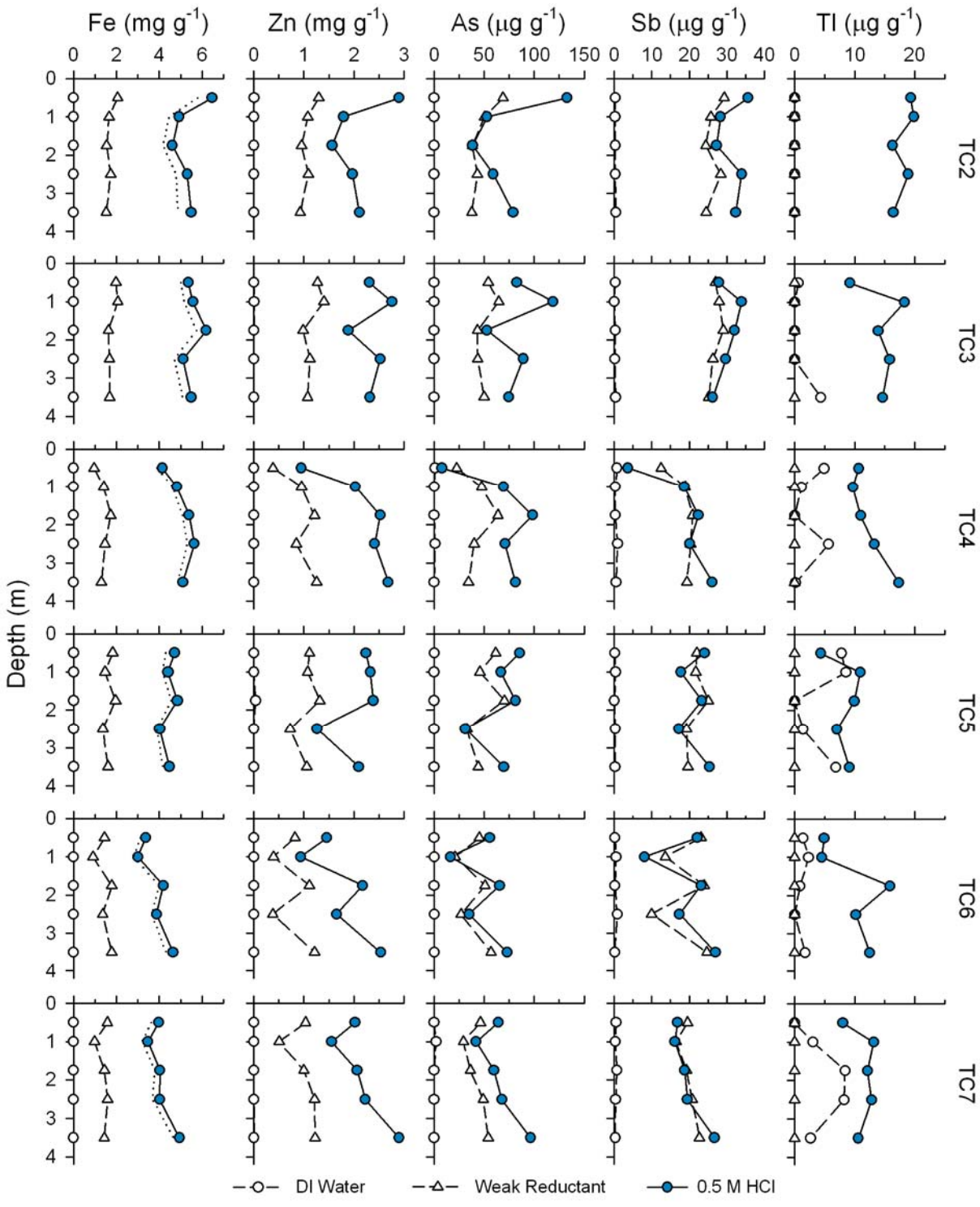

Figure 5.13 Solid-phase iron (Fe), zinc (Zn), arsenic (As), antimony (Sb), and thallium (Tl) concentrations for 2008 cores samples determined by selective extractions. Dotted line on Fe plots represents Fe(II) measured in 0.5 M HCl filtrate.

Chapter 6:

Conclusions

6.1 Summary of Findings

Sulfate reduction is effective for passive treatment of acid mine drainage (AMD) and tailings pore water characterized by near-neutral pH conditions. Laboratory batch experiments into AMD remediation (Chapter 2) demonstrated that dissimilatory sulfate reduction in the presence of organic carbon (Equation 1.6) and zero-valent iron (ZVI; Equation 1.9) can support extensive removal of SO_4, Fe and metals via metal-sulfide precipitation (Equation 1.7). These results build upon previous research by Tuttle et al. (1969), Dvorak et al. (1992), Christensen et al. (1996), Waybrant et al. (1998), Cocos et al. (2002) and Giber et al. (2004) which demonstrated the utility of organic carbon for passive AMD remediation. Gibert et al. (2003) reported that the addition of ZVI to organic carbon mixtures supported effective metal removal, however, treatment was primarily attributed to the precipitation of metal hydroxide phases with increasing pH. An evaluation of the effect of ZVI and organic carbon proportions on AMD treatment had not been evaluated prior to this thesis. The laboratory batch experiments discussed in Chapter 2 demonstrated that small proportions of ZVI could support enhanced sulfate reduction rates (SRRs) and effective AMD treatment. The precipitation of Fe-sulfides was observed in all mixtures that contained organic carbon.

This mechanism dominated metal removal under sulfate-reducing conditions. Production of carbonate alkalinity and hydroxide ions generated via DSR and anaerobic ZVI corrosion (Equation 1.8), respectively, neutralized acidity and promoted increases in pH to near-neutral conditions. Neutral conditions are favorable to growth of many species of sulfate-reducing bacteria (SRB) and thereby sustain sulfate reduction and treatment. The removal of Fe(II) under sulfate-reducing conditions, combined with alkalinity production, also supported a shift in the potential acidity of drainage from net acid generating to net neutralizing. These results generally agree with previous studies which utilized organic carbon, however, results presented in this thesis demonstrate that augmenting organic carbon mixtures with ZVI can enhance the remediation of AMD. Reactive mixtures amended with small proportions of ZVI ($\leq$ 10 dry wt. %) supported modest increases in sulfate-reduction rates (SRRs). The addition of ZVI enhanced AMD remediation; however, organic carbon was essential for SRB growth, sulfate reduction and therefore AMD treatment.

The application of sulfate reduction to the management of water quality at active mine sites was evaluated at the Greens Creek mine, Alaska, USA. This investigation began with an interdisciplinary study of mechanisms controlling pore-water chemistry in the sulfide- and carbonate-rich tailings deposit (Chapter 3). Research into mechanisms controlling water quality at mine sites chararcterized by near-neutral pH conditions is limited. Heikkinen et al. (2009) reported elevated concentrations of SO_4, Fe, Zn and Ni in neutral mine drainage (NMD) from a sulfidic tailings deposit in western Finland. Several sites exhibiting acidic pH conditions near the tailings surface and increasing pH with depth have been studied (Blowes and Jambor, 1990; Moncur et al., 2005; Gunsinger et al., 2006a). Pore-water concentrations of metals generally decrease with increasing pH, however,

elevated concentrations of metals (e.g. Fe, Zn and Ni) and trace elements (e.g. As, Sb and Tl) may persist under these conditions. Mineralogical assessment of tailings deposited at the Greens Creek mine revealed that the dominat phases were pyrite [FeS_2] and dolomite [$CaMg(CO_3)_2$]. The dissolution of these and other phases, including sphalerite [(Zn,Fe)S], galena [PbS], tetrahedrite [$(Cu,Fe,Zn,Ag)_{12}Sb_4S_{13}$] and calcite [$CaCO_3$], were the primary controls on pore-water chemistry within the tailings storage facility. Sulfide-mineral oxidation at the tailings surface (Equation 1.1) resulted in large increases in pore-water SO_4 concentrations. Near-neutral pH conditions were maintained via dolomite dissolution (Equation 1.3), however, this reaction resulted in a stoichiometric excess of SO_4 to Ca, and gypsum [$CaSO_4 \cdot 2H_2O$] was therefore an ineffective control on pore-water SO_4 concentrations. A number of metal(loid)s, including Fe, Zn, Sb, As, Mo, Se and Tl, remained mobile in tailings pore-water below the oxidation zone. Several of these elements exhibit elevated toxicity and the potential for transport and discharge may contribute to water quality degradation. The precipitation of secondary metal-sulfide minerals had the potential to limit migration of SO_4, Fe, Zn and several trace elements observed in pore-water at the Greens Creek mine. Most probable number (MPN) enumerations indicated that SRB were present within the tailings facility. However, similar to results reported by Benner et al. (2000) and Praharaj and Fortin (2008), DSR in tailings facilities is likely limited by the availability of organic carbon. Therefore, organic carobn amendment of tailings had the potential to induce sulfate reduction and improve the quality of tailings pore water and drainage.

Amendment of unoxidized tailings with organic carbon was evaluated as a technique for managing pore-water quality (Chapters 4 and 5). Hulshof et al. (2006) demonstrated that the addition of horizontal layers of organic carbon within tailings

impoundments could induce sulfate reduction and minimize the transport of sulfide-mineral oxidation products. Amendment of tailings with a small and disperse mass of organic carbon led to effective management of pore-water quality. The addition of 5 and 10 vol. % organic carbon supported growth of SRB within the vadose zone of the Greens Creek tailings deposit. Amendments containing varied mixtures of peat, spent brewing grain (SBG) and municipal biosolids (MB) were evaluated in a series of field trial cells. Zero-valent iron was not evaluated in this study due to limited availability at this remote study site. Organic carbon amendments containing peat + SBG and peat + SBG + MB supported SO_4 removal. Decreases in aqueous concentrations of SO_4 and S_2O_3 were accompanied by H_2S production, enrichment in ^{34}S-SO_4 and undersaturation of pore-water with respect to gypsum. The addition of organic carbon to tailings supported growth or iron reducing bacteria (IRB) and the reductive mobilization of Fe and As. Subsequent removal of mobilized Fe and As was observed under sulfate-reducing conditions. Removal of Fe and Zn was attributed to the precipitation of secondary sulfide phases, similar to those observed by Benner et al. (1999) and Labrenz et al. (2000). Decreases in aqueous Tl concentrations were attributed to sorption or (co)precipitation with sedondary Fe and Zn sulfide minerals. The precipitation of Tl_2S has been reported previously (Laforte et al., 2005), however, this phase was not observed during mineralogical investigation of reaction products. Removal of Sb likely resulted from sulfide precipitation, or reduction of Sb(V) to Sb(III) which is less mobile in the presence of Fe(III) (oxy)hydroxide phases (Chen et al., 2003; Leuz et al., 2006). Removal of Fe and S_2O_3 under sulfate-reducing conditions, combined with carbonate alkalinity production, altered the pore-water chemistry such that drainage will consume, rather than generate, acid under oxidized conditions. This novel technique for managing pore-water quality in mine tailings deposits

therefore has potential to improve drainage quality, reduce reliance on traditional active treatment systems, and therefore minimize costs associated with mine water treatment.

6.2 Scientific Contributions

Research presented in this thesis contributed information related to several aspects of mine drainage geochemistry and treatment. New scientific contributions resulting from this thesis include:

- Demonstrating that the performance of organic-carbon bearing permeable reactive barriers can be enhanced by adding a small proportion of zero-valent iron.
- Investigating mechanisms controlling pore-water quality in a dry-stacked tailings deposit which is characterized by neutral mine drainage.
- Illustrating the importance of methodological considerations when performing acid-base accounting analyses.
- Describing (bio)geochemical conditions which promote the mobility of metal(loid)s such as Sb, As, Mo, Se and Tl under neutral mine drainage conditions.
- Demonstrating that sulfate reduction may be achieved in the vadose zone of a mine tailings deposit.
- Illustrating that a decrease in mass transport of sulfide-mineral oxidation products can be achieved by amending mine tailings with organic carbon.
- Demonstrating that treatment of Sb and Tl in mine water can be achieved using passive treatment systems which support sufate reduction.

6.3 Recommendations

Amendment of tailings with organic carbon during deposition resulted in decreases in mass transport of sulfide-mineral oxidation products. This passive approach to water-quality management can improve drainage quality and reduce mass loading to receiving waters.

Locally available organic carbon sources used in laboratory and field experiments proved effective in supporting sulfate reduction. However, the initial reactivity of the organic carbon source(s) and the chosen amendment rate are important factors when considering this passive treatment technology. Organic carbon sources which contribute a large initial mass of labile organic carbon (e.g. municipal biosolids) should be used sparingly. Such materials support the rapid development of reducing conditions; however, reductive Fe mobilization occurred more rapidly in the presence of labile organic carbon. Enhanced reductive dissolution resulted in higher concentrations of Fe and As in tailings pore water. Due to the potential for reductive Fe mobilization, the application of this technology to the oxidized zone of tailings impoundments is not recommended. This challenge may be overcome by utilizing organic carbon materials which contribute labile organic carbon via in situ degradation of cellulose. Spent brewing grain was effective in this regard, and dissimilatory sulfate reduction was sustained over the four-year duration of the field trial experiments (Chapters 4 and 5). Furthermore, organic carbon amendment rates between 5 and 10 vol. % are recommended based on findings from this study. Higher amendment rates may be considered when using organic carobn sources which contain small initial masses of labile organic carbon. Refractory organic carbon sources, such as peat, were ineffective in supporting sulfate reduction. Therefore, mixtures of materials which have differing labile organic carbon contents are recommended for use in passive in situ systems for treatment of mine drainage. The addition of ZVI to these mixtures can enhance sulfate reduction rates; however, this material may not be readily available at remote sites. Combining alternative reclamation strategies, such as cover systems, with organic carbon amendment of tailings has potential to improve drainage quality and reduce demand on active treatment systems.

6.3 Future Research

Augmenting organic carbon mixtures with ZVI supported modest increases in sulfate-reduction rates and metal removal over a limited time period. However, ZVI is expected to provide long term benefits to treatment which may improve the cost-effectiveness of PRBs for the remediation of AMD. Declines in sulfate reduction rates are commonly observed as the initial pool of labile organic carbon becomes limited. Long-term rates of sulfate reduction therefore become limited by rates of carbon degradation. Production of H_2 via anaerobic ZVI corrosion has potential to sustain treatment by supporting sulfate reduction by hydrogenotrophic SRB, such as *Desulfobacter hydrogenophilus* of *Desulfovibrio desulficurans*. Long-term evaluation of AMD remediation using ZVI and organic carbon mixtures under dynamic flow conditions is required to provide more information of the benefits of ZVI. Such a study would ideally monitor SRB population dynamics to examine the effect of carbon limitation on SRB activity in the presence and absence of ZVI. This research would provide more information on the long-term benefits of ZVI addition to organic carbon PRBs used for AMD remediation.

Neutral mine drainage is beginning to receive more attention from the scientific community. Nonetheless, a limited body of research is available on mechanisms controlling drainage quality under near-neutral pH conditions. Characterization of additional tailings deposits exhibiting NMD would contribute to understanding of mechanisms controlling the transport and attenuation of trace elements, such as Sb, Mo, Tl and V, which have received relatively little attention in the literature. Information gathered from such research will assist decision makers and regulators in the prediction and management of mine-water quality.

Organic carbon amendment of unoxidized tailings has potential for cost-effective treatment or management of tailings pore-water and drainage quality. However, research described in this thesis, and by Hulshof et al. (2006), are the only field-scale evaluations of this migration control technique. Future research in this area should focus on evaluating carbon addition to tailings characterized by differing mineralogy, hydrology, and degrees of oxidation. Combining this technique with sulfide oxidation-control measures, such as cover systems, has the potential for enhanced management of pore-water and drainage quality. Additional field-scale evaluations which examine these issues are required to improve techniques for passive in situ management of tailings pore water and drainage.

References

Abraitis, P.K., Pattrick, R.A.D., Kelsall, G.H., Vaughan, D.J., 2004a. Acid leaching and dissolution of major sulphide ore materials: Processes and galvanic effects in complex systems. Mineral. Mag. 68, 343–351.

Abraitis, P.K., Pattrick, R.A.D., Vaughan, D.J., 2004b. Variations in the compositional, textural and electrical properties of natural pyrite: A review. Int. J. Miner. Process. 74, 41–59.

Al, T.A., Martin, C.J., Blowes, D.W., 2000. Carbonate-mineral/water interactions in sulfide-rich mine tailings. Geochim. Cosmochim. Acta 64, 3933–3948.

Alexander, M. 1965. Most-probable-number method for microbial populations. In: Black, C.A. (Ed.). Methods of Soil Analysis Part 2: Chemical and Microbiological Properties. 9: 1467–1471.

Allison, J.D., Brown, D.S., Novo-Gradac, K.L., 1990. MINTEQA2/PRODEFA2, A Geochemical Assessment Model for Environmental Systems, Version 3.0 User's Manual. Environmental Research Laboratory, Office of Research and Development, US EPA, Athens, GA.

Amirbahman, A., Schowenberger, R., Johnson, C., Sigg, L., 1998. Aqueous- and solid-phase biogeochemistry of a calcareous aquifer system downgradient from a municipal solid waste landfill, Winterhur, Switzerland. Environ. Sci. Technol. 32, 1933–1940.

Arakaki, T., Morse, J.W., 1993. Adsorption and coprecipitation of divalent metals with mackinawite (FeS). Appl. Geochem. 57, 3635–3640.

Baker, M.J., Blowes, D.W., Ptacek, C.J., 1998. Laboratory development of permeable reactive mixtures for the removal of phosphorus from onsite wastewater disposal systems. Environ. Sci. Technol. 32, 2308–2316.

Balistrieri, L.S., Murray, J.W., Paul, B., 1994. The geochemical cycling of trace elements in a biogenic meromictic lake. Geochim. Cosmochim. Acta 58, 3993-4008.

Ball, J.W., Nordstrom, D.K., 1991. User's manual for WATEQ4F with revised thermodynamic database and test cases for calculating speciation of major, trace and redox elements in natural waters. US Geol. Surv. Open-File Rep. 91–83.

Benner, S.G., Blowes, D.W. Ptacek, C.J., 1997. A full-scale porous reactive wall for prevention of acid mine drainage. Ground Water Monit. Remed. 17, 99–107.

Benner, S.G., Blowes, D.W., Gould, W.D., Herbert Jr., R.B., Ptacek, C.J., 1999. Geochemistry of a permeable reactive barrier for metals and acid mine drainage. Environ. Sci. Technol. 33, 2793–2799.

Benner, S.G., Gould, W.D., Blowes, D.W., 2000. Microbial populations associated with the generation and treatment of acid mine drainage. Chem. Geol. 169, 435–448.

Benner S.G., Blowes D.W., Ptacek C.J., Mayer K.U., 2002. Rates of sulfate reduction and metal sulfide precipitation in a permeable reactive barrier. Appl. Geochem. 17, 301–320.

Blowes, D.W., Jambor, J.L., 1990. The pore-water geochemistry and the mineralogy of the vadose zone of sulfide tailings: Waite Amulet, Quebec, Canada. Appl. Geochem. 5, 327–346.

Blowes, D.W., Ptacek, C.J., Jambor, J.L., 1997. In-situ remediation of chromate contaminated groundwater using permeable reactive walls. Environ. Sci. Technol. 31, 3348–3357.

Blowes, D.W., Jambor, J.L., Hanton-Fong, C.J., Lortie, L., Gould, W.D., 1998. Geochemical mineralogical and microbiological characterization of a sulphide-bearing carbonate-rich gold-mine tailings impoundment, Joutel, Quebec. Appl. Geochem. 13, 687–705.

Blowes, D.W., Ptacek, C.J., Benner, S.G., McRae, C.W.T., Bennett, T.A., Puls, R.W., 2000. Treatment of inorganic contaminants using permeable reactive barriers. J. Contam. Hydrol. 45, 123–137.

Blowes, D.W. 2002. Tracking hexavalent Cr in groundwater. Science 295, 2024–2025.

Blowes, D.W., Ptacek, C.J., Jambor, J.L., Weisener, C.G., 2003. The geochemistry of acid mine drainage. In: Sherwood-Lollar, B. (Ed.), Environmental Geochemistry. In: Holland, H.D., Turekian, K.K. (Eds.), Treatise on Geochemistry, vol. 9. Elsevier-Pergamon, Oxford, pp. 149–204.

Boudreau, B.P., Westrich J.T., 1984. The dependence of bacterial sulfate reduction on sulfate concentration in marine sediments. Geochim. Cosmochim. Acta 48, 2503–2516.

Brock, T.P., Smith, D.W., Madigan, M.T., 1984. Biology of Microorganisms. Prentice Hall, New York.

Bunker, G., Stern, E.A., 1984. Experimental study of multiple scattering in X-ray adsorption near-edge structure. Phys. Rev. Lett. 52, 1990–1993.

Chang, I.S., Shin, P.K., Him, B.K., 2000. Biological treatment of acid mine drainage under sulphate-reducing conditions with solid waste materials as subtrate. Water Res. 34, 1269–1277.

Chapelle, F.H., 1993. Groundwater Microbiology and Geochemistry. John Wiley and Sons, West Sussex.

Cheam, V., 2000. Comment on "Thallium speciation in the great lakes". Environ. Sci. Technol. 34, 2367–2370.

Chen, Y.-W., Deng, T.-L., Filella, M., Belzile, N. 2003. Distribution and early diagenesis of antimony species in sediments and porewaters of freshwater lakes. Environ. Sci. Technol. 37, 1163–1168.

Cochran, W.G., 1950. Estimation of bacterial densities by means of the most probable number. Biometrics 6, 105–116.

Christensen, B., Laake, M., Lien, T., 1996. Treatment of acid mine water by sulphate-reducing bacteria; Results from a bench scale experiment. Water Res. 30, 1617–1624.

Cocos, I.A., Zagury, G.J., Clement, B., Samson, R., 2002. Multiple factor design for reactive mixture selection for use in reactive walls in mine drainage treatment. Water Res. 36, 167–177.

Costa, M.C., Santos, E.S., Barros, R.J., Pires, C., Martins, M., 2009. Wine wastes as carbon source for biological treatment of acid mine drainage. Chemosphere 75, 831–836.

Dixit, S., Herring, J.G., 2003. Comparison of arsenic(V) and arsenic(III) sorption onto iron oxide minerals: implications for arsenic mobility. Environ. Sci. Technol. 37, 4182–4189.

Dvorak, D.H., Hedin, R.S., Edenborn, H.M., McIntire, P.E., 1992. Treatment of metal-contaminated water using bacterial sulfate reduction: Results from pilot-scale reactors. Biotechnol. Bioeng. 40, 609–616.

Ehrlich, H.L., 2002. Geomicrobiology. Fourth Ed. Marcel Dekker, New York.

Farquhar, M.L., Charnock, J.M., Livens, F.R., Vaughan, D.J. 2002. Mechanisms of arsenic uptake from aqueous solution by interaction with goethite, lepidocrocite, mackinawite, and pyrite: An X-ray absorption spectroscopy study. Environ. Sci. Technol. 36, 1757–1762.

Fetter, C.W., 2000. Applied Hydrogeology. Prentice Hall, New York.

Filella, M., Belzile, N., Chen, Y-W., 2002. Antimony in the environment: A review focused on natural waters: II. Relevant solution chemistry. Earth-Sci. Rev. 59, 265–285.

Fleet, M.E., 2005. XANES spectroscopy of sulfur in earth materials. Can. Mineral. 43, 1811–1838.

Freeze, A.R., Cherry, J.A., 1979. Groundwater. Prentice Hall, New York.

Friedman, G.M., Sanders, J.E., 1978. Principles of Sedimentology. Freeman, New York.

Gallegos, T.J., Sung, P.H., Hayes, K.F., 2007. Spectroscopic investigation of the uptake of arsenite from solution by synthetic mackinawite. Environ. Sci. Technol. 41, 7781–7786.

Geets, J., Borremans, B., Vangronsveld, J., Diels, L., van der Lelie, D., 2005. Molecular monitoring of SRB community structure and dynamics in batch experiments to examine the applicability of in situ precipitation of heavy metals for groundwater remediation. J. Soils Sed. 5, 149–163.

Gerzabek, M.H., Haberhauer, G., Kirchmann, H., 2001. Soil organic matter pools and carbon-13 natural abundances in particle-size fractions of a long-term agricultural field experiment receiving organic amendments. Soil Sci. Soc. Am. J., 65, 352–358.

Gibbs, M.M., 1979. A simple method for the rapid determination of iron in natural waters. Water Res. 13, 295–297.

Gibert, O., de Pablo, J., Cortina, J.L., Ayora, C., 2003. Evaluation of municipal compost/limestone/iron mixtures as filling material for permeable reactive barriers for in-situ acid mine drainage treatment. J. Chem. Technol. Biotechnol. 78, 489–496.

Gibert, O., de Pablo, J., Cortina, J.L., Ayora, C., 2004. Chemical characterization of natural organic substrates for biological mitigation of acid mine drainage. Water Res. 38, 4186–4196.

Gibert, O., de Pablo, J., Cortina, J.L., Ayora, C., 2005. Municipal compost-based mixture for acid mine drainage bioremediation: Metal retention mechanisms. Appl. Geochem. 20, 1648–1657.

Giesemann, A., Jager, H.J., Norman, A.-L., Krouse, H.R., Brand, W.A. 1994. On-line sulfur-isotope determination using an elemental analyzer coupled to a mass spectrometer. Anal. Chem. 66, 2816–2819.

Goldhaber, M.B., 1983. Experimental study of metastable sulfur oxyanion formation during pyrite oxidation at pH 6-9 and 30°C. Am. J. Sci. 283, 193–217.

Gould, W.D., Stichbury, M., Francis, M., Lortie, L., Blowes, D.W., 2003. An MPN method for the enumeration of iron-reducing bacteria. In:Graeme, S., Beckett, P., Conroy, H. (Eds.),

Proceedings of Sudbury ’03, Mining and the Environment III. Laurentian University, Sudbury, pp. 153–157.

Gould, W.D., Kapoor, A. 2003. The microbiology of acid mine drainage. In: Environmental Aspects of Mine Wastes, Short Course Series Vol. 31, Jambor, J.L., Blowes, D.W., and Ritchie, A.I.M. (Eds.), Mineralogical Association of Canada, Ottawa, 2003. pp. 203–226.

Gu, B., Liang, L., Dickey, M.J., Yin, X., Dai, S., 1998. Reductive precipitation of uranium VI by zero-valent iron. Environ. Sci. Technol. 32, 3366–3373.

Gu, B., Phelps, T.J., Liang, L., Dickey, M.J., Roh, Y., Kinsall, B.L., Palumbo, A.V., Jacobs, G.K., 1999. Biochemical dynamics in zero-valent iron columns: Implications for permeable reactive barriers. Environ. Sci. Technol. 33, 2170–2177.

Gunsinger, M.R., Ptacek, C.J., Blowes, D.W., Jambor, J.L., 2006a. Evaluation of long-term sulfide oxidation processes within pyrrhotite-rich tailings, Lynn Lake, Manitoba. J. Contam. Hydrol. 83, 149–170.

Gunsinger, M.R., Ptacek, C.J., Blowes, D.W., Jambor, J.L., Moncur, M.C., 2006b. Mechanisms controlling acid neutralization and metal mobility within a Ni-rich tailings impoundment. Appl. Geochem. 21, 1301–1321.

Guo, Q., 2008. Some aspects of Arsenic and Antimony Geochemistry in High Temperature Granitic Melt – Aqueous Fluid System and in Low Temperature Permeable Reactive Barrier – Groundwater System, Ph.D. Thesis, University of Waterloo, Waterloo, Ontario, Canada.

Haas, C.N., 1996. Moment analysis of tracer experiments. J. Environ. Eng. 122, 1121–1123.

Habicht, K.S., Canfield, D.E., Rethmeier, 1998. J. Sulfur isotope fractionation during bacterial reduction and disproportionation of thiosulfate and sulfite. Geochim. Cosmochim. Acta 62, 2585–2595.

Hao, F.P., Silvester, E., Senior, G.D., 2000. Spectroscopic characterization of ethyl xanthate oxidation products and analysis by ion interaction chromatography. Anal. Chem. 72, 4836–4845.

Harder, W., Dijkhuizen, L., 1983. Physiological responses to nutrient limitation. Ann. Rev. Microbiol. 37. 1–23.

Hedin, R.S., Hammack, R.W., Hyman D.M., 1989. Potential importance of sulfate reduction processes in wetlands constructed to treat mine drainage. In: Hammer, D.A. (Ed.), Constructed Wetlands for Wastewater Treatment, Lewis Publishers, Chelsea, MI, pp. 508–514.

Heikkinen, P.M., Räisänen, M.L., Johnson, R.H., 2009. Geochemical characterisation of seepage and drainage water quality from two sulphide mine tailings impoundments: Acid mine drainage versus neutral mine drainage. Mine Water Environ. 28, 30–49.

Hemsi, P.S., Shackelford, C.D., Figueroa, L.A., 2005. Modeling the influence of decomposing organic solids on sulfate reduction rates for iron precipitation. Environ. Sci. Technol. 39, 3215–3225.

Herbert, R.B., Jr., Benner, S.G., Blowes, D.W., 2000. Solid phase iron-sulfur geochemistry of a reactive barrier for treatment of mine drainage. Appl. Geochem. 15, 1331–1343.

Herbert, R.B., Jr., 2003. Zinc immobilization by zerovalent Fe: surface chemistry and mineralogy of reaction products. Mineral. Mag. 67, 1285–1298.

Heron, G., Crouzet, C., Bourg, A.C., Christensen, T.H., 1994. Speciation of Fe(II) and Fe(III) in contaminated aquifer sediments using chemical extraction techniques. Environ. Sci.Technol. 28, 1698–1705.

Holmström, H.; Öhlander, B., 1999. Oxygen penetration and subsequent reactions in flooded sulphidic mine tailings: A study at Stekenjokk, northern Sweden. Appl. Geochem. 14, 747–759.

Howarth, R.W., 1979. Pyrite: Its rapid formation in a salt marsh and its importance in ecosystem metabolism. Science 203, 49–51.

Huerta-Diaz, M.A., Tessier, A., Carignan, R., 1998. Geochemistry of trace metals associated with reduced sulfur in freshwater sediments. Appl. Geochem. 13, 213–233.

Hulshof, A.H.M., Blowes, D.W., Ptacek, C.J., Gould, W.D., 2003. Microbial and nutrient investigations into the use of in situ layers for treatment of tailings effluent. Environ. Sci. Technol. 37, 5027–5033.

Hulshof, A.H.M., Blowes, D.W., Gould, W.D., 2006. Evaluation of in situ layers for treatment of acid mine drainage: A field comparison. Water Res. 40, 1816–1826.

Jambor, J.L., Blowes, D.W., 1998. Theory and applications of mineralogy in environmental studies of sulfide-bearing mine wastes. In: Modern Approaches to Ore and Environmental Mineralogy, Short Course Series Vol. 27, Cabri, L.J., and Vaughan, D.J. (Eds.), Mineralogical Association of Canada, Ottawa, 1998. pp. 367–401.

Jambor, J.L., 2003. Mine-waste mineralogy and mineralogical perspectives of acid-base accounting. In: Jambor, J.L., Blowes, D.W., Ritchie, A.I.M. (Eds.), Environmental Aspects of Mine Wastes, Short Course Series, vol. 31. Mineral. Assoc. Can. Ottawa, ON, pp. 117–145.

Jambor, J.L., Raudseff, M., Mountjoy, K., 2005. Mineralogy of permeable reactive barriers for the attenuation of subsurface contaminants. Can. Mineral. 43, 2117-2140.

Jarvis, A.P., Moustafa, M., Orme, P.H.A., Younger, P.L., 2006. Effective remediation of grossly polluted acidic, and metal-rich, spoil heap drainage using a novel, low-cost, permeable reactive barrier in Northumberland, UK. Environ. Pollut. 143, 261–268.

Jeong, H.Y., Klaue, B., Blum, J.D., Hayes, K.F., 2007. Sorption of mercuric ion by synthetic nanocrystalline mackinawite (FeS). Environ. Sci. Technol. 41, 7699–7705.

Johnson, D.B., Hallberg K.B., 2005. Acid mine drainage remediation options: A review. Sci. Tot. Environ. 338, 3–14.

Jørgensen, B.B. 1990. A thiosulfate shunt in the sulfur cycle of marine sediments. Science, 249, 152–154.

Jørgensen, B.B., Bak, F. 1991. Pathways and microbiology of thiosulfate transformations and sulfate reduction in a marine sediment (Kattegat, Denmark). Appl. Environ. Microbiol. 57, 847–856.

Jurjovec, J., Ptacek, C.J., Blowes, D.W., 2002. Acid neutralization mechanisms and metal release in mine tailings: A laboratory column experiment. Geochim. Cosmochim. Acta 66, 1511–1523.

Karri, S., Sierra-Alvarez, R., Field, J.A., 2005. Zero-valent iron as an electron donor for methanogenesis and sulfate reduction in anaerobic sludge. J. Biotechnol. Bioeng. 92, 810–819.

Kocar, B.D., Fendorf, S. 2009 Thermodynamic constraints on reductive reactions influencing the biogeochemistry of arsenic in soils and sediments. Environ. Sci. Technol. 43, 4871–4877.

Koren, D.W., Gould, W.D., Bédard, P., 2000. Biological removal of ammonia and nitrate from simulated mine and mill effluents. Hydromet. 56, 127–144.

Labrenz, M., Druschel, G.K., Thomsen-Ebert, T., Gilbert, B., Welch, S.A., Kemner, K.M., Logan, G.A., Summons, R.E., De Stasio, G., Bond, P.L., Lai, B., Kelly, S.D., Banfield, J.F. 2000. Formation of sphalerite (ZnS) deposits in natural biofilms of sulfate-reducing bacteria. Science 1744–1747.

Laforte, L., Tessier, A., Gobiel, C., Carignan, R. 2005. Thallium diagenesis in lacustrine sediments. Geochim. Cosmochim. Acta 69, 5295–5306.

Leuz, A.-K., Mönch, H., Johnson, C.A. 2006. Sorption of Sb(III) and Sb(V) to goethite: Influence of Sb(III) on oxidation and mobilization. Environ. Sci. Technol. 40, 7277–7282.

Li, D., Bancroft, G.M., Kasrai, M, Fleet, M.E., Feng, X., Tan, K., 1995. S K- and L-edge X-ray adsorption spectroscopy of metal sulfides and sulfates: Applications in mineralogy and geochemistry. Can. Mineral. 33, 949–960.

Light, T.S., 1972. Standard solution for redox potential measurements. Anal. Chem. 44, 1038–1039.

Lin, T.-S., Nriagu, J., 1999. Thallium speciation in the great lakes. Environ. Sci. Technol. 33, 3394–3397.

Lindsay, M.B.J., Ptacek, C.J., Blowes, D.W., Gould, W.D., 2008. Zero-valent iron and organic carbon mixtures for remediation of acid mine drainage: Batch experiments. Appl. Geochem. 23, 2214–2225.

Lindsay, M.B.J., Blowes, D.W., Condon, P.D., Ptacek, C.J., 2009a. Managing pore-water quality in mine tailings by inducing microbial sulfate reduction. Environ. Sci. Technol. 43, 7086–7091.

Lindsay, M.B.J., Condon, P.D., Jambor, J.L., Lear, K.G., Blowes, D.W., Ptacek, C.J., 2009b. Mineralogical, geochemical, and microbial investigation of a sulfide-rich tailings deposit characterized by neutral drainage. Appl. Geochem. 24, 2212–2221.

Lindsay, S.S., Baedecker, M.J., 1988. Determination of aqueous sulfide in contaminated and natural water using the methylene blue method. In: Collins, A.G., Johnson, A.I. (Eds.), Ground-Water Contamination: Field Methods, ASTM, Philadelphia, pp. 349-357.

Liu, R., Wolfe, A.L., Dzombak, D.A., Stewart, B.W., Capo, R.C. 2008. Comparison of dissolution under oxic acid drainage conditions for eight sedimentary and hydrothermal pyrite samples. Environ. Geol. 56, 171–182.

Logan, M.V., Reardon, K.F., Figueroa, L.A., McLain, J.E.T., Ahmann, D.M., 2005. Microbial community activities during establishment, performance, and decline of bench-scale passive treatment systems for mine drainage. Water Res. 39, 4537–4551.

Londry, K.L., Des Marais, 2003. D.J. Stable carbon isotope fractionation by sulfate-reducing bacteria. Appl. Environ. Microbiol. 69, 2942–2949.

Lotens, J.P., Wesker, E., 1987. The behaviour of sulphur in the oxidative leaching of sulphidic minerals. Hydrometallurgy, 18: 39–54.

Lovley, D.R., Phillips, E.J.P., 1998. Novel mode of microbial energy metabolism: organic carbon oxidation coupled to dissimilatory reduction of iron or manganese. Appl. Environ. Microbiol. 54, 1472–1480.

Ludwig, R.D., McGregor, R.G., Blowes, D.W., Benner, S.G., Mountjoy, K., 2002. A permeable reactive barrier for treatment of heavy metals. Ground Water 40, 59–66.

Luther III, G.W. 1987. Pyrite oxidation and reduction: Molecular orbital theory considerations. Geochim. Cosmochi. Acta, 51: 3193–3199.

Machemer, S.D., Wildeman, T.R., 1992. Adsorption compared with sulfide precipitation as metal removal processes from acid mine drainage in a constructed wetland. J. Contam. Hydrol. 9, 115–131.

MacPherson, R., Miller, J.D.A., 1963. Nutritional studies on Desulfovibrio desulfuricans using defined media. J. Gen. Microbiol. 31, 365–373.

Masscheleyn, P.H., Delaune, R.D., Patrick Jr., W.H. 1991. Heavy metals in the environment: Arsenic and selenium chemistry as affected by sediment redox potential and pH. J. Environ. Qual. 20, 522–527.

Moncur, M.C., Ptacek, C.J., Blowes, D.W., Jambor, J.L., 2005. Release, transport and attenuation of metals from an old tailings impoundment. Appl. Geochem. 10, 639–659.

Moncur, M.C., Ptacek, C.J., Blowes, D.W., Jambor, J.L. 2006. Spatial variations in water composition at a northern Canadian lake impacted by acid mine drainage. Appl. Geochem. 21, 1799–1817.

Moses, C.O., Nordstrom, D.K., Herman, J.S., Mills, A.L. 1987. Aqueous pyrite oxidation by dissolved oxygen and by dissolved ferric iron. Geochim. Cosmochi. Acta, 51: 1561–1571.

Moses, C.O., Herman, J.S., 1991. Pyrite oxidation at circumneutral pH. Geochim. Cosmochim. Acta, 55: 471–482.

Mullet, M., Boursiquot, S., Abdelmoula, M., Genin, J-M., Ehrhardt, J-J., 2002. Surface chemistry and structural properties of mackinawite prepared by reaction of sulfide ions with metallic iron. Geochem. Cosmochim. Acta. 66, 829–836.

Neretin, L.N., Bottcher, M.E., Jorgensen, B.B., Volkov, I.I., Luschen, H., Hilgenfeldt, K., 2004. Pyritization processes and greigite formation in the advancing sulfidization front in the Upper Pleistocene sediments of the Black Sea. Geochim. Cosmochim. Acta. 68, 2081–2093.

Nevin, K.P., Lovley, D.R., 2002. Mechanisms for Fe(III) oxide reduction in sedimentary environments. Geomicrobiol. J. 19, 141–159.

Nordstrom, D.K., 1977. Thermochemical redox equilibria in ZoBell's solution. Geochim. Cosmochim. Acta 41, 1835–1841.

Nordstrom, D.K., and Southam 1997. Geomicrobiology of sulfide mineral oxidation. Rev. Mineral., 35: 361–390.

Nordstrom, D.K., Alpers, C.N., 1999. Geochemistry of acid mine water. In: Plumlee, G.S., Logsdon, M.J. (Eds.), The Environmental Geochemistry of Mineral Deposits. Part A: Processes, Techniques, and Health Issues, Rev. Econ. Geol., 6A, pp. 133–160.

Nordstrom, D.K., Alpers, C.N., Ptacek, C.J., Blowes, D.W. 2000. Negative pH and extremely acidic mine waters from Iron Mountain, California. Environ. Sci. Technol. 34, 254–258.

Nordstrom, D.K., 2003. Effects of microbiological and geochemical interactions in mine drainage. In: Environmental Aspects of Mine Wastes, Short Course Series Vol. 31, Jambor, J.L., Blowes, D.W., and Ritchie, A.I.M. (Eds.), Mineralogical Association of Canada, Ottawa, 2003. pp. 227–238.

Pallud, C., Van Cappellen, P. 2006. Kinetics of microbial sulfate reduction in estuarine sediments. Geochim. Cosmochim. Acta 70, 1148–1162.

Papelis C., Hayes K. F., Leckie J. O., 1988. HYDRAQL: A Program for the Computation of Chemical Equilibrium Composition of Aqueous Batch Systems Including Surface-Complexation Modeling of Ion Adsorption at the Oxide/Solution Interface. Technical Report 306, Stanford University, Stanford, pp. 1–130.

Posfai, M., Buseck, P.R., Bazylinski, D.A., Frankel, R.B., 1998. Reaction sequence of iron sulfide minerals in bacteria and their use as biomarkers. Science. 280, 880–883.

Postgate, J.R., 1984. The Sulphate-Reducing Bacteria. Second Ed. Cambridge University Press, Cambridge.

Praharaj, T., Fortin, D., 2008. Seasonal variations of microbial sulfate and iron reduction in alkaline Pb-Zn mine tailings (Ontario, Canada). Appl. Geochem. 23, 3728–3740.

Pruden, A., Messner, N., Pereyra, L., Hanson, R.E., Hiibel, S.R., Reardon, K.F., 2007. The effect of inoculum on the performance of sulfate-reducing columns treating heavy metal contaminated water. Water Res. 41, 904–914.

Ptacek, C.J., 1992. Experimental determination of siderite solubility in high ionic-strength solutions. PhD Thesis, University of Waterloo, Waterloo, Ontario.

Pugh, C.E., Hossner, L.R., Dixon, J.B. 1984. Oxidation rate of iron sulfides as affected by surface area, morphology, oxygen concentration, and autotrophic bacteria. Soil. Sci. 137, 309–314.

Ravel, B., Newville, M., 2005. ATHENA, ARTEMIS, HEPHAESTUS: data analysis for X-ray adsorption spectroscopy using IFEFFIT. J. Synchrotron Rad. 12, 537–541.

Reynolds, W.D., Elrick, D.W., 1991. Determination of hydraulic conductivity using a tension infiltrometer. Soil. Sci. Soc. J. Am. 55, 633–639.

Ribet, I., Ptacek, C.J., Blowes, D.W., Jambor, J.L., 1995. The potential for metal release by reductive dissolution of weathered mine tailings. J. Contam. Hydrol. 17, 239–273.

Rickard, D., Luther III, G.W., 2007. Chemistry of iron sulfides. Chem. Rev. 107, 514–562.

Rickard, D., Morse, J.W., 2005. Acid volatile sulfide (AVS). Marine Chem. 97, 141–197.

Schippers, A., Sand, W. 1999. Bacterial leaching of sulfides proceeds by two indirect methods via thiosulfate or via polysulfides and sulfur. Appl. Environ. Microbiol., 65: 319–321.

Schnurer, J., Rosswall, T., 1982. Fluorescein diacetate hydrolysis as a measure of total microbial activity in soil and litter. Appl. Environ. Microbiol. 43, 1256–1261.

Shepard, F.P., 1954. Nomenclature based on sand-silt-clay ratios. J. Sedimentary Petrology 24, 151–158.

Shokes, T.E., Moller, G., 1999. Removal of dissolved heavy metals from acid rock drainage using iron metal. Environ. Sci. Technol. 33, 282–287.

Sidenko, N.V., Sherriff, B.L., 2005. The attenuation of Ni, Zn and Cu, by secondary Fe phases of different crystallinity from surface and ground water of two sulfide mine tailings in Manitoba, Canada. Appl. Geochem. 20, 1180–1194.

St-Jean, G. 2003. Automated quantitative and isotopic (^{13}C) analysis of dissolved inorganic carbon and dissolved organic carbon in continuous-flow using a total organic carbon analyser. Rapid Commun. Mass Spectrom. 17, 419–428.

Standard Methods for the Examination of Water and Wastewater (SMEWW), 2005. American Public Health Association, Washington, D.C.

Starr, R.C., Ingleton, R.A. 1992. A new method for collecting core samples without a drill rig. Ground Water Monit. Remed. 41, 91–95.

Strebel, O., Böttcher, J., Fritz, P. 1990. Use of isotope fractionation of sulfate-sulfur and sulfate-oxygen to assess bacterial desulfurication in a sandy aquifer. J. Hydrol. 121, 155–172.

Stumm, W., Morgan, J.J., 1996. Aquatic Chemistry: Chemical Equilibria and Rates in Natural Waters. John Wiley & Sons, New York.

Suzuki, I. 1999. Oxidation of inorganic sulfur compounds: Chemical and enzymatic reactions. Can. J. Microbiol. 45; 97–105.

Taylor, C. D., Newkirk, S.R., Hall, T.E., Lear, K.G., Premo, W.R., Leventhal, J.S., Meier, A.L., Johnson, C.A., Harris. A.G., 1999. The Greens Creek deposit, southeastern Alaska: a

VMS-SEDEX hybrid. In: Mineral Deposits, Processes to Processing, Stanley, C.J., et al. (Eds). Balkema, Rotterdam. pp. 597–600.

Tuttle, J.H., Dugan, P.R., Randles, C.I., 1969. Microbial sulfate reduction and its potential utility as an acid mine water abatement procedure. Appl. Microbiol. 17, 297–302.

Van Damme, P.A., Hamel, C., Ayala, A., Bervoets, L. 2008. Macroinvertebrate community response to acid mine drainage in rivers of the High Andes (Bolivia). Environ. Pollut. 156, 1061–1068.

Vaněk, A., Chrastný, V., Mihaljevič, M., Drahota, P., Grygar, T., Komárek, M., 2009. Lithogenic thallium behaviour in soils with different land use. J. Geochem. Explor. 102, 7–12.

Vaughan, D.J., Rosso, K.M., 2006. Chemical bonding in sulfide minerals. Rev. Miner. Geochem. 61, 231–264.

Vink, B.W. 1993. The behaviour of thallium in the (sub)surface environment in terms of Eh and pH. Chem. Geol. 109, 119–123.

Watson, J.H.P, Cressey, B.A., Roberts, A.P., Ellwood, D.C., Harnock, J.M., Soper, A.K., 2000. Structural and magnetic studies on heavy-metal-adsorbing iron sulphide nonoparticles produced by sulphate-reducing bacteria. J. Magn. Magn. Mater. 214, 13–30.

Waybrant, K.R., Blowes, D.W., Ptacek, C.J., 1998. Selection of reactive mixtures for use in permeable reactive walls for treatment of mine drainage. Environ. Sci. Technol. 32, 1972–1979.

Waybrant, K.R., Ptacek, C.J., Blowes, D.W., 2002. Treatment of mine drainage using permeable reactive barriers: Column experiments. Environ. Sci. Technol. 36, 1349-1356.

Weisener, C.G., Sale, K.S., Smyth, D.J.A., Blowes, D.W., 2005. Field column study using zerovalent iron for mercury removal from contaminated groundwater. Environ. Sci. Technol. 39, 6306–6312.

Westerhoff, P., James, J., 2003. Nitrate removal in zero-valent iron packed columns. Water Res. 37, 1818–1830.

White, C., Sayer, J.A., Gadd, G.M., 1997. Microbial solubilization and immobilization of toxic metals: key biogeochemical processes for treatment of contamination. FEMS Microbiol. Rev. 20, 503–516.

Wilkin, R.T., McNeil, M.S., 2003. Laboratory evaluation of zero-valent iron to treat water impacted by acid mine drainage. Chemosphere 53, 715–725.

Wolthers, M., Van der Gaast, S.J., Rickard, D., 2003. The structure of disordered mackinawite. Am. Mineral. 88, 2007–2015.

Xu, Y., Schoonen, M.A.A. 1995. The stability of thiosulfate in the presence of pyrite in low-temperature aqueous solutions. Geochim. Cosmochim. Acta. 59, 4605–4622.

Appendix A:

Summary of Data Presented in Chapter 2

Table A.1 Summary of general chemistry and anion concentrations for batch experiments.

Sample	Time	pH	Eh	Aqueous Concentration (mg L^{-1})						
	(days)		(mV)	Alk	SO_4	NO_3-N	NH_3-N	o-PO_4	H_2S	DOC
RM1a	0.0	4.50	102	44	3651	4.2	0.33	0.07	0.01	-0.4
	0.9	6.21	-51	144	3555	0.8	108			175
	5.0	6.20	-83	358	3772				0.01	
	12.8	6.41	-237	950	3104	-0.2	115		0.04	350
	15.8	6.57	-257	900	3017			14	0.09	
	20.7	6.65	-238	1055	2599	-0.2	115			179
	25.7	6.69	-221	1183	2308			10	0.06	
	29.8	6.66	-207	1363	1911	-0.2	86			149
	34.8	6.63	-218	1714	894			29	0.20	
	41.8	6.56	-228	2172	-1	-0.2	93		0.21	485
	53.8	6.65	-232	1961	-1			33	0.10	
RM1b	0.0	4.88	-34	53	3681					
	0.9	6.29	-235	155	3764					
	5.8	6.41	-220	293	3826					
	10.8	6.47	-214	643	3707					
	15.8	6.50	-211	631	3142					
	21.7	6.68	-208	1143	2830					
	27.7	6.68	-208	1300	2430					
	39.8	6.60	-243	2226	262					
	48.7	6.45	-234	2184	10					
	57.7	6.53	-238	2466	-1					
RM1c	0.0	4.88	-34	53	3681					
	0.9	6.34	-240	114	3636					
	5.9	6.48	-225	239	3830					
	10.8	6.57	-221	430	3783					
	14.9	6.59	-227	407	3352					
	19.8	6.71	-228	745	3130					
	24.9	6.84	-223	899	2810					
	31.8	6.78	-243	1600	1140					
	38.8	6.66	-238	2292	1					
	56.9	6.63	-241	2476	10					
RM2	0.0	4.80	66	34	3556	4.6	1.02	0.09	0.01	-0.4
	0.9	6.30	-235	159	3653	1.5	105			216
	5.9	6.38	-230	300	3626			1.4		
	10.8	6.48	-219	522	3571	-0.2	108		0.04	296
	14.9	6.54	-200	741	3246			9.9		
	19.8	6.72	-236	1081	2911	-0.2	150			200
	24.9	6.78	-220	1163	2497			7.4		
	31.8	6.74	-211	1506	1887	-0.2	88		0.05	137
	38.8	6.72	-222	2257	167			33		
	56.9	6.71	-239	1963	-1	0.2	36		0.16	440
RM3	0.0	4.79	59	34	3582	4.6	0.18	0.07	0.01	-0.2
	0.9	6.28	-239	153	3551	1.8	94			176
	5.9	6.41	-237	275	3686			1.1		
	10.9	6.47	-236	504	3553	-0.2	105		0.03	343
	14.9	6.61	-206	674	3186			7.0		
	19.8	6.77	-242	952	2846	-0.2	138			171
	24.9	6.81	-228	1130	2443			6.3		
	31.8	6.74	-230	1454	1784	-0.2	70		0.06	140
	38.8	6.71	-224	2189	116			31	-	
	56.8	6.66	-238	1912	-1	-0.2	16		0.13	559

Table A.1 Continued.

Sample	Time (days)	pH	Eh (mV)	Aqueous Concentration (mg L^{-1})						
				Alk	SO_4	NO_3-N	NH_3-N	o-PO_4	H_2S	DOC
RM4a	0.0	4.50	102	44	3651	4.2	0.33	0.07	0.01	-0.4
	1.0	6.18	-115	191	3614	1.8	91			175
	5.1	6.26	-135	298	3728			0.52	0.02	
	12.9	6.39	-232	675	3270	-0.2	97		0.06	255
	15.9	6.57	-259	674	3257			8.3	0.05	
	20.8	6.74	-233	825	2832	-0.2	105			113
	25.8	6.80	-225	870	2638			4.6	0.03	
	29.9	6.81	-219	991	2408	-0.2	128			95
	34.8	6.78	-228	1230	1792			7.8	0.04	
	41.9	6.72	-239	1971	1	-0.2	61		0.04	234
	53.8	6.75	-235	1961	3			9.2	0.03	
RM4b	0.0	4.80	-59	54	3701					
	0.9	6.30	-242	150	3724					
	5.8	6.36	-218	287	3841					
	10.8	6.39	-207	567	3717					
	15.8	6.50	-230	495	3175					
	21.8	6.63	-218	975	2920					
	27.7	6.77	-224	1170	2540					
	39.8	6.67	-247	2083	277					
	48.8	6.69	-234	2566	1					
	57.8	6.81	-235	2152	3					
RM4c	0.0	4.80	-59	54	3701					
	0.9	6.31	-242	120	3604					
	5.9	6.40	-225	216	3777					
	10.9	6.48	-216	407	3855					
	15.8	6.54	-230	350	3481					
	21.8	6.66	-215	738	3180					
	27.8	6.78	-216	907	2740					
	39.9	6.73	-254	1456	840					
	48.7	6.60	-238	2365	1					
	57.8	6.65	-236	2287	-1					
RM5	0.0	4.80	66	34	3556	4.6	1.02	0.09	0.01	-0.4
	1.0	6.17	-255	64	3405	3.6	0.9			21
	5.9	7.18	-273	76	3455			0.09		
	10.9	7.32	-306	87	3443	-0.2	3.4		0.01	15
	15.0	7.39	-246	77	3442			0.11		
	19.9	7.45	-275	85	3542	-0.2	4.4			19
	25.0	7.48	-337	83	3334			0.13		
	32.0	7.50	-260	59	3454	-0.2	3.3		0.00	18
	39.0	7.61	-251	45	3390			0.16		
	57.0	7.54	-249	43	3720	-0.2	3.5		0.01	31

Table A.2 Summary of metal and cation concentrations for batch experiments.

Reactive	Time	Aqueous Concentration (mg L^{-1})											
Mixture	(days)	Ca	Mg	K	Na	Al	Cd	Co	Fe	Mn	Ni	Pb	Zn
RM1a	0.0	431	40	316	45	20	11	4.9	738	21	8.3	1.1	99
	0.9	583	141	326	94	1.27	2.8	3.1	511	16	4.3	-0.03	43
	5.0	632	147	336	97	0.68	0.71	2.6	479	15	3.1	-0.03	27
	12.8	752	156	350	103	-0.04	-0.01	3.0	360	12	-0.01	-0.03	0.20
	15.8	686	157	328	96	-0.04	-0.01	0.04	306	10	-0.01	-0.03	0.14
	20.7	655	141	320	96	-0.04	-0.01	-0.01	194	7.9	-0.01	-0.03	0.13
	25.7	669	146	319	97	-0.04	-0.01	-0.01	153	6.5	-0.01	-0.03	0.03
	29.8	637	152	306	102	-0.04	-0.01	-0.01	109	5.3	0.04	0.17	0.23
	34.8	489	163	219	82	-0.04	-0.01	-0.01	29	2.8	-0.01	-0.03	0.11
	41.8	405	193	193	78	-0.04	-0.01	-0.01	20	2.2	0.03	-0.03	0.12
	53.8	400	133	230	90	-0.04	-0.01	-0.01	25	2.0	-0.01	-0.03	0.09
RM1b	0.0	431	38	309	45	7.07	9.02	4.97	687	20	13.65	0.36	100
	0.8	576	130	318	97	0.26	1.45	2.59	379	14	5.34	-0.03	35
	5.7	673	143	345	98	0.35	0.32	2.12	340	14	3.92	-0.03	16
	10.8	703	199	338	80	-0.04	0.05	1.37	338	12	2.33	-0.03	3.0
	15.7	734	203	307	81	-0.04	-0.01	0.06	303	11	-0.01	-0.03	0.15
	21.7	651	159	317	100	-0.04	-0.01	0.02	179	7.0	-0.01	-0.03	0.10
	27.7	647	154	314	96	-0.04	-0.01	0.01	139	5.7	-0.01	-0.03	0.10
	39.7	477	157	249	97	-0.04	0.01	-0.01	8	1.9	-0.01	-0.03	0.08
	48.8	473	148	255	93	-0.04	-0.01	0.02	21	2.3	-0.01	-0.03	0.11
	57.7	464	141	255	94	-0.04	-0.01	0.01	26	2.3	-0.01	-0.03	0.24
RM1c	0.0	431	38	309	45	7.07	9.02	4.97	687	20	13.65	0.36	100
	0.9	575	116	318	84	0.45	1.78	2.85	424	16	5.95	-0.03	39
	5.8	640	122	339	87	0.33	0.60	2.34	397	15	4.70	-0.03	19
	10.8	669	175	336	74	0.11	0.10	1.92	391	14	3.66	-0.03	9.9
	15.8	704	173	306	75	-0.04	-0.01	0.24	372	12	-0.01	-0.03	0.24
	21.7	634	135	328	88	-0.04	-0.01	0.02	283	9.4	-0.01	-0.03	0.12
	27.7	607	135	314	87	-0.04	-0.01	0.02	206	7.4	-0.01	-0.03	0.10
	39.8	508	140	280	90	-0.04	0.01	-0.01	52	3.4	-0.01	-0.03	0.18
	48.7	426	125	257	84	-0.04	-0.01	-0.01	27	2.4	-0.01	-0.03	0.21
	57.7	422	120	264	84	-0.04	-0.01	0.01	64	2.8	-0.01	-0.03	0.31
RM2	0.0	433	40	311	46	7.0	9.3	5.1	696	20	8.8	0.82	98
	0.9	548	130	316	91	0.89	2.4	3.1	454	15	4.8	-0.03	42
	5.9	651	134	338	93	0.53	0.36	2.2	380	14	1.8	-0.03	17
	10.8	678	136	336	91	0.18	0.09	1.7	377	13	1.1	-0.03	4.0
	14.9	641	161	268	81	-0.04	-0.01	0.18	317	11	-0.01	-0.03	0.37
	19.8	647	172	279	84	-0.04	-0.01	-0.01	247	9.1	-0.01	-0.03	0.17
	24.9	664	159	288	97	-0.04	-0.01	-0.01	201	7.5	-0.01	-0.03	0.16
	31.8	634	193	269	75	-0.04	-0.01	-0.01	119	5.0	-0.01	-0.03	0.10
	38.8	416	140	236	89	-0.04	-0.01	-0.01	17	1.9	-0.01	-0.03	0.04
	56.9	458	140	255	93	-0.04	-0.01	-0.01	43	2.4	-0.01	-0.03	0.26
RM3	0.0	430	38	313	46	7.7	10	5.1	681	20	8.4	0.66	96
	0.9	570	126	329	94	0.46	2.4	3.1	455	15	4.5	-0.03	41
	5.9	644	127	339	94	0.29	0.35	2.2	390	14	1.7	-0.03	17
	10.9	677	128	339	96	-0.04	0.07	1.6	401	14	0.81	-0.03	3.6
	14.9	625	151	266	79	-0.04	-0.01	0.10	325	11	-0.01	-0.03	0.18
	19.8	626	161	277	83	-0.04	-0.01	-0.01	253	9.4	-0.01	-0.03	0.18
	24.9	650	147	291	97	-0.04	-0.01	-0.01	213	7.9	-0.01	-0.03	0.12
	31.8	598	180	267	76	-0.04	-0.01	-0.01	119	5.2	-0.01	-0.03	0.09
	38.8	410	135	244	91	-0.04	-0.01	-0.01	22	2.2	-0.01	-0.03	0.06
	56.8	466	128	262	91	-0.04	-0.01	-0.01	64.5	2.9	-0.01	-0.03	0.27

Table A.2 Continued.

Reactive	Time	Aqueous Concentration (mg L^{-1})											
Mixture	(days)	Ca	Mg	K	Na	Al	Cd	Co	Fe	Mn	Ni	Pb	Zn
RM4	0.0	431	40	316	45	19.6	11	4.9	738	21	8.3	1.1	99
	1.0	582	123	329	93	1.22	3.7	3.3	533	17	5.0	-0.03	50
	5.1	629	131	335	91	0.53	1.7	2.7	475	15	3.6	-0.03	34
	12.9	699	137	341	94	0.15	0.02	2.6	431	13	0.60	-0.03	1.8
	15.9	669	138	324	93	-0.04	-0.01	0.06	392	12	-0.01	-0.03	0.28
	20.8	621	123	323	91	-0.04	-0.01	0.03	286	9.6	-0.01	-0.03	0.08
	25.8	626	126	324	94	-0.04	-0.01	-0.01	244	7.7	-0.01	-0.03	0.13
	29.9	612	136	315	99	-0.04	-0.01	-0.01	207	6.7	0.04	-0.03	0.45
	34.8	508	140	237	77	-0.04	-0.01	-0.01	118	4.5	-0.01	-0.03	0.11
	41.9	370	163	211	72	-0.04	-0.01	-0.01	34	2.1	-0.01	-0.03	0.09
	53.8	367	112	243	88	-0.04	-0.01	-0.01	64	2.3	-0.01	-0.03	0.11
RM4b	0.0	423	38	309	45	7.35	10.65	4.95	693	21	21.00	0.28	100
	0.9	603	136	333	98	-0.19	1.82	2.71	389	15	10.80	-0.03	35
	5.8	685	142	344	100	0.24	0.51	2.29	355	15	7.73	-0.03	18
	10.8	706	197	342	81	-0.04	0.07	1.53	346	13	5.11	-0.03	3.2
	15.8	736	199	307	80	-0.04	-0.01	0.09	306	11	-0.01	-0.03	0.18
	21.8	660	155	326	98	-0.04	-0.01	-0.01	211	8.3	-0.01	-0.03	0.16
	27.7	665	153	322	95	-0.04	-0.01	-0.01	155	6.5	-0.01	-0.03	0.11
	39.8	448	160	243	103	-0.04	-0.01	-0.01	6	1.8	-0.01	-0.03	0.12
	48.8	420	143	239	92	-0.04	-0.01	-0.01	15	1.9	-0.01	-0.03	0.12
	57.8	395	139	232	96	-0.04	-0.01	0.01	17	1.8	-0.01	-0.03	0.30
RM4c	0.0	423	38	309	45	7.35	10.65	4.95	693	21	21.00	0.28	100
	0.9	578	117	330	95	0.36	2.19	2.99	448	17	12.30	-0.03	39
	5.9	652	124	337	96	0.29	0.72	2.46	410	16	8.67	-0.03	22
	10.9	671	170	337	77	-0.04	0.06	1.91	405	15	6.56	-0.03	8.9
	15.8	705	176	302	79	-0.04	-0.01	0.43	391	14	0.30	-0.03	0.35
	21.8	633	133	325	95	-0.04	-0.01	0.02	302	10	-0.01	-0.03	0.22
	27.8	614	131	325	92	-0.04	-0.01	0.02	221	7.9	-0.01	-0.03	0.11
	39.9	471	141	273	98	-0.04	-0.01	-0.01	37	3.5	-0.01	-0.03	0.16
	48.7	416	125	261	89	-0.04	-0.01	-0.01	31	2.8	-0.01	-0.03	0.14
	57.8	413	117	264	88	-0.04	-0.01	0.02	66	3.0	-0.01	-0.03	0.26
RM5	0.0	433	40	311	46	7.0	9.3	5.1	696	20	8.8	0.82	98
	1.0	469	39	321	74	-0.04	6.1	4.3	651	23	7.9	-0.03	75
	5.9	450	36	302	69	-0.04	2.4	3.2	659	25	4.3	-0.03	36
	10.9	452	36	300	70	-0.04	1.0	2.7	665	26	3.1	-0.03	20
	15.0	426	44	245	59	-0.04	0.47	2.4	650	25	2.6	-0.03	12
	19.9	453	47	300	57	-0.04	0.19	2.2	626	25	2.5	-0.03	8.2
	25.0	471	46	276	70	-0.04	0.07	2.0	654	27	1.4	-0.03	5.2
	32.0	477	47	280	57	-0.04	-0.01	1.7	616	25	0.90	-0.03	2.9
	39.0	459	40	300	68	-0.04	-0.01	1.4	493	24	0.47	-0.03	1.9
	57.0	489	41	306	71	-0.04	-0.01	1.2	478	26	0.01	-0.03	1.7

Table A.3 Saturation indices for batch samples calculated using MINTEQA2.

		Mineral Saturation Indices (Sis) Calculated with MINTEQA2												
Reactive Mixture	**Time (d)**	**$Al(OH)_3$ (amorph.)**	**Anhydrite [$CaSO_4$]**	**Aragonite [$CaCO_3$]**	**Calcite [$CaCO_3$]**	**Dolomite [$CaMg(CO_3)_2$]**	**Ferrihydrite [$Fe(OH)_3$]**	**FeS ppt.**	**Gibbsite [$Al(OH)_3$]**	**Goethite [α-FeOOH]**	**Greigite [Fe_3S_4]**	**Gypsum [$CaSO_4{:}2H_2O$]**	**Mackinawite [$Fe_{1+x}S$]**	**Pyrite [FeS_2]**
RM1	0.0	-2.03	-0.31	-5.23	-5.10	-9.98	-5.14	-6.03	0.66	0.79	-14.86	-0.10	-5.30	4.45
	0.9	0.73	-0.19	-0.97	-0.83	-1.57	-2.77	-3.97	3.41	3.16	-11.58	0.02	-3.24	3.61
	5.0	0.46	-0.15	-0.56	-0.42	-0.78	-3.44	-3.42	3.15	2.46	-10.44	0.07	-2.69	3.72
	12.8	-5.32	-0.15	0.19	0.33	0.67	-5.60	-0.01	-2.63	0.29	-1.81	0.07	0.72	5.54
	15.8	-5.40	-0.18	0.32	0.45	0.94	-5.49	0.46	-2.72	0.44	-0.45	0.04	1.20	5.88
	20.7	-5.43	-0.23	0.47	0.61	1.26	-5.16	0.29	-2.74	0.75	-0.31	-0.02	1.03	6.39
	25.7	-5.46	-0.26	0.60	0.73	1.49	-4.86	0.76	-2.77	1.06	2.28	-0.04	1.50	8.02
	29.8	-5.43	-0.34	0.63	0.77	1.57	-4.88	-0.02	-2.75	1.03	-0.23	-0.12	0.71	7.09
	34.8	-5.42	-0.67	0.68	0.81	1.64	-5.74	0.33	-2.74	0.19	1.45	-0.46	1.07	8.03
	41.8	-5.38	-9.63	0.70	0.83	1.72	-6.31	0.02	-2.71	-0.37	0.06	-9.42	0.75	7.25
	53.8	-5.44	-9.65	0.74	0.88	1.89	-5.98	-0.25	-2.76	-0.04	-1.27	-9.43	0.48	6.46
RM2	0.0	-1.59	-0.31	-4.77	-4.63	-9.06	-4.87	-6.05	1.09	1.06	-16.15	-0.09	-5.32	3.22
	0.9	0.61	-0.20	-0.87	-0.73	-1.35	-5.66	-3.86	3.29	0.26	-17.29	0.02	-3.13	-2.29
	5.9	0.38	-0.14	-0.41	-0.28	-0.49	-5.43	-2.67	3.06	0.50	-12.25	0.08	-1.94	0.35
	10.8	-0.11	-0.13	-0.05	0.09	0.22	-4.99	-0.74	2.57	0.94	-4.10	0.09	0.00	4.62
	14.9	-5.39	-0.16	0.17	0.30	0.57	-4.58	-0.03	-2.71	1.36	-0.48	0.05	0.71	6.80
	19.8	-5.49	-0.20	0.53	0.67	1.32	-4.81	0.24	-2.81	1.12	-0.52	0.02	0.97	6.25
	24.9	-5.53	-0.23	0.66	0.80	1.59	-4.44	0.22	-2.85	1.50	0.06	-0.02	0.95	6.87
	31.8	-5.53	-0.34	0.77	0.90	1.80	-4.65	0.09	-2.86	1.32	0.19	-0.13	0.83	7.18
	38.8	-5.48	-1.43	0.86	0.99	2.11	-5.83	0.10	-2.80	0.10	0.68	-1.21	0.83	7.73
	56.9	-5.54	-9.61	0.88	1.01	2.16	-5.62	-0.23	-2.88	0.38	-1.51	-9.41	0.51	6.04
RM3	0.0	-1.56	-0.31	-4.78	-4.65	-9.09	-5.02	-5.81	1.12	0.91	-15.39	-0.09	-5.08	3.47
	0.9	0.32	-0.20	-0.88	-0.74	-1.38	-5.78	-3.88	3.00	0.15	-17.51	0.02	-3.15	-2.48
	5.9	0.11	-0.14	-0.43	-0.29	-0.51	-5.44	-2.96	2.79	0.50	-13.64	0.08	-2.23	-0.48
	10.9	-5.36	-0.13	-0.08	0.06	0.17	-5.26	-1.17	-2.68	0.67	-6.42	0.08	-0.44	3.17
	14.9	-5.43	-0.18	0.19	0.32	0.62	-4.44	-0.03	-2.75	1.50	-0.70	0.04	0.71	6.58
	19.8	-5.53	-0.21	0.52	0.65	1.31	-4.73	0.28	-2.85	1.21	-0.58	0.00	1.01	6.10
	24.9	-5.56	-0.25	0.68	0.81	1.63	-4.46	0.33	-2.88	1.48	0.18	-0.03	1.06	6.76
	31.8	-5.53	-0.37	0.74	0.87	1.76	-4.95	0.19	-2.86	1.01	-0.06	-0.16	0.93	6.73
	38.8	-5.47	-1.59	0.84	0.97	2.09	-5.77	0.12	-2.79	0.17	0.53	-1.37	0.85	7.54
	56.8	-5.50	-9.61	0.82	0.96	2.05	-5.56	-0.23	-2.84	0.44	-1.66	-9.40	0.51	5.89
RM4	0.0	-2.03	-0.31	-5.23	-5.10	-9.98	-5.14	-6.11	0.66	0.79	-15.17	-0.10	-5.38	4.29
	1.0	0.70	-0.19	-0.88	-0.74	-1.39	-3.92	-4.12	3.38	2.01	-14.32	0.03	-3.38	1.16
	5.1	0.38	-0.15	-0.58	-0.44	-0.82	-4.12	-3.42	3.06	1.78	-12.21	0.07	-2.69	1.95
	12.9	-0.15	-0.15	-0.02	0.12	0.27	-5.46	-0.34	2.54	0.44	-3.07	0.07	0.40	4.94
	15.9	-5.40	-0.16	0.16	0.30	0.62	-5.39	0.21	-2.72	0.54	-1.67	0.06	0.94	5.17
	20.8	-5.48	-0.22	0.41	0.55	1.16	-4.61	0.52	-2.80	1.30	0.56	-0.01	1.25	6.82
	25.8	-5.54	-0.24	0.52	0.66	1.38	-4.35	0.29	-2.86	1.57	0.02	-0.03	1.03	6.70
	29.9	-5.54	-0.28	0.59	0.73	1.52	-4.31	-0.06	-2.86	1.61	-1.12	-0.06	0.67	6.28
	34.8	-5.53	-0.41	0.64	0.77	1.57	-4.80	-0.02	-2.86	1.15	-0.93	-0.20	0.72	6.34
	41.9	-5.48	-9.66	0.79	0.93	1.98	-5.74	-0.59	-2.81	0.20	-2.98	-9.44	0.15	5.41
	53.8	-5.51	-3.20	0.81	0.94	2.08	-5.31	-0.33	-2.83	0.64	-2.08	-2.99	0.41	5.79
RM5	0.0	-1.59	-0.31	-4.77	-4.63	-9.06	-4.87		1.09	1.06		-0.09		
	1.0	-5.39	-0.28	-2.02	-1.89	-3.59	-6.16		-2.72	-0.22		-0.07		
	5.9	-5.90	-0.29	-0.76	-0.63	-1.08	-3.43		-3.22	2.52		-0.07		
	10.9	-6.01	-0.29	-0.56	-0.42	-0.68	-3.58		-3.33	2.35		-0.07		
	15.0	-6.09	-0.29	-0.56	-0.43	-0.74	-2.37		-3.42	3.58		-0.08		
	19.9	-6.15	-0.27	-0.43	-0.29	-0.42	-2.70		-3.47	3.24		-0.06		
	25.0	-6.17	-0.27	-0.38	-0.25	-0.38	-3.63		-3.49	2.31		-0.06		
	32.0	-6.23	-0.25	-0.49	-0.36	-0.60	-2.26		-3.56	3.71		-0.04		
	39.0	-6.30	-0.27	-0.51	-0.37	-0.58	-1.91		-3.63	4.04		-0.05		
	57.0	-6.30	-0.22	-0.56	-0.43	-0.70	-2.07		-3.63	3.93		-0.01		

Table A.3 Continued.

Reactive Mixture	Time (d)	Mineral Saturation Indices (Sis) Calculated with MINTEQA2													
		Quartz [SiO_2]	Siderite [$FeCO_3$]	Rhodochrosite [$MnCO_3$]	MnS (green)	Smithsonite [$ZnCO_3$]	ZnS (amorph.)	Sphalerite [ZnS]	Wurtzite [ZnS]	Greenockite [CdS]	Aglesite [$PbSO_4$]	Galena [PbS]	Millerite [NiS]	Native S	Lepidocrocite [γ-FeOOH]
RM1	0.0	-1.60	-2.58	-4.61	-15.28	-4.48	-1.92	0.64	-1.29	3.67	-0.47	-0.90	-3.92	-1.93	-1.62
	0.9	-0.22	1.36	-0.61	-13.16	-0.73	-0.06	2.50	0.57	5.30	-6.71	-4.87	-2.07	-4.83	0.75
	5.0	0.22	1.68	-0.29	-12.62	-0.61	0.32	2.88	0.95	5.32	-6.87	-4.40	-1.72	-5.31	0.08
	12.8	0.78	2.15	0.20	-9.19	-2.22	1.65	4.21	2.28	0.98	-7.38	-1.21	-4.97	-6.90	-2.08
	15.8	0.76	2.24	0.30	-8.70	-2.47	1.77	4.33	2.40	1.07	-7.56	-0.90	-4.53	-7.00	-1.97
	20.7	0.83	2.19	0.33	-8.79	-2.31	1.81	4.37	2.44	1.17	-7.70	-0.93	-4.62	-6.33	-1.64
	25.7	0.88	2.17	0.33	-8.30	-3.65	0.96	3.52	1.59	1.08	-8.21	-0.80	-4.12	-5.17	-1.34
	29.8	0.90	2.04	0.27	-9.02	-1.91	2.04	4.60	2.67	1.18	-7.93	-1.06	-4.77	-5.32	-1.36
	34.8	0.95	1.54	0.07	-8.36	-3.71	1.10	3.65	1.72	0.83	-9.22	-1.14	-3.91	-4.71	-2.22
	41.8	1.03	1.39	-0.03	-8.62	-3.53	1.11	3.66	1.74	0.79	-18.08	-1.18	0.41	-5.17	-2.79
	53.8	1.03	1.56	0.00	-9.02	-2.72	1.49	4.04	2.11	1.07	-17.49	-0.98	-4.50	-5.69	-2.46
RM2	0.0	-1.27	-2.14	-4.16	-15.29	-4.02	-1.92	0.64	-1.29	3.59	-0.60	-1.02	-3.89	-3.15	-1.35
	0.9	0.05	1.45	-0.51	-13.04	-0.62	0.09	2.65	0.72	5.40	-6.73	-4.74	-1.89	-10.86	-2.14
	5.9	0.37	1.72	-0.19	-11.80	-0.67	0.94	3.50	1.57	5.77	-6.91	-3.63	-1.16	-9.39	-1.91
	10.8	0.56	2.03	0.09	-9.89	-0.98	2.26	4.82	2.89	5.96	-7.13	-1.87	0.42	-7.06	-1.47
	14.9	0.69	2.16	0.22	-9.17	-1.87	1.96	4.52	2.59	1.07	-7.33	-1.25	-4.97	-5.58	-1.06
	19.8	0.81	2.36	0.45	-8.89	-1.98	1.91	4.46	2.54	1.24	-7.67	-1.11	-4.83	-6.39	-1.29
	24.9	0.86	2.37	0.46	-8.90	-1.91	1.95	4.50	2.58	1.30	-7.81	-1.13	-4.85	-5.76	-0.92
	31.8	0.89	2.20	0.35	-8.95	-2.19	1.71	4.25	2.33	1.20	-8.04	-1.13	-4.79	-5.29	-1.13
	38.8	0.99	1.46	0.06	-8.52	-3.92	0.73	3.28	1.36	0.94	-9.92	-1.05	-4.04	-4.78	-2.31
	56.9	1.05	1.86	0.15	-9.12	-1.81	2.09	4.62	2.71	1.12	-17.45	-1.18	-4.77	-6.07	-2.10
RM3	0.0	-1.23	-2.17	-4.18	-15.04	-4.04	-1.67	0.88	-1.05	3.87	-0.70	-0.88	-3.66	-3.13	-1.50
	0.9	0.07	1.42	-0.53	-13.05	-0.65	0.07	2.63	0.70	5.38	-6.73	-4.76	-1.94	-11.02	-2.26
	5.9	0.35	1.73	-0.18	-12.09	-0.68	0.64	3.19	1.27	5.49	-6.89	-3.94	-1.49	-9.92	-1.91
	10.9	0.55	2.03	0.09	-10.33	-1.00	1.81	4.36	2.43	5.81	-7.11	-2.32	-0.17	-8.07	-1.74
	14.9	0.66	2.21	0.28	-9.17	-1.81	1.96	4.51	2.59	1.14	-7.34	-1.28	-5.01	-5.79	-0.92
	19.8	0.78	2.38	0.48	-8.84	-1.96	1.95	4.50	2.57	1.29	-7.66	-1.09	-4.82	-6.58	-1.21
	24.9	0.83	2.42	0.51	-8.80	-1.93	1.99	4.54	2.62	1.32	-7.84	-1.07	-4.78	-5.97	-0.93
	31.8	0.88	2.20	0.36	-8.84	-2.26	1.74	4.28	2.36	1.19	-8.07	-1.05	-4.69	-5.84	-1.43
	38.8	1.00	1.57	0.10	-8.57	-3.69	0.87	3.42	1.49	0.99	-9.91	-1.00	-4.14	-4.99	-2.25
	56.8	1.10	1.99	0.17	-9.23	-1.72	2.06	4.59	2.67	1.09	-17.37	-1.29	-4.90	-6.22	-2.04
RM4	0.0	-1.60	-2.58	-4.61	-15.36	-4.48	-2.00	0.56	-1.37	3.59	-0.47	-0.98	-4.00	-2.01	-1.62
	1.0	0.00	1.47	-0.52	-13.32	-0.59	-0.16	2.40	0.47	5.27	-6.74	-5.08	-2.19	-7.14	-0.40
	5.1	0.24	1.67	-0.29	-12.62	-0.51	0.42	2.98	1.05	5.68	-6.84	-4.39	-1.66	-7.07	-0.60
	12.9	0.65	2.09	0.11	-9.55	-1.35	2.26	4.82	2.89	5.27	-7.20	-1.50	0.49	-7.18	-1.94
	15.9	0.64	2.24	0.25	-9.00	-2.03	1.96	4.51	2.59	1.10	-7.33	-1.09	-4.82	-7.46	-1.87
	20.8	0.73	2.36	0.41	-8.66	-2.49	1.70	4.26	2.33	1.27	-7.61	-0.84	-4.56	-6.14	-1.09
	25.8	0.78	2.38	0.40	-8.91	-2.06	1.87	4.43	2.50	1.33	-7.68	-1.05	-4.79	-6.01	-0.83
	29.9	0.81	2.36	0.40	-9.25	-1.40	2.19	4.75	2.82	1.36	-7.77	-1.37	-5.12	-6.08	-0.79
	34.8	0.86	2.19	0.30	-9.12	-2.03	1.77	4.32	2.39	1.30	-7.95	-1.19	-4.90	-6.05	-1.28
	41.9	1.09	1.77	0.09	-9.48	-2.04	1.61	4.16	2.24	1.24	-17.35	-1.33	-5.04	-6.40	-2.22
	53.8	1.13	2.07	0.16	-9.45	-1.91	1.70	4.25	2.33	1.27	-10.91	-1.37	-5.08	-6.28	-1.79
RM5	0.0	-1.27	-2.14	-4.16		-4.02					-0.60				-1.35
	1.0	-0.17	0.53	-1.41		-1.43					-6.55				-2.64
	5.9	-0.04	1.81	-0.09		-0.48					-6.75				0.09
	10.9	-0.06	2.02	0.13		-0.53					-6.84				-0.06
	15.0	-0.14	2.03	0.14		-0.73					-6.84				1.15
	19.9	-0.22	2.12	0.23		-0.81					-6.90				0.82
	25.0	-0.30	2.17	0.30		-0.97					-6.93				-0.11
	32.0	-0.47	2.03	0.16		-1.34					-6.86				1.26
	39.0	-0.50	1.94	0.14		-1.53					-6.86				1.62
	57.0	-0.55	1.84	0.09		-1.64					-6.81				1.46

Table A.4 Most-probable number populations of acid-producing (fermentative) bacteria (APB), iron-reducing bacteria (IRB) and sulfate-reducing bacteria (SRB), and fluorescein diacetate (FDA) hydrolysis rates for solid-phase samples.

Reactive	MPN Population (cells g^{-1})			FDA
Mixture	APB	IRB	SRB	(nmol FDA h^{-1} g^{-1})
RM1a	4.9E+03	1.7E+05	7.9E+06	3.54
RM1b	3.3E+03	2.1E+05	1.1E+07	4.17
RM1c	6.8E+03	7.0E+05	7.9E+06	3.30
RM2	4.9E+03	4.9E+05	7.0E+06	3.28
RM3	1.3E+03	1.7E+06	1.1E+07	3.48
RM4a	2.4E+03	3.3E+05	1.7E+07	2.77
RM4b	3.3E+03	2.2E+05	7.9E+06	3.87
RM4c	4.9E+02	7.9E+04	4.6E+07	4.27
RM5	2.4E+02	3.3E+02	0.0E+00	0.21

Appendix B:

Summary of Data Presented in Chapter 3

Table B.1 Summary of whole-rock digestion data for core samples collected in February and March 2005. Astersisks denote replicate analyses.

Borehole	Depth Interval (m)	SiO_2 wt. %	Al_2O_3 wt. %	$Fe_2O_{3(T)}$ wt. %	MnO wt. %	MgO wt. %	CaO wt. %
BH1	1.8 - 2.1	21.75	3.94	13.06	0.25	5.58	9.20
	2.1 - 2.4	18.97	3.42	18.74	0.35	6.29	11.34
	3.2 - 3.4	19.11	3.18	16.46	0.34	6.77	12.72
BH2	2.6 - 3.0	18.73	2.83	12.85	0.24	5.55	9.99
	5.6 - 6.1	14.13	2.31	12.57	0.37	5.66	9.76
	5.6 - 6.1*	14.02	2.35	12.57	0.37	5.67	9.77
	7.2 - 7.6	19.00	3.04	10.42	0.30	6.80	11.20
	8.5 - 9.1	23.43	3.60	16.41	0.36	6.65	11.20
	11.6 - 12.2	23.18	3.54	17.01	0.27	5.34	9.88
	14.6 - 15.2	23.18	4.51	10.13	0.39	6.38	10.34
	17.7 - 18.3	26.85	4.23	11.52	0.20	4.00	7.13
	19.2 - 19.8	36.17	5.02	10.08	0.16	4.33	7.94
BH3	2.6 - 3.0	24.06	4.20	13.54	0.34	6.19	10.51
	5.6 - 6.1	17.93	3.15	15.68	0.32	5.82	10.72
	7.2 - 7.6	47.27	8.58	10.39	0.22	4.56	5.26
	8.7 - 9.1	22.84	4.25	10.69	0.22	4.61	8.06
	10.2 - 10.7	22.97	4.29	10.53	0.21	4.57	8.19
	11.7 - 12.2	20.42	3.98	11.77	0.20	4.34	7.79
	14.8 - 15.2	24.65	4.16	10.63	0.20	4.11	7.88
	16.3 - 16.8	28.54	4.20	10.67	0.17	4.72	8.69
	17.8 - 18.3	17.81	2.79	15.55	0.11	2.31	4.58
	20.7 - 21.5	25.39	4.02	10.74	0.16	4.92	8.86
	22.2 - 23.0	29.48	4.85	9.22	0.18	4.33	7.98
	22.2 - 23.0*	29.32	4.82	9.30	0.19	4.33	7.96
	23.8 - 24.5	38.36	5.52	8.69	0.15	4.97	9.03
BH4	2.6 - 3.0	23.05	3.61	12.48	0.25	5.37	8.71
	5.6 - 6.1	26.05	3.30	14.33	0.29	5.08	8.90
	7.2 - 7.6	16.12	2.29	13.42	0.32	8.69	14.68
	10.2 - 10.7	17.84	2.59	14.87	0.37	7.74	13.72
	11.7 - 12.2	17.94	2.91	13.88	0.37	7.14	12.00
	13.3 - 13.7	20.41	3.05	14.91	0.39	8.33	13.04
	14.8 - 15.2	21.64	3.86	11.97	0.36	5.28	10.01
BH5	1.1 - 1.5	22.21	3.36	10.44	0.32	5.15	8.84
	2.6 - 3.0	41.42	5.01	9.53	0.27	4.04	6.40
	4.1 - 4.6	34.23	4.20	12.43	0.35	5.17	8.34
	5.6 - 6.1	32.01	5.02	12.97	0.35	5.72	9.34
	7.2 - 7.6	37.01	5.12	7.38	0.27	7.01	11.37
	10.2 - 10.7	42.33	5.30	12.31	0.43	5.30	7.51
	11.7 - 12.2	39.30	4.65	13.26	0.30	5.03	7.64
	14.8 - 15.2	27.00	4.30	10.55	0.46	6.98	11.48
	16.3 - 16.8	35.06	4.98	10.04	0.45	6.05	9.28
	19.2 - 19.9	28.96	4.53	6.86	0.37	6.11	10.31

Table B.1 Continued.

Borehole	Depth Interval (m)	Na_2O wt. %	K_2O wt. %	TiO_2 wt. %	P_2O_5 wt. %	LOI wt. %	TOTAL wt. %	Ba ppm
BH1	1.8 - 2.1	0.26	0.82	0.23	0.32	19.78	75.20	66272
	2.1 - 2.4	0.26	0.56	0.16	0.22	21.76	82.07	48607
	3.2 - 3.4	0.25	0.62	0.18	0.42	21.90	81.95	32841
BH2	2.6 - 3.0	0.18	0.44	0.15	0.40	17.75	69.10	82245
	5.6 - 6.1	0.14	0.47	0.11	0.27	17.44	63.22	96675
	5.6 - 6.1*	0.14	0.44	0.11	0.28	17.44	63.15	96461
	7.2 - 7.6	0.14	0.57	0.14	0.24	17.67	69.52	63486
	8.5 - 9.1	0.22	0.66	0.19	0.37	20.98	84.08	35501
	11.6 - 12.2	0.23	0.47	0.18	0.33	19.18	79.63	62938
	14.6 - 15.2	0.19	0.77	0.23	0.58	18.63	75.33	76789
	17.7 - 18.3	0.22	0.74	0.22	0.49	14.04	69.65	111540
	19.2 - 19.8	0.22	1.06	0.31	0.81	16.47	82.56	41647
BH3	2.6 - 3.0	0.34	0.68	0.21	0.41	19.98	80.46	42368
	5.6 - 6.1	0.17	0.54	0.16	0.35	17.88	72.71	74955
	7.2 - 7.6	0.38	1.62	0.63	0.32	16.21	95.44	26408
	8.7 - 9.1	0.22	0.76	0.25	0.51	15.25	67.65	121220
	10.2 - 10.7	0.25	0.66	0.24	0.51	15.74	68.16	110200
	11.7 - 12.2	0.20	0.65	0.19	0.58	15.56	65.69	128150
	14.8 - 15.2	0.17	0.72	0.20	0.60	14.13	67.45	98751
	16.3 - 16.8	0.19	0.74	0.22	0.60	14.59	73.33	89032
	17.8 - 18.3	0.15	0.52	0.14	0.39	14.20	58.54	191090
	20.7 - 21.5	0.14	0.76	0.22	0.76	14.75	70.71	101930
	22.2 - 23.0	0.17	0.90	0.26	0.92	16.10	74.40	73038
	22.2 - 23.0*	0.18	0.90	0.26	0.92	16.10	74.28	73222
	23.8 - 24.5	0.24	1.17	0.32	1.02	18.19	87.67	32338
BH4	2.6 - 3.0	0.17	0.35	0.21	0.36	15.90	70.45	95642
	5.6 - 6.1	0.19	0.57	0.16	0.30	18.85	78.04	56960
	7.2 - 7.6	0.19	0.43	0.11	0.18	16.31	72.74	29536
	10.2 - 10.7	0.20	0.57	0.13	0.30	17.90	76.24	34720
	11.7 - 12.2	0.18	0.38	0.15	0.28	18.18	73.41	44037
	13.3 - 13.7	0.23	0.62	0.18	0.26	19.84	81.27	19814
	14.8 - 15.2	0.17	0.61	0.21	0.39	16.31	70.81	83129
BH5	1.1 - 1.5	0.14	0.70	0.19	0.45	19.01	70.81	78524
	2.6 - 3.0	0.71	0.86	0.24	0.32	12.99	81.81	57572
	4.1 - 4.6	0.21	0.86	0.21	0.38	17.97	84.36	29131
	5.6 - 6.1	0.19	0.88	0.27	0.46	17.44	84.63	38679
	7.2 - 7.6	0.89	0.80	0.26	0.56	17.57	88.23	20618
	10.2 - 10.7	0.40	0.99	0.28	0.35	18.01	93.21	16404
	11.7 - 12.2	0.22	0.97	0.22	0.34	19.19	91.12	20049
	14.8 - 15.2	0.12	0.78	0.22	0.55	20.29	82.72	32774
	16.3 - 16.8	0.14	1.02	0.24	0.44	19.78	87.46	24785
	19.2 - 19.9	0.10	0.83	0.23	0.67	17.64	76.63	56797

Table B.2 Summary of aqua-regia digestion data for core samples collected in February and March 2005. Astersisks denote replicate analyses.

Borehole	Depth Interval (m)	V ppm	Cr ppm	Mn ppm	Fe wt. %	Co ppm	Ni ppm	Cu ppm	Zn ppm	As ppm	Se ppm	Sr ppm
BH1	1.8 - 2.1	90	56.1	2010	13.2	8.6	89	1280	>10000	2170	22.9	102.2
	2.1 - 2.4	37	27.4	2480	16.3	6.6	102	1560	>10000	2350	18.9	56.0
	3.2 - 3.4	48	28.6	2500	14.6	6.0	89	1550	>10000	2270	23.6	61.8
BH2	2.6 - 3.0	86	65.0	1810	14.7	6.2	84	2100	>10000	1500	18.5	58.6
	5.6 - 6.1	76	61.9	2990	14.4	6.5	130	1540	>10000	3500	20.0	64.1
	7.2 - 7.6	77	60.2	2290	12.4	6.6	92	1210	>10000	1380	18.0	88.4
	8.5 - 9.1	97	72.8	2640	14.0	6.3	89	1530	>10000	1560	24.1	66.3
	11.6 - 12.2	92	69.2	1930	14.6	8.1	135	1390	>10000	1960	22.0	40.3
	14.6 - 15.2	119	63.5	3120	11.3	6.7	85	1490	7570	1370	23.0	71.2
	17.7 - 18.3	108	44.4	1580	9.6	7.2	58	1420	>10000	593	18.6	62.1
	19.2 - 19.8	95	41.8	1240	9.6	8.6	69	1420	>10000	473	25.3	65.7
BH3	2.6 - 3.0	86	68.3	2470	13.2	7.4	92	1400	>10000	1400	20.8	79.9
	5.6 - 6.1	89	62.4	2330	13.7	6.1	96	1210	>10000	1820	24.9	73.4
	7.2 - 7.6	55	51.9	1650	9.1	25.0	133	605	>10000	560	13.6	84.5
	8.7 - 9.1	112	55.4	1690	9.7	7.6	64	1420	>10000	539	22.1	91.7
	10.2 - 10.7	112	46.8	1660	10.0	7.1	60	1390	>10000	691	22.0	65.6
	11.7 - 12.2	109	42.3	1560	10.4	5.9	57	1230	>10000	603	19.9	77.9
	14.8 - 15.2	119	48.6	1630	11.5	6.1	62	1780	>10000	598	18.1	54.4
	16.3 - 16.8	117	46.2	1360	9.8	5.9	55	1150	7210	420	17.9	63.7
	17.8 - 18.3	76	30.1	906	12.7	4.3	50	1220	9560	689	14.6	53.4
	20.7 - 21.5	84	24.4	1300	9.5	6.5	68	977	7030	425	22.2	53.0
	22.2 - 23.0	81	26.0	1500	9.3	7.5	70	2900	>10000	561	24.2	43.1
	23.8 - 24.5	75	32.1	1140	7.7	8.4	61	934	>10000	298	24.5	73.0
	23.8 - 24.5*	102	44.8	1190	8.1	9.0	65	969	>10000	310	25.2	75.2
BH4	2.6 - 3.0	94	78.0	1970	11.9	8.0	98	1040	>10000	1750	21.8	58.4
	5.6 - 6.1	78	52.2	2180	14.0	6.1	87	1740	>10000	1550	17.9	67.5
	7.2 - 7.6	67	48.5	2320	13.2	4.8	85	1450	>10000	1400	16.3	127.6
	10.2 - 10.7	79	53.9	2780	13.0	4.1	74	1460	>10000	1610	22.1	111.7
	11.7 - 12.2	78	69.9	2700	14.3	6.4	97	1780	>10000	1590	19.1	66.9
	13.3 - 13.7	73	79.0	2870	14.1	7.0	94	1480	>10000	1630	16.8	92.6
	14.8 - 15.2	95	65.7	3070	11.7	7.9	104	1230	>10000	1610	28.9	69.3
BH5	1.1 - 1.5	99	61.7	2520	11.9	6.6	87	1360	>10000	1350	30.5	66.7
	2.6 - 3.0	66	43.1	2120	8.0	8.2	64	809	>10000	823	18.5	68.6
	4.1 - 4.6	87	55.7	2750	13.0	7.1	90	1600	>10000	2150	26.4	58.5
	5.6 - 6.1	97	64.4	2610	12.5	8.4	100	1270	>10000	1780	29.6	52.8
	7.2 - 7.6	93	63.6	2300	12.4	6.0	97	1260	>10000	2210	28.5	61.7
	10.2 - 10.7	69	52.5	3050	11.8	10.8	79	973	>10000	1340	18.0	65.1
	11.7 - 12.2	76	47.5	2200	12.1	7.6	85	973	9070	1690	24.4	69.1
	14.8 - 15.2	112	59.7	3560	11.5	6.8	98	976	9990	2430	33.4	60.1
	16.3 - 16.8	105	81.5	3470	10.7	10.8	140	950	>10000	1710	25.1	66.7
	16.3 - 16.8*	73	58.1	3330	10.6	10.8	138	954	>10000	1740	24.5	56.6
	19.2 - 19.9	111	60.5	3050	8.7	8.5	109	877	8120	998	28.5	85.5

Table B.2 Continued

Borehole	Depth Interval (m)	Mo ppm	Ag ppm	Cd ppm	Sn ppm	Sb ppm	Ba ppm	W ppm	Au ppb	Tl ppm	Pb ppm	U ppm
BH1	1.8 - 2.1	65.7	264	100	5.5	349	7.8	3.3	563	106	>10000	6.1
	2.1 - 2.4	84.8	223	152	7.7	381	6.5	2.9	199	110	>10000	5.5
	3.2 - 3.4	77.0	254	139	6.2	403	7.3	3.5	186	126	>10000	6.6
BH2	2.6 - 3.0	68.4	234	140	8.0	325	7.0	3.0	201	94	>10000	6.8
	5.6 - 6.1	91.1	268	119	6.4	503	5.4	3.5	669	137	>10000	6.7
	7.2 - 7.6	66.6	221	103	5.6	282	7.4	2.6	208	84	9490	6.3
	8.5 - 9.1	80.2	178	103	6.1	316	7.1	3.3	301	92	>10000	7.0
	11.6 - 12.2	78.6	271	133	7.8	389	5.4	4.5	129	118	>10000	6.1
	14.6 - 15.2	81.3	251	55	5.1	393	7.9	3.9	74	55	7830	10.6
	17.7 - 18.3	46.9	151	100	6.1	423	9.2	2.7	80	34	8150	9.0
	19.2 - 19.8	39.9	194	131	3.8	388	10.8	2.4	48	24	8470	9.1
BH3	2.6 - 3.0	66.1	188	101	4.7	367	8.3	3.3	228	85	>10000	7.5
	5.6 - 6.1	90.4	239	150	7.0	466	7.9	2.8	144	114	>10000	7.3
	7.2 - 7.6	29.2	86	69	2.3	105	7.9	1.5	41	30	5100	3.1
	8.7 - 9.1	50.8	232	85	8.2	366	11.8	2.6	81	30	9320	10.9
	10.2 - 10.7	54.6	185	117	5.6	443	7.9	2.8	84	45	>10000	10.1
	11.7 - 12.2	48.3	131	98	6.2	341	10.7	3.4	115	43	7860	9.0
	14.8 - 15.2	49.8	169	101	8.3	519	7.9	3.2	216	37	8130	9.4
	16.3 - 16.8	39.6	126	55	5.8	338	9.5	2.5	122	32	6180	7.9
	17.8 - 18.3	46.4	86	66	4.9	169	14.8	3.0	359	66	6570	5.6
	20.7 - 21.5	47.6	172	55	3.3	206	18.0	2.5	129	30	5010	9.0
	22.2 - 23.0	62.1	283	192	4.6	1080	21.5	3.5	247	18	>10000	17.0
	23.8 - 24.5	28.4	139	98	2.0	241	9.2	1.6	54	14	6580	8.3
	23.8 - 24.5*	30.0	150	101	2.1	252	10.1	1.7	73	16	6690	8.6
BH4	2.6 - 3.0	73.9	171	111	6.5	286	11.4	3.9	682	109	9970	7.3
	5.6 - 6.1	63.2	212	99	7.0	293	6.8	3.9	630	104	8120	5.7
	7.2 - 7.6	65.3	192	131	6.7	240	8.1	2.7	483	96	>10000	5.0
	10.2 - 10.7	86.6	276	137	6.2	361	11.3	3.5	205	90	>10000	7.6
	11.7 - 12.2	71.3	184	121	7.3	284	17.3	3.3	612	90	>10000	6.1
	13.3 - 13.7	70.0	191	89	5.3	253	6.6	2.7	297	84	>10000	5.5
	14.8 - 15.2	103.6	328	150	5.1	505	10.9	3.7	777	86	>10000	9.8
BH5	1.1 - 1.5	95.4	317	133	6.4	549	7.4	3.7	198	71	>10000	11.1
	2.6 - 3.0	58.9	213	86	4.0	283	8.0	2.9	289	47	>10000	6.6
	4.1 - 4.6	93.0	288	128	6.4	569	5.7	5.1	429	118	>10000	8.5
	5.6 - 6.1	87.1	270	108	6.2	456	8.3	4.2	76	93	>10000	10.0
	7.2 - 7.6	96.5	292	126	6.5	520	5.1	3.4	86	105	>10000	8.1
	10.2 - 10.7	52.6	178	71	5.8	284	5.8	5.5	443	58	8890	6.1
	11.7 - 12.2	56.1	172	61	6.5	253	6.3	4.8	110	48	7790	6.1
	14.8 - 15.2	95.4	272	74	5.0	401	5.4	4.7	99	90	>10000	10.1
	16.3 - 16.8	75.1	211	87	5.2	323	11.2	4.3	90	81	>10000	7.7
	16.3 - 16.8*	74.6	212	90	5.1	315	12.9	4.4	57	81	>10000	7.5
	19.2 - 19.9	70.8	207	61	5.8	287	13.1	3.7	40	36	9480	9.0

Table B.3 Summary of solid-phase carbon and sulfur speciation data for core samples collected in February and March 2005. Asterisks denote replicate analyses.

Borehole	Depth	Carbon Content (wt. % as C)				Sulfur Content (wt. % as C)		
	Interval (m)	Total	Carbonate	Graphitic	Organic	Total-S	Sulfate-S	Sulfide-S
BH1	1.5 - 1.7	3.74	3.18	0.23	0.33	19.42	9.81	9.61
	1.5 - 1.7*	3.76	3.20			19.59	6.78	12.81
	1.8 - 2.1	3.80	3.20	0.11	0.50	18.19	7.83	10.37
	2.1 - 2.4	4.06	3.43	0.12	0.51	22.50	7.36	15.14
	2.1 - 2.4*	4.08	3.46			22.68	7.57	15.10
	3.2 - 3.4	4.68	3.96	0.29	0.44	20.68	8.99	11.69
BH2	1.1 - 1.5	3.70	3.08	0.14	0.48	23.14	7.74	15.40
	2.6 - 3.0	3.92	3.46	0.16	0.30	21.82	10.61	11.21
	4.1 - 4.6	4.70	3.57	0.19	0.94	22.86	8.17	14.69
	4.1 - 4.6*	4.67	3.54			22.54	9.19	13.35
	5.6 - 6.1	4.10	3.74	0.23	0.13	21.51	10.17	11.34
	7.2 - 7.6	4.70	4.27	0.22	0.21	17.61	7.96	9.64
	8.5 - 9.1	4.49	3.96	0.43	0.10	18.96	5.87	13.08
	10.1 - 10.7	4.52	3.78	0.32	0.42	18.88	8.67	10.21
	11.6 - 12.2	3.67	3.24	0.26	0.17	21.54	7.34	14.21
	13.1 - 13.7	3.75	3.20	0.13	0.42	24.27	7.72	16.55
	16.2 - 16.8	4.60	3.87	0.14	0.59	14.84	6.45	8.39
	17.7 - 18.3	2.90	2.42	0.31	0.18	15.32	8.17	7.15
	19.2 - 19.8	3.06	2.47	0.39	0.20	13.56	6.41	7.15
BH3	1.1 - 1.5	3.64	3.16	0.09	0.39	15.96	8.33	7.63
	2.6 - 3.0	4.01	3.49	0.19	0.33	18.22	8.15	10.08
	2.6 - 3.0*	3.97	3.47			17.66	8.12	9.54
	4.1 - 4.6	4.29	3.74	0.19	0.36	18.27	9.89	8.38
	5.6 - 6.1	4.25	3.78	0.25	0.22	20.36	8.09	12.27
	7.2 - 7.6	1.90	1.94	0.18	-0.23	8.39	3.65	4.74
	8.7 - 9.1	3.50	2.98	0.17	0.35	15.58	8.05	7.53
	10.2 - 10.7	3.49	3.01	0.15	0.34	15.85	8.06	7.79
	11.7 - 12.2	3.38	2.76	0.16	0.46	17.04	8.50	8.55
	14.8 - 15.2	3.16	2.61	0.22	0.32	17.62	8.29	9.34
	16.3 - 16.8	3.46	2.89	0.17	0.40	14.43	7.13	7.30
	17.8 - 18.3	1.89	1.44	0.14	0.30	20.98	12.33	8.65
	19.2 - 19.9	3.80	3.36	0.09	0.35	14.58	7.77	6.81
	20.7 - 21.5	3.65	3.04	0.19	0.42	13.84	7.36	6.48
	22.2 - 23.0	3.23	2.57	0.28	0.38	15.26	6.84	8.41
	22.2 - 23.0*	3.22	2.59	0.28	0.36	14.95	7.50	7.45
	23.8 - 24.5	3.56	2.79	0.31	0.47	10.98	5.00	5.98

Table B.3 Continued.

Borehole	Depth	Carbon Content (wt. % as C)				Sulfur Content (wt. % as C)		
	Interval (m)	Total	Carbonate	Graphitic	Organic	Total-S	Sulfate-S	Sulfide-S
BH4	2.6 - 3.0	3.60	3.12	0.20	0.28	17.42	8.30	9.13
	5.6 - 6.1	3.65	3.01	0.23	0.41	19.25	9.14	10.11
	7.2 - 7.6	5.68	5.03	0.09	0.56	18.02	8.27	9.75
	9.2 - 9.6	5.45	4.95	0.13	0.37	18.84	9.72	9.12
	10.2 - 10.7	5.32	4.64	0.30	0.38	18.79	7.64	11.15
	11.7 - 12.2	4.76	4.18	0.11	0.47	19.49	6.87	12.62
	13.3 - 13.7	5.24	4.56	0.21	0.47	17.74	5.08	12.66
	14.8 - 15.2	3.90	3.32	0.13	0.45	16.97	6.20	10.77
BH5	1.1 - 1.5	3.97	3.38	0.50	0.10	17.08	8.55	8.53
	2.6 - 3.0	2.84	2.36	0.13	0.36	10.38	5.95	4.43
	4.1 - 4.6	3.66	3.10	0.10	0.46	16.06	8.18	7.87
	5.6 - 6.1	3.91	3.28	0.26	0.36	16.10	6.95	9.15
	7.2 - 7.6	4.28	3.57	0.36	0.35	17.06	7.43	9.63
	7.2 - 7.6*	4.28	3.54			17.29	7.54	9.75
	8.7 - 9.1	3.05	4.01	0.12	-1.08	11.61	6.14	5.47
	10.2 - 10.7	3.38	2.64	0.12	0.61	14.03	6.96	7.07
	11.7 - 12.2	3.52	2.87	0.12	0.53	14.79	6.44	8.35
	14.8 - 15.2	4.99	4.38	0.53	0.09	14.93	6.31	8.62
	16.3 - 16.8	4.24	3.44	0.30	0.51	13.24	5.22	8.02
	17.8 - 18.3	3.53	3.94	0.58	-0.99	10.81	6.10	4.71
	19.2 - 19.9	4.75	4.01	0.20	0.53	12.04	5.92	6.13
	20.7 - 21.5	4.40	3.48	0.20	0.72	18.44	7.65	10.79

Table B.4 Summary of acid-base accounting data for core samples collected in February and March 2005. Asterisks denote replicate analyses.

Borehole	Depth	Paste	HCl	NaOH	Equivalent Mass (kg $CaCO_3$ t^{-1})			NP:AP
	Interval (m)	pH	mL	mL	AP	NP	NNP	
BH1	1.8 - 2.1	7.56	65	4.10	324	118	-206	0.36
	2.1 - 2.4	7.63	85	4.05	473	171	-302	0.36
	3.2 - 3.4	7.77	68	5.20	365	112	-253	0.31
BH2	2.6 - 3.0	7.70	70	6.00	350	107	-243	0.31
	5.6 - 6.1	7.71	70	6.05	354	107	-248	0.30
	7.2 - 7.6	7.87	72	6.00	301	113	-189	0.37
	8.5 - 9.1	7.73	66	4.30	409	118	-291	0.29
	11.6 - 12.2	7.54	66	3.80	444	124	-319	0.28
	14.6 - 15.2	7.63	65	5.65	255	99	-156	0.39
	17.7 - 18.3	7.39	45	3.20	223	77	-146	0.35
	19.2 - 19.8	7.02	50	3.60	223	85	-138	0.38
BH3	2.6 - 3.0	7.32	62	4.20	315	109	-206	0.35
	5.6 - 6.1	7.53	70	4.00	383	132	-251	0.35
	7.2 - 7.6	7.91	45	2.70	148	83	-65	0.56
	8.7 - 9.1	7.68	45	3.70	235	71	-164	0.30
	10.2 - 10.7	7.74	50	3.80	243	83	-161	0.34
	11.7 - 12.2	7.69	55	4.50	267	87	-180	0.33
	14.8 - 15.2	7.78	55	3.75	292	96	-195	0.33
	16.3 - 16.8	7.70	57	4.10	228	97	-131	0.43
	16.3 - 16.8*	7.71	57	4.20	228	96	-132	0.42
	17.8 - 18.3	7.23	45	2.10	270	91	-179	0.34
	20.7 - 21.5	7.63	60	4.90	202	95	-107	0.47
	22.2 - 23.0	7.58	65	5.40	263	102	-161	0.39
	23.8 - 24.5	7.53	50	3.85	187	82	-105	0.44
BH4	2.6 - 3.0	8.01	60	4.00	285	106	-179	0.37
	5.6 - 6.1	7.65	60	5.50	316	88	-228	0.28
	7.2 - 7.6	7.78	80	7.70	305	112	-193	0.37
	10.2 - 10.7	7.87	70	4.40	348	127	-221	0.37
	11.7 - 12.2	7.88	70	6.05	394	107	-288	0.27
	13.3 - 13.7	7.88	85	5.45	396	153	-242	0.39
	14.8 - 15.2	7.72	65	4.40	337	114	-222	0.34
BH5	1.1 - 1.5	7.21	60	3.40	267	114	-153	0.43
	2.6 - 3.0	7.55	50	4.35	138	76	-62	0.55
	4.1 - 4.6	7.23	60	4.20	246	104	-142	0.42
	5.6 - 6.1	7.44	60	3.70	286	110	-176	0.38
	5.6 - 6.1*	7.90	65	4.35	286	115	-171	0.40
	7.2 - 7.6	8.08	60	5.25	113	91	-23	0.80
	10.2 - 10.7	7.48	45	4.70	221	58	-162	0.26
	11.7 - 12.2	7.08	50	2.45	261	100	-161	0.38
	14.8 - 15.2	7.65	70	7.50	269	89	-181	0.33
	16.3 - 16.8	7.08	72	4.50	251	131	-119	0.52
	19.2 - 19.9	7.79	56	4.35	191	92	-100	0.48

Table B.5 Summary of most probable number populations of sulfate-reducing bacteria (SRB), iron-reducing bacteria (IRB), acid-producing (fermentative) bacteria (APB), neutrophilic sulfur-oxidizing bacteria (nSOB), acidophilic sulfur-oxidizing bacteria (aSOB) and iron-oxidizing bacteria (IOB) for core samples collected in February and March 2005..

Borehole	Depth	Most Probable Number Population (cells g^{-1} tailings)					
	Interval (m)	SRB	IRB	APB	nSOB	aSOB	IOB
BH1	1.5 - 1.7	7.9E+01	2.3E+01	1.7E+02	1.3E+05	3.3E+03	7.9E+01
	3.1 - 3.2	4.1E+01	2.3E+01	0.0E+00	6.8E+02	0.0E+00	2.4E+02
BH2	1.1 - 1.5	1.4E+01	5.2E+02	0.0E+00	0.0E+00	0.0E+00	2.3E+01
	4.1 - 4.6	2.1E+01	5.2E+02	0.0E+00	2.0E+04	0.0E+00	3.3E+01
	7.2 - 7.6	1.3E+02	1.3E+02	0.0E+00	2.0E+02	0.0E+00	2.4E+02
	10.2 - 10.7	1.3E+04	1.7E+03	0.0E+00	1.6E+04	9.3E+01	2.4E+02
	13.3 - 13.7	1.3E+03	1.7E+03	0.0E+00	0.0E+00	0.0E+00	4.8E+01
	16.3 - 16.8	9.2E+02	1.6E+03	4.8E+01	9.2E+05	1.4E+03	2.3E+01
	19.2 - 19.9	4.5E-01	2.3E+01	0.0E+00	7.6E+00	0.0E+00	2.3E+01
BH3	1.1 - 1.5	1.6E+03	3.3E+02	1.1E+03	2.3E+06	2.2E+03	2.3E+01
	4.1 - 4.6	3.3E+02	3.3E+01	2.0E+00	3.5E+06	0.0E+00	2.4E+02
	7.2 - 7.6	2.2E+02	2.3E+01	2.2E+03	1.3E+01	0.0E+00	2.4E+02
	10.2 - 10.7	1.4E+01	3.3E+01	1.1E+02	4.5E+00	0.0E+00	2.4E+02
	11.7 - 12.2	6.8E+02	5.2E+02	4.8E+03	2.3E+05	7.3E+01	1.3E+02
	16.3 - 16.8	1.1E+02	2.3E+01	2.4E+02	9.4E+02	0.0E+00	4.8E+01
	19.2 - 19.9	7.9E+02	2.2E+04	1.4E+03	3.5E+06	0.0E+00	7.9E+01
	22.2 - 23.0	1.3E+02	2.3E+01	1.4E+02	1.3E+05	0.0E+00	1.3E+02
BH4	2.6 - 3.0	2.2E+03	2.3E+01	0.0E+00	0.0E+00	0.0E+00	1.3E+02
	5.6 - 6.1	1.3E+01	2.3E+01	0.0E+00	0.0E+00	0.0E+00	3.3E+01
	8.7 - 9.1	7.9E+01	2.3E+01	0.0E+00	4.8E+01	0.0E+00	2.4E+02
	11.7 - 12.2	3.3E+01	2.3E+01	0.0E+00	0.0E+00	0.0E+00	2.4E+02
	14.8 - 15.2	1.3E+01	2.3E+01	0.0E+00	0.0E+00	0.0E+00	2.4E+02
BH5	1.1 - 1.5	1.68E+05	5.18E+02	3.49E+05	5.42E+07	3.49E+03	7.00E+01
	4.1 - 4.6	1.75E+02	2.31E+01	6.80E+00	1.30E+06	0.00E+00	2.31E+01
	5.6 - 6.1	4.10E+01	2.31E+01	2.00E+00	7.00E+05	0.00E+00	4.83E+01
	7.2 - 7.6	7.92E+01	1.68E+02	0.00E+00	0.00E+00	0.00E+00	1.30E+02
	8.7 - 9.1	1.07E+03	2.31E+02	1.39E+02	4.50E+03	0.00E+00	2.40E+02
	11.7 - 12.2	7.92E+01	1.68E+02	4.50E+00	1.37E+01	0.00E+00	2.40E+02
	14.8 - 15.2	4.83E+02	5.18E+01	6.80E+00	7.60E+00	0.00E+00	2.40E+02
	17.8 - 18.3	4.83E+01	7.92E+02	4.50E+00	4.10E+02	0.00E+00	2.40E+02
	19.2 - 19.9	4.83E+02	2.31E+01	2.00E+00	4.83E+04	0.00E+00	2.40E+02
	20.7 - 21.5	1.30E+02	7.92E+02	1.20E+01	1.71E+06	0.00E+00	7.92E+01

Table B.6 Summary of field parameters for pore-water samples collected in 2005 and 2007. Alkalinity is given in mg L^{-1} as $CaCO_3$.

Lysimeter ID	Depth (m)	Sampling Date	Temp. (°C)	pH	E_h (mV)	Alkalinity (mg L^{-1})
TC2-BE	0.50	12-Oct-05	9.1	7.19	195	250
TC2-BW	0.50	11-Oct-05	8.7	7.24	182	282
TC2-CE	0.75	12-Oct-05	8.7	7.04	172	276
TC2-CW	0.75	11-Oct-05	9.0	7.44	163	186
TC2-DE	1.00	12-Oct-05	8.8	7.12	158	282
TC2-DW	1.00	11-Oct-05	8.9	7.93	175	200
TC2-EE	1.25	12-Oct-05	9.3	7.52	180	152
TC2-EW	1.25	11-Oct-05	9.2	7.66	195	90
TC2-FW	1.50	11-Oct-05	9.8	7.64	155	160
TC2-GE	1.75	12-Oct-05	9.4	7.49	210	38
TC2-GW	1.75	11-Oct-05	9.9	8.12	187	52
TC2-HE	2.00	12-Oct-05	10.1	8.23	195	48
TC2-IE	2.50	12-Oct-05	10.4	7.50	198	72
TC2-IW	2.50	11-Oct-05	10.0	7.48	199	58
TC2-JW	3.00	11-Oct-05	10.3	7.74	195	46
TC2-KE	3.50	12-Oct-05	10.4	7.35	193	44
TC2-KW	3.50	11-Oct-05	10.0	7.37	185	132
TC2-LE	4.00	12-Oct-05	10.5	8.14	201	38
TC2-AE	0.25	25-Sep-07	11.4	6.68	319	320
TC2-BE	0.50	25-Sep-07	12.5	6.93	191	580
TC2-CE	0.75	25-Sep-07	14.0	7.05	200	720
TC2-DE	1.00	25-Sep-07	12.9	6.94	283	480
TC2-DW	1.00	26-Sep-07	11.9	7.16	230	460
TC2-EW	1.25	26-Sep-07	12.3	7.26	284	400
TC2-FW	1.50	26-Sep-07	11.9	7.23	240	480
TC2-GE	1.75	25-Sep-07	13.0	7.22	139	360
TC2-HW	2.00	26-Sep-07	11.8	7.8	295	180
TC2-IE	2.50	25-Sep-07	13.9	7.41	235	120
TC2-IW	2.50	26-Sep-07	11.5	7.39	406	80
TC2-KE	3.50	25-Sep-07	12.9	7.72	324	100
TC2-KW	3.50	26-Sep-07	13.0	7.61	-52	160
TC2-LE	4.00	25-Sep-07	12.6	7.97	338	100

Table B.7 Summary of anion data for pore-water samples collected in 2005 and 2007.

Lysimeter	Depth	Sampling	Aqueous Concentration (mg L^{-1})						DOC	NH_3-N
ID	(m)	Date	Br	Cl	NO_3-N	NO_2-N	SO_4	S_2O_3	(mg/L)	(mg/L)
TC2-BE	0.50	12-Oct-05	-1.0	1.3	-0.25	-0.25	2160	101	1.4	0.6
TC2-BW	0.50	11-Oct-05	-1.0	1.3	-0.25	-0.25	3330	-5.0	2.2	16
TC2-CE	0.75	12-Oct-05	-1.0	1.3	-0.25	-0.25	1740	-5.0	1.9	0.6
TC2-CW	0.75	11-Oct-05	-1.0	1.3	-0.25	-0.25	1810	-5.0	1.5	1.4
TC2-DE	1.00	12-Oct-05	-1.0	1.3	-0.25	-0.25	4160	239	4.9	3.5
TC2-DW	1.00	11-Oct-05	-1.0	2.9	-0.25	-0.25	1890	185	14	0.2
TC2-EE	1.25	12-Oct-05	-1.0	1.3	-0.25	-0.25	2620	140	3.2	3.4
TC2-EW	1.25	11-Oct-05	-1.0	1.3	-0.25	-0.25	1570	474	12	5.4
TC2-FW	1.50	11-Oct-05	-1.0	1.3	-0.25	-0.25	1770	35	7.7	4.7
TC2-GE	1.75	12-Oct-05	-1.0	3.6	-0.25	-0.25	1960	715	78	3.5
TC2-GW	1.75	11-Oct-05	-1.0	9.2	-0.25	-0.25	2270	1290	31	6.2
TC2-HE	2.00	12-Oct-05	-1.0	5.3	-0.25	-0.25	2170	1330		7.9
TC2-IE	2.50	12-Oct-05	-1.0	3.6	-0.25	-0.25	2330	1040	32	5.4
TC2-IW	2.50	11-Oct-05	-1.0	9.0	-0.25	-0.25	2040	1720	76	8.1
TC2-JW	3.00	11-Oct-05	-1.0	3.3	-0.25	-0.25	1390	977	22	5.7
TC2-KE	3.50	12-Oct-05	-1.0	8.5	-0.25	-0.25	1960	1800	63	7.1
TC2-KW	3.50	11-Oct-05	-1.0	9.7	-0.25	-0.25	2100	1780	90	7.3
TC2-LE	4.00	12-Oct-05	-1.0	9.4	-0.25	-0.25	2030	1940	79	6.8
TC2-AE	0.25	25-Sep-07	-0.4	-1.0	-0.1	-0.1	4180	-2.0	-1.3	-1.0
TC2-BE	0.50	25-Sep-07	-4.0	-10	-1.0	1.1	8970	69	-1.3	-1.0
TC2-CE	0.75	25-Sep-07	-4.0	-10	-1.0	-1.0	5310	23.5	-1.3	-1.0
TC2-DE	1.00	25-Sep-07	-4.0	-10	-1.0	-1.0	6450	-20	-1.3	-1.0
TC2-DW	1.00	26-Sep-07	-0.4	3.2	-0.1	-0.1	2170	5.8	-1.3	1.3
TC2-EW	1.25	26-Sep-07	-0.4	6.1	-0.1	-0.1	2320	-2.0	-1.3	1.5
TC2-FW	1.50	26-Sep-07	-0.4	4.0	-0.1	-0.1	2130	4.9	-1.3	1.1
TC2-GE	1.75	25-Sep-07	-0.4	4.2	-0.1	-0.1	1990	-2.0	4.8	1.7
TC2-HW	2.00	26-Sep-07	-0.4	2.2	-0.1	-0.1	2680	3.1	1.9	2.5
TC2-IE	2.50	25-Sep-07	-0.4	-1.0	-0.1	-0.1	1750	-2.0	5.0	1.3
TC2-IW	2.50	26-Sep-07	-0.4	2.4	-0.1	-0.1	2200	481	3.9	11
TC2-KE	3.50	25-Sep-07	-0.4	1.6	-0.1	-0.1	2720	129	-1.3	3.2
TC2-KW	3.50	26-Sep-07	-0.4	4.7	-0.1	-0.1	2170	262	-1.3	40
TC2-LE	4.00	25-Sep-07	-4.0	1.5	-1.0	-1.0	2420	315	-1.3	7.2

Table B.8 Summary of major cation data for pore-water samples collected in 2005 and 2007.

Lysimeter	Depth	Sampling	Aqueous Concentration (mg L^{-1})							
ID	(m)	Date	Al	Ca	Fe	Mg	K	Si	Na	Sr
TC2-BE	0.50	12-Oct-05	-0.25	546	3.0	298	-5.0	6.2	-15	0.33
TC2-BW	0.50	11-Oct-05	-0.25	486	4.2	482	13	9.0	-15	0.41
TC2-CE	0.75	12-Oct-05	0.27	558	4.6	94	5.7	12	-15	-0.25
TC2-CW	0.75	11-Oct-05	-0.25	594	7.8	72	5.2	9.9	-15	0.92
TC2-DE	1.00	12-Oct-05	-0.25	526	5.6	672	11	6.7	-15	0.33
TC2-DW	1.00	11-Oct-05	-0.25	537	0.54	268	16	16	18	0.52
TC2-EE	1.25	12-Oct-05	-0.25	518	0.54	318	9.6	9.5	-15	0.45
TC2-EW	1.25	11-Oct-05	-0.25	627	-0.25	249	17	9.9	-15	0.72
TC2-FW	1.50	11-Oct-05	-0.25	544	0.99	160	14	12	-15	0.36
TC2-GE	1.75	12-Oct-05	-0.25	642	-0.25	228	19	7.9	21	0.72
TC2-GW	1.75	11-Oct-05	-0.25	711	-0.25	295	29	6.8	70	0.87
TC2-HE	2.00	12-Oct-05	-0.25	733	-0.25	265	23	10	40	0.89
TC2-IE	2.50	12-Oct-05	0.26	665	-0.25	288	21	8.1	33	0.93
TC2-IW	2.50	11-Oct-05	-0.25	842	-0.25	276	35	5.0	67	1.1
TC2-JW	3.00	11-Oct-05	-0.25	809	-0.25	125	27	5.9	19	1.1
TC2-KE	3.50	12-Oct-05	-0.25	841	-0.25	226	34	5.8	63	1.1
TC2-KW	3.50	11-Oct-05	-0.25	826	0.54	306	27	7.2	70	1.4
TC2-LE	4.00	12-Oct-05	-0.25	843	-0.25	261	25	5.4	69	1.3
TC2-AE	0.25	25-Sep-07	-0.50	473	11.90	649	-10	11	-30	5.9
TC2-BE	0.50	25-Sep-07	-0.50	439	27.30	2250	-10	11	-30	1.4
TC2-CE	0.75	25-Sep-07	-0.50	481	13.90	1260	-10	12	-30	0.8
TC2-DE	1.00	25-Sep-07	-0.50	496	3.01	1440	-10	11	-30	0.8
TC2-DW	1.00	26-Sep-07	-0.50	552	10.02	261	-10	14	-30	-0.5
TC2-EW	1.25	26-Sep-07	-0.50	560	15.10	346	-10	11	-30	-0.5
TC2-FW	1.50	26-Sep-07	-0.50	586	12.40	253	-10	13	-30	-0.5
TC2-GE	1.75	25-Sep-07	-0.50	609	13.80	216	-10	13	-30	-0.5
TC2-HW	2.00	26-Sep-07	-0.50	481	-0.50	361	-10	17	-30	-0.5
TC2-IW	2.50	26-Sep-07	-0.50	539	-0.50	289	2.1	11	-30	0.7
TC2-KE	3.50	25-Sep-07	-0.50	553	-0.50	432	-10	9.5	-30	-0.5
TC2-KW	3.50	26-Sep-07	-0.50	566	-0.50	253	2.2	16	49	1.0
TC2-LE	4.00	25-Sep-07	-0.50	549	-0.50	333	-10	9	-30	0.6

Table B.9 Summary of trace element data for pore-water samples collected in 2005 and 2007.

Lysimeter	Depth	Sampling	Aqueous Concentration ($\mu g\ L^{-1}$)						
ID	(m)	Date	Sb	As	Ba	Cd	Cr	Co	Cu
TC2-BE	0.50	12-Oct-05	21	2.8	9.6	-2.0	6.7	-5.0	-1.0
TC2-BW	0.50	11-Oct-05	28	9.1	9.0	-2.0	11	-5.0	-1.0
TC2-CE	0.75	12-Oct-05	19	5.7	11	-2.0	7.6	-5.0	2.3
TC2-CW	0.75	11-Oct-05	25	8.1	15	-2.0	7.4	-5.0	-1.0
TC2-DE	1.00	12-Oct-05	12	23	11	-2.0	7.9	-5.0	-1.0
TC2-DW	1.00	11-Oct-05	39	13	12	-2.0	9.3	-5.0	-1.0
TC2-EE	1.25	12-Oct-05	32	8.6	14	-2.0	2.6	-5.0	-1.0
TC2-EW	1.25	11-Oct-05	31	5.1	17	-2.0	2.6	-5.0	5.4
TC2-FW	1.50	11-Oct-05	27	10	16	-2.0	3.6	-5.0	-1.0
TC2-GE	1.75	12-Oct-05	34	3.5	17	-2.0	1.9	-5.0	-1.0
TC2-GW	1.75	11-Oct-05	52	6.5	21	-2.0	16	-5.0	12
TC2-HE	2.00	12-Oct-05	47	5.6	20	-2.0	3.7	-5.0	2.7
TC2-IE	2.50	12-Oct-05	29	3.1	18	-2.0	5.0	-5.0	9.5
TC2-IW	2.50	11-Oct-05	62	7.0	36	-2.0	15	-5.0	114
TC2-JW	3.00	11-Oct-05	56	5.6	26	-2.0	4.2	-5.0	41
TC2-KE	3.50	12-Oct-05	56	3.4	35	-2.0	11	-5.0	67
TC2-KW	3.50	11-Oct-05	64	6.6	26	4.9	19	-5.0	76
TC2-LE	4.00	12-Oct-05	49	4.5	34	-2.0	12	-5.0	172
TC2-AE	0.25	25-Sep-07	-0.50	3.0	7.7	45	2.4	25	26
TC2-BE	0.50	25-Sep-07	-0.50	8.8	7.3	1.5	4.2	-2.5	11
TC2-CE	0.75	25-Sep-07	-0.50	18	5.0	1.3	8.1	-2.5	5.2
TC2-DE	1.00	25-Sep-07	0.76	4.7	6.9	1.8	3.2	2.6	10
TC2-DW	1.00	26-Sep-07	3.6	21	8.6	-1.0	4.1	-2.5	2.8
TC2-EW	1.25	26-Sep-07	3.9	12	11	-1.0	2.8	-2.5	2.6
TC2-FW	1.50	26-Sep-07	18	15	10	-1.0	2.6	-2.5	1.0
TC2-GE	1.75	25-Sep-07	26	18	8.1	-1.0	4.4	-2.5	2.1
TC2-HW	2.00	26-Sep-07	20	12	8.4	-1.0	2.0	-2.5	-0.5
TC2-IE	2.50	25-Sep-07	-0.50	9.6	8.1	1.0	3.7	-2.5	-0.5
TC2-IW	2.50	26-Sep-07	22	3.8	26	-1.0	2.4	-2.5	2.7
TC2-KE	3.50	25-Sep-07	18	6.4	12	-1.0	1.5	-2.5	1.4
TC2-KW	3.50	26-Sep-07	60	43	12	-1.0	2.9	-2.5	-0.5
TC2-LE	4.00	25-Sep-07	31	5.4	17	1.0	4.3	-2.5	-0.5

Table B.9 Continued.

Lysimeter	Depth	Sampling	Aqueous Concentration (μg L^{-1})							
ID	(m)	Date	Pb	Mn	Mo	Ni	Se	Ag	Tl	Zn
TC2-BE	0.50	12-Oct-05	-1.0	552	7.8	53	-5.0	-1.0	75	11700
TC2-BW	0.50	11-Oct-05	-1.0	1440	8.4	81	7.2	-1.0	66	22700
TC2-CE	0.75	12-Oct-05	-1.0	312	8.0	45	-5.0	-1.0	30	5260
TC2-CW	0.75	11-Oct-05	-1.0	3990	-5.0	126	12	-1.0	43	39200
TC2-DE	1.00	12-Oct-05	-1.0	656	20.8	64	-5.0	-1.0	48	8730
TC2-DW	1.00	11-Oct-05	-1.0	479	13.5	27	5.9	-1.0	48	519
TC2-EE	1.25	12-Oct-05	-1.0	968	8.5	38	-5.0	-1.0	53	882
TC2-EW	1.25	11-Oct-05	-1.0	918	7.7	26	8.2	9.0	72	1180
TC2-FW	1.50	11-Oct-05	-1.0	820	8.1	30	5.2	-1.0	70	576
TC2-GE	1.75	12-Oct-05	-1.0	404	8.7	29	5.1	2.1	71	93
TC2-GW	1.75	11-Oct-05	7.1	797	10.7	22	12	12	103	66
TC2-HE	2.00	12-Oct-05	-1.0	219	10.6	32	7.9	9.9	135	27
TC2-IE	2.50	12-Oct-05	19.1	833	8.9	41	6.5	26	97	828
TC2-IW	2.50	11-Oct-05	969	873	-5.0	23	17	121	144	780
TC2-JW	3.00	11-Oct-05	188	859	7.6	22	12	66	144	165
TC2-KE	3.50	12-Oct-05	358	600	6.9	39	12	96	121	201
TC2-KW	3.50	11-Oct-05	937	1270	5.8	37	20	73	141	5770
TC2-LE	4.00	12-Oct-05	-1.0	-0.5	-5.0	-1.5	11	170	-0.50	62
TC2-AE	0.25	25-Sep-07	1.3	33950	-2.5	1001	6.7	-0.5	315	176500
TC2-BE	0.50	25-Sep-07	-0.5	13100	13	194	8.7	-0.5	53	66500
TC2-CE	0.75	25-Sep-07	-0.5	2290	16	102	6.3	-0.5	19	23600
TC2-DE	1.00	25-Sep-07	-0.5	7990	7.0	251	7.2	-0.5	41	64200
TC2-DW	1.00	26-Sep-07	-0.5	283	11	45	-2.5	-0.5	32	8520
TC2-EW	1.25	26-Sep-07	0.6	393	6.6	28	3.0	-0.5	80	12400
TC2-FW	1.50	26-Sep-07	-0.5	240	14	30	-2.5	0.6	55	7960
TC2-GE	1.75	25-Sep-07	-0.5	222	4.3	41	-2.5	-0.5	69	3890
TC2-HW	2.00	26-Sep-07	-0.5	766	8.2	20	-2.5	-0.5	65	32
TC2-IE	2.50	25-Sep-07	-0.5	588	3.7	25	-2.5	-0.5	70	1510
TC2-IW	2.50	26-Sep-07	5.2	448	12	22	-2.5	4.8	49	473
TC2-KE	3.50	25-Sep-07	-0.5	501	6.8	26	2.5	-0.5	33	206
TC2-KW	3.50	26-Sep-07	0.7	547	7.4	20	-2.5	-0.5	-0.25	43
TC2-LE	4.00	25-Sep-07	1.0	451	8.7	15	-2.5	0.6	43	60

Table B.10 Saturation indices calculated with MINTEQA2 for pore-water samples collected in 2005 and 2007.

			Saturation Index Calclated by MINTEQA2														
Lysimeter ID	Depth (m)	Sampling Date	$Al(OH)_3$ amorphous	Anhydrite [$CaSO_4$]	Aragonite [$CaCO_3$]	Barite [$BaSO_4$]	Calcite [$CaCO_3$]	Dolomite [$CaMg(CO_3)_2$]	Epsomite [$MgSO_4{\cdot}7H_2O$]	Ferrihydrite [$Fe(OH)_3$]	Gibbsite [$Al(OH)_3$]	Goethite [α-FeOOH]	Gypsum [$CaSO_4{\cdot}2H_2O$]	Siderite [$FeCO_3$]	Rhodochrosite [$MnCO_3$]	Smithsonite [$ZnCO_3$]	Lepidocrocite [γ-FeOOH]
TC2-BE	0.50	12-Oct-05	-1.21	-0.32	0.09	0.48	0.29	0.46	-2.37	-1.20	1.63	4.09	-0.03	-2.86	-0.95	-0.30	2.32
TC2-BW	0.50	11-Oct-05	-1.25	-0.28	0.05	0.59	0.25	0.63	-2.07	-1.15	1.60	4.13	0.01	-2.65	-0.51	-0.03	2.38
TC2-CE	0.75	12-Oct-05	0.36	-0.31	0.04	0.54	0.24	-0.17	-2.87	-1.59	3.20	3.69	-0.02	-2.48	-1.26	-0.71	1.93
TC2-CW	0.75	11-Oct-05	-1.42	-0.27	0.27	0.70	0.47	0.15	-2.98	-0.35	1.43	4.94	0.02	-2.07	0.06	0.36	3.17
TC2-DE	1.00	12-Oct-05	-1.16	-0.23	-0.08	0.68	0.13	0.49	-1.91	-1.05	1.69	4.23	0.05	-1.89	-1.01	-0.59	2.47
TC2-DW	1.00	11-Oct-05	-1.90	-0.36	0.74	0.54	0.94	1.70	-2.45	-0.97	0.95	4.31	-0.07	-3.86	-0.41	-1.16	2.55
TC2-EE	1.25	12-Oct-05	-1.52	-0.28	0.15	0.73	0.35	0.64	-2.29	-1.58	1.32	3.72	0.00	-3.86	-0.60	-1.35	1.94
TC2-EW	1.25	11-Oct-05	-1.65	-0.37	0.22	0.57	0.42	0.57	-2.57	-1.65	1.20	3.65	-0.08	-4.70	-0.65	-1.21	1.87
TC2-FW	1.50	11-Oct-05	-1.65	-0.33	0.40	0.68	0.60	0.81	-2.66	-1.13	1.19	4.19	-0.04	-3.16	-0.47	-1.33	2.39
TC2-GE	1.75	12-Oct-05	-1.50	-0.29	-0.34	0.66	-0.14	-0.59	-2.53	-1.91	1.34	3.40	-0.01	-5.25	-1.55	-2.84	1.61
TC2-GW	1.75	11-Oct-05	-2.14	-0.25	0.42	0.72	0.62	1.01	-2.44	-0.62	0.69	4.71	0.03	-4.72	-0.57	-2.36	2.90
TC2-HE	2.00	12-Oct-05	-2.26	-0.24	0.51	0.68	0.71	1.13	-2.49	-0.56	0.57	4.77	0.04	-5.07	-1.05	-2.69	2.96
TC2-IE	2.50	12-Oct-05	-0.14	-0.25	-0.05	0.68	0.14	0.08	-2.42	-1.93	2.69	3.42	0.03	-4.81	-0.97	-1.64	1.60
TC2-IW	2.50	11-Oct-05	-1.52	-0.24	-0.07	0.86	0.13	-0.08	-2.53	-1.78	1.31	3.55	0.04	-4.75	-1.08	-1.77	1.74
TC2-JW	3.00	11-Oct-05	-1.78	-0.31	0.15	0.65	0.34	0.03	-2.93	-1.28	1.06	4.07	-0.03	-4.78	-0.86	-2.22	2.25
TC2-KE	3.50	12-Oct-05	-1.42	-0.24	-0.30	0.83	-0.11	-0.62	-2.62	-2.10	1.41	3.25	0.04	-4.82	-1.47	-2.58	1.42
TC2-KW	3.50	11-Oct-05	-1.42	-0.25	0.16	0.72	0.36	0.44	-2.48	-1.82	1.41	3.51	0.03	-3.97	-0.69	-0.69	1.70
TC2-LE	4.00	12-Oct-05	-2.19	-0.24	0.39	0.82	0.59	0.82	-2.56	-0.49	0.64	4.86	0.04	-5.02	-3.57	-2.47	3.03
TC2-AE	0.25	25-Sep-07	-0.05	-0.27	-0.48	0.48	-0.29	-0.26	-1.96	-1.71	2.77	3.67	0.00	-4.47	0.35	0.38	1.81
TC2-BE	0.50	25-Sep-07	-0.19	-0.26	-0.13	0.46	0.05	1.01	-1.40	1.12	2.62	6.55	0.01	0.32	0.28	0.27	4.64
TC2-CE	0.75	25-Sep-07	-0.32	-0.28	0.26	0.21	0.44	1.51	-1.72	-0.98	2.48	4.50	-0.01	-2.04	-0.17	0.15	2.54
TC2-DE	1.00	25-Sep-07	-0.20	-0.23	-0.07	0.42	0.11	0.89	-1.62	-2.12	2.60	3.33	0.04	-4.60	0.08	0.29	1.40
TC2-DW	1.00	26-Sep-07	-0.30	-0.30	0.38	0.40	0.57	0.99	-2.46	-0.99	2.52	4.41	-0.02	-2.94	-1.00	-0.21	2.53
TC2-EW	1.25	26-Sep-07	-0.40	-0.29	0.42	0.47	0.61	1.19	-2.35	-0.23	2.41	5.19	-0.02	-3.38	-0.82	-0.01	3.30
TC2-FW	1.50	26-Sep-07	-0.36	-0.28	0.50	0.47	0.69	1.19	-2.48	-0.62	2.46	4.78	-0.01	-2.86	-0.99	-0.17	2.90
TC2-GE	1.75	25-Sep-07	-0.39	-0.27	0.42	0.32	0.60	0.95	-2.58	-0.58	2.41	4.86	-0.01	-1.14	-1.11	-0.54	2.94
TC2-HW	2.00	26-Sep-07	-0.90	-0.31	0.51	0.46	0.70	1.46	-2.26	-1.61	1.92	3.80	-0.03	-6.40	-0.36	-2.48	1.92
TC2-IW	2.50	26-Sep-07	-0.49	-0.32	-0.17	0.86	0.02	-0.05	-2.41	-2.23	2.33	3.16	-0.04	-8.50	-1.27	-1.90	1.29
TC2-KE	3.50	25-Sep-07	-0.87	-0.27	0.26	0.54	0.44	0.97	-2.22	-1.53	1.94	3.91	0.00	-6.93	-0.83	-1.90	1.99
TC2-KW	3.50	26-Sep-07	-0.76	-0.29	0.40	0.50	0.59	1.03	-2.49	-2.39	2.05	3.05	-0.02	-0.73	-0.67	-2.46	1.13
TC2-LE	4.00	25-Sep-07	-1.10	-0.29	0.51	0.67	0.69	1.36	-2.35	-1.00	1.71	4.43	-0.02	-7.14	-0.64	-2.23	2.52

Appendix C:

Summary of Data Presented in Chapters 4 and 5

Table C.1 Summary of pore-water data for lysimeter samples collected in November 2004.

Lysimeter ID	Depth (m)	Sample Date	Temp. (°C)	pH	Eh (mV)	Alk. (mg L^{-1})	H_2S (μg L^{-1})	$\delta^{34}S$-SO_4 (‰)	$\delta^{13}C$-DIC (‰)
TC2-DE	1.00	16-Nov-04	6.1	8.43	241	35			
TC2-DW	1.00	16-Nov-04	5.8	8.77	342	43			
TC2-EE	1.25	16-Nov-04	5.9	8.20	339	50			
TC2-FE	1.50	16-Nov-04	6.3	6.77	375	28			
TC2-FW	1.50	16-Nov-04	5.4	8.40	342	48			
TC2-GE	1.75	16-Nov-04	5.7	8.52	327	40			
TC2-GW	1.75	16-Nov-04	5.9	8.41	329	58			
TC2-HW	2.00	16-Nov-04	6.2	8.68	349	48			
TC2-IE	2.50	16-Nov-04	7.8	8.05	334	25			
TC2-JW	3.00	16-Nov-04	6.7	8.33	326	55			
TC2-KE	3.50	16-Nov-04	7.3	7.83	325	54			
TC2-KW	3.50	16-Nov-04	6.5	8.41	336	58			
TC2-LE	4.00	16-Nov-04	7.3	8.72	325	28			
TC3-DE	1.00	17-Nov-04	5.9	8.09	351	96			
TC3-DW	1.00	17-Nov-04	6.4	7.45	313	128			
TC3-EE	1.25	17-Nov-04	5.8	7.71	325	120			
TC3-FE	1.50	17-Nov-04	7.1	7.39	356	110			
TC3-FW	1.50	17-Nov-04	5.9	8.22	333	78			
TC3-GE	1.75	17-Nov-04	5.7	8.34	357	63			
TC3-GW	1.75	17-Nov-04	6.5	7.17	244	130			
TC3-HW	2.00	17-Nov-04	6.2	7.21	231	130			
TC3-IE	2.50	17-Nov-04	6.8	7.85	328	113			
TC3-IW	2.50	17-Nov-04	9.4	7.32	256	143			
TC3-JW	3.00	17-Nov-04	7.0	7.36	224	138			
TC3-KE	3.50	17-Nov-04		7.23	220	133			
TC3-KW	3.50	17-Nov-04	7.6	7.98	349	118			
TC3-LE	4.00	17-Nov-04	6.3	7.72	296	80			
TC4-DE	1.00	18-Nov-04	5.2	8.01	355	95			
TC4-DW	1.00	18-Nov-04	4.8	8.29	208	115			
TC4-EE	1.25	18-Nov-04	5.4	7.48	268	135			
TC4-FE	1.50	18-Nov-04	5.4	7.70	330	118			
TC4-FW	1.50	18-Nov-04	5.8	8.10	120	125			
TC4-GE	1.75	18-Nov-04	6.9	8.38	194	105			
TC4-HW	2.00	18-Nov-04	6.6	7.59	208	158			
TC4-IE	2.50	18-Nov-04	7.1	7.54	211	140			
TC4-IW	2.50	18-Nov-04	6.3	7.37	202	218			
TC4-JW	3.00	18-Nov-04	6.6	8.17	267	143			
TC4-KE	3.50	18-Nov-04	7.9	7.53	347	65			
TC4-KW	3.50	18-Nov-04	7.4	8.55	331	83			
TC4-LE	4.00	18-Nov-04	6.7	7.77	213	150			

Table C.1 Continued.

Lysimeter ID	Depth (m)	Sample Date	Temp. (°C)	pH	Eh (mV)	Alk. (mg L^{-1})	H_2S (μg L^{-1})	$\delta^{34}S\text{-}SO_4$ (‰)	$\delta^{13}C\text{-}DIC$ (‰)
TC5-DE	1.00	19-Nov-04	6.4	7.54	286	470			
TC5-DW	1.00	19-Nov-04	4.4	8.86	352	308			
TC5-EE	1.25	19-Nov-04	4.8	7.45	311	265			
TC5-FE	1.50	19-Nov-04	4.8	8.73	358	155			
TC5-FW	1.50	19-Nov-04	5.3	8.77	356	255			
TC5-GE	1.75	19-Nov-04	5.2	7.69	269	463			
TC5-GW	1.75	19-Nov-04	4.9	8.10	354				
TC5-HW	2.00	19-Nov-04	5.9	7.53	328	295			
TC5-IE	2.50	19-Nov-04	6.1	8.75	346	180			
TC5-IW	2.50	19-Nov-04	5.7	8.16	350	145			
TC5-KE	3.50	19-Nov-04	6.7	8.34	343	87			
TC5-LE	4.00	19-Nov-04	7.0	8.00	357	128			
TC6-DE	1.00	20-Nov-04	9.6	7.85	229	298			
TC6-DW	1.00	20-Nov-04	5.8	8.62	356	113			
TC6-EE	1.25	20-Nov-04	6.7	7.68	294	145			
TC6-FE	1.50	20-Nov-04	6.7	8.09	339	173			
TC6-FW	1.50	20-Nov-04	8.4	8.34	345	243			
TC6-GE	1.75	20-Nov-04	7.2	8.49	344	143			
TC6-GW	1.75	20-Nov-04	7.6	7.64	355	185			
TC6-HW	2.00	20-Nov-04	7.4	7.82	356	180			
TC6-IE	2.50	20-Nov-04	8.4	8.57	326	280			
TC6-IW	2.50	20-Nov-04	9.9	7.62	354	225			
TC6-JW	3.00	20-Nov-04	8.4	8.71	324	265			
TC6-KE	3.50	20-Nov-04	9.1	8.15	352	155			
TC6-KW	3.50	20-Nov-04	8.3	8.13	343	103			
TC6-LE	4.00	20-Nov-04	8.2	8.38	322	98			
TC7-DE	1.00	20-Nov-04	5.2	8.56	356	400			
TC7-DW	1.00	21-Nov-04	5.3	7.60	286	373			
TC7-EE	1.25	21-Nov-04	5.5	7.47	354	273			
TC7-FE	1.50	21-Nov-04	5.9	7.26	201	520			
TC7-FW	1.50	21-Nov-04	5.5	7.82	181	620			
TC7-GE	1.75	21-Nov-04	7.4	8.31	271	570			
TC7-GW	1.75	21-Nov-04	6.5	7.79	339	373			
TC7-HW	2.00	21-Nov-04	6.2	7.95	223	415			
TC7-IE	2.50	21-Nov-04	6.4	8.29	199	567			
TC7-IW	2.50	21-Nov-04	6.6	7.91	343	375			
TC7-JW	3.00	21-Nov-04	6.8	8.41	350	415			
TC7-KE	3.50	21-Nov-04	8.7	8.00	338	130			
TC7-KW	3.50	21-Nov-04	6.7	8.41	413	88			
TC7-LE	4.00	21-Nov-04	7.6	8.02	338	130			

Table C.1 Continued.

Lysimeter	Aqueous Concentration (mg L^{-1})								
ID	Br	Cl	NO_3-N	NO_2-N	SO_4	S_2O_3	o-PO_4	NH_3-N	DOC
TC2-DE	-0.8	6.89	5.38	-0.2	1870	1050	0.013	5.9	
TC2-DW	-0.8	11.4	11.3	-0.2	1910	1630	0.008	5.1	85
TC2-EE	-0.8	11.5	9.37	-0.2	1870	1640	0.012	6.1	89
TC2-FE	-1	11	10.6	-0.25	2110	981	0.016	5.6	92
TC2-FW	-0.8	10	8.56	-0.2	1860	1770	0.009	6.0	80
TC2-GE	-0.8	12.5	10.4	-0.2	1990	1890	0.009	7.4	95
TC2-GW	-1	12.5	10.3	-0.25	1930	1910	0.011	5.9	100
TC2-HW	-0.8	11.1	8.17	-0.2	1860	1810	0.008	7.5	87
TC2-IE	-1	9.19	7.74	-0.25	1860	905	0.008	5.4	70
TC2-JW	-0.8	9.67	3.11	-0.2	1920	1690	0.011	6.1	81
TC2-KE	-0.8	12	7	-0.2	1890	1810	0.013	6.9	83
TC2-KW	-0.8	8.97	4.34	-0.2	1890	1620	0.011	7.8	72
TC2-LE	-0.8	11	8.5	-0.2	1650	1850	0.009	6.2	80
TC3-DE	-0.8	8.51	3.9	-0.2	2010	1310	0.047	7.1	62
TC3-DW	-0.8	9.29	5.26	-0.2	2100	1445	0.022	6.8	73
TC3-EE	-0.8	6.7	5.53	-0.2	2090	1890	0.005	7.6	63
TC3-FE	-0.8	8.51	0.937	-0.2	2050	1460	0.009	6.5	57
TC3-FW	-0.8	9.13	-0.2	-0.2	2080	1770	0.004	6.8	67
TC3-GE	-0.8	7.7	1.02	-0.2	1990	1490	0.005	7.0	50
TC3-GW	-0.8	8.35	-0.2	-0.2	2000	1440	0.010	7.1	60
TC3-HW	-0.8	8.52	-0.2	-0.2	2020	1760	0.010	6.9	67
TC3-IE	-0.8	10.4	-0.2	-0.2	2380	2060	0.004	6.9	75
TC3-IW	-0.8	9.24	-0.2	-0.2	2080	1640	0.033	7.2	62
TC3-JW	-0.8	9.72	-0.2	-0.2	2120	1610	0.026	7.4	74
TC3-KE	-0.8	8.78	-0.2	-0.2	2100	1240	0.008	5.8	65
TC3-KW	-0.8	9.1	-0.2	-0.2	2100	1400	0.021	7.0	67
TC3-LE	-0.8	9.75	-0.2	-0.2	2100	1680	0.030	6.7	68
TC4-DE	-0.8	9.82	0.46	-0.2	2070	1370	1.182	6.0	190
TC4-DW	-0.8	10.1	-0.2	-0.2	2010	1270	0.006	6.0	220
TC4-EE	-0.8	9.77	0.222	-0.2	2060	1420	0.007	5.7	210
TC4-FE	-0.8	8.94	-0.2	-0.2	2040	1470	0.004	5.8	140
TC4-FW	-0.8	9.68	-0.2	-0.2	2010	1380	0.007	6.5	250
TC4-GE	-0.8	11	-0.2	-0.2	2070	1530	0.000	6.7	300
TC4-HW	-0.8	10.7	-0.2	-0.2	2050	1500		5.3	230
TC4-IE	-0.8	9.14	-0.2	-0.2	2010	1320	0.018	5.0	150
TC4-IW	-0.8	10.3	-0.2	-0.2	2040	1400	0.005	5.6	180
TC4-JW	-0.8	8.78	-0.2	-0.2	2040	1730	0.049	6.0	190
TC4-KE	-0.8	7.92	-0.2	-0.2	1980	1930	0.007	6.4	8.3
TC4-KW	-0.8	10.2	-0.2	-0.2	2070	2050	0.016	7.2	67
TC4-LE	-0.8	9.72	0.756	-0.2	1960	2080			

Table C.1 Continued.

Lysimeter	Aqueous Concentration (mg L^{-1})								
ID	Br	Cl	NO_3-N	NO_2-N	SO_4	S_2O_3	o-PO_4	NH_3-N	DOC
TC5-DE	15.6	22.7	-0.2	-0.2	2100	1400	0.009	120	410
TC5-DW	6.96	16.7	-0.2	-0.2	2070	1240	0.005	67	250
TC5-EE	3.92	15.1	-0.2	-0.2	2020	1190	0.005	54	200
TC5-FE	1.87	12	-0.2	-0.2	1980	1200	0.014	33	150
TC5-FW	3.16	14.9	-0.2	-0.2	2080	1240	0.010	59	230
TC5-GE	9.53	19.5	-0.2	-0.2	2070	1290	0.023	84	330
TC5-GW	7.04	18.5	-0.2	-0.2	2060	1400	0.015	75	290
TC5-HW	3.18	14.6	-0.2	-0.2	2060	1210	0.013	48	210
TC5-IE	4.71	13.9	-0.2	-0.2	2110	1380	0.018	44	170
TC5-IW	0.965	8.94	-0.2	-0.2	1990	1390	0.012	22	100
TC5-KE	-0.8	14	-0.2	-0.2	2350	1500	0.010	13	130
TC5-LE	-0.8	13.2	1.37	0.277	2870	1660	0.010	14	120
TC6-DE	6.4	19.1	-0.2	-0.2	1675	1086	0.012	51	260
TC6-DW	-0.8	11.3	-0.2	-0.2	1970	1320	0.015	20	130
TC6-EE	-0.8	10.3	-0.2	-0.2	1920	1580	0.017	21	99
TC6-FE	1.57	10.2	-0.2	-0.2	1970	1640	0.013	31	140
TC6-FW	3.06	13.4	-0.2	-0.2	1980	1390	0.006	38	200
TC6-GE	-0.8	13.2	-0.2	-0.2	2120	1640	0.008	19	150
TC6-GW	1.01	15.2	-0.2	-0.2	2000	1560	0.007	23	190
TC6-HW	-0.8	13.5	-0.2	-0.2	1950	1390	0.009	17	260
TC6-IE	4.48	18.5	-0.2	-0.2	2010	1260	0.018	46	270
TC6-IW	2.14	12.8	-0.2	-0.2	2030	1310	0.009	35	260
TC6-JW	2.39	17.7	-0.2	-0.2	2020	1270	0.006	29	310
TC6-KE	-0.8	12.4	-0.2	-0.2	2110	1530	0.013	19	120
TC6-KW	-0.8	12.9	-0.2	-0.2	2630	1630	0.008	12	110
TC6-LE	-0.8	10.8	-0.2	-0.2	2980	2040	0.010	14	140
TC7-DE	8.26	27.3	-0.2	-0.2	2060	1390	0.017	72	420
TC7-DW	5.47	22.1	-0.2	-0.2	2050	1390	0.009	63	330
TC7-EE	2.78	18.8	-0.2	-0.2	1950	1360	0.000	41	260
TC7-FE	12.8	30.3	-0.2	-0.2	2000	1500	0.010	110	530
TC7-FW	11.7	28.9	-0.2	-0.2	2590	1950	0.000	110	480
TC7-GE	13.1	31.8	-0.2	-0.2	2040	1360	0.003	120	540
TC7-GW	8.68	22.9	-0.2	-0.2	2060	1450	0.000	67	340
TC7-HW	10.3	28.1	-0.2	-0.2	2110	1650	0.007	69	440
TC7-IE	14.6	27.5	-0.2	-0.2	2040	1440	0.005	130	570
TC7-IW	7.97	24.1	-0.2	-0.2	2030	1560	0.006	67	340
TC7-JW	11.2	27.4	-0.2	-0.2	2880	2070	0.007	100	640
TC7-KE	-0.8	6.33	-0.2	-0.2	2010	1260	0.010	9.0	73
TC7-KW	-0.8	4.32	-0.2	-0.2	2440	1320	0.000	7.9	43
TC7-LE	-0.8	13.8	-0.2	-0.2	2330	1560	0.005	16	150

Table C.1 Continued.

Lysimeter	Aqueous Concentration (mg L^{-1})						
ID	Al	Ca	Fe	Mg	K	Si	Na
TC2-DE	0.06	870	-0.05	220	29	6.1	50
TC2-DW	0.09	1000	-0.05	270	36	6.7	80
TC2-EE	0.12	900	-0.05	240	32	5.9	72
TC2-FE	0.08	1100	-0.05	270	34	7.4	77
TC2-FW	-0.05	830	-0.05	200	29	5.7	56
TC2-GE	-0.05	1000	-0.05	330	42	8.5	84
TC2-GW	-0.05	800	-0.05	250	36	5.5	74
TC2-HW	0.08	980	-0.05	230	37	7.6	77
TC2-IE	-0.05	1000	-0.05	250	30	4.6	57
TC2-JW	0.06	980	-0.05	280	31	7.2	68
TC2-KE	-0.05	1100	-0.05	240	41	4.9	73
TC2-KW	0.08	870	-0.05	250	24	8.1	60
TC2-LE	-0.05	960	-0.05	130	41	7.6	74
TC3-DE	-0.05	820	-0.05	320	25	11	55
TC3-DW	0.09	800	-0.05	320	22	6.1	64
TC3-EE	-0.05	910	-0.05	360	25	10	61
TC3-FE	0.14	830	-0.05	310	23	5.9	56
TC3-FW	-0.05	860	-0.05	360	23	6.1	56
TC3-GE	0.08	750	-0.05	270	22	12	41
TC3-GW	0.08	900	0.58	300	30	6.5	61
TC3-HW	-0.05	880	1.3	330	22	7.7	57
TC3-IE	-0.05	800	-0.05	330	26	7.7	63
TC3-IW	-0.05	860	0.097	350	31	7.1	61
TC3-JW	0.07	760	0.29	280	28	5.6	59
TC3-KE	-0.05	800	-0.05	300	23	5.6	56
TC3-KW	0.07	800	-0.05	330	28	13	58
TC3-LE	-0.05	900	-0.05	300	23	4.8	60
TC4-DE	0.07	850	-0.05	300	27	8.5	53
TC4-DW	-0.05	810	-0.05	280	28	12	54
TC4-EE	0.08	910	0.07	300	32	7.5	56
TC4-FE	0.06	770	-0.05	260	23	6.3	41
TC4-FW	0.05	860	0.77	290	33	15	45
TC4-GE	0.08	910	-0.05	320	34	13	53
TC4-HW	-0.05	880	0.29	300	32	8.4	53
TC4-IE	0.10	840	0.15	270	29	7.0	46
TC4-IW	-0.05	960	1.9	300	32	9.6	58
TC4-JW	0.09	890	-0.05	330	31	15	57
TC4-KE	0.11	1000	-0.05	280	19	11	48
TC4-KW	0.07	970	-0.05	340	29	11	68
TC4-LE	0.07	1000	0.19	280	33	7.6	65

Table C.1 Continued.

Lysimeter	Aqueous Concentration (mg L^{-1})						
ID	Al	Ca	Fe	Mg	K	Si	Na
TC5-DE	-0.05	870	-0.05	270	87	6.4	60
TC5-DW	-0.05	860	-0.05	280	67	18	53
TC5-EE	-0.05	700	-0.05	210	51	5.1	57
TC5-FE	-0.05	560	-0.05	170	24	8.8	37
TC5-FW	0.08	900	-0.05	300	69	17	59
TC5-GE	-0.05	900	-0.05	270	82	6.7	58
TC5-GW	-0.05	910	-0.05	280	75	10	61
TC5-HW	0.06	880	-0.05	270	56	7.4	60
TC5-IE	0.08	900	-0.05	260	52	15	47
TC5-IW	-0.05	960	-0.05	240	38	12	38
TC5-KE	-0.05	810	-0.05	400	32	9.3	86
TC5-LE	-0.05	880	-0.05	560	36	8.2	84
TC6-DE	-0.05	920	0.07	250	56	8.0	55
TC6-DW	0.09	730	-0.05	210	31	10	48
TC6-EE	0.16	960	-0.05	250	35	7.5	51
TC6-FE	-0.05	960	-0.05	280	40	10	44
TC6-FW	0.06	920	-0.05	230	40	10	42
TC6-GE	0.12	890	-0.05	310	42	8.9	70
TC6-GW	-0.05	870	-0.05	270	39	5.4	61
TC6-HW	-0.05	910	-0.05	270	37	8.2	60
TC6-IE	-0.05	900	-0.05	270	57	13	55
TC6-IW	-0.05	870	-0.05	240	43	7.9	55
TC6-JW	0.11	840	-0.05	280	41	9.5	45
TC6-KE	0.08	900	-0.05	280	36	12	61
TC6-KW	-0.05	800	-0.05	450	29	7.4	74
TC6-LE	-0.05	930	-0.05	600	30	10	78
TC7-DE	-0.05	890	-0.05	300	59	14	56
TC7-DW	-0.05	850	-0.05	270	56	7.4	64
TC7-EE	-0.05	800	-0.05	230	44	6.4	53
TC7-FE	0.07	960	1.8	300	75	11	63
TC7-FW	-0.05	930	0.28	340	83	14	64
TC7-GE	-0.05	890	-0.05	310	76	17	55
TC7-GW	-0.05	930	0.07	290	64	7.9	57
TC7-HW	-0.05	1000	-0.05	340	74	11	70
TC7-IE	-0.05	920	0.08	330	89	22	67
TC7-IW	-0.05	920	-0.05	300	60	11	61
TC7-JW	-0.05	920	-0.05	360	80	16	75
TC7-KE	-0.05	920	-0.05	250	19	10	25
TC7-KW	-0.05	860	-0.05	210	19	16	17
TC7-LE	-0.05	870	-0.05	480	34	8.2	78

Table C.1 Continued.

Lysimeter	Aqueous Concentration (μg L^{-1})											
ID	Sb	As	Ba	Cd	Cu	Pb	Mn	Mo	Ni	Se	Tl	Zn
TC2-DE	70	-10	34	-4.0	189	6.5	807	18	18	168	18	39
TC2-DW	53	-10	40	-4.0	16	-4	55	22	16	247	25	23
TC2-EE	48	-10	44	-4.0	165	-4	414	9.3	18	239	53	20
TC2-FE	49	-10	59	-4.0	123	-4	462	18	23	243	28	24
TC2-FW	49	-10	43	-4.0	111	-4	278	8.2	20	215	50	12
TC2-GE	50	-10	35	-4.0	20	-4	119	19	16	267	51	30
TC2-GW	50	-10	47	-4.0	205	-4	218	5.0	18	252	50	18
TC2-HW	52	-10	49	-4.0	17	-4	35	22	18	244	34	22
TC2-IE	37	-10	57	-4.0	20	-4	27	21	19	178	26	24
TC2-JW	59	-10	51	-4.0	109	-4	209	10	18	192	58	21
TC2-KE	55	-10	62	-4.0	134	-4	511	15	20	229	82	29
TC2-KW	49	-10	51	-4.0	101	-4	125	12	17	183	41	23
TC2-LE	49	-10	51	-4.0	23	-4	5.5	49	18	248	53	24
TC3-DE	60	-10	27	6.1	33	-4	1070	10	28	136	20	91
TC3-DW	55	-10	31	19	63	29	2900	8.7	59	199	32	10300
TC3-EE	60	-10	42	9.6	87	6.1	2100	6.9	40	160	31	1720
TC3-FE	61	-10	47	16	136	-4	2300	11	40	145	25	2870
TC3-FW	46	-10	43	11	17	-4	1610	13	31	138	51	1710
TC3-GE	47	-10	29	6.9	12	-4	481	11	22	90	32	61
TC3-GW	71	-10	33	6.4	85	-4	1930	5.8	45	45	38	9460
TC3-HW	62	-10	48	7.6	104	209	2590	8.2	58	88	41	8800
TC3-IE	60	-10	46	4.9	132	5.8	1630	7.3	31	125	62	452
TC3-IW	56	-10	50	-4.0	121	-4	2030	8.3	37	50	45	2350
TC3-JW	51	-10	49	7.6	73	20	2190	10	39	74	65	3980
TC3-KE	51	-10	49	-4.0	52	-4	2050	16	42	39	58	6540
TC3-KW	53	-10	41	0.0	36	-4	849	15	26	71	47	213
TC3-LE	41	-10	55	18	61	-4	1180	15	22	181	78	568
TC4-DE	58	-10	42	8.1	81	-4	1390	10	28	124	21	287
TC4-DW	69	-10	33	4.4	14	-4	1240	12	36	116	16	448
TC4-EE	72	-10	37	30	67	9	2560	11	45	123	28	7950
TC4-FE	64	-10	39	28	78	-4	2350	13	39	116	26	3520
TC4-FW	45	-10	32	4.9	10	-4	619	16	33	73	15	104
TC4-GE	59	-10	32	8.7	13	-4	754	15	30	82	25	166
TC4-HW	67	-10	47	8.0	66	-4	2550	16	42	28	32	1950
TC4-IE	55	-10	49	5.3	36	-4	1460	29	29	38	32	608
TC4-IW	80	-10	46	14	86	12	2760	14	57	36	33	7900
TC4-JW	69	-10	42	7.1	15	-4	1490	15	42	61	43	486
TC4-KE	58	-10	47	4.6	27	-4	551	16	22	123	44	53
TC4-KW	57	-10	45	6.1	41	-4	408	13	22	187	38	22
TC4-LE	74	-10	71	7.7	95	36	1210	13	35	192	43	1040

Table C.1 Continued.

Lysimeter	Aqueous Concentration (μg L^{-1})											
ID	Sb	As	Ba	Cd	Cu	Pb	Mn	Mo	Ni	Se	Tl	Zn
TC5-DE	79	-10	40	13	127	167	2310	12	45	37	42	5960
TC5-DW	54	-10	35	-4.0	12	-4	25	19	36	78	29	19
TC5-EE	56	-10	32	20	73	45	2100	9.0	45	77	37	10500
TC5-FE	38	-10	36	4.4	13	-4	109	18	27	94	24	17
TC5-FW	44	-10	35	-4.0	12	-4	81	21	23	81	32	17
TC5-GE	57	-10	46	10	123	-4	1850	14	39	36	52	1660
TC5-GW	61	-10	42	9.9	76	-4	1080	14	31	66	47	106
TC5-HW	49	-10	45	11	75	-4	2170	24	47	74	48	4380
TC5-IE	48	-10	37	6.0	14	-4	242	21	23	59	42	18
TC5-IW	58	-10	51	7.4	90	-4	748	18	29	63	32	26
TC5-KE	55	-10	41	7.0	67	-4	349	14	18	238	36	18
TC5-LE	60	-10	56	5.6	87	-4	770	16	23	278	46	47
TC6-DE	74	-10	39	11	80	-4	1380	14	37	74	37	898
TC6-DW	52	-10	37	6.2	15	-4	150	18	23	129	22	17
TC6-EE	66	-10	42	24	171	9.4	1710	6.8	35	90	40	1110
TC6-FE	75	-10	39	8.5	111	8.1	641	14	31	83	37	58
TC6-FW	61	-10	36	9.9	41	-4	704	12	30	64	37	60
TC6-GE	57	-10	38	7.1	113	-4	575	6.9	23	97	38	19
TC6-GW	63	-10	39	13	183	67	1570	6.8	31	32	44	1320
TC6-HW	65	-10	38	17	169	4.2	1620	6.5	35	18	36	425
TC6-IE	55	-10	37	6.1	30	-4	147	15	23	0	39	17
TC6-IW	63	-10	47	14	107	-4.0	1440	13	32	23	44	299
TC6-JW	62	-10	42	6.0	14	-4.0	28	43	22	13	26	19
TC6-KE	65	-10	53	9.2	122	-4	547	15	25	37	41	20
TC6-KW	64	-10	41	9.0	146	-4.0	1030	6.1	24	25	46	27
TC6-LE	74	-10	44	6.6	103	-4	426	10	26	425	53	38
TC7-DE	75	-10	40	7.5	14	-4.0	367	20	35	62	31	231
TC7-DW	76	-10	41	13	108	-4.0	1920	11	43	78	34	1800
TC7-EE	76	-10	45	15	148	-4.0	1830	14	38	71	33	1130
TC7-FE	102	-10	43	23	146	180	2310	13	58	25	37	6040
TC7-FW	79	-10	45	14	87	-4.0	1410	14	48	26	47	477
TC7-GE	68	-10	36	10	18	-4.0	613	21	43	16	36	777
TC7-GW	75	-10	45	16	128	10	1510	10	42	34	40	2060
TC7-HW	83	-10	42	12	140	17	1260	9.0	42	21	47	897
TC7-IE	76	-10	42	7.2	31	-4.0	340	23	41	19	49	30
TC7-IW	77	-10	47	13	123	4.5	991	17	33	21	48	102
TC7-JW	77	-10	42	7.0	27	-4.0	281	17	28	13	50	23
TC7-KE	54	-10	49	8.4	99	-4.0	981	16	31	21	27	45
TC7-KW	52	-10	29	6.4	12	-4.0	263	18	26	27	19	23
TC7-LE	67	-10	54	7.9	182	-4.0	526	11	28	323	43	25

Table C.2 Saturation indices calculated for pore-water samples collected in 2004.

Lysimeter ID	Saturation Indices (SIs) Calculated by MINTEQA2														
	$Al(OH)_3$ (amorph)	Anhydrite [$CaSO_4$]	Aragonite [$CaCO_3$]	Barite [$BaSO_4$]	Calcite [$CaCO_3$]	Dolomite [$CaMg(CO_3)_2$]	Epsomite [$MgSO_4{\cdot}7H_2O$]	Ferrihydrite [$Fe(OH)_3$]	Lepidocrocite [γ-FeOOH]	$Fe_3(OH)_8$	FeS (ppt)	Hydroxylapatite [$Ca_5(PO_4)_3(OH)$]	Gibbsite [$Al(OH)_3$]	Goethite [α-FeOOH]	Greigite [Fe_3S_4]
TC2-DE	-1.5	-0.2	0.6	0.9	0.8	1.1	-2.6	-0.9	2.6	-7.6	-8.2	3.7	1.4	4.2	-9.5
TC2-EE	-1.0	-0.2	0.5	1.0	0.7	1.0	-2.6	-1.4	2.1	-10.6	-10.1	2.7	1.9	3.8	-12.1
TC2-FE	0.0	-0.1	-1.0	1.1	-0.8	-2.2	-2.5	-4.4	-0.8	-18.7	-11.5	-2.6	2.9	0.8	-17.0
TC2-GE	-2.4	-0.2	0.7	0.9	1.0	1.5	-2.4	-0.9	2.6	-9.3	-9.6	3.5	0.5	4.2	-10.3
TC2-KE	-1.7	-0.2	0.3	1.1	0.5	0.5	-2.6	-2.1	1.4	-12.0	-10.0	1.8	1.1	3.1	-12.8
TC2-LE	-2.6	-0.2	0.8	1.0	1.0	1.2	-2.9	-0.5	3.1	-8.0	-9.4	4.4	0.2	4.8	-9.4
TC2-DW	-1.6	-0.2	1.0	0.9	1.2	1.9	-2.5	-0.3	3.2	-7.9	-9.6	4.1	1.2	4.8	-9.3
TC2-FW	-2.2	-0.3	0.7	1.0	0.9	1.2	-2.6	-1.0	2.5	-9.5	-9.9	3.0	0.7	4.2	-11.1
TC2-GW	-2.3	-0.3	0.7	1.1	0.9	1.4	-2.5	-1.0	2.6	-9.2	-9.8	3.1	0.6	4.2	-11.2
TC2-HW	-1.6	-0.2	1.0	1.0	1.2	1.8	-2.6	-0.6	3.0	-8.7	-9.8	3.9	1.2	4.6	-9.9
TC2-JW	-1.5	-0.2	0.7	1.0	0.9	1.4	-2.5	-1.2	2.3	-10.0	-9.8	3.1	1.4	4.0	-11.4
TC2-KW	-1.4	-0.2	0.8	1.1	1.0	1.5	-2.5	-1.1	2.4	-9.9	-10.0	3.2	1.5	4.1	-11.4
TC3-DE	-1.9	-0.3	0.7	0.8	0.9	1.4	-2.4	-1.9	1.6	-12.1	-10.7	3.8	0.9	3.3	-13.8
TC3-EE	-1.6	-0.2	0.4	1.0	0.6	0.9	-2.4	-2.6	0.9	-13.5	-10.9	-0.6	1.3	2.5	-16.5
TC3-FE	-0.2	-0.2	0.1	1.0	0.3	0.2	-2.4	-3.0	0.5	-14.9	-11.7	-1.1	2.7	2.2	-18.4
TC3-GE	-1.3	-0.3	0.7	0.9	0.9	1.4	-2.5	-1.4	2.1	-11.1	-11.5	1.6	1.6	3.7	-16.4
TC3-IE	-1.7	-0.2	0.5	1.1	0.7	1.1	-2.4	-2.2	1.3	-12.5	-10.5	-0.5	1.1	3.0	-14.6
TC3-KE	-1.4	-0.2	0.1	1.0	0.3	0.3	-2.5	-1.9	1.6	-9.0	-7.2	-1.9	1.4	3.6	-9.2
TC3-LE	-1.6	-0.2	0.3	1.1	0.5	0.6	-2.4	-2.3	1.2	-11.9	-9.4	2.0	1.3	2.9	-12.3
TC3-DW	-0.4	-0.2	0.1	0.9	0.4	0.4	-2.4	-2.9	0.6	-13.9	-11.0	0.3	2.5	2.3	-17.9
TC3-FW	-2.1	-0.2	0.7	1.0	0.9	1.5	-2.4	-1.4	2.1	-10.4	-11.4	1.1	0.8	3.8	-17.8
TC3-GW	-0.2	-0.2	-0.1	0.9	0.2	-0.1	-2.5	-2.1	1.4	-10.0	-8.4	-1.7	2.7	3.1	-12.9
TC3-HW	-1.1	-0.2	0.0	1.0	0.2	0.0	-2.4	-1.8	1.8	-8.7	-7.6	-1.7	1.7	3.4	-10.5
TC3-IW	-1.4	-0.2	0.2	1.0	0.4	0.5	-2.4	-2.7	0.8	-12.0	-8.8	0.4	1.5	2.6	-12.7
TC3-JW	-0.5	-0.3	0.1	1.1	0.3	0.2	-2.5	-2.0	1.5	-9.4	-7.7	0.0	2.4	3.2	-10.6
TC3-KW	-1.1	-0.2	0.7	1.0	0.9	1.4	-2.4	-2.2	1.3	-12.9	-10.6	2.3	1.8	3.0	-13.3
TC4-DE	-1.0	-0.2	0.6	1.0	0.8	1.2	-2.4	-2.0	1.6	-12.3	-11.1	7.8	1.9	3.2	-15.3
TC4-EE	-0.4	-0.2	0.3	1.0	0.5	0.5	-2.4	-2.5	1.0	-11.8	-10.2	-0.9	2.4	2.6	-17.4
TC4-FE	-0.8	-0.3	0.3	1.0	0.6	0.7	-2.5	-2.4	1.1	-12.9	-11.6	-1.0	2.1	2.7	-19.1
TC4-GE	-1.4	-0.2	1.0	0.9	1.2	2.1	-2.4	-1.4	2.2	-8.0	-8.5	-2.4	1.5	3.9	-12.9
TC4-IE	-0.4	-0.2	0.3	1.1	0.5	0.6	-2.5	-2.1	1.4	-9.6	-7.5	0.3	2.4	3.1	-9.9
TC4-KE	-0.4	-0.2	0.0	1.0	0.2	0.0	-2.5	-3.1	0.4	-15.1	-10.8	-0.5	2.4	2.1	-15.0
TC4-LE	-0.9	-0.2	0.7	1.2	0.9	1.3	-2.5	-1.5	2.1	-8.0	-7.7	-2.6	2.0	3.7	-10.4
TC4-DW	-2.1	-0.2	0.9	1.0	1.1	1.8	-2.4	-1.5	2.0	-8.6	-8.0	1.9	0.8	3.6	-10.6
TC4-FW	-1.2	-0.2	0.8	0.9	1.0	1.6	-2.5	-0.5	3.0	-3.8	-5.0	1.6	1.6	4.6	-4.7
TC4-HW	-1.5	-0.2	0.4	1.0	0.7	0.9	-2.5	-1.7	1.8	-8.5	-7.5	-3.6	1.4	3.5	-10.4
TC4-IW	-1.3	-0.2	0.4	1.0	0.6	0.8	-2.5	-1.3	2.2	-7.0	-7.1	-1.5	1.6	3.9	-10.1
TC4-JW	-1.1	-0.2	1.0	1.0	1.2	2.0	-2.4	-1.8	1.7	-10.5	-9.6	4.4	1.7	3.4	-13.5
TC4-KW	-1.7	-0.2	1.1	1.0	1.3	2.3	-2.4	-0.9	2.6	-9.3	-10.2	4.3	1.2	4.3	-12.2
TC5-DE	-1.4	-0.2	0.8	1.0	1.0	1.6	-2.5	-2.9	0.7	-13.2	-10.3	-0.5	1.5	2.3	-16.5
TC5-EE	-1.3	-0.3	0.4	1.0	0.7	0.9	-2.5	-2.7	0.8	-13.3	-10.9	-1.5	1.6	2.4	-17.8
TC5-FE	-2.5	-0.3	1.3	1.1	1.5	2.5	-2.6	-0.5	3.0	-8.8	-10.1	3.9	0.4	4.6	-10.6
TC5-GE	-1.5	-0.2	1.0	1.1	1.2	1.9	-2.5	-2.5	1.1	-12.0	-9.8	1.6	1.4	2.7	-15.1

Table C.2 Continued.

Lysimeter ID	Saturation Indices (SIs) Calculated by MINTEQA2														
	$Al(OH)_3$ (amorph)	Anhydrite [$CaSO_4$]	Aragonite [$CaCO_3$]	Barite [$BaSO_4$]	Calcite [$CaCO_3$]	Dolomite [$CaMg(CO_3)_2$]	Epsomite [$MgSO_4 \cdot 7H_2O$]	Ferrihydrite [$Fe(OH)_3$]	Lepidocrocite [γ-FeOOH]	$Fe_3(OH)_8$	FeS (ppt)	Hydroxylapatite [$Ca_5(PO_4)_3(OH)$]	Gibbsite [$Al(OH)_3$]	Goethite [α-FeOOH]	Greigite [Fe_3S_4]
TC5-IE	-1.8	-0.2	1.6	1.0	1.8	3.1	-2.5	-0.6	2.9	-8.9	-10.4	5.1	1.1	4.6	-11.9
TC5-KE	-2.2	-0.2	0.8	1.0	1.0	1.8	-2.3	-1.4	2.1	-10.8	-10.6	2.4	0.7	3.8	-13.7
TC5-LE	-1.9	-0.2	0.7	1.2	0.9	1.7	-2.1	-2.0	1.5	-12.4	-10.8	1.2	1.0	3.2	-14.0
TC5-DW	-2.7	-0.2	1.8	1.0	2.1	3.7	-2.4	-0.5	3.0	-8.7	-10.1	3.5	0.2	4.6	-10.2
TC5-FW	-1.7	-0.2	1.7	1.0	1.9	3.5	-2.4	-0.7	2.9	-9.2	-10.1	4.3	1.2	4.5	-10.4
TC5-GW	-1.9	-0.2	1.2	1.0	1.4	2.3	-2.5	-1.8	1.7	-12.0	-11.4	2.6	1.0	3.3	-16.5
TC5-HW	-0.6	-0.2	0.6	1.1	0.8	1.2	-2.5	-2.9	0.6	-14.2	-11.0	0.0	2.3	2.3	-16.7
TC5-IW	-2.0	-0.2	1.0	1.1	1.2	1.9	-2.5	-1.7	1.8	-11.7	-11.0	2.8	0.8	3.4	-14.7
TC6-DE	-1.9	-0.3	1.1	1.0	1.3	2.2	-2.6	-1.7	2.5	-9.1	-11.1	1.7	0.9	3.6	-14.4
TC6-EE	-0.4	-0.2	0.5	1.1	0.7	1.0	-2.6	-2.5	0.7	-12.6	-11.6	1.4	2.5	2.7	-18.0
TC6-FE	-2.0	-0.2	1.0	1.0	1.2	2.0	-2.5	-1.8	1.9	-11.8	-7.5	2.5	0.9	3.4	-11.8
TC6-GE	-1.3	-0.2	1.2	0.9	1.4	2.5	-2.4	-1.0	1.8	-9.7	-10.2	3.0	1.5	4.2	-15.6
TC6-IE	-2.6	-0.2	1.7	1.0	1.9	3.3	-2.5	-0.9	2.2	-9.3	-7.9	4.6	0.3	4.3	-10.8
TC6-KE	-1.3	-0.2	1.1	1.0	1.3	2.1	-2.5	-1.7	1.5	-11.7	-10.9	2.8	1.6	3.6	-15.4
TC6-LE	-2.4	-0.1	1.0	1.1	1.2	2.3	-2.1	-1.3	1.5	-10.1	-10.8	2.7	0.5	4.0	-15.0
TC6-DW	-1.5	-0.3	1.1	1.0	1.4	2.3	-2.6	-0.8	0.8	-9.5	-10.4	4.0	1.4	4.3	-16.6
TC6-FW	-1.5	-0.2	1.3	1.1	1.6	2.6	-2.6	-1.4	2.0	-10.8	-7.7	2.1	1.3	3.8	-12.2
TC6-GW	-1.5	-0.2	0.5	1.0	0.7	1.1	-2.5	-2.6	1.6	-13.8	-11.1	-0.4	1.3	2.7	-16.9
TC6-HW	-1.7	-0.2	0.7	1.0	0.9	1.4	-2.5	-2.4	1.4	-13.3	-9.3	0.8	1.1	2.9	-15.1
TC6-IW	-1.6	-0.2	0.7	1.0	0.8	1.3	-2.6	-2.7	1.2	-14.2	-11.6	0.0	1.2	2.6	-17.8
TC6-JW	-1.6	-0.2	1.7	1.1	1.9	3.4	-2.5	-0.6	2.0	-8.4	-10.9	3.2	1.2	4.7	-14.0
TC6-KW	-2.1	-0.2	0.7	0.9	0.9	1.6	-2.2	-1.7	2.1	-11.5	-11.8	1.3	0.8	3.5	-14.4
TC7-DE	-2.4	-0.2	1.7	1.0	2.0	3.5	-2.4	-1.0	2.5	-10.0	-11.1	4.4	0.5	4.2	-14.4
TC7-EE	-1.3	-0.3	0.5	1.1	0.7	1.0	-2.5	-2.8	0.7	-14.4	-11.6	-6.0	1.5	2.3	-18.0
TC7-FE	-0.3	-0.2	0.7	1.0	0.9	1.3	-2.5	-1.6	1.9	-7.8	-7.5	-1.1	2.5	3.6	-11.8
TC7-GE	-2.2	-0.2	1.7	0.9	1.9	3.4	-2.5	-1.7	1.8	-10.3	-10.2	1.3	0.6	3.5	-15.6
TC7-IE	-2.2	-0.2	1.7	1.0	1.9	3.4	-2.4	-1.3	2.2	-7.8	-7.9	1.7	0.7	3.9	-10.8
TC7-KE	-2.0	-0.2	0.8	1.0	1.0	1.6	-2.5	-2.0	1.5	-12.2	-10.9	1.8	0.9	3.2	-15.4
TC7-LE	-1.9	-0.2	0.7	1.1	0.9	1.7	-2.3	-2.0	1.5	-12.0	-10.8	0.4	0.9	3.3	-15.0
TC7-DW	-1.4	-0.2	0.8	1.0	1.0	1.5	-2.5	-2.7	0.8	-12.9	-10.4	-0.1	1.4	2.4	-16.6
TC7-FW	-1.6	-0.2	1.2	1.1	1.4	2.4	-2.4	-1.6	2.0	-7.8	-7.7	-4.8	1.2	3.6	-12.2
TC7-GW	-1.7	-0.2	1.0	1.0	1.2	2.0	-2.5	-1.9	1.6	-11.7	-11.1	-4.6	1.2	3.3	-16.9
TC7-HW	-1.9	-0.2	1.3	1.0	1.5	2.6	-2.4	-2.1	1.4	-10.4	-9.3	1.3	1.0	3.1	-15.1
TC7-IW	-1.8	-0.2	1.1	1.0	1.3	2.3	-2.5	-2.3	1.2	-13.0	-11.6	0.7	1.1	2.9	-17.8
TC7-JW	-2.3	-0.1	1.6	1.1	1.8	3.3	-2.3	-1.5	2.0	-11.2	-10.9	2.4	0.6	3.7	-14.0
TC7-KW	-2.3	-0.1	0.9	0.9	1.1	1.7	-2.5	-1.4	2.1	-12.2	-11.8	-2.4	0.6	3.8	-14.4

Table C.2 Continued.

	Saturation Indices (SIs) Calculated using MINTEQA2														
Lysimeter ID	**Gypsum [$CaSO_4{\cdot}2H_2O$]**	**Mackinawite [$Fe_{1+x}S$]**	**Pyrite [FeS_2]**	**Quartz [SiO_2]**	**Siderite [$FeCO_3$]**	**SiO_2 (amorph)**	**Rhodochrosite [$MnCO_3$]**	**MnS (green)**	**Chalcopyrite [$CuFeS_2$]**	**Smithsonite [$ZnCO_3$]**	**$Zn(OH)_2$**	**ZnS (amorph)**	**Sphalerite [ZnS]**	**Wurtzite [ZnS]**	**Cerrusite [$PbCO_3$]**
TC2-DE	0.1	-7.4	15.7	0.6	-6.8	-0.4	-0.5	-9.4	16.3	-2.6	2.4	5.1	3.0	6.5	-1.5
TC2-EE	0.1	-9.3	17.0	0.6	-8.5	-0.4	-0.8	-10.0	14.5	-2.9	1.8	4.6	2.5	6.3	-2.6
TC2-FE	0.2	-10.7	14.8	0.7	-9.4	-0.3	-2.4	-12.0	12.9	-4.4	-0.1	2.7	0.6	4.8	-3.3
TC2-GE	0.1	-8.8	17.8	0.8	-8.5	-0.3	-1.2	-9.8	14.2	-2.7	2.6	5.4	3.3	6.6	-2.6
TC2-KE	0.1	-9.2	15.9	0.5	-8.1	-0.5	-1.0	-10.5	14.5	-3.0	1.4	4.2	2.1	5.8	-2.6
TC2-LE	0.1	-8.7	18.2	0.7	-8.6	-0.3	-2.5	-10.8	14.2	-2.8	2.7	5.4	3.3	6.8	-2.6
TC2-DW	0.1	-8.9	18.8	0.7	-8.7	-0.4	-1.4	-9.8	14.0	-2.8	2.6	5.4	3.3	6.9	-2.6
TC2-FW	0.0	-9.2	17.7	0.6	-8.5	-0.4	-0.9	-9.8	14.5	-3.1	1.8	4.6	2.5	6.5	-2.5
TC2-GW	0.0	-9.0	17.3	0.6	-8.2	-0.5	-0.9	-10.0	14.8	-2.8	1.9	4.7	2.6	6.5	-2.5
TC2-HW	0.1	-9.1	18.6	0.7	-8.8	-0.3	-1.6	-10.1	13.8	-2.7	2.6	5.4	3.3	6.8	-2.6
TC2-JW	0.1	-9.1	17.0	0.7	-8.3	-0.4	-1.0	-10.1	14.5	-2.8	2.0	4.8	2.7	6.4	-2.6
TC2-KW	0.1	-9.2	17.4	0.7	-8.5	-0.3	-1.1	-10.1	14.3	-2.7	2.1	4.9	2.8	6.5	-2.6
TC3-DE	0.0	-10.0	16.5	0.9	-8.6	-0.2	-0.3	-9.9	13.0	-2.1	2.1	4.9	2.8	7.3	-2.5
TC3-EE	0.1	-10.2	14.3	0.8	-8.1	-0.2	-0.3	-10.7	12.9	-1.0	2.4	5.2	3.1	6.9	-1.5
TC3-FE	0.1	-11.0	13.8	0.6	-8.4	-0.4	-0.5	-11.4	11.9	-1.1	1.9	4.6	2.6	6.6	-2.6
TC3-GE	0.0	-10.8	15.5	0.9	-9.0	-0.1	-0.6	-10.7	10.9	-2.3	1.5	4.3	2.2	7.6	-2.5
TC3-IE	0.1	-9.8	15.3	0.7	-8.0	-0.3	-0.3	-10.3	13.6	-1.5	2.3	5.0	3.0	7.0	-1.5
TC3-KE	0.0	-6.5	13.5	0.4	-4.3	-0.6	-0.6	-10.9	16.0	-0.7	2.6	5.3	3.3	5.9	-2.7
TC3-LE	0.1	-8.7	15.4	0.5	-7.4	-0.5	-0.6	-10.2	14.9	-1.7	2.6	5.4	3.3	5.8	-2.6
TC3-DW	0.0	-10.3	12.9	0.6	-7.6	-0.4	-0.3	-11.3	12.2	-0.5	2.4	5.2	3.1	6.7	-0.8
TC3-FW	0.1	-10.7	14.0	0.6	-8.2	-0.4	-0.1	-10.9	10.7	-0.8	2.2	5.0	2.9	7.5	-2.5
TC3-GW	0.1	-7.7	12.8	0.6	-4.9	-0.4	-0.8	-11.8	15.0	-0.7	2.1	4.9	2.8	6.4	-0.3
TC3-HW	0.1	-6.8	13.5	0.7	-4.4	-0.4	-0.6	-11.3	16.2	-0.7	2.4	5.2	3.1	6.4	0.0
TC3-IW	0.0	-8.1	13.5	0.6	-5.9	-0.4	-0.5	-10.8	15.1	-1.1	2.3	5.1	3.0	6.3	-2.6
TC3-JW	0.0	-6.9	13.6	0.6	-4.8	-0.5	-0.5	-10.9	16.2	-0.9	2.5	5.3	3.2	6.5	-1.0
TC3-KW	0.0	-9.8	16.6	0.9	-8.6	-0.1	-0.4	-9.9	13.3	-1.7	2.6	5.3	3.3	6.0	-2.6
TC4-DE	0.1	-10.4	15.8	0.8	-8.6	-0.3	-0.3	-10.3	12.8	-1.7	2.1	4.9	2.8	7.3	-2.5
TC4-EE	0.1	-9.4	11.9	0.7	-6.4	-0.3	-0.3	-11.7	12.8	-0.5	2.0	4.8	2.7	6.8	-1.3
TC4-FE	0.0	-10.8	13.0	0.6	-7.9	-0.4	-0.2	-11.4	11.4	-0.7	1.9	4.7	2.6	7.0	-2.6
TC4-GE	0.1	-7.7	12.8	0.9	-5.9	-0.1	-0.2	-10.3	14.0	-1.7	2.0	4.8	2.7	7.6	-2.5
TC4-IE	0.1	-6.7	13.8	0.7	-4.9	-0.4	-0.5	-10.6	16.4	-1.6	2.2	5.0	2.9	6.5	-2.6
TC4-KE	0.1	-10.1	15.4	0.9	-8.7	-0.2	-1.2	-10.9	13.0	-2.9	1.3	4.0	2.0	6.4	-2.7
TC4-LE	0.1	-6.9	13.8	0.7	-4.9	-0.3	-0.3	-10.6	16.2	-1.1	2.4	5.2	3.1	7.0	-0.7
TC4-DW	0.1	-7.3	14.5	0.9	-6.0	-0.1	0.0	-9.5	15.4	-1.3	3.0	5.9	3.8	7.4	-2.5
TC4-FW	0.1	-4.2	14.2	1.0	-3.0	0.0	-0.4	-9.9	18.5	-2.0	2.4	5.2	3.1	7.2	-2.5
TC4-HW	0.1	-6.8	13.5	0.7	-4.6	-0.3	-0.1	-10.5	16.3	-1.0	2.5	5.3	3.2	6.8	-2.6
TC4-IW	0.1	-6.4	13.0	0.8	-3.6	-0.3	-0.2	-11.2	16.4	-0.4	2.4	5.2	3.1	6.6	-1.2
TC4-JW	0.1	-8.8	14.5	1.0	-7.1	0.0	0.1	-9.9	13.4	-1.2	2.6	5.4	3.3	7.4	-2.5
TC4-KW	0.1	-9.4	16.9	0.9	-8.4	-0.2	-0.4	-9.6	13.3	-2.6	1.9	4.7	2.6	7.7	-2.6
TC5-DE	0.1	-9.6	13.0	0.6	-6.5	-0.4	0.1	-11.2	13.2	-0.2	2.3	5.1	3.0	6.7	0.0
TC5-EE	0.0	-10.2	13.1	0.6	-7.1	-0.5	-0.1	-11.5	12.3	-0.2	2.4	5.2	3.1	6.8	-0.6
TC5-FE	0.0	-9.4	18.7	0.8	-8.5	-0.3	-0.7	-9.9	13.4	-2.7	2.0	4.8	2.7	7.8	-2.6
TC5-GE	0.1	-9.0	13.4	0.7	-6.3	-0.4	0.2	-10.9	14.0	-0.7	2.1	4.9	2.8	7.0	-2.5

Table C.2 Continued.

	Saturation Indices (SIs) Calculated using MINTEQA2														
Lysimeter ID	**Gypsum [$CaSO_4 \cdot 2H_2O$]**	**Mackinawite [$Fe_{1+x}S$]**	**Pyrite [FeS_2]**	**Quartz [SiO_2]**	**Siderite [$FeCO_3$]**	**SiO_2 (amorph)**	**Rhodochrosite [$MnCO_3$]**	**MnS (green)**	**Chalcopyrite [$CuFeS_2$]**	**Smithsonite [$ZnCO_3$]**	**$Zn(OH)_2$**	**ZnS (amorph)**	**Sphalerite [ZnS]**	**Wurtzite [ZnS]**	**Cerrusite [$PbCO_3$]**
TC5-IE	0.1	-9.7	17.7	1.0	-8.5	0.0	-0.3	-9.7	12.7	-2.7	1.7	4.5	2.4	8.0	-2.6
TC5-KE	0.1	-9.9	16.4	0.8	-8.5	-0.2	-0.6	-10.3	13.1	-2.7	1.4	4.2	2.1	7.5	-2.5
TC5-LE	0.1	-10.1	16.4	0.7	-8.5	-0.3	-0.4	-10.2	13.3	-2.4	1.6	4.4	2.3	7.1	-2.6
TC5-DW	0.1	-9.3	19.0	1.1	-8.5	0.1	-1.1	-10.3	13.4	-2.9	1.9	4.7	2.6	7.1	-2.6
TC5-FW	0.1	-9.4	18.9	1.1	-8.6	0.0	-0.7	-9.8	13.4	-2.8	2.0	4.8	2.7	6.9	-2.6
TC5-GW	0.1	-10.7	15.3	0.9	-8.2	-0.2	0.1	-10.7	12.1	-1.8	1.3	4.1	2.0	7.4	-2.5
TC5-HW	0.1	-10.2	14.1	0.7	-7.6	-0.3	-0.1	-11.0	12.6	-0.5	2.4	5.2	3.1	6.7	-2.5
TC5-IW	0.1	-10.2	16.1	0.9	-8.5	-0.1	-0.2	-10.2	12.9	-2.5	1.3	4.1	2.0	7.4	-2.5
TC6-DE	0.0	-10.3	16.7	0.7	-5.3	-0.3	-0.1	-10.4	11.7	0.0	1.9	4.7	2.6	7.9	1.4
TC6-EE	0.1	-10.9	14.1	0.7	-7.3	-0.3	-0.5	-11.3	12.1	-0.2	1.6	4.4	2.3	6.8	1.6
TC6-FE	0.1	-6.8	12.1	0.8	-8.1	-0.2	-0.5	-11.8	15.7	-2.7	1.8	4.5	2.5	6.5	1.1
TC6-GE	0.1	-9.5	13.6	0.8	-8.3	-0.3	-0.4	-10.9	12.2	-0.6	1.7	4.5	2.4	7.5	1.1
TC6-IE	0.1	-7.2	13.2	0.9	-7.8	-0.1	-0.7	-10.6	15.4	-2.7	0.9	3.7	1.6	7.5	0.4
TC6-KE	0.1	-10.2	15.1	0.9	-8.5	-0.2	-0.5	-10.5	12.6	-2.6	1.2	4.0	1.9	7.1	1.0
TC6-LE	0.1	-10.1	15.4	0.8	-8.2	-0.2	-0.7	-10.7	13.2	-2.3	1.0	3.8	1.7	7.1	0.9
TC6-DW	0.0	-9.6	13.1	0.8	-8.6	-0.2	-0.9	-11.2	13.2	-2.6	1.9	4.7	2.6	6.9	0.5
TC6-FW	0.1	-7.0	12.1	0.8	-8.1	-0.2	-0.2	-11.2	15.5	-2.6	1.2	4.0	1.9	7.1	1.1
TC6-GW	0.1	-10.4	14.2	0.5	-8.1	-0.5	-0.5	-11.2	12.1	-2.1	1.9	4.7	2.6	7.0	1.5
TC6-HW	0.1	-8.6	12.4	0.7	-8.3	-0.3	-0.3	-10.9	14.2	-0.4	1.9	4.6	2.6	7.2	1.5
TC6-IW	0.1	-10.8	14.2	0.7	-8.1	-0.4	-0.4	-11.2	11.8	-2.6	0.8	3.6	1.5	7.1	1.4
TC6-JW	0.1	-10.1	16.6	0.8	-7.7	-0.3	-1.4	-10.4	12.4	-2.6	1.0	3.8	1.7	7.6	-0.3
TC6-KW	0.1	-11.1	18.1	0.7	-8.3	-0.4	-0.5	-10.1	11.3	-2.6	1.8	4.6	2.5	7.6	1.3
TC7-DE	0.1	-10.3	16.7	1.0	-8.3	-0.1	0.0	-10.4	11.7	-1.7	1.9	4.7	2.6	7.9	-2.6
TC7-EE	0.0	-10.9	14.1	0.7	-8.0	-0.4	-0.2	-11.3	12.1	-1.1	1.6	4.4	2.3	6.8	-2.5
TC7-FE	0.1	-6.8	12.1	0.8	-3.3	-0.2	0.0	-11.8	15.7	-0.3	1.8	4.5	2.5	6.5	0.0
TC7-GE	0.0	-9.5	13.6	1.0	-6.6	0.0	0.2	-10.9	12.2	-1.0	1.7	4.5	2.4	7.5	-2.6
TC7-IE	0.1	-7.2	13.9	1.2	-5.0	0.1	-0.1	-10.6	15.4	-2.5	0.9	3.7	1.6	7.5	-2.6
TC7-KE	0.1	-10.2	15.1	0.8	-8.2	-0.2	-0.2	-10.5	12.6	-2.3	1.2	4.0	1.9	7.1	-2.6
TC7-LE	0.1	-10.1	15.4	0.7	-8.2	-0.3	-0.6	-10.7	13.2	-2.6	1.0	3.8	1.7	7.1	-2.6
TC7-DW	0.1	-9.6	13.1	0.7	-6.7	-0.3	0.0	-11.2	13.2	-0.8	1.9	4.7	2.6	6.9	-2.5
TC7-FW	0.1	-7.0	12.1	1.0	-3.8	0.0	0.2	-11.2	15.5	-1.2	1.2	4.0	1.9	7.1	-2.5
TC7-GW	0.1	-10.4	14.2	0.7	-7.3	-0.3	0.1	-11.3	12.1	-0.6	1.9	4.7	2.6	7.0	-1.2
TC7-HW	0.1	-8.6	12.4	0.9	-5.7	-0.2	0.2	-10.9	14.2	-0.9	1.9	4.6	2.6	7.2	-1.0
TC7-IW	0.1	-10.8	14.2	0.9	-7.9	-0.2	0.0	-11.2	11.8	-1.8	0.8	3.6	1.5	7.1	-1.6
TC7-JW	0.2	-10.1	16.6	1.0	-8.2	0.0	-0.2	-10.4	12.4	-2.6	1.0	3.8	1.7	7.6	-2.6
TC7-KW	0.1	-11.1	18.1	1.0	-9.9	0.0	-0.7	-10.1	11.3	-2.6	1.8	4.6	2.5	7.6	-2.5

Table C.2 Continued.

Lysimeter ID	Saturation Indices (SIs) Calculated using MINTEQA2											
	Anglesite [$PbSO_4$]	Galena [PbS]	$Pb(OH)_2$	$NiCO_3$	$Ni(OH)_2$	Millerite [NiS]	Orpiment [As_2S_3]	Realgar [As_4S_4]	Stibnite [Sb_2S_3]	Sb_2O_4	Native S	Tl_2S
TC2-DE	-3.8	4.4	-1.4	-7.1	-0.4	0.2	-19.0	-16.3	0.1	8.2	10.7	-6.1
TC2-EE	-4.9	3.0	-2.9	-7.1	-0.8	0.0	-18.6	-17.7	0.2	11.0	13.8	-5.5
TC2-FE	-3.9	1.9	-4.8	-7.8	-2.8	-1.2	-16.3	-16.1	2.5	9.4	13.1	-8.2
TC2-GE	-5.1	3.6	-2.4	-7.1	-0.3	0.5	-18.3	-17.7	0.6	11.2	14.1	-4.8
TC2-KE	-4.7	2.7	-3.3	-7.1	-1.4	-0.3	-18.3	-17.0	0.5	9.9	12.7	-5.8
TC2-LE	-5.2	3.8	-2.0	-7.0	-0.1	0.8	-18.9	-18.1	0.0	11.5	14.4	-4.5
TC2-DW	-5.3	3.8	-2.1	-7.1	-0.1	0.7	-18.7	-18.4	0.4	12.3	15.1	-5.0
TC2-FW	-5.0	3.3	-2.7	-7.1	-0.5	0.2	-18.6	-18.0	0.2	11.5	14.3	-5.1
TC2-GW	-5.1	3.1	-2.7	-7.1	-0.6	0.0	-19.0	-17.9	-0.1	11.1	13.8	-5.3
TC2-HW	-5.3	3.7	-2.3	-7.1	-0.2	0.6	-18.5	-18.4	0.4	12.4	15.2	-4.9
TC2-JW	-5.1	3.1	-2.7	-7.1	-0.8	0.1	-18.8	-17.7	0.2	10.9	13.6	-5.2
TC2-KW	-5.1	3.2	-2.7	-7.1	-0.7	0.1	-18.8	-17.9	0.0	11.3	14.1	-5.4
TC3-DE	-5.0	2.6	-3.2	-6.9	-1.0	-0.3	-18.8	-17.9	0.2	11.4	14.0	-6.6
TC3-EE	-3.7	2.9	-2.7	-6.8	-1.3	-1.0	-19.7	-17.3	-0.7	9.7	12.0	-7.3
TC3-FE	-4.5	1.2	-4.1	-6.8	-1.8	-1.5	-20.3	-17.7	-1.3	10.2	12.3	-8.3
TC3-GE	-5.1	2.2	-2.8	-7.0	-0.6	-0.9	-21.5	-19.1	-2.7	11.8	13.8	-6.6
TC3-IE	-3.8	3.2	-2.5	-6.8	-1.4	-0.7	-19.2	-17.3	-0.2	10.1	12.6	-6.3
TC3-KE	-4.5	1.4	-4.2	-6.6	-2.7	-1.0	-18.9	-14.8	-0.3	4.9	7.8	-7.5
TC3-LE	-4.6	2.6	-3.6	-7.0	-1.5	-0.4	-17.8	-16.2	0.8	8.3	11.6	-5.9
TC3-DW	-2.8	2.9	-2.3	-6.6	-1.6	-1.4	-20.6	-17.1	-1.7	8.6	10.7	-8.1
TC3-FW	-5.0	1.4	-3.0	-6.8	-0.7	-1.4	-23.0	-19.1	-4.2	10.8	12.2	-7.0
TC3-GW	-2.0	3.5	-2.0	-6.8	-2.1	-1.6	-19.8	-15.3	-0.7	5.8	8.0	-8.3
TC3-HW	-1.8	4.1	-1.8	-6.7	-1.9	-1.2	-18.9	-14.8	0.1	5.3	7.9	-7.8
TC3-IW	-4.6	1.6	-4.2	-6.8	-2.3	-1.0	-18.5	-15.3	0.2	6.4	9.2	-7.4
TC3-JW	-2.9	3.3	-2.6	-6.8	-2.0	-1.0	-18.5	-14.8	0.3	5.2	8.1	-7.0
TC3-KW	-5.0	2.6	-3.4	-6.9	-1.4	-0.2	-18.1	-17.5	0.7	11.0	14.0	-5.9
TC4-DE	-4.9	2.2	-3.4	-6.9	-1.0	-0.7	-19.6	-18.1	-0.7	11.3	13.6	-7.1
TC4-EE	-3.4	2.2	-2.8	-6.8	-1.6	-1.9	-21.5	-16.7	-2.4	7.3	8.9	-8.4
TC4-FE	-4.7	1.0	-3.8	-6.8	-1.3	-1.8	-22.0	-18.1	-3.0	9.9	11.4	-8.3
TC4-GE	-5.4	2.0	-2.9	-6.8	-0.7	-0.8	-21.4	-16.2	-2.4	6.3	8.1	-6.7
TC4-IE	-4.7	2.1	-4.0	-6.9	-1.9	-0.8	-17.9	-14.4	1.0	5.1	8.1	-7.1
TC4-KE	-4.4	2.4	-3.7	-7.1	-1.9	-0.6	-17.7	-16.8	1.2	10.0	13.1	-6.8
TC4-LE	-3.1	3.8	-1.9	-6.8	-1.5	-0.9	-19.4	-15.3	-0.3	6.0	8.3	-6.8
TC4-DW	-5.3	2.8	-3.1	-6.8	-0.6	-0.1	-18.8	-15.5	0.3	6.7	9.2	-6.4
TC4-FW	-5.1	2.7	-3.4	-6.8	-1.0	-0.1	-18.1	-13.5	0.6	2.8	5.9	-6.7
TC4-HW	-4.8	1.8	-4.0	-6.7	-1.6	-0.9	-19.0	-14.9	0.0	5.3	7.8	-7.3
TC4-IW	-3.4	2.5	-2.9	-6.6	-1.8	-1.4	-19.9	-14.8	-0.7	4.9	6.9	-8.0
TC4-JW	-5.3	2.2	-3.3	-6.7	-0.9	-0.5	-19.9	-16.8	-0.8	8.7	10.8	-6.1
TC4-KW	-5.5	2.9	-2.6	-7.0	-0.6	-0.1	-20.0	-18.5	-1.0	11.6	14.0	-5.4
TC5-DE	-2.6	3.4	-2.0	-6.7	-2.1	-1.8	-20.0	-16.5	-0.8	8.1	10.1	-7.6
TC5-EE	-2.9	2.9	-2.4	-6.7	-1.8	-1.8	-20.6	-17.1	-1.7	8.7	10.7	-7.9
TC5-FE	-5.7	3.1	-2.9	-6.9	-0.5	0.1	-18.8	-18.6	0.0	12.4	15.5	-5.2
TC5-GE	-5.3	1.2	-4.3	-6.8	-1.9	-1.6	-19.7	-16.3	-0.7	7.6	9.9	-6.9

Table C.2 Continued.

Lysimeter ID	Saturation Indices (SIs) Calculated using MINTEQA2											
	Anglesite [$PbSO_4$]	Galena [PbS]	$Pb(OH)_2$	$NiCO_3$	$Ni(OH)_2$	Millerite [NiS]	Orpiment [As_2S_3]	Realgar [As_4S_4]	Stibnite [Sb_2S_3]	Sb_2O_4	Native S	Tl_2S
TC5-IE	-5.9	2.7	-2.8	-7.0	-0.6	-0.2	-20.0	-18.9	-1.0	12.4	14.9	-4.9
TC5-KE	-5.1	2.5	-3.0	-7.1	-1.0	-0.5	-19.8	-18.3	-0.9	11.4	13.8	-6.1
TC5-LE	-5.0	2.4	-3.4	-7.0	-1.4	-0.6	-18.9	-17.9	0.1	11.4	14.0	-6.2
TC5-DW	-6.3	3.1	-3.0	-6.9	-0.4	0.2	-18.6	-18.6	0.6	12.9	15.8	-4.6
TC5-FW	-6.1	3.1	-3.0	-7.0	-0.7	0.1	-18.4	-18.6	0.5	12.7	15.7	-4.6
TC5-GW	-5.5	1.5	-3.8	-6.9	-1.3	-1.4	-20.7	-18.5	-1.6	11.5	13.5	-6.5
TC5-HW	-4.9	1.3	-4.4	-6.7	-1.9	-1.4	-19.4	-17.1	-0.6	9.2	11.8	-7.3
TC5-IW	-5.3	2.2	-3.3	-6.9	-1.0	-0.7	-19.8	-18.3	-0.8	11.5	13.8	-6.3
TC6-DE	-1.4	1.9	0.2	-6.5	-1.7	-1.0	-19.1	-19.1	-1.5	2.9	14.5	-5.9
TC6-EE	-0.8	1.1	0.3	-6.5	-1.3	-1.7	-18.5	-17.7	-0.9	4.8	12.4	-7.8
TC6-FE	-1.6	3.0	0.2	-6.5	-1.0	-2.1	-18.9	-14.9	-1.1	7.2	6.4	-8.3
TC6-GE	-1.9	1.0	0.7	-6.4	-0.4	-1.6	-20.2	-17.7	-2.7	8.2	10.6	-6.7
TC6-IE	-3.0	1.7	-0.1	-8.7	-3.0	-1.0	-18.2	-15.7	-0.6	7.8	8.6	-5.8
TC6-KE	-1.7	1.8	0.4	-6.8	-1.4	-0.9	-18.7	-18.1	-1.5	7.9	12.9	-7.1
TC6-LE	-1.7	2.0	0.7	-5.8	0.2	-0.8	-18.4	-17.9	-0.9	7.2	13.0	-6.6
TC6-DW	-2.5	1.1	0.3	-6.4	0.0	-1.7	-18.5	-16.6	-0.9	8.9	10.2	-7.6
TC6-FW	-2.0	0.8	0.4	-6.6	-1.2	-1.8	-19.1	-15.1	-1.5	7.8	6.6	-7.2
TC6-GW	-0.8	2.1	0.1	-6.9	-2.0	-1.9	-19.8	-18.2	-2.3	6.8	12.1	-7.5
TC6-HW	-1.0	2.7	0.3	-7.2	-2.0	-1.6	-19.4	-16.2	-1.8	7.3	8.5	-6.9
TC6-IW	-0.9	2.0	0.0	-7.0	-2.5	-1.8	-19.6	-18.3	-2.0	6.8	12.5	-7.1
TC6-JW	-3.8	1.9	-0.7	-7.3	-1.5	0.9	-18.2	-18.5	-0.6	7.9	14.2	-5.6
TC6-KW	-1.1	2.8	0.7	-7.0	-1.4	-0.1	-19.3	-19.5	-0.4	7.4	16.7	-6.3
TC7-DE	-6.2	1.9	-3.4	-6.9	-0.9	-1.0	-20.7	-19.1	-1.5	12.8	14.5	-5.9
TC7-EE	-4.9	1.1	-4.3	-6.8	-1.9	-1.7	-20.1	-17.7	-0.9	10.5	12.4	-7.8
TC7-FE	-2.5	3.0	-2.2	-6.6	-2.2	-2.1	-20.5	-14.9	-1.1	4.9	6.4	-8.3
TC7-GE	-6.1	1.0	-3.8	-6.7	-1.5	-1.6	-21.8	-17.7	-2.7	9.0	10.6	-6.7
TC7-IE	-6.1	1.7	-3.8	-6.7	-1.4	-1.0	-19.8	-15.7	-0.6	6.5	8.6	-5.8
TC7-KE	-5.1	1.8	-3.4	-6.8	-1.5	-0.9	-20.3	-18.1	-1.5	10.7	12.9	-7.1
TC7-LE	-5.1	2.0	-3.4	-6.8	-1.4	-0.8	-20.0	-17.9	-0.9	10.8	13.0	-6.6
TC7-DW	-5.1	1.1	-4.4	-6.7	-1.8	-1.7	-20.1	-16.6	-0.9	8.2	10.2	-7.6
TC7-FW	-5.5	0.8	-4.4	-6.7	-1.8	-1.8	-20.7	-15.1	-1.5	4.9	6.6	-7.2
TC7-GW	-4.0	2.1	-2.8	-6.7	-1.8	-1.9	-21.4	-18.2	-2.3	10.6	12.1	-7.5
TC7-HW	-4.1	2.7	-2.4	-6.7	-1.6	-1.6	-21.1	-16.2	-1.8	6.9	8.5	-6.9
TC7-IW	-4.5	2.0	-3.1	-6.8	-1.8	-1.8	-21.2	-18.3	-2.0	10.9	12.5	-7.1
TC7-JW	-5.9	1.9	-3.6	-6.9	-1.4	-0.9	-19.8	-18.5	-0.6	12.2	14.2	-5.6
TC7-KW	-5.2	2.8	-2.9	-6.9	-0.7	-0.1	-19.3	-19.5	-0.4	14.1	16.7	-6.3

Table C.3 Summary of pore-water data for lysimeter samples collected in October 2006.

Lysimeter ID	Depth (m)	Sample Date	Temp. (°C)	pH	Eh (mV)	Alk. (mg L^{-1})	H_2S (μg L^{-1})	$\delta^{34}S$-SO_4 (‰)	$\delta^{13}C$-DIC (‰)
TC2-BE	0.50	20-Oct-06	8.6	7.08	242	104	7		
TC2-CW	0.75	15-Oct-06	11.8	7.18	108	378	66		
TC2-DE	1.00	20-Oct-06	10.2	7.16	177	164	8	-10.27	
TC2-DW	1.00	15-Oct-06	10.0	7.34	80	430	70	-8.15	-11.10
TC2-EW	1.25	15-Oct-06	11.3	7.37	99	153	20		
TC2-FW	1.50	15-Oct-06	12.2	7.43	56	45	23	-9.39	-9.42
TC2-GE	1.75	20-Oct-06	10.2	7.60	239	78	15		
TC2-HE	2.00	20-Oct-06	10.7	8.10	263	38	-2		
TC2-HW	2.00	15-Oct-06	12.1	7.75	0	52	-2	-4.97	-10.28
TC2-IE	2.50	20-Oct-06	10.6	7.55	184	40	-2		
TC2-IW	2.50	15-Oct-06	10.3	7.39	95	46	8		
TC2-KE	3.50	12-Oct-06	9.8	7.51	194	24	-2	-8.10	-8.01
TC2-KW	3.50	15-Oct-06	11.3	7.66	12	98	-2		
TC2-LE	4.00	20-Oct-06	9.7	7.90	225	24	-2	-9.16	-12.24
TC3-BW	0.50	23-Oct-06	8.0	7.28	248	450	13		
TC3-DE	1.00	13-Oct-06	8.8	7.11	100	520	240	-12.57	-9.11
TC3-EE	1.25	15-Oct-06	9.4	7.29	128	430	460		
TC3-EW	1.25	13-Oct-06	8.5	7.25	117	440	1020		
TC3-FE	1.50	15-Oct-06	9.9	7.27	111	440	77		
TC3-FW	1.50	13-Oct-06	8.7	7.28	122	440	21		
TC3-GE	1.75	15-Oct-06	8.7	7.38	149	440	140		
TC3-GW	1.75	13-Oct-06	9.3	7.41	139	330	110		-12.11
TC3-HE	2.00	15-Oct-06	10.0	7.22	133	430	120	-2.20	-13.39
TC3-HW	2.00	13-Oct-06	9.2	7.26	120	310	33	-8.73	
TC3-IE	2.50	13-Oct-06	9.2	7.39	100	330	110		
TC3-JW	3.00	13-Oct-06	9.5	7.30	145	330	150	-0.98	-12.60
TC3-KE	3.50	13-Oct-06	9.0	7.34	132	340	62		
TC3-KW	3.50	13-Oct-06	8.4	7.34	169	400	110		
TC3-LE	4.00	15-Oct-06	9.6	7.40	141	320	16	-2.70	-13.25
TC4-BW	0.50	23-Oct-06	7.3	7.17	224	1000	10		
TC4-CE	0.75	12-Oct-06	9.0	7.25	89	520	13		
TC4-DE	1.00	12-Oct-06	9.7	7.18	77	700	44		
TC4-DW	1.00	11-Oct-06	12.9	7.16	78	800	14	2.63	-22.43
TC4-EE	1.25	12-Oct-06	9.3	7.27	103	720	16		
TC4-FW	1.50	12-Oct-06	9.1	7.19	105	1340	41	3.94	-22.53
TC4-GW	1.75	12-Oct-06	7.9	7.15	94	1760	740	4.36	
TC4-HE	2.00	12-Oct-06	10.2	7.16	65	1760		3.23	-23.57
TC4-HW	2.00	12-Oct-06	8.9	7.49	104	2060	9		
TC4-IW	2.50	11-Oct-06	13.2	7.02	89	1800	1050	3.14	
TC4-JW	3.00	12-Oct-06	8.9	7.25	139	1220	18	8.48	-22.64
TC4-KE	3.50	12-Oct-06	10.2	7.27	78	680	32		
TC4-KW	3.50	11-Oct-06	13.4	7.71	65	500	33		
TC4-LE	4.00	12-Oct-06	9.5	7.75	94	680	200	3.84	-21.98

Table C.3 Continued.

Lysimeter ID	Depth (m)	Sample Date	Temp. (°C)	pH	Eh (mV)	Alk. (mg L^{-1})	H_2S (μg L^{-1})	$\delta^{34}S$-SO_4 (‰)	$\delta^{13}C$-DIC (‰)
TC5-BW	0.50	10-Oct-06	13.0	7.26	65	780	3		
TC5-CE	0.75	11-Oct-06	10.7	7.33	69	520	9		
TC5-CW	0.75	10-Oct-06	12.6	7.42	56	620	-2		
TC5-DE	1.00	11-Oct-06	10.9	7.49	85	740	7	8.76	-17.58
TC5-DW	1.00	10-Oct-06	12.0	7.38	64	760	3		
TC5-FE	1.50	11-Oct-06	11.7	7.59	70	400	9		
TC5-FW	1.50	10-Oct-06	13.1	7.40	46	540	3	2.50	-16.88
TC5-GE	1.75	11-Oct-06	11.3	7.45	79	680	39		
TC5-GW	1.75	10-Oct-06	12.7	7.41	70	580	8		
TC5-HE	2.00	11-Oct-06	11.3	7.40	78	480	9	6.27	-17.28
TC5-HW	2.00	10-Oct-06	12.5	7.33	84	560	9		
TC5-IE	2.50	11-Oct-06	11.2	7.33	121	420	9		
TC5-JW	3.00	10-Oct-06	13.4	7.26	45	340	7	-2.26	-14.45
TC5-LE	4.00	11-Oct-06	11.8	7.51	150	220	58	2.89	-13.12
TC6-BW	0.50	23-Oct-06	7.0	7.36	182	2200	-2		
TC6-CE	0.75	9-Oct-06	9.5	7.23	110	1140	10		
TC6-EW	1.25	9-Oct-06	9.4	7.23	123	760	26	0.89	-20.65
TC6-FE	1.50	9-Oct-06	10.3	7.45	102	760	36		
TC6-FW	1.50	9-Oct-06	9.3	7.28	131	700	10		
TC6-GE	1.75	9-Oct-06	10.1	7.33	119	840	11	8.30	-17.27
TC6-GW	1.75	9-Oct-06	9.2	7.26	107	820	16		
TC6-HE	2.00	9-Oct-06	10.4	7.31	112	740	75	6.04	-18.54
TC6-HW	2.00	10-Oct-06	10.3	7.35	59	1340	45	8.85	
TC6-IE	2.50	9-Oct-06	10.3	7.56	118	1680	10		
TC6-JW	3.00	9-Oct-06	9.7	7.57	139	1180	7	0.08	-21.11
TC6-KE	3.50	10-Oct-06	10.4	7.72	55	1280	88		
TC6-KW	3.50	9-Oct-06	9.5	7.82	156	1700	190		
TC6-LE	4.00	10-Oct-06	10.9	7.75	52	880	380	6.89	-18.28
TC7-BW	0.50	23-Oct-06	7.6	7.02	215	1260	-2		
TC7-CE	0.75	8-Oct-06	9.3	7.25	106	2480	12		
TC7-DE	1.00	8-Oct-06	8.7	7.26	101	1800	78	13.21	-18.96
TC7-DW	1.00	8-Oct-06	8.1	7.24	104	1860	7	9.48	
TC7-EE	1.25	8-Oct-06	10.0	7.20	109	2200	10		
TC7-EW	1.25	9-Oct-06	9.2	7.21	140	1380	41	9.11	-19.33
TC7-FW	1.50	8-Oct-06	8.3	7.36	92	2040	240		
TC7-GE	1.75	8-Oct-06	10.5	7.33	88	3240	300		-17.04
TC7-GW	1.75	8-Oct-06	9.8	7.33	112	1980	100		
TC7-IE	2.50	8-Oct-06	10.8	7.17	128	380	8		
TC7-IW	2.50	8-Oct-06	10.1	7.72	78	1820	36		
TC7-JW	3.00	8-Oct-06	9.4	7.50	79	2300	10		
TC7-KE	3.50	8-Oct-06	10.5	7.70	130	2360	42		
TC7-KW	3.50	8-Oct-06	9.7	7.91	53	1880	3100	7.25	-18.50
TC7-LE	4.00	8-Oct-06	11.3	7.36	108	960	160	-1.81	-18.79

Table C.3 Continued.

Lysimeter	Aqueous Concentration (mg L^{-1})								
ID	Br	Cl	NO_3-N	NO_2-N	SO_4	S_2O_3	o-PO_4	NH_3-N	DOC
TC2-BE	-0.4	-1.0	-0.1	-0.1	1940	11	0.011	0	0
TC2-CW	-0.4	2.7	-0.1	-0.1	3000	2.4		1.5	1.1
TC2-DE	-0.4	-1.0	-0.1	-0.1	2600	5.0	0.006	1.4	1.2
TC2-DW	-0.4	1.9	-0.1	-0.1	3290	32	0.004	1.6	1.9
TC2-EW	-0.4	4.2	-0.1	-0.1	3340	-2	0.007	2.5	2.5
TC2-FW	-0.4	1.4	-0.1	-0.1	2240	-2	0.010	0	2.2
TC2-GE	-0.4	3.1	-0.1	-0.1	3500	-2	0.010	3	1.2
TC2-HE	-0.4	2.4	-0.1	-0.1	3040	47	0.007	3.05	7.7
TC2-HW	-0.4	2.1	-0.1	-0.1	2680	162	0.025	3.6	8.1
TC2-IE	-0.4	1.3	-0.1	-0.1	2220	83	0.010	3	1.5
TC2-IW	-0.4	4.1	-0.1	-0.1	1900	798	0.063	5.9	27
TC2-KE	-0.4	1.7	-0.1	-0.1	2210	534	0.011	4.9	7.7
TC2-KW	-0.4	8.2	-0.1	-0.1	1740	1100	0.009	7.4	56
TC2-LE	-0.4	1.7	-0.1	-0.1	2160	736	0.008	4.4	7.1
TC3-BW	-0.4	1.5	0.20	-0.1	3270	29	0.006	0	1
TC3-DE	-0.4	1.7	-0.1	-0.1	3750	40		0	1
TC3-EE	-0.4	2.0	-0.1	-0.1	2860	15	0.009	3.1	2.5
TC3-EW	-0.4	2.4	-0.1	-0.1	3350	14	0.009	0	2.6
TC3-FE	-0.4	2.3	-0.1	-0.1	3340	41	0.007	3.3	3
TC3-FW	-0.4	2.2	-0.1	-0.1	3190	-2		0	2.2
TC3-GE	-0.4	4.6	-0.1	-0.1	2520	92	0.010	6.25	12
TC3-GW	-0.4	4.8	-0.1	-0.1	2620	16	0.007	4.6	12
TC3-HE	-0.4	3.0	-0.1	-0.1	2290	31	0.006	4.3	5.8
TC3-HW	-0.4	1.5	-0.1	-0.1	2910	-2	0.009	0	1.2
TC3-IE	-0.4	4.8	-0.1	-0.1	2580	58		5	16
TC3-JW	-0.4	2.5	-0.1	-0.1	2330	15	0.009	1.7	2.7
TC3-KE	-0.4	7.4	-0.1	-0.1	2600	40	0.006	5.2	19
TC3-KW	-0.4	6.2	-0.1	-0.1	2500	74	0.007	5.2	16
TC3-LE	-0.4	6.9	-0.1	-0.1	2505	0.82	0.006	6	16
TC4-BW	-0.4	4.6	-0.1	-0.1	3380	7.9	0.011	21	23
TC4-CE	-0.4	4.3	-0.1	-0.1	2780	-2	0.007	15	16
TC4-DE	-0.4	8.0	-0.1	-0.1	2540	-2	0.007	21	94
TC4-DW	-0.4	7.4	-0.1	-0.1	2330	-2	0.009	21	84
TC4-EE	-0.4	8.2	-0.1	-0.1	2040	-2	0.006	17	190
TC4-FW	-0.4	12	-0.1	-0.1	2060	-2	0.017	29	240
TC4-GW	-0.4	11	-0.1	-0.1	1250	-2	0.095	43	290
TC4-HE	-0.4	16	-0.1	-0.1	1260	-2	0.245	53	430
TC4-HW	-0.4	6.3	-0.1	-0.1	23	-2	0.075	69	85
TC4-IW	-0.4	-1.0	-0.1	-0.1	1540	-2	0.033	54	
TC4-JW	-0.4	4.7	-0.1	-0.1	2015	-2	0.010	51.5	16
TC4-KE	-0.4	3.1	-0.1	-0.1	3220	-2	0.007	48	9.8
TC4-KW	-0.4	15	-0.1	-0.1	2400	6.1	0.010	32	260
TC4-LE	-0.4	7.1	-0.1	-0.1	819	36	0.015	60	200

Table C.3 Continued.

Lysimeter	Aqueous Concentration (mg L^{-1})								
ID	Br	Cl	NO_3-N	NO_2-N	SO_4	S_2O_3	o-PO_4	NH_3-N	DOC
TC5-BW	-0.4	6.5	-0.1	-0.1	4140	-2		71	4.4
TC5-CE	-0.4	4.2	-0.1	-0.1	3450	-2	0.074	42	8.2
TC5-CW	-0.4	7.2	-0.1	-0.1	4160	-2	0.012	82	14
TC5-DE	-0.4	9.4	-0.1	-0.1	2330	-2	0.033	130	24
TC5-DW	-0.4	6.8	-0.1	-0.1	3490	-2	0.589	110	14
TC5-FE	-0.4	9.3	-0.1	-0.1	3430	-2	0.011	180	71
TC5-FW	-0.4	8.6	-0.1	-0.1	2800	-2	0.011	100	44
TC5-GE	-0.4	9.8	-0.1	-0.1	2750	-2	0.098	180	37
TC5-GW	-0.4	9.9	-0.1	-0.1	2800	-2	0.007	140	40
TC5-HE	-0.4	8.7	-0.1	-0.1	2840	-2	0.009	160	37
TC5-HW	-0.4	7.7	-0.1	-0.1	3910	-2	0.010	93	14
TC5-IE	-0.4	4.2	-0.1	-0.1	2830	-2		110	5.9
TC5-JW	-0.4	3.9	-0.1	-0.1	3470	-2	0.010	62	4.9
TC5-LE	-0.4	7.0	-0.1	-0.1	3070	13	0.009	170	27
TC6-BW	-0.4	4.5	-0.1	-0.1	2000	8.3	0.024	97	8.7
TC6-CE	-0.4	4.8	-0.1	-0.1	3240	-2	0.172	120	19
TC6-EW	-0.4	6.6	-0.1	0.65	3420	-2	0.018	120	14
TC6-FE	-0.4	8.3	-0.1	-0.1	2700	-2	0.717	200	38
TC6-FW	-0.4	6.6	-0.1	-0.1	2980	-2	0.047	87	11
TC6-GE	-0.4	11	-0.1	-0.1	2890	-2	0.019	130	44
TC6-GW	-0.4	8.3	-0.1	-0.1	2890	-2		200	24
TC6-HE	-0.4	7.9	-0.1	-0.1	2880	-2	0.024	110	8.8
TC6-HW	-0.4	2.4	-0.1	-0.1	1480	-2	0.037	170	6.3
TC6-IE	-0.4	2.3	-0.1	-0.1	508	-2		120	10
TC6-JW	-0.4	-1.0	-0.1	-0.1	1020	-2	0.049	91	7.15
TC6-KE	-0.4	1.9	-0.1	1.4	981	5.9	0.015	96	19
TC6-KW	-0.4	5.6	-0.1	-0.1	138	45	0.027	160	57
TC6-LE	-0.4	-1.0	-0.1	-0.1	1040	19	0.016	140	47
TC7-BW	-0.4	3.9	-0.1	-0.1	2250	2.6	0.010	72	7.4
TC7-CE	-0.4	-1.0	-0.1	-0.1	600	-2	0.033	130	10
TC7-DE	-0.4	9.8	-0.1	-0.1	2130	-2		250	150
TC7-DW	-0.4	-1.0	-0.1	-0.1	1750	-2	0.007	73	6.8
TC7-EE	-0.4	1.4	-0.1	-0.1	398	-2	0.017	140	45
TC7-EW	-0.4	-1.0	-0.1	-0.1	1810	-2		160	22
TC7-FW	-0.4	3.9	-0.1	-0.1	1180	-2	1.038	200	40
TC7-GE	-0.4	8.7	-0.1	-0.1	42	-2	1.642	280	130
TC7-GW	-0.4	-1.0	-0.1	-0.1	1370	-2		230	75
TC7-IE	-0.4	-1.0	-0.1	-0.1	863	-2	0.009	8.8	2.3
TC7-IW	-0.4	-1.0	-0.1	-0.1	438	-2	0.195	150	18.5
TC7-JW	-0.4	4.0	-0.1	-0.1	616	-2	1.266	170	32
TC7-KE	-0.4	-1.0	-0.1	-0.1	19	12	0.052	165	36
TC7-KW	-0.4	1.6	-0.1	-0.1	98	5.8	0.216	150	48
TC7-LE	-0.4	2.2	-0.1	0.6	1830	6.6	0.030	72	6

Table C.3 Continued.

Lysimeter	Aqueous Concentrations (mg L^{-1})						
ID	Al	Ca	Fe	Mg	K	Si	Na
TC2-BE	-0.5	509	8.1	141	-10	10	-30
TC2-CW	-0.5	393	4.0	375	-10	5.5	-30
TC2-DE	-0.5	476	5.1	353	-10	10	-30
TC2-DW	-0.5	424	6.1	522	12	12	-30
TC2-EW	-0.5	380	4.6	474	-10	8.9	-30
TC2-FW	-0.5	376	9.9	498	-10	6.8	-30
TC2-GE	-0.5	434	6.1	553	10	15	-30
TC2-HE	-0.5	465	-0.5	425	-10	16	-30
TC2-HW	-0.5	436	-0.5	347	13	14	-30
TC2-IE	-0.5	479	-0.5	207	-10	13	-30
TC2-IW	-0.5	547	-0.5	208	20	5.5	-30
TC2-KE	-0.5	553	-0.5	290	16	11	-30
TC2-KW	-0.5	590	-0.5	161	35	8.3	53
TC2-LE	-0.5	575	-0.5	279	18	11	-30
TC3-BW	-0.5	456	9.0	528	11	8.3	-30
TC3-DE	-0.5	468	14	651	-10	16	-30
TC3-EE	-0.5	423	6.7	420	-10	8.5	-30
TC3-EW	-0.5	474	8.8	577	-10	5.6	-30
TC3-FE	-0.5	412	5.5	536	16	6.9	-30
TC3-FW	-0.5	490	7.8	563	-10	6.9	-30
TC3-GE	-0.5	462	3.4	337	12	7.8	-30
TC3-GW	-0.5	500	7.2	384	14	8.8	32
TC3-HE	-0.5	474	7.1	284	11	9.4	-30
TC3-HW	-0.5	490	14	475	-10	5.9	-30
TC3-IE	-0.5	468	4.4	345	16	5.6	34
TC3-JW	-0.5	502	6.0	293	10	5.8	-30
TC3-KE	-0.5	501	4.2	380	20	5.4	50
TC3-KW	-0.5	496	4.1	344	19	2.5	42
TC3-LE	-0.5	412	5.2	290	16	10	42
TC4-BW	-0.5	477	13	728	16	11	-30
TC4-CE	-0.5	508	18	456	11	9.5	-30
TC4-DE	-0.5	481	5.9	434	20	15	42
TC4-DW	-0.5	472	7.0	340	21	18	32
TC4-EE	-0.5	555	17	407	27	14	46
TC4-FW	-0.5	505	17	510	22	23	41
TC4-GW	-0.5	400	5.4	465	24	26	40
TC4-HE	-0.5	365	1.8	493	27	25	53
TC4-HW	-0.5	71	8.9	526	13	18	-30
TC4-IW	-0.5	517	2.8	414	29	23	33
TC4-JW	-0.5	360	14	499	19	12	-30
TC4-KE	-0.5	479	18	592	22	10	-30
TC4-KW	-0.5	426	2.5	329	27	15	42
TC4-LE	-0.5	146	0.8	310	29	10	38

Table C.3 Continued.

Lysimeter	Aqueous Concentrations (mg L^{-1})						
ID	Al	Ca	Fe	Mg	K	Si	Na
TC5-BW	-0.5	441	14	754	26	9.4	31
TC5-CE	-0.5	437	14	521	19	12	-30
TC5-CW	-0.5	431	14	785	30	8.4	-30
TC5-DE	-0.5	428	17	316	43	15	45
TC5-DW	-0.5	452	14	593	35	14	-30
TC5-FE	-0.5	392	5.2	373	60	16	43
TC5-FW	-0.5	484	12	395	34	15	46
TC5-GE	-0.5	413	12	277	48	13	42
TC5-GW	-0.5	475	15	360	47	10	49
TC5-HE	-0.5	463	13	314	51	11	46
TC5-HW	-0.5	385	11	556	13	6.4	32
TC5-IE	-0.5	440	16	363	35	10	-30
TC5-JW	-0.5	363	9.6	452	21	2.5	-30
TC5-LE	-0.5	406	1.8	301	50	5.7	35
TC6-BW	-0.5	353	14	566	17	18	-30
TC6-CE	-0.5	365	16	726	19	18	-30
TC6-EW	-0.5	463	20	570	30	16	30
TC6-FE	-0.5	341	6.1	387	56	17	33
TC6-FW	-0.5	440	14	438	34	15	30
TC6-GE	-0.5	460	15	410	45	16	53
TC6-GW	-0.5	344	14	380	58	15	48
TC6-HE	-0.5	414	17	434	44	16	34
TC6-HW	-0.5	251	8.0	311	48	15	-30
TC6-IE	-0.5	74	2.7	325	34	14	50
TC6-JW	-0.5	137	2.9	318	24	12	31
TC6-KE	-0.5	61	1.0	404	32	8.4	53
TC6-KW	-0.5	26	0.8	255	35	8.5	54
TC6-LE	-0.5	75	1.2	259	42	12	48
TC7-BW	-0.5	574	34	315	21	18	-30
TC7-CE	-0.5	176	13	503	17	15	-30
TC7-DE	-0.5	313	15	508	51	23	43
TC7-DW	-0.5	287	29	558	18	17	-30
TC7-EE	-0.5	188	18	372	25	17	-30
TC7-EW	-0.5	305	17	411	39	21	-30
TC7-FW	-0.5	204	8.3	426	51	21	43
TC7-GE	-0.5	97	4.7	372	49	20	-30
TC7-GW	-0.5	202	2.6	409	59	20	46
TC7-IE	-0.5	275	8.2	85	-10	7.4	-30
TC7-IW	-0.5	62	5.9	350	31	12	-30
TC7-JW	-0.5	134	3.7	432	43	19	33
TC7-KE	-0.5	36	2.3	330	35	13	-30
TC7-KW	-0.5	23	0.0	294	36	18	-30
TC7-LE	-0.5	255	12	409	13	11	-30

Table C.3 Continued.

Lysimeter	Aqueous Concentration (μg L^{-1})											
ID	Sb	As	Ba	Cd	Cu	Pb	Mn	Mo	Ni	Se	Tl	Zn
TC2-BE	1.0	4.8	7.7	-4	-2	-2	8260	-10	129	-10	27	49900
TC2-CW	5.1	4.2	7.7	-4	-2	-2	2470	-10	62	-10	88	35800
TC2-DE	3	7.2	7.2	-4	-2	-2	1020	-10	57	11	27	23800
TC2-DW	37	5.4	7.4	-4	-2	-2	528	18	32	-10	32	3910
TC2-EW	10	8.7	9.2	-4	-2	-2	879	-10	24	-10	63	3140
TC2-FW	20	12	8.2	-4	-2	-2	156	15	23	-10	60	3230
TC2-GE	37	7.6	8.8	-4	-2	-2	632	-10	23	-10	70	506
TC2-HE	27	10	8.5	-4	-2	-2	388	-10	17	-10	37	35
TC2-HW	23	7.7	7.6	-4	-2	-2	305	-10	11	-10	38	11
TC2-IE	8.0	6.2	11	-4	-2	-2	706	-10	21	-10	34	157
TC2-IW	30	1.5	31	-4	12	52	556	-10	21	-10	59	509
TC2-KE	24	7.3	16	-4	-2	-2	446	-10	21	-10	21	109
TC2-KW	68	1.5	20	-4	-2	5.2	891	-10	21	-10	-0.5	79
TC2-LE	32	4.7	17	-4	-2	-2	357	-10	22	-10	19	25
TC3-BW	17	10	41	-4	-2	-2	3460	-10	117	-10	-0.5	28800
TC3-DE	1.0	19	6.7	-4	-2	-2	1070	18	24	-10	-0.5	478
TC3-EE	4.4	19	7.5	-4	-2	-2	268	-10	36	-10	23	6110
TC3-EW	1.0	33	6.0	-4	-2	-2	556	10	63	-10	44	10900
TC3-FE	6.7	12	10	-4	-2	-2	263	11	40	-10	35	11200
TC3-FW	7.6	1.5	8.1	-4	-2	-2	238	-10	41	-10	65	13100
TC3-GE	4.2	13	7.7	-4	-2	-2	256	-10	32	-10	33	6860
TC3-GW	5.7	12	8.2	-4	-2	-2	249	-10	25	-10	11	2910
TC3-HE	8.1	36	12	-4	-2	-2	259	-10	41	-10	50	7940
TC3-HW	1.0	28	7.7	-4	-2	-2	345	-10	37	-10	47	10500
TC3-IE	12	7.5	10	-4	-2	-2	313	-10	33	-10	31	5830
TC3-JW	6.7	4.7	9.4	-4	-2	3.3	301	-10	34	-10	35	7310
TC3-KE	5.0	4.0	11	-4	-2	-2	316	-10	34	-10	46	10500
TC3-KW	11	7.4	10	-4	-2	-2	308	-10	32	-10	36	9100
TC3-LE	24	18	9.0	-4	-2	-2	286	12	16	-10	-0.5	119
TC4-BW	22	95	58	-4	-2	-2	2070	11	130	-10	26	13000
TC4-CE	1.0	23	8.3	-4	-2	-2	3455	-10	76	-10	43	17450
TC4-DE	1.0	1.5	10	-4	-2	-2	202	-10	14	-10	-0.5	9.0
TC4-DW	0.5	8.2	7.4	-2	-1	-1	229	5.6	30	-5	2.5	29
TC4-EE	1.0	56	11	-4	-2	-2	251	-10	25	-10	5.3	1230
TC4-FW	2.7	42	10	-4	-2	-2	212	-10	17	-10	-0.5	23
TC4-GW	5.1	16	24	-4	-2	-2	204	-10	12	72	-0.5	13
TC4-HE	3.1	1.5	179	-4	-2	-2	117	-10	11	66	-0.5	17
TC4-HW	1.0	117	6090	-4	-2	-2	41	41	1.5	-10	-0.5	100
TC4-IW	1.8	0.8	16	-2	-1	-1	204	-5	22	1.9	-0.25	1.3
TC4-JW	1.0	82	8.0	-4	-2	-2	106	17	22	-10	11	1030
TC4-KE	21	52	9.1	-4	-2	-2	184	-10	34	-10	83	6020
TC4-KW	4.9	31	11	-2	-1	-1	389	8.9	18	-5	28	594
TC4-LE	1.0	4.5	14	-4	-2	-2	125	12	4.9	-10	-0.5	9

Table C.3 Continued.

Lysimeter	Aqueous Concentration (μg L^{-1})											
ID	Sb	As	Ba	Cd	Cu	Pb	Mn	Mo	Ni	Se	Tl	Zn
TC5-BW	18	27	8.2	-2	-1	-1	1380	19	54	-5	26	4320
TC5-CE	1.3	59	9.2	-2	-1	-1	1940	12	51	-5	8.2	3780
TC5-CW	0.5	71	7.2	-2	-1	-1	299	17	25	5.8	7.9	696
TC5-DE	0.5	293	7.5	-2	1.0	-1	193	18	31	-5	-0.25	141
TC5-DW	3.0	148	6.9	-2	-1	-1	226	16	31	5.5	15	376
TC5-FE	0.5	70	8.6	-2	-1	-1	236	12	28	-5	-0.25	38
TC5-FW	0.5	102	8.2	-2	-1	-1	204	9.4	24	-5	9.5	285
TC5-GE	0.5	54	8.9	-2	-1	-1	269	11	24	-5	-0.25	7.2
TC5-GW	3.4	107	10	-2	-1	-1	207	10	35	-5	44	2340
TC5-HE	0.5	75	8.7	-2	-1	-1	235	8.5	34	-5	24	1400
TC5-HW	0.5	83	7.8	-2	-1	-1	205	8.9	34	-5	82	5670
TC5-IE	1.1	128	8.8	-2	-1	-1	1040	7.9	47	-5	43	4290
TC5-JW	0.5	34	6.3	-2	-1	-1	554	-5	43	-5	107	10700
TC5-LE	13	7.4	11	-2	-1	1.8	387	-5	41	-5	29	4160
TC6-BW	20	148	32	-4	-2	-2	686	55	30	-10	2.6	1900
TC6-CE	6.7	39	8.4	-2	-1	-1	233	-5	17	-5	-0.25	37
TC6-EW	0.02	63	9.0	-2	-1	-1	208	15	22	-5	-0.25	16
TC6-FE	1.6	29	11	-2	-1	-1	277	8.0	18	10	-0.25	4.1
TC6-FW	6.7	117	8.1	-2	-1	-1	243	9.3	25	-5	14	813
TC6-GE	3.3	153	10	-2	-1	-1	159	15	32	-5	16	959
TC6-GW	1.8	125	8.7	-2	-1	-1	139	12	20	-5	1.1	198
TC6-HE	0.5	195	8.3	-2	-1	-1	161	9.1	18	-5	-0.25	5.7
TC6-HW	0.5	74	13	-2	-1	-1	74	17	12	-5	-0.25	8.3
TC6-IE	1.8	195	12	-2	-1	-1	63	33	6.9	5.1	11	360
TC6-JW	0.5	98	19	-2	-1	-1	489	27	9.4	-5	3.8	780
TC6-KE	3.9	71	11	-2	-1	-1	37	45	5.5	-5	6.9	121
TC6-KW	9.2	48	54	-2	-1	-1	20	40	3.2	5.3	4.7	176
TC6-LE	27	41	10	-2	-1	-1	41	43	5.0	-5	-0.25	8.5
TC7-BW	12	179	33	-4	-2	-2	5130	14	117	-10	27	12900
TC7-CE	0.5	112	13	-2	-1	-1	418	29	11	6.3	2.5	1160
TC7-DE	5.8	55	13	-2	-1	-1	171	-5	15	11	-0.25	9.1
TC7-DW	0.5	586	9.4	-2	-1	-1	326	21	24	9.8	3.1	932
TC7-EE	1.6	254	44	-2	1.8	-1	1200	14	28	6.2	10	3950
TC7-EW	1.4	149	8.6	-2	-1	-1	154	10	14	5.7	-0.25	7.6
TC7-FW	1.6	15	14	-2	-1	-1	194	-5	8.9	10	-0.25	8.4
TC7-GE	2.7	157	6150	-2	-1	-1	106	18	5.0	6.9	-0.25	8.0
TC7-GW	1.8	22	14	-2	1.9	-1	142	-5	9.3	8.1	-0.25	8.5
TC7-IE	0.5	128	11	-2	-1	-1	3800	-5	101	5.4	5.3	21300
TC7-IW	0.5	140	199	-2	-1	-1	37	30	4.0	11	-0.25	9.2
TC7-JW	1.1	65	45	-2	8.3	-1	263	20	9.2	-5	-0.25	61
TC7-KE	19	53	523	-2	-1	-1	21	54	3.1	-5	-0.25	35
TC7-KW	0.5	14	49	-2	-1	-1	35	28	2.2	56	-0.25	2.7
TC7-LE	5.3	38	10	-2	-1	-1	116	11	13	11	-0.25	6.5

Table C.4 Saturation indices calculated for pore-water samples collected in 2006.

	Saturation Indices (SIs) Calculated by MINTEQA2														
Lysimeter ID	$Al(OH)_3$ (amorph)	Anhydrite [$CaSO_4$]	Aragonite [$CaCO_3$]	Barite [$BaSO_4$]	Calcite [$CaCO_3$]	Dolomite [$CaMg(CO_3)_2$]	Epsomite [$MgSO_4{\cdot}7H_2O$]	Ferrihydrite [$Fe(OH)_3$]	Lepidocrocite [γ-FeOOH]	$Fe_3(OH)_8$	FeS (ppt)	Hydroxylapatite [$Ca_5(PO_4)_3(OH)$]	Gibbsite [$Al(OH)_3$]	Goethite [α-FeOOH]	Greigite [Fe_3S_4]
TC2-BE	-1.1	-0.3	-0.1	0.4	0.1	-0.1	-2.7	-1.1	2.5	-6.7	-6.4	-4.2	1.7	4.2	-6.3
TC2-DE	-1.2	-0.3	-0.2	0.4	0.0	0.1	-2.3	-1.2	2.3	-6.1	-5.4	-5.1	1.6	4.1	-5.2
TC2-GE	-1.6	-0.3	0.3	0.6	0.5	1.3	-2.0	-0.5	3.0	-5.5	-5.6	-3.2	1.2	4.8	-2.3
TC2-HE	-2.2	-0.3	0.9	0.5	1.1	2.3	-2.2	-1.0	2.5	-7.9	-9.1	-1.4	0.7	4.4	-13.0
TC2-IE	-1.6	-0.3	0.3	0.6	0.5	0.8	-2.5	-2.0	1.5	-8.9	-7.7	-2.5	1.2	3.4	-12.1
TC2-KE	-1.5	-0.3	0.3	0.7	0.5	0.9	-2.4	-2.0	1.5	-9.1	-7.8	-2.5	1.3	3.3	-12.2
TC2-LE	-1.9	-0.3	0.8	0.7	1.0	1.8	-2.4	-1.3	2.3	-7.8	-8.4	-1.2	0.9	4.1	-12.4
TC2-CW	-1.3	-0.4	-0.4	0.5	-0.3	-0.3	-2.2	-1.0	2.5	-4.3	-3.6	-8.0	1.5	4.4	-1.8
TC2-DW	-1.4	-0.3	-0.4	0.5	-0.2	-0.2	-2.0	-0.9	2.6	-3.7	-2.8	-5.4	1.4	4.4	0.1
TC2-EW	-1.5	-0.4	-0.3	0.6	-0.1	0.0	-2.1	-0.8	2.7	-3.8	-3.4	-4.8	1.4	4.6	-1.0
TC2-FW	-1.6	-0.5	-0.4	0.3	-0.2	-0.2	-2.2	0.0	3.5	-0.7	-2.0	-3.8	1.3	5.4	1.8
TC2-HW	-1.9	-0.3	-3.0	0.4	-2.8	-5.5	-2.3	-1.7	1.8	-5.0	-4.6	-1.0	1.0	3.7	-8.9
TC2-IW	-1.4	-0.3	-0.1	0.9	0.1	0.0	-2.6	-1.9	1.6	-7.1	-4.4	-0.5	1.4	3.4	-4.1
TC2-KW	-1.7	-0.3	-0.7	0.7	-0.5	-1.3	-2.7	-1.7	1.9	-5.0	-4.6	-1.7	1.1	3.7	-8.9
TC3-DE	-1.1	-0.3	-0.6	0.5	-0.4	-0.4	-1.9	-1.0	2.5	-4.1	-1.9	-8.4	1.7	4.2	4.1
TC3-EE	-1.3	-0.4	-0.3	0.5	-0.1	0.0	-2.1	-0.7	2.8	-3.8	-3.3	-4.4	1.5	4.6	0.6
TC3-FE	-1.3	-0.3	-0.4	0.6	-0.2	-0.1	-2.0	-0.8	2.8	-3.7	-3.3	-5.2	1.5	4.6	-0.4
TC3-GE	-1.4	-0.3	-0.1	0.5	0.2	0.3	-2.3	-0.9	2.6	-4.8	-4.0	-3.6	1.5	4.4	-1.0
TC3-HE	-1.3	-0.3	-0.2	0.6	0.0	-0.1	-2.4	-0.9	2.7	-4.3	-3.5	-4.8	1.6	4.5	-0.2
TC3-IE	-1.4	-0.3	-0.2	0.6	0.0	0.0	-2.3	-0.5	3.0	-2.8	-2.9	-6.6	1.5	4.8	0.8
TC3-KE	-1.3	-0.3	-0.1	0.6	0.1	0.2	-2.2	-0.6	2.9	-3.7	-3.7	-4.3	1.5	4.7	-0.9
TC3-LE	-1.4	-0.4	-0.1	0.5	0.1	0.2	-2.3	-0.7	2.8	-4.2	-3.5	-4.3	1.4	4.6	0.5
TC3-BW	-1.3	-0.3	0.0	1.2	0.2	0.6	-2.0	-0.5	3.0	-5.2	-6.0	-5.0	1.6	4.8	-4.3
TC3-EW	-1.2	-0.3	-0.3	0.4	-0.1	0.0	-2.0	-0.2	3.4	-1.9	-2.5	-4.7	1.6	5.1	2.4
TC3-FW	-1.3	-0.3	-0.3	0.5	-0.1	0.1	-2.0	-0.5	3.1	-2.9	-3.5	-7.4	1.6	4.8	-1.0
TC3-GW	-1.4	-0.3	0.0	0.5	0.2	0.4	-2.2	-0.4	3.1	-3.3	-3.3	-3.8	1.4	4.9	0.9
TC3-HW	-1.3	-0.3	-0.3	0.5	-0.1	0.0	-2.1	0.7	4.2	0.6	-2.1	-4.3	1.6	6.0	3.1
TC3-JW	-1.3	-0.3	-0.1	0.5	0.1	0.2	-2.3	-0.4	3.1	-3.3	-3.4	-3.8	1.5	4.9	0.7
TC3-KW	-1.3	-0.3	0.0	0.6	0.2	0.4	-2.3	0.2	3.7	-1.8	-3.3	-4.1	1.5	5.5	1.7
TC4-CE	-0.3	-0.3	-0.4	0.5	-0.2	-0.3	-2.1	0.1	3.6	-0.6	-2.4	-4.6	2.6	5.4	0.7
TC4-DE	-0.2	-0.3	-0.5	0.5	-0.3	-0.5	-2.2	-1.4	2.2	-4.8	-1.2	-4.9	2.6	4.0	6.2
TC4-EE	-0.3	-0.4	-0.2	0.5	0.0	0.0	-2.3	-0.4	3.2	-2.3	-2.6	-4.2	2.6	4.9	1.3
TC4-HE	-0.2	-0.7	-0.6	1.4	-0.4	-0.5	-2.4	-2.2	1.3	-7.0	-3.3	-0.6	2.6	3.2	-2.0
TC4-KE	-0.3	-0.3	-0.4	0.5	-0.2	-0.2	-2.0	0.0	3.5	-0.9	-2.0	-4.8	2.5	5.3	2.1
TC4-LE	-0.7	-1.1	-0.2	0.3	0.0	0.5	-2.6	-0.9	2.7	-4.1	-1.2	-3.1	2.1	4.5	8.4
TC4-BW	-0.1	-0.3	0.5	1.3	0.7	1.7	-1.9	-0.6	2.9	-5.1	-5.3	-4.9	2.7	4.6	-3.0
TC4-DW	-0.3	-0.4	0.6	0.3	0.7	1.5	-2.4	-1.4	2.1	-5.0	-2.2	-4.6	2.5	4.0	2.6
TC4-FW	-0.2	-0.4	0.8	0.4	1.0	2.1	-2.2	-1.0	2.5	-4.1	-1.7	-3.7	2.6	4.3	5.7
TC4-GW	-0.1	-0.7	0.8	0.6	1.0	2.1	-2.4	-1.7	1.8	-6.1	-0.5	-1.9	2.7	3.5	10.2
TC4-HW	-0.5	-3.1	0.5	1.3	0.7	2.4	-4.0	-0.6	2.9	-3.2	-2.6	-4.0	2.4	4.7	2.2
TC4-IW	-0.2	-0.5	0.8	0.4	1.0	2.1	-2.5	-2.3	1.3	-7.6	-1.4	-3.3	2.6	3.2	7.1
TC4-JW	-0.3	-0.6	0.6	0.3	0.8	1.9	-2.2	-0.5	3.0	-3.3	-3.2	-4.8	2.6	4.8	1.2
TC4-KW	-0.9	-0.4	0.9	0.5	1.0	2.2	-2.4	-0.7	2.8	-3.2	-2.8	-2.4	1.9	4.8	0.7

Table C.4 Continued.

Lysimeter ID	Saturation Indices (SIs) Calculated by MINTEQA2														
	$Al(OH)_3$ (amorph)	Anhydrite [$CaSO_4$]	Aragonite [$CaCO_3$]	Barite [$BaSO_4$]	Calcite [$CaCO_3$]	Dolomite [$CaMg(CO_3)_2$]	Epsomite [$MgSO_4{\cdot}7H_2O$]	Ferrihydrite [$Fe(OH)_3$]	Lepidocrocite [γ-FeOOH]	$Fe_3(OH)_8$	FeS (ppt)	Hydroxylapatite [$Ca_5(PO_4)_3(OH)$]	Gibbsite [$Al(OH)_3$]	Goethite [α-FeOOH]	Greigite [Fe_3S_4]
TC5-CE	-0.4	-0.3	0.4	0.6	0.6	1.4	-2.1	-0.4	3.1	-1.9	-2.5	-1.7	2.4	5.0	0.5
TC5-DE	-0.6	-0.4	0.8	0.4	1.0	1.9	-2.4	0.0	3.5	-1.2	-2.1	-1.7	2.3	5.3	3.0
TC5-FE	-0.7	-0.4	0.5	0.5	0.7	1.6	-2.2	-0.6	2.9	-3.0	-2.3	-3.2	2.1	4.7	2.1
TC5-GE	-0.5	-0.4	0.7	0.5	0.8	1.7	-2.4	-0.3	3.3	-1.8	-0.7	-0.6	2.3	5.1	8.4
TC5-HE	-0.5	-0.3	0.5	0.5	0.7	1.4	-2.3	-0.2	3.3	-1.6	-2.4	-3.7	2.3	5.2	1.2
TC5-IE	-0.4	-0.3	0.4	0.5	0.5	1.2	-2.3	0.1	3.6	-1.2	-2.9	-7.1	2.4	5.5	0.9
TC5-LE	-0.6	-0.3	0.2	0.6	0.4	0.9	-2.3	-0.8	2.7	-4.8	-4.4	-3.5	2.2	4.6	-1.7
TC5-BW	-0.4	-0.3	0.5	0.5	0.7	1.8	-1.9	-0.4	3.1	-1.8	-2.5	-8.0	2.4	5.1	0.0
TC5-CW	-0.6	-0.3	0.5	0.4	0.7	1.9	-1.9	0.0	3.5	-0.6	-2.4	-4.0	2.2	5.4	-0.1
TC5-DW	-0.5	-0.3	0.6	0.4	0.8	2.0	-2.1	-0.5	3.1	-2.0	-2.3	1.2	2.3	5.0	1.1
TC5-FW	-0.6	-0.3	0.6	0.4	0.8	1.7	-2.3	-0.6	3.0	-2.1	-2.2	-3.4	2.2	4.9	1.0
TC5-GW	-0.6	-0.3	0.6	0.5	0.8	1.7	-2.3	0.1	3.6	-0.6	-2.1	-4.0	2.2	5.5	1.8
TC5-HW	-0.5	-0.4	0.4	0.5	0.6	1.5	-2.0	0.0	3.6	-0.9	-2.4	-4.7	2.3	5.5	1.2
TC5-JW	-0.5	-0.4	0.1	0.4	0.3	0.9	-2.1	-0.2	3.3	-1.0	-2.1	-4.9	2.3	5.2	0.4
TC6-CE	-0.3	-0.5	0.5	0.4	0.7	1.9	-2.0	-0.8	2.7	-3.6	-2.5	-1.6	2.6	4.5	2.6
TC6-FE	-0.5	-0.5	0.6	0.6	0.8	1.8	-2.2	-0.9	2.7	-4.0	-1.7	1.5	2.3	4.5	6.2
TC6-GE	-0.4	-0.4	0.6	0.5	0.8	1.8	-2.2	-0.5	3.0	-3.2	-3.1	-3.2	2.5	4.8	0.6
TC6-HE	-0.4	-0.4	0.5	0.5	0.7	1.6	-2.2	-0.5	3.1	-2.8	-0.9	-3.2	2.5	4.9	9.1
TC6-IE	-0.6	-1.6	0.6	0.0	0.8	2.3	-2.8	-0.9	2.6	-4.5	-3.6	-9.1	2.2	4.4	-0.2
TC6-KE	-0.8	-1.5	0.5	0.3	0.7	2.3	-2.5	-0.8	2.7	-3.3	-2.3	-5.5	2.1	4.5	1.9
TC6-LE	-0.8	-1.3	0.5	0.3	0.7	2.0	-2.6	-0.8	2.7	-3.4	-1.1	-4.6	2.0	4.5	6.8
TC6-BW	-0.3	-0.6	0.9	0.9	1.1	2.6	-2.2	-0.6	2.9	-4.5	-5.1	-3.3	2.6	4.6	-4.1
TC6-EW	-0.3	-0.3	0.5	0.5	0.7	1.5	-2.0	-0.5	3.0	-3.0	-1.7	-4.0	2.6	4.8	6.1
TC6-FW	-0.3	-0.4	0.5	0.5	0.7	1.5	-2.2	-0.6	2.9	-3.6	-3.3	-2.4	2.5	4.7	0.3
TC6-GW	-0.3	-0.5	0.4	0.5	0.6	1.4	-2.2	-0.6	2.9	-3.2	-2.5	-8.0	2.6	4.7	2.5
TC6-HW	-0.4	-0.8	0.7	0.4	0.9	2.0	-2.5	-0.9	2.7	-3.1	-0.7	-3.0	2.4	4.5	7.6
TC6-JW	-0.6	-1.1	0.6	0.5	0.8	2.2	-2.6	-0.8	2.8	-4.4	-4.1	-2.7	2.3	4.6	-1.5
TC6-KW	-0.8	-2.6	0.4	0.2	0.6	2.3	-3.4	-0.7	2.9	-4.7	-3.1	-5.6	2.0	4.6	4.2
TC7-CE	-0.3	-1.3	0.7	0.0	0.9	2.4	-2.7	-0.7	2.8	-3.4	-2.8	-4.4	2.6	4.6	1.2
TC7-DE	-0.3	-0.6	0.7	0.5	0.9	2.2	-2.2	-0.9	2.6	-3.9	-1.0	-8.2	2.6	4.4	8.0
TC7-EE	-0.3	-1.4	0.7	0.4	0.9	2.2	-3.0	-0.6	2.9	-3.1	-3.0	-5.0	2.6	4.7	0.3
TC7-GE	-0.4	-2.7	0.7	1.6	0.9	2.5	-4.0	-1.3	2.2	-5.0	-0.7	0.1	2.4	4.0	9.5
TC7-IE	-0.2	-0.7	0.1	0.4	0.3	0.3	-3.1	-0.6	3.0	-3.3	-3.9	-4.6	2.6	4.8	-2.3
TC7-KE	-0.7	-3.4	0.6	0.2	0.8	2.6	-4.3	-0.6	2.9	-4.1	-2.8	-4.7	2.1	4.7	3.8
TC7-LE	-0.5	-0.7	0.6	0.4	0.8	1.9	-2.3	-0.3	3.2	-2.3	-0.4	-3.4	2.4	5.1	11.0
TC7-BW	0.0	-0.3	0.6	1.0	0.8	1.4	-2.4	0.3	3.8	-2.0	-4.2	-4.8	2.8	5.5	-0.2
TC7-DW	-0.2	-0.7	0.7	0.3	0.9	2.2	-2.2	0.0	3.5	-1.2	-2.1	-5.8	2.6	5.3	2.8
TC7-EW	-0.2	-0.7	0.6	0.3	0.8	1.9	-2.3	-0.8	2.7	-4.3	-1.9	-8.2	2.6	4.5	6.5
TC7-FW	-0.3	-1.0	0.8	0.4	1.0	2.3	-2.5	-1.0	2.5	-4.1	-1.4	0.8	2.5	4.3	6.7
TC7-GW	-0.4	-0.9	0.7	0.4	0.9	2.3	-2.5	-1.6	1.9	-6.2	-1.9	-8.5	2.5	3.7	6.1
TC7-IW	-0.7	-1.8	0.7	1.2	0.9	2.6	-2.9	-0.1	3.4	-1.6	-1.0	-1.9	2.1	5.2	7.6
TC7-JW	-0.5	-1.4	0.8	0.6	1.0	2.7	-2.7	-1.1	2.5	-4.2	-2.5	1.0	2.3	4.2	1.8
TC7-KW	-0.9	-2.8	0.5	0.0	0.7	2.6	-3.5	-1.4	2.2	-5.1	-3.3	-2.8	1.9	3.9	-1.1

Table C.4 Continued.

Lysimeter ID	Saturation Indices (SIs) Calculated by MINTEQA2														
	Gypsum [$CaSO_4{\cdot}2H_2O$]	Mackinawite [$Fe_{1+x}S$]	Pyrite [FeS_2]	Quartz [SiO_2]	Siderite [$FeCO_3$]	SiO_2 (amorph)	Rhodochrosite [$MnCO_3$]	MnS (green)	Chalcopyrite [$CuFeS_2$]	Smithsonite [$ZnCO_3$]	$Zn(OH)_2$	ZnS (amorph)	Sphalerite [ZnS]	Wurtzite [ZnS]	Cerrusite [$PbCO_3$]
TC2-BE	0.0	-5.7	15.2	0.6	-3.4	-0.5	0.1	-10.4	0.2	-1.1	3.4	6.2	4.1	5.6	-2.4
TC2-DE	0.0	-4.7	14.1	0.6	-2.7	-0.4	-0.9	-11.1	-0.2	-1.3	3.3	6.1	4.0	5.6	-2.4
TC2-GE	0.0	-4.9	17.5	0.8	-3.8	-0.2	-0.6	-9.9	-1.4	-2.2	3.0	5.7	3.7	6.1	-2.3
TC2-HE	0.0	-8.4	13.8	0.9	-5.7	-0.1	-0.3	-11.2	-2.3	-2.6	0.5	3.2	1.2	6.3	-2.3
TC2-IE	0.0	-7.0	11.8	0.9	-4.3	-0.1	-0.6	-11.5	-1.9	-2.7	0.9	3.6	1.6	5.8	-2.3
TC2-KE	0.0	-7.1	12.0	0.8	-4.4	-0.2	-0.8	-11.7	-2.1	-2.9	0.7	3.4	1.4	5.8	-2.3
TC2-LE	0.0	-7.6	13.0	0.8	-4.9	-0.2	-0.5	-11.5	-2.5	-2.9	0.3	3.1	1.0	6.2	-2.3
TC2-CW	-0.1	-2.9	13.8	0.3	-1.5	-0.7	-0.7	-10.2	-0.2	-1.1	3.9	6.6	4.6	5.6	-2.5
TC2-DW	-0.1	-2.1	14.3	0.7	-1.3	-0.3	-1.3	-10.3	-1.2	-1.7	3.6	6.3	4.3	5.9	-2.5
TC2-EW	-0.1	-2.6	14.2	0.6	-1.5	-0.4	-1.0	-10.3	-1.1	-1.8	3.3	6.0	4.0	5.8	-2.4
TC2-FW	-0.2	-1.3	14.1	0.2	-0.4	-0.9	-1.8	-10.9	-1.2	-1.5	3.4	6.1	4.1	5.9	-2.5
TC2-HW	-0.1	-3.8	8.6	0.9	-4.6	-0.1	-4.1	-11.5	-6.2	-3.4	0.0	2.7	0.7	5.9	-4.6
TC2-IW	-0.1	-3.6	13.2	0.5	-2.7	-0.5	-1.1	-10.3	-1.8	-2.4	2.7	5.4	3.4	5.9	-0.7
TC2-KW	-0.1	-3.9	8.8	0.7	-2.3	-0.4	-1.5	-11.2	-3.2	-2.6	0.8	3.5	1.5	5.9	-1.9
TC3-DE	0.0	-1.2	16.6	0.8	-1.3	-0.3	-1.2	-9.4	-2.5	-3.4	3.1	5.8	3.8	5.7	-2.7
TC3-EE	-0.1	-2.5	15.7	0.5	-1.7	-0.5	-1.5	-10.5	-0.8	-1.6	3.9	6.6	4.5	5.8	-2.4
TC3-FE	-0.1	-2.5	14.7	0.4	-1.5	-0.6	-1.6	-10.9	-0.6	-1.4	3.8	6.5	4.5	5.8	-2.4
TC3-GE	-0.1	-3.3	15.7	0.6	-2.3	-0.4	-1.3	-10.5	-0.6	-1.4	4.0	6.7	4.6	6.0	-2.3
TC3-HE	-0.1	-2.8	15.3	0.5	-1.7	-0.5	-1.5	-10.7	-0.7	-1.6	3.8	6.5	4.5	5.8	-2.4
TC3-IE	0.0	-2.1	15.1	0.3	-1.3	-0.7	-1.4	-10.4	-0.8	-1.4	3.9	6.6	4.6	6.0	-2.4
TC3-KE	0.0	-2.9	15.1	0.3	-1.7	-0.7	-1.3	-10.8	-0.5	-1.3	3.8	6.6	4.5	5.9	-2.4
TC3-LE	-0.1	-2.8	16.2	0.6	-2.1	-0.4	-1.3	-10.2	-2.4	-3.1	2.4	5.2	3.1	5.9	-2.4
TC3-BW	0.0	-5.3	16.4	0.4	-3.3	-0.6	-0.2	-10.4	0.1	-1.0	3.6	6.4	4.3	5.8	-2.3
TC3-EW	0.0	-1.7	16.0	-0.1	-0.9	-1.1	-1.3	-10.4	-0.7	-1.5	4.0	6.8	4.7	5.8	-2.4
TC3-FW	0.0	-2.8	14.6	0.3	-1.3	-0.7	-1.6	-11.2	-0.5	-1.3	3.6	6.3	4.3	5.8	-2.4
TC3-GW	0.0	-2.6	16.2	0.5	-1.8	-0.5	-1.3	-10.4	-1.0	-1.7	3.7	6.5	4.4	6.0	-2.3
TC3-HW	0.0	-1.4	16.0	-0.7	-0.1	-1.8	-1.4	-10.9	-0.6	-1.4	3.6	6.4	4.3	5.8	-2.4
TC3-JW	0.0	-2.7	16.1	0.2	-1.7	-0.8	-1.3	-10.5	-0.6	-1.5	3.9	6.7	4.6	5.9	-1.8
TC3-KW	0.0	-2.6	17.0	-0.5	-1.5	-1.6	-1.2	-10.6	-0.5	-1.3	3.9	6.7	4.6	5.9	-2.3
TC4-CE	0.0	-1.7	14.3	0.0	-0.2	-1.1	-0.6	-10.3	-0.5	-1.2	3.5	6.3	4.2	4.5	-2.4
TC4-DE	-0.1	-0.5	17.3	0.9	-1.4	-0.2	-1.9	-9.2	-5.5	-6.2	1.0	3.7	1.6	4.2	-3.8
TC4-EE	-0.1	-1.9	15.2	0.5	-0.9	-0.5	-1.6	-10.8	-1.5	-2.3	3.0	5.8	3.7	4.5	-2.4
TC4-HE	-0.4	-2.6	13.2	1.1	-2.1	0.1	-2.1	-10.9	-3.6	-4.3	1.4	4.1	2.0	4.4	-2.5
TC4-KE	0.0	-1.3	14.7	0.1	-0.3	-0.9	-1.9	-11.1	-1.0	-1.7	3.5	6.2	4.2	4.5	-2.5
TC4-LE	-0.8	-0.5	19.5	0.7	-2.3	-0.3	-1.3	-7.8	-6.7	-6.9	0.6	3.3	1.3	4.1	-5.0
TC4-BW	-0.1	-4.6	16.4	0.5	-2.2	-0.6	0.0	-10.6	0.0	-1.7	3.2	6.0	3.9	4.5	-2.3
TC4-DW	-0.1	-1.5	15.3	0.9	-0.4	-0.1	-0.9	-10.1	-2.7	-4.5	1.7	4.4	2.4	4.2	-2.7
TC4-FW	-0.2	-0.9	17.6	1.0	-0.3	-0.1	-0.8	-9.7	-3.3	-5.3	1.6	4.3	2.3	4.3	-2.4
TC4-GW	-0.4	0.2	20.0	1.2	-0.7	0.1	-0.8	-8.1	-6.6	-8.7	-0.2	2.6	0.5	3.3	-5.0
TC4-HW	-2.8	-1.9	16.1	0.9	-0.3	-0.1	-1.2	-11.0	-1.8	-3.7	2.1	4.8	2.8	4.8	-2.3
TC4-IW	-0.2	-0.6	18.1	1.0	-0.9	0.0	-0.9	-8.8	-6.5	-8.8	-0.8	1.9	-0.2	3.4	-4.4
TC4-JW	-0.3	-2.4	16.2	0.5	-0.6	-0.5	-1.1	-11.1	-0.9	-2.7	2.8	5.6	3.5	4.5	-2.3
TC4-KW	-0.1	-2.0	14.5	0.8	-0.8	-0.2	-0.4	-9.7	-1.0	-2.1	3.2	5.9	3.9	4.8	-2.6

Table C.4 Continued.

Lysimeter ID	Saturation Indices (SIs) Calculated by MINTEQA2														
	Gypsum [$CaSO_4{\cdot}2H_2O$]	Mackinawite [$Fe_{1+x}S$]	Pyrite [FeS_2]	Quartz [SiO_2]	Siderite [$FeCO_3$]	SiO_2 (amorph)	Rhodochrosite [$MnCO_3$]	MnS (green)	Chalcopyrite [$CuFeS_2$]	Smithsonite [$ZnCO_3$]	$Zn(OH)_2$	ZnS (amorph)	Sphalerite [ZnS]	Wurtzite [ZnS]	Cerrusite [$PbCO_3$]
TC5-CE	0.0	-1.7	13.9	0.5	0.2	-0.5	-0.1	-10.2	-0.5	-1.9	3.1	5.8	3.7	4.5	-2.6
TC5-DE	-0.1	-1.4	15.6	0.6	0.1	-0.4	-0.8	-10.4	-1.7	-3.1	2.3	5.0	3.0	4.7	-2.6
TC5-FE	-0.1	-1.6	15.2	0.9	-0.7	-0.2	-0.8	-9.9	-2.4	-3.5	2.1	4.9	2.8	4.7	-2.6
TC5-GE	-0.1	0.0	18.2	0.6	0.1	-0.4	-0.7	-8.9	-4.4	-5.9	1.0	3.8	1.7	4.4	-3.1
TC5-HE	0.0	-1.7	14.5	0.4	0.1	-0.6	-0.9	-10.8	-0.9	-2.2	2.9	5.6	3.6	4.6	-2.6
TC5-IE	-0.1	-2.2	15.2	0.1	-0.3	-0.9	-0.4	-10.5	-0.5	-1.8	3.1	5.8	3.8	4.5	-2.6
TC5-LE	-0.1	-3.6	15.4	0.4	-2.4	-0.6	-0.9	-10.3	-0.5	-1.4	3.7	6.4	4.4	4.7	-2.1
TC5-BW	-0.1	-1.8	13.3	0.3	0.6	-0.8	-0.1	-10.6	-0.4	-2.1	2.7	5.4	3.4	4.3	-2.6
TC5-CW	-0.1	-1.7	13.1	0.2	0.7	-0.9	-0.7	-11.3	-1.1	-2.5	1.9	4.6	2.6	4.5	-2.6
TC5-DW	-0.1	-1.6	14.1	0.6	0.3	-0.4	-0.8	-10.9	-1.4	-2.9	2.3	5.0	2.9	4.5	-2.6
TC5-FW	-0.1	-1.4	13.6	0.7	0.3	-0.3	-0.9	-10.8	-1.5	-2.9	2.2	4.9	2.9	4.5	-2.6
TC5-GW	-0.1	-1.4	14.4	0.2	0.6	-0.8	-0.9	-11.0	-0.6	-2.0	3.0	5.7	3.6	4.5	-2.6
TC5-HW	-0.1	-1.7	14.4	-0.1	0.4	-1.1	-1.0	-11.2	-0.3	-1.8	3.1	5.8	3.8	4.4	-2.6
TC5-JW	-0.1	-1.4	12.9	-0.4	0.7	-1.4	-0.8	-11.1	-0.2	-1.5	3.2	5.9	3.8	4.3	-2.7
TC6-CE	-0.2	-1.7	16.2	0.8	-0.4	-0.2	-0.8	-10.4	-2.5	-4.3	1.7	4.4	2.4	4.5	-2.6
TC6-FE	-0.2	-1.0	18.1	0.9	-0.9	-0.1	-0.6	-8.9	-4.6	-6.1	0.8	3.6	1.5	4.4	-3.1
TC6-GE	-0.1	-2.4	15.4	0.7	-0.6	-0.3	-1.0	-11.0	-1.0	-2.6	2.8	5.5	3.4	4.6	-2.6
TC6-HE	-0.1	-0.1	19.4	0.6	-0.4	-0.4	-1.0	-8.9	-5.3	-6.8	0.5	3.3	1.2	4.1	-3.7
TC6-IE	-1.4	-2.9	15.5	0.9	-1.1	-0.1	-0.9	-10.9	-1.2	-3.0	2.5	5.2	3.2	4.8	-2.6
TC6-KE	-1.2	-1.6	15.1	0.7	-0.3	-0.4	-1.1	-10.6	-1.8	-3.2	2.5	5.2	3.2	4.9	-2.6
TC6-LE	-1.1	-0.4	17.5	0.8	-0.5	-0.2	-1.1	-9.1	-4.6	-5.8	1.1	3.9	1.8	4.5	-3.3
TC6-BW	-0.3	-4.4	15.0	0.9	-1.5	-0.2	-0.1	-11.3	-0.6	-2.5	2.0	4.8	2.7	4.7	-2.3
TC6-EW	0.0	-1.0	18.1	0.6	-0.5	-0.4	-1.0	-9.7	-3.5	-5.1	1.6	4.3	2.3	4.4	-2.7
TC6-FW	-0.1	-2.6	15.6	0.7	-0.9	-0.3	-0.9	-10.8	-1.1	-2.7	2.7	5.4	3.4	4.5	-2.6
TC6-GW	-0.2	-1.7	16.0	0.7	-0.4	-0.3	-1.1	-10.7	-1.7	-3.4	2.4	5.2	3.1	4.5	-2.6
TC6-HW	-0.5	0.0	17.5	0.8	0.3	-0.2	-1.1	-9.6	-4.3	-6.1	1.0	3.7	1.7	4.3	-3.0
TC6-JW	-0.8	-3.4	15.4	0.8	-1.5	-0.2	-0.1	-10.3	-0.9	-2.4	2.7	5.5	3.4	4.8	-2.6
TC6-KW	-2.3	-2.4	19.0	0.7	-2.0	-0.3	-1.3	-9.9	-2.5	-3.9	2.7	5.5	3.4	4.8	-2.8
TC7-CE	-1.0	-2.1	15.3	0.7	0.1	-0.3	-0.3	-10.7	-0.8	-2.9	2.6	5.4	3.3	4.5	-2.6
TC7-DE	-0.4	-0.3	18.8	1.0	-0.2	0.0	-0.8	-9.2	-4.7	-6.6	0.7	3.5	1.4	4.2	-3.3
TC7-EE	-1.1	-2.3	14.8	0.7	0.2	-0.4	0.1	-10.5	-0.2	-2.4	2.8	5.6	3.5	4.4	-2.6
TC7-GE	-2.4	0.0	19.4	1.0	-0.2	0.0	-0.8	-8.7	-5.7	-7.9	0.0	2.8	0.7	3.6	-4.3
TC7-IE	-0.5	-3.1	13.9	0.3	-0.8	-0.7	0.2	-10.4	0.2	-1.2	3.4	6.1	4.0	4.4	-2.6
TC7-KE	-3.1	-2.1	17.9	0.8	-1.2	-0.2	-1.3	-10.4	-2.6	-4.3	2.0	4.7	2.7	4.8	-2.7
TC7-LE	-0.4	0.4	20.1	0.4	-0.2	-0.6	-1.0	-8.7	-5.8	-7.4	0.2	3.0	0.9	3.9	-4.3
TC7-BW	0.0	-3.4	16.8	-0.3	-0.7	-1.4	0.4	-10.6	0.0	-2.0	2.8	5.6	3.5	4.3	-2.3
TC7-DW	-0.4	-1.4	15.8	0.3	0.7	-0.7	-0.5	-10.9	-0.9	-2.9	2.5	5.2	3.2	4.6	-2.6
TC7-EW	-0.4	-1.2	18.9	0.9	-0.8	-0.2	-0.9	-9.5	-4.2	-6.2	0.9	3.7	1.6	4.3	-3.0
TC7-FW	-0.7	-0.6	18.1	1.0	-0.2	0.0	-0.6	-9.2	-4.2	-6.1	1.0	3.8	1.7	4.4	-2.9
TC7-GW	-0.7	-1.2	18.5	1.0	-1.2	0.0	-0.8	-9.0	-4.9	-6.9	0.6	3.3	1.3	4.1	-3.5
TC7-IW	-1.5	-0.3	18.1	0.7	0.1	-0.3	-1.1	-9.7	-3.7	-5.3	1.4	4.1	2.1	4.7	-2.8
TC7-JW	-1.1	-1.8	15.5	1.0	-0.3	0.0	-0.3	-10.1	-2.1	-4.0	1.9	4.7	2.6	4.7	-2.6
TC7-KW	-2.5	-2.6	14.1	1.0	-1.0	0.0	-1.0	-10.7	-3.6	-4.9	0.4	3.2	1.1	5.2	-2.7

Table C.4 Continued.

	Saturation Indices (SIs) Calculated by MINTEQA2												
Lysimeter ID	**Anglesite [$PbSO_4$]**	**Galena [PbS]**	**$Pb(OH)_2$**	**$NiCO_3$**	**$Ni(OH)_2$**	**Millerite [NiS]**	**Orpiment [As_2S_3]**	**Realgar [As_4S_4]**	**Stibnite [Sb_2S_3]**	**Sb_2O_4**	**$Sb(OH)_3$**	**Native S**	**Tl_2S**
TC2-BE	-4.2	1.7	-4.4	-6.2	-2.1	-0.7	-14.0	-13.5	-2.3	1.9	-1.0	8.5	-8.0
TC2-DE	-4.1	2.0	-4.2	-6.6	-2.4	-0.8	-13.6	-12.3	-1.4	0.6	-0.6	6.5	-7.8
TC2-GE	-4.5	2.9	-3.8	-6.9	-2.4	-0.2	-11.8	-13.2	2.6	5.9	0.5	10.1	-5.6
TC2-HE	-5.0	1.3	-3.3	-7.0	-2.1	-1.9	-18.0	-16.2	-4.0	7.6	0.4	9.9	-7.2
TC2-IE	-4.4	1.4	-3.7	-6.9	-2.5	-1.8	-16.8	-13.9	-3.5	2.6	-0.1	6.5	-7.9
TC2-KE	-4.5	1.4	-3.8	-6.9	-2.4	-1.8	-16.5	-13.9	-2.3	3.9	0.4	6.8	-8.3
TC2-LE	-4.9	1.4	-3.4	-6.9	-2.1	-1.8	-18.0	-15.4	-3.2	5.9	0.5	8.3	-8.0
TC2-CW	-3.9	2.4	-3.9	-6.6	-2.4	-0.2	-13.2	-11.0	0.1	-1.2	-0.3	4.4	-6.5
TC2-DW	-3.9	3.2	-3.7	-6.9	-2.2	0.2	-11.6	-10.1	3.0	-0.3	0.5	4.1	-6.6
TC2-EW	-4.0	2.8	-3.7	-6.9	-2.5	-0.2	-12.2	-10.6	1.0	-0.5	0.0	4.6	-6.3
TC2-FW	-4.0	2.9	-3.4	-7.0	-2.3	-0.1	-12.3	-10.0	1.2	-1.3	0.3	3.1	-6.3
TC2-HW	-3.5	2.4	-2.4	-9.5	-1.6	-0.9	-17.4	-11.1	-3.4	-2.5	0.3	0.2	-7.7
TC2-IW	-2.4	4.7	-1.9	-7.0	-2.4	-0.2	-13.4	-11.2	2.3	0.3	0.5	4.6	-6.2
TC2-KW	-3.1	2.9	-2.0	-7.3	-1.6	-1.0	-18.7	-11.8	-2.3	-1.4	0.8	0.4	-11.5
TC3-DE	-3.9	3.8	-4.3	-7.1	-2.6	0.8	-7.0	-8.5	1.8	-4.9	-1.8	5.4	-9.6
TC3-EE	-4.0	3.1	-3.9	-6.8	-2.3	0.2	-10.0	-10.2	1.8	-0.5	-0.4	5.8	-6.9
TC3-FE	-3.9	2.9	-3.9	-6.8	-2.3	0.0	-11.3	-10.4	1.3	-0.7	-0.2	4.9	-6.8
TC3-GE	-4.2	3.1	-3.9	-6.8	-2.2	0.1	-10.7	-10.9	1.4	0.4	-0.3	6.6	-6.4
TC3-HE	-4.1	2.9	-4.0	-6.7	-2.4	0.1	-9.8	-10.1	2.0	0.1	-0.1	5.8	-6.4
TC3-IE	-4.0	3.2	-3.7	-6.8	-2.1	0.2	-11.4	-10.4	2.1	-0.4	0.1	4.9	-6.5
TC3-KE	-4.1	2.8	-3.9	-6.8	-2.2	-0.2	-12.5	-11.4	0.8	-0.1	-0.3	5.7	-6.5
TC3-LE	-4.2	3.3	-3.8	-7.1	-2.6	0.0	-9.8	-10.5	3.1	1.3	0.2	6.6	-9.9
TC3-BW	-4.2	2.1	-4.2	-6.3	-1.9	-0.4	-12.9	-13.3	0.7	5.0	0.3	9.3	-11.0
TC3-EW	-3.9	3.1	-4.0	-6.6	-2.0	0.4	-9.5	-9.7	0.6	-2.2	-1.0	5.3	-6.4
TC3-FW	-4.0	2.6	-3.9	-6.8	-2.2	-0.4	-13.9	-11.7	0.6	-0.2	-0.1	5.0	-6.5
TC3-GW	-4.2	3.2	-3.8	-6.9	-2.3	0.1	-10.5	-10.8	1.9	0.4	-0.3	6.5	-7.2
TC3-HW	-4.0	2.7	-3.9	-6.8	-2.3	-0.3	-11.0	-10.3	-0.8	-2.1	-1.0	5.1	-6.7
TC3-JW	-3.6	3.5	-3.4	-6.8	-2.4	0.0	-11.5	-11.2	1.9	0.5	-0.2	6.4	-6.5
TC3-KW	-4.2	2.9	-4.0	-6.8	-2.3	-0.1	-11.3	-11.5	2.1	1.8	0.1	7.2	-6.5
TC4-CE	-3.9	2.5	-3.9	-6.6	-1.9	-0.2	-12.0	-10.1	-1.7	-3.2	-1.0	3.6	-7.1
TC4-DE	-5.1	3.5	-5.2	-7.3	-2.8	1.4	-7.3	-8.6	1.0	-8.2	-3.2	5.5	-8.7
TC4-EE	-4.1	3.0	-3.8	-7.0	-2.4	-0.1	-9.7	-9.5	0.0	-2.7	-1.0	4.7	-8.3
TC4-HE	-4.1	3.4	-3.8	-7.4	-2.8	-0.1	-11.8	-9.9	1.8	-3.3	-0.5	3.5	-10.2
TC4-KE	-3.9	2.9	-3.8	-6.9	-2.3	-0.1	-10.3	-9.3	2.0	-0.9	0.3	3.7	-6.2
TC4-LE	-7.4	3.2	-5.9	-7.6	-2.5	2.0	-5.2	-8.7	-0.4	-9.0	-4.5	7.6	-7.1
TC4-BW	-4.7	1.8	-4.9	-6.2	-2.4	-0.7	-9.9	-11.5	2.0	4.1	0.4	8.5	-7.4
TC4-DW	-5.1	2.5	-5.0	-6.7	-3.5	0.0	-9.0	-9.0	1.3	-4.7	-1.5	4.6	-8.4
TC4-FW	-5.2	3.3	-5.1	-7.0	-3.6	0.2	-5.2	-8.0	1.7	-5.8	-2.5	6.2	-9.0
TC4-GW	-8.1	2.3	-7.9	-7.2	-3.8	1.6	-0.9	-6.4	0.4	-12.7	-5.7	7.4	-7.3
TC4-HW	-7.4	2.5	-4.9	-8.1	-4.5	-1.8	-7.6	-8.9	1.2	-2.4	-1.1	5.6	-9.3
TC4-IW	-7.2	2.1	-7.2	-6.8	-4.2	1.2	-5.7	-8.3	0.7	-10.3	-4.5	6.5	-8.9
TC4-JW	-5.0	2.3	-4.9	-6.9	-3.4	-0.9	-8.5	-9.6	0.7	-1.5	-1.0	6.2	-7.4
TC4-KW	-5.4	2.4	-4.2	-6.9	-3.0	-0.4	-10.6	-9.7	0.8	-1.6	-0.4	4.3	-6.2

Table C.4 Continued.

	Saturation Indices (SIs) Calculated by MINTEQA2												
Lysimeter ID	**Anglesite [$PbSO_4$]**	**Galena [PbS]**	**$Pb(OH)_2$**	**$NiCO_3$**	**$Ni(OH)_2$**	**Millerite [NiS]**	**Orpiment [As_2S_3]**	**Realgar [As_4S_4]**	**Stibnite [Sb_2S_3]**	**Sb_2O_4**	**$Sb(OH)_3$**	**Native S**	**Tl_2S**
TC5-CE	-4.9	1.8	-4.7	-6.5	-2.7	-0.6	-10.8	-9.3	-1.0	-3.5	-0.9	3.3	-8.3
TC5-DE	-5.3	2.2	-4.6	-6.7	-3.0	-0.4	-8.0	-8.6	-0.5	-3.4	-1.3	4.7	-8.5
TC5-FE	-5.0	2.8	-4.3	-6.7	-2.7	0.1	-8.7	-8.9	0.0	-3.7	-1.3	4.6	-8.2
TC5-GE	-5.7	3.2	-5.2	-6.8	-3.1	1.0	-5.1	-7.7	0.4	-7.3	-3.1	5.9	-9.1
TC5-HE	-5.0	2.0	-4.5	-6.7	-2.9	-0.6	-10.3	-9.3	-1.5	-3.8	-1.3	3.9	-7.1
TC5-IE	-4.8	1.8	-4.6	-6.5	-2.7	-0.7	-10.3	-10.0	-1.4	-1.7	-1.0	5.1	-6.9
TC5-LE	-4.1	3.0	-3.5	-6.6	-2.4	-0.1	-12.2	-11.7	1.4	1.8	0.1	6.7	-6.7
TC5-BW	-5.0	1.3	-4.8	-6.4	-3.1	-1.0	-12.2	-9.8	0.5	-1.4	0.2	2.9	-7.7
TC5-CW	-5.0	1.2	-4.6	-6.8	-3.2	-1.4	-12.4	-9.7	-3.6	-4.5	-1.3	2.6	-8.7
TC5-DW	-5.1	1.8	-4.7	-6.7	-3.2	-0.8	-9.5	-8.8	0.1	-2.8	-0.6	3.5	-7.5
TC5-FW	-5.1	1.9	-4.5	-6.8	-3.2	-0.8	-10.1	-8.7	-1.7	-4.9	-1.3	2.9	-7.9
TC5-GW	-5.1	1.7	-4.6	-6.6	-3.0	-0.8	-10.6	-9.3	-0.5	-2.4	-0.5	3.6	-6.7
TC5-HW	-4.9	1.6	-4.6	-6.6	-3.1	-1.0	-11.0	-9.6	-2.3	-3.7	-1.3	3.8	-6.4
TC5-JW	-4.6	1.5	-4.5	-6.5	-3.0	-0.9	-12.4	-9.5	-3.0	-5.2	-1.4	2.1	-6.6
TC6-CE	-5.1	2.4	-5.1	-7.0	-3.5	-0.5	-8.0	-9.0	2.7	-1.8	-0.6	5.6	-12.6
TC6-FE	-5.7	3.2	-5.2	-7.0	-3.2	0.8	-5.5	-8.4	0.9	-6.1	-2.9	6.7	-9.1
TC6-GE	-5.1	2.0	-4.9	-6.7	-3.1	-0.7	-8.7	-9.4	1.0	-0.9	-0.5	5.5	-7.2
TC6-HE	-6.1	2.9	-5.9	-7.0	-3.3	1.1	-2.5	-7.1	0.2	-8.0	-3.9	7.2	-8.9
TC6-IE	-6.4	2.0	-5.0	-7.4	-3.9	-1.3	-8.2	-9.4	0.8	-1.0	-0.8	6.0	-6.9
TC6-KE	-6.1	2.5	-4.7	-7.5	-3.7	-0.9	-8.4	-8.6	1.7	-2.8	-0.7	4.3	-6.8
TC6-LE	-6.6	3.3	-5.1	-7.5	-3.6	0.5	-5.2	-7.6	1.6	-6.5	-2.5	5.5	-8.4
TC6-BW	-5.4	1.2	-5.1	-6.8	-3.2	-1.9	-10.8	-11.1	0.7	2.9	0.4	7.0	-9.4
TC6-EW	-5.1	3.2	-5.1	-6.9	-3.2	0.4	-5.4	-8.3	-0.7	-6.8	-3.4	6.8	-9.7
TC6-FW	-5.0	2.1	-4.9	-6.9	-3.1	-0.7	-8.8	-9.6	1.9	0.0	-0.2	5.8	-7.4
TC6-GW	-5.0	2.4	-5.0	-7.0	-3.3	-0.5	-7.3	-8.6	1.8	-2.3	-0.8	5.4	-9.2
TC6-HW	-6.0	3.1	-5.5	-7.1	-3.7	0.4	-4.2	-6.9	0.5	-8.7	-3.3	5.1	-9.1
TC6-JW	-5.9	1.9	-4.8	-7.3	-3.5	-1.3	-9.7	-10.3	-1.2	-1.4	-1.3	6.4	-8.1
TC6-KW	-7.3	3.2	-4.9	-7.8	-3.9	-0.3	-5.9	-9.7	1.3	-2.3	-2.3	9.0	-5.9
TC7-CE	-6.2	1.7	-5.5	-7.2	-4.0	-1.5	-8.3	-8.9	0.1	-3.2	-1.3	5.1	-8.7
TC7-DE	-6.2	3.0	-6.0	-7.1	-3.7	0.6	-3.3	-7.3	1.4	-7.8	-3.5	6.7	-8.9
TC7-EE	-6.2	1.3	-5.5	-6.8	-3.7	-1.4	-8.6	-8.9	0.1	-2.2	-0.8	4.8	-7.9
TC7-GE	-9.2	2.3	-7.2	-7.5	-4.5	0.5	-0.8	-6.2	0.3	-10.6	-4.8	7.0	-8.1
TC7-IE	-5.0	1.3	-4.7	-6.2	-2.5	-0.8	-11.2	-10.2	-2.9	-2.5	-1.3	4.8	-9.2
TC7-KE	-8.2	2.8	-5.1	-7.8	-4.3	-0.8	-6.7	-9.4	2.1	-1.7	-1.4	7.6	-9.0
TC7-LE	-7.0	2.6	-6.5	-7.1	-3.6	1.2	-3.1	-7.5	0.9	-8.2	-4.0	7.5	-8.5
TC7-BW	-4.8	1.4	-5.2	-6.2	-2.8	-1.1	-9.7	-11.0	1.1	3.0	0.1	7.8	-7.7
TC7-DW	-5.6	1.7	-5.4	-6.9	-3.5	-1.2	-7.1	-8.2	-0.1	-3.3	-1.3	4.8	-8.6
TC7-EW	-5.8	3.1	-5.6	-7.1	-3.7	0.4	-3.4	-7.8	1.1	-5.7	-3.1	7.7	-9.3
TC7-FW	-6.2	3.1	-5.6	-7.3	-3.8	0.2	-5.2	-8.1	0.9	-7.5	-3.3	6.3	-8.9
TC7-GW	-6.7	2.8	-6.2	-7.3	-4.0	0.5	-4.0	-7.9	0.6	-8.0	-3.9	7.4	-8.6
TC7-IW	-6.8	3.1	-5.0	-7.7	-4.0	-0.2	-4.8	-7.7	0.2	-6.5	-2.9	6.1	-8.6
TC7-JW	-6.4	2.3	-5.2	-7.3	-3.8	-0.9	-7.7	-8.6	1.3	-3.5	-1.2	4.9	-9.8
TC7-KW	-7.5	2.2	-4.8	-8.0	-4.1	-1.6	-10.6	-9.7	-0.4	-3.8	-1.3	4.3	-9.5

Table C.5 Summary of pore-water data for lysimeter samples collected in October 2006.

Lysimeter ID	Depth (m)	Sample Date	Temp. (°C)	pH	Eh (mV)	Alk. (mg L^{-1})	H_2S (μg L^{-1})	$\delta^{34}S$-SO_4 (‰)	$\delta^{13}C$-DIC (‰)
TC2-AW	0.25	23-Aug-08	13.9	6.95	290	940	2	-13.89	
TC2-BE	0.50	21-Aug-08	13.8	6.78	245	490	5	-13.98	-1.86
TC2-CE	0.75	21-Aug-08	13.4	6.99	203	680	2	-14.30	-1.96
TC2-DE	1.00	21-Aug-08	12.9	6.91	255	540	4	-14.35	-3.04
TC2-DW	1.00	22-Aug-08	12.9	7.14	257	620	18	-12.05	
TC2-EE	1.25	21-Aug-08	12.5	7.07	194	660	105		
TC2-EW	1.25	22-Aug-08	12.5	7.22	272	580	-2		
TC2-FW	1.50	21-Aug-08	12.0	7.09	226	510	23	-12.42	-5.5
TC2-GE	1.75	21-Aug-08	11.7	7.31	192	470	18		
TC2-HE	2.00	21-Aug-08	11.4	7.31	188	270	12	-10.01	-8.77
TC2-HW	2.00	21-Aug-08	11.4	7.39	173	320	25	-10.30	-10.68
TC2-JW	3.00	22-Aug-08	9.6	7.52	319	120	16		
TC2-KE	3.50	21-Aug-08	9.2	7.55	385	70	208	-6.90	-10.24
TC3-AW	0.25	24-Aug-08	13.9	6.90	233	800	169	-14.66	
TC3-BW	0.50	20-Aug-08	13.8	6.90	226	520	287	-13.95	-4.13
TC3-CE	0.75	23-Aug-08	13.4	7.10	243	640	143		
TC3-DE	1.00	20-Aug-08	12.9	7.06	319	740	81		-3.88
TC3-EE	1.25	20-Aug-08	12.5	6.96	211	660	3		
TC3-EW	1.25	20-Aug-08	12.5	7.26	171	720	32		
TC3-FW	1.50	20-Aug-08	12.0	7.16	198	620	23	-11.64	-8.33
TC3-GE	1.75	20-Aug-08	11.7	7.15	199	560	5		
TC3-GW	1.75	20-Aug-08	11.7	7.29	157	440	30		
TC3-HE	2.00	20-Aug-08	11.4	7.08	323	450	8	-13.61	-8.77
TC3-IE	2.50	20-Aug-08	10.5	7.35	224	380			-12.22
TC3-JW	3.00	20-Aug-08	9.6	7.32	226	350		-3.91	-11.36
TC3-KW	3.50	20-Aug-08	9.2	7.27	240	260	13	-0.45	-12.42
TC3-LE	4.00	20-Aug-08	8.9	7.33	296	320	9	1.08	-12.28
TC4-AE	0.25	24-Aug-08	13.9	6.94	272	900	113	-14.43	
TC4-CE	0.75	19-Aug-08	13.4	7.09	247	660	-2	-9.84	
TC4-DW	1.00	19-Aug-08	12.9	7.22	145	1580	1	1.63	-22.88
TC4-EW	1.25	19-Aug-08	12.5	7.16	140	1620	1014	5.08	
TC4-FW	1.50	19-Aug-08	12.0	7.30	149	2220	762	20.18	-21.49
TC4-GE	1.75	19-Aug-08	11.7	7.20	257	2160	214	20.78	
TC4-HE	2.00	19-Aug-08	11.4	7.27	133	3300	6413	6.72	-22.79
TC4-HW	2.00	19-Aug-08	11.4	7.27	146	1680	-2	4.45	-19.09
TC4-IE	2.50	19-Aug-08	10.5	7.56	238	3280	39		-19.71
TC4-JW	3.00	19-Aug-08	9.6	7.61	200	2720	22	23.52	-21.4
TC4-KE	3.50	19-Aug-08	9.2	7.42	199	1560	49	4.78	-20.6
TC4-KW	3.50	19-Aug-08	9.2	7.66	197	2560	55	7.53	-21.03
TC4-LE	4.00	19-Aug-08	8.9	7.64	276	2300	125		-20.93

Table C.5 Continued.

Lysimeter ID	Depth (m)	Sample Date	Temp. (°C)	pH	Eh (mV)	Alk. (mg L^{-1})	H_2S (μg L^{-1})	$\delta^{34}S$-SO_4 (‰)	$\delta^{13}C$-DIC (‰)
TC5-BW	0.50	19-Aug-08	13.8	6.97	234	820	159	-12.21	-1.56
TC5-CE	0.75	18-Aug-08	13.4	7.11	173	840	3		
TC5-DE	1.00	18-Aug-08	12.9	7.45	164	960	39	-2.45	-18.39
TC5-EW	1.25	18-Aug-08	12.5	7.31	131	940	-2		
TC5-GE	1.75	18-Aug-08	11.7	7.29	146	960	3		
TC5-GW	1.75	18-Aug-08	11.7	7.30	185	740	-2		-18.11
TC5-HE	2.00	18-Aug-08	11.4	7.30	166	720		7.36	-19.37
TC5-HW	2.00	18-Aug-08	11.4	7.31	165	780	-2	-2.31	
TC5-IE	2.50	18-Aug-08	10.5	7.33	195	760	-2		-17.45
TC5-IW	2.50	18-Aug-08	10.5	7.33	192	640	1		
TC5-JW	3.00	18-Aug-08	9.6	7.04	206	380	4	-13.03	-11.66
TC5-LE	4.00	18-Aug-08	8.9	7.46	162	360	-2	4.31	-17.04
TC6-AE	0.25	24-Aug-08	13.9	6.85	398	740	22	-14.99	
TC6-BW	0.50	17-Aug-08	13.8	6.77	167	700	1	-13.57	-2.79
TC6-CE	0.75	18-Aug-08	13.4	6.97	209	900	10		
TC6-DW	1.00	17-Aug-08	12.9	6.89	150	800	-2	-12.39	-5.81
TC6-EW	1.25	17-Aug-08	12.5	7.18	126	1120	2		
TC6-FE	1.50	17-Aug-08	12.0	7.27	137	920	3	-0.01	-15.99
TC6-GE	1.75	17-Aug-08	11.7	7.28	127	800	4		
TC6-HE	2.00	17-Aug-08	11.4	7.36	121	800	-2		
TC6-HW	2.00	17-Aug-08	11.4	7.65	139	2060	4	10.08	-17.9
TC6-IE	2.50	17-Aug-08	10.5	7.48	153	1280			-21.66
TC6-JW	3.00	17-Aug-08	9.6	7.14	164	920	3		-15.37
TC6-KE	3.50	17-Aug-08	9.2	7.38	132	1100	2		
TC6-KW	3.50	18-Aug-08	9.2	7.71	187	1640	1	18.77	-21.18
TC6-LE	4.00	17-Aug-08	8.9	7.54	130	1180	11	17.09	-20.39
TC7-AE	0.25	16-Aug-08	13.9	6.67	402	380	-2		
TC7-BW	0.50	16-Aug-08	13.8	7.24	154	2100	23	-6.77	-6.98
TC7-CE	0.75	16-Aug-08	13.4	6.83	183	720	2		
TC7-CW	0.75	16-Aug-08	13.4	6.99	154	1160	2		
TC7-DE	1.00	16-Aug-08	12.9	7.40	159	2680	2	11.20	-20.27
TC7-EW	1.25	16-Aug-08	12.5	7.46	196	2300	2		-18.14
TC7-FW	1.50	16-Aug-08	12.0	7.54	147	2480	-2	27.19	
TC7-GE	1.75	16-Aug-08	11.7	7.54	129	4060	68		
TC7-GW	1.75	17-Aug-08	11.7	7.43	128	2060	54	17.11	
TC7-IW	2.50	16-Aug-08	10.5	7.22	144	1060	2		-14.42
TC7-JW	3.00	16-Aug-08	9.6	7.51	173	1560	-2	7.36	-18.68
TC7-KE	3.50	16-Aug-08	9.2	7.72	186	2790	4		-15.44
TC7-KW	3.50	17-Aug-08	9.2	7.71	250	1760	9	7.19	-17.78
TC7-LE	4.00	16-Aug-08	8.9	7.16	150	640	2		-15.73

Table C.5 Continued.

Lysimeter	Aqueous Concentration (mg L^{-1})								
ID	Br	Cl	NO_3-N	NO_2-N	SO_4	S_2O_3	o-PO_4	NH_3-N	DOC
TC2-AW	-1	-1	-2		10830	325	0.035	0.26	-1
TC2-BE	-1	-1	-2		4547	81	0.008	-0.1	-1
TC2-CE	-1	-1	-2		5461	126	0.007	-0.1	-1
TC2-DE	-1	-1	-2		4757	-2	0.006	-0.1	-1
TC2-DW	-1	-1	-2		2345	-2	0.007	0.16	1.3
TC2-EE	-1	1.8	-2		4688	-2	0.011	-0.1	
TC2-EW	-1	-1	-2		3018	-2	0.008	0.26	1.5
TC2-FW	-1	-1	-2		1346	1.7	0.007	0.14	1.1
TC2-GE	-1	-1	-2		2254	-2	0.009	0.23	1.7
TC2-HE	-1	-1	-2		1833	-2	0.016	0.26	1.3
TC2-HW	-1	2.1	-2		3441	-2	0.007	2.7	2.5
TC2-JW	-1	3.0	-2		2630	-2	0.006	2.7	
TC2-KE	-1	3.6	-2		3769	34	0.008	1.41	3.2
TC3-AW	-1	-1	-2		10568	52		-0.1	1.6
TC3-BW	-1	-1	-2		4325	32		-0.1	1.3
TC3-CE	-1	-1	-2		3529	33	0.010	0.18	1.9
TC3-DE	-1	-1	-2		5967	-2	0.041	-0.1	2.0
TC3-EE	-1	2.4	-2		3405	3.3	0.047	-0.1	2.7
TC3-EW	-1	-1	-2		5714	2.6	0.008	-0.1	2.6
TC3-FW	-1	1.8	-2		4394	2.3	0.008	0.42	2.2
TC3-GE	-1	1.7	-2		2971	-2		-0.1	2.5
TC3-GW	-1	2.4	-2		2991	-2	0.008	2.0	
TC3-HE	-1	-1	-2		2027	-2	0.052	-0.1	1.9
TC3-IE	-1	2.4	-2		2589	-2	0.057	0.64	4.7
TC3-JW	-1	2.9	-2		2773	-2	0.007	1.7	3.7
TC3-KW	-1	3.3	-2		1779	-2	0.007	2.6	3.2
TC3-LE	-1	3.1	-2		2453	-2	0.061	-0.1	4.1
TC4-AE	-1	-1	-2		9079	17		5	5.7
TC4-CE	-1	-1	-2		3569	-2		19	9.3
TC4-DW	-1	3.9	-2		5216	-2	0.081	50	79
TC4-EW	-1	6.7	-2		3415	-2	0.097	63	140
TC4-FW	-1	3.9	-2		1301	-2	0.394	60	280
TC4-GE	-1	5.5	-2		1145	-2	0.359	68	220
TC4-HE	-1	5.7	-2		1757	3.0	0.962	109	340
TC4-HW	-1	2.6	-2		2805	-2	0.094	60	6.7
TC4-IE	1.1	3.4	-2		1.1	-2	0.041	81	320
TC4-JW	-1	3.3	-2		398	-2	0.072	58	7.4
TC4-KE	-1	2.5	-2		2069	14	0.007		3.8
TC4-KW	1.9	6.2	-2		77	4.6	0.008	90	
TC4-LE	1.6	5.0	-2		36	8.2	0.004	98	220

Table C.5 Continued.

Lysimeter	Aqueous Concentration (mg L^{-1})								
ID	Br	Cl	NO_3-N	NO_2-N	SO_4	S_2O_3	o-PO_4	NH_3-N	DOC
TC5-BW	-1	-1	-2		5249	9.1	0.005	2.6	
TC5-CE	-1	-1	-2		4942	-2	0.022	5	3.6
TC5-DE	-1	-1	-2		4536	-2	1.176	54	12
TC5-EW	-1	-1	-2		4952	-2	0.008	32	11
TC5-GE	-1	6.9	-2		3520	-2	0.039	80	14
TC5-GW	-1	7.0	-2		3380	-2	0.005	104	16
TC5-HE	-1	5.9	-2		3139	-2	0.011	125	10
TC5-HW	-1	-1	-2		3455	-2	0.003	100	5.7
TC5-IE	-1	-1	-2		3622	-2	0.011	100	3.9
TC5-IW	-1	7.5	-2		2222	-2	0.003	136	11
TC5-JW	-1	-1	-2		5938	-2	0.003	42	2.1
TC5-LE	-1	-1	-2		2409	-2	0.009	107	11
TC6-AE	-1	-1	-2		6972	-2	0.052	0.68	
TC6-BW	-1	-1	-2		7989	-2	0.011	3.7	3.8
TC6-CE	-1	-1	-2		4773	-2	0.074	4.5	
TC6-DW	-1	-1	-2		6127	-2	0.017	3.7	2.1
TC6-EW	-1	-1	-2		4504	-2	0.010	50	3.3
TC6-FE	-1	-1	-2		2650	-2	0.118	116	5.8
TC6-GE	-1	-1	-2		3305	-2	0.077	80	9.5
TC6-HE	-1	-1	-2		2526	-2	0.061	60	2.8
TC6-HW	-1	-1	-2		2292	-2	0.254	92	9.5
TC6-IE	-1	-1	-2		3936	-2	0.107	47	8.6
TC6-JW	-1	-1	-2		3799	-2	0.037	40	6.7
TC6-KE	-1	3.2	-2		4506	-2	0.072	73	6.2
TC6-KW	-1	3.5	-2		2151	-2	0.046	40	7.5
TC6-LE	-1	4.8	-2		2691	-2	0.069	139	6.2
TC7-AE	-1	-1	-2		5359	-2	0.028	0.52	5.3
TC7-BW	-1	-1	-2		5519	-2	0.078	38	1.6
TC7-CE	-1	1.6	-2		6375	-2	0.014	75	7.7
TC7-CW	-1	3.0	-2		5126	-2	0.012	32	
TC7-DE	-1	5.2	-2		2666	-2	1.749	115	11
TC7-EW	-1	3.7	-2		435	-2	0.225	143	11
TC7-FW	-1	4.6	-2		959	-2	1.502	194	15
TC7-GE	-1	4.8	-2		0.55	-2	2.867	150	69
TC7-GW	-1	4.5	-2		1041	-2	2.225	156	
TC7-IW	-1	1.4	-2		2182	-2	0.037	37	4
TC7-JW	-1	3.0	-2		1444	-2	0.538	81	5.9
TC7-KE	-1	5.1	-2		18	1.2	0.007	60	22
TC7-KW	-1	3.6	-2		824	1.2	0.029	87	10
TC7-LE	-1	2.3	-2		1999	-2	0.008	21	1.4

Table C.5 Continued.

Lysimeter	Aqueous Concentration (mg L^{-1})							
ID	Al	Ca	Fe	Mg	K	Si	Na	Zn
TC2-AW	0.17	455	7.9	2103	3	2.2	8.8	45
TC2-BE	0.47	474	26.8	1187	7	2.7	8.9	89
TC2-CE	0.15	459	21.2	1685	1	1.8	8.8	36
TC2-DE	0.21	465	6.3	1200	1	1.2	7.6	61
TC2-DW	0.11	564	10.5	393	4	1.1	8.4	12
TC2-EE	0.29	523	23.0	1381	2	1.1	7.7	18
TC2-EW	0.08	500	12.9	622	6	2.2	6.8	16
TC2-FW	0.24	586	12.9	241	3	1.1	7.2	14
TC2-GE	0.28	569	11.2	458	4	1.5	6.5	5.6
TC2-HE	0.25	648	17.7	352	4	1.0	7.6	2.3
TC2-HW	0.11	479	12.3	828	6	2.3	7.9	3.0
TC2-JW	0.18	475	2.2	404	17	4.6	5.7	0.51
TC2-KE	0.01	445	0.1	876	7	3.3	4.5	-0.02
TC3-AW	0.29	453	9.6	2761	4	2.7	9.4	48
TC3-BW	0.26	542	17.4	1173	2	1.3	8.6	49
TC3-CE	0.02	523	4.8	815	5	1.8	10	34
TC3-DE	0.21	439	29.5	1618	3	11	9.8	44
TC3-EE	0.09	481	25.1	911	4	1.6	8.7	26
TC3-EW	0.14	442	11.6	1616	5	2.2	6.4	19
TC3-FW	0.17	465	13.0	1163	5	2.3	6.9	15
TC3-GE	0.21	469	24.4	757	7	2.1	7.5	13
TC3-GW	0.04	459	10.4	706	10	3.0	7.2	-0.17
TC3-HE	0.24	456	17.1	397	3	1.4	7.4	24
TC3-IE	-0.04	471	7.8	599	14	5.6	5.4	4.1
TC3-JW	0.06	452	6.7	693	9	5.0	5.4	7.0
TC3-KW	0.33	515	4.0	309	13	11	4.4	9.1
TC3-LE	0.02	475	6.3	490	16	8.9	5.0	3.5
TC4-AE	0.19	456	7.1	1972	3	2.0	12	55
TC4-CE	0.23	495	19.6	962	7	2.8	10	41
TC4-DW	0.02	367	8.6	1489	20	13	15	-0.13
TC4-EW	-0.11	332	1.6	1068	61	30	24	-0.26
TC4-FW	0.01	171	2.9	685	26	26	25	-0.19
TC4-GE	-0.07	199	2.9	624	26	26	23	-0.17
TC4-HE	-0.13	147	0.1	1097	24	25	22	-0.31
TC4-HW	-0.12	241	10.4	912	10	8.5	18	0.03
TC4-IE	0.05	36	2.3	647	23	15	12	-0.11
TC4-JW	0.08	39	4.5	631	17	14	11	-0.08
TC4-KE	0.07	176	7.3	794	9	4.0	8.5	1.82
TC4-KW	0.17	38	1.5	498	32	44	14	-0.14
TC4-LE	-0.12	30	1.3	465	28	29	8.5	-0.13

Table C.5 Continued.

Lysimeter	Aqueous Concentration (mg L^{-1})							
ID	Al	Ca	Fe	Mg	K	Si	Na	Zn
TC5-BW	0.11	468	10.8	1389	8	2.4	11	11
TC5-CE	0.21	461	27.2	1375	8	3.8	9.6	13
TC5-DE	-0.04	417	8.3	1192	26	8.9	11	0.44
TC5-EW	0.20	441	19.6	1516	17	5.1	8.4	1.4
TC5-GE	0.09	466	19.9	780	42	35	9.6	-0.04
TC5-GW	0.20	454	18.8	709	42	36	7.9	1.5
TC5-HE	0.05	433	11.0	634	40	33	8.2	2.2
TC5-HW	0.27	468	11.4	907	23	16	7.2	5.9
TC5-IE	0.14	418	14.1	873	17	9.6	7.6	4.0
TC5-IW	0.01	379	10.9	392	46	42	7.8	2.5
TC5-JW	0.08	489	22.4	1397	7	3.6	6.2	51
TC5-LE	0.06	367	9.2	445	38	28	4.1	3.7
TC6-AE	0.15	449	3.5	1180	4	1.3	8.3	251
TC6-BW	0.48	486	45.3	1956	3	2.5	13	140
TC6-CE	0.14	557	25.6	1330	5	1.7	14	15
TC6-DW	0.34	469	46.4	1604	4	2.0	11	36
TC6-EW	0.09	400	21.5	1297	9	3.4	12	0.71
TC6-FE	0.12	360	10.6	747	15	4.4	12	0.25
TC6-GE	0.16	397	18.0	901	23	6.1	10	0.10
TC6-HE	0.20	255	11.6	699	9	4.5	9.7	0.57
TC6-HW	0.09	74	0.5	951	19	7.6	11	-0.10
TC6-IE	0.15	214	4.0	1129	28	12	12	1.3
TC6-JW	0.19	291	9.9	962	14	6.7	8.8	38
TC6-KE	0.30	284	15.1	1310	25	37	10	0.1411
TC6-KW	0.07	75	4.3	809	26	15	8.2	-0.22
TC6-LE	0.09	109	3.4	778	41	26	5.8	0.21
TC7-AE	0.40	459	0.0	1070	3	1.1	7.3	266
TC7-BW	-0.02	464	7.9	1664	9	3.2	21	-0.06
TC7-CE	0.58	460	42.6	1596	2	1.7	10	117.9
TC7-CW	0.27	447	22.5	1425	16	5.3	12	37
TC7-DE	0.09	144	2.3	1188	24	8.0	16	-0.21
TC7-EW	0.06	69	0.2	486	30	12	11	0.24
TC7-FW	0.16	80	1.5	636	42	26	15	-0.13
TC7-GE	0.03	37	3.3	714	37	15	14	-0.19
TC7-GW	-0.03	118	2.6	539	39	16	14	-0.14
TC7-IW	0.16	461	16.1	477	10	3.4	13	0.81
TC7-JW	0.10	184	2.1	737	19	11	13	-0.04
TC7-KE	0.03	25	0.0	444	41	19	8.0	0.17
TC7-KW	0.12	56	0.4	518	19	9.6	7.9	0.17
TC7-LE	0.14	444	21.0	403	7	3.8	8.4	0.25

Table C.5 Continued.

Lysimeter	Aqueous Concentration (μg L^{-1})										
ID	Sb	As	Ba	Cd	Cu	Pb	Mn	Mo	Ni	Se	Tl
TC2-AW	38	9.0	44	25	21	8.1	17930	13	769	-8	1.6
TC2-BE	1.3	4.2	2.9	1.2	2.4	8.6	20750	7.6	532	-8	89
TC2-CE	2.8	46	7.1	1.2	9.4	12	8784	19	386	-8	23
TC2-DE	2.2	1.0	2.5	3.03	4.1	5.6	7585	4.6	310	-8	56
TC2-DW	2.6	15	4.4	0.66	4.4	55	306	10	24	-8	31
TC2-EE	19	13	6.1	0.23	15	14	2050	14	50	-8	35
TC2-EW	3.5	11	4.8	1.88	0.21	2.1	307	8.0	29	-8	62
TC2-FW	7.0	10	4.3	0.76	2.8	26	298	10	28	-8	55
TC2-GE	25	26	2.8	0.34	8.5	29	146	10	16	-8	52
TC2-HE	6.6	76	1.7	0.10	2.8	2.2	169	6.7	13	-8	25
TC2-HW	13	13	6.7	0.72	1.1	13	854	8.9	11	-8	67
TC2-JW	11	0.5	5.5	0.27	3.7	5.3	610	6.9	5.0	-8	94
TC2-KE	23	3.6	7.2	0.31	22	13	506	10	3.7	-8	27
TC3-AW	36	9.1	31	23	4.4	5.0	13350	14	648	-8	1.5
TC3-BW	0.44	28	9.9	0.31	6.2	2.8	10530	9.1	319	-8	23
TC3-CE	16	5.0	31	2.0	6.0	6.5	1287	11	129	-8	0.21
TC3-DE	1.6	45	1.8	0.13	0.94	3.4	7279	10	203	-8	13
TC3-EE	1.7	30	1.8	0.35	2.6	1.7	1729	11	57	-8	31
TC3-EW	1.8	9.1	0.8	0.45	0.82	2.7	1756	17	59	-8	69
TC3-FW	2.7	12	3.1	0.74	5.0	3.4	387	14	32	-8	60
TC3-GE	2.7	68	1.6	0.15	1.7	6.1	505	8.4	29	-8	42
TC3-GW	0.9	26	1.6	0.10	0.94	4.9	176	12	1.9	-8	0.07
TC3-HE	1.4	10	2.8	0.48	0.53	2.2	1936	6.1	72	-8	45
TC3-IE	5.7	13	2.9	0.18	0.94	18	242	8.3	14	-8	50
TC3-JW	1.9	0.8	2.4	0.17	2.3	5.0	200	9.3	18	-8	46
TC3-KW	4.3	0.5	5.6	0.13	6.2	5.5	252	6.2	15	-8	59
TC3-LE	22	5.2	0.9	0.10	0.47	5.5	248	11	6.6	-8	41
TC4-AE	20	11	40	18	3.5	17	31770	16	1029	-8	0.53
TC4-CE	1.2	32	5.8	0.10	3.6	12	13370	13	264	-8	49
TC4-DW	1.5	19	1.5	0.12	1.7	2.5	195	4.7	0.7	-8	2.9
TC4-EW	0.84	6.5	11	0.09	5.9	6.2	141	1.1	0.57	-8	0.04
TC4-FW	1.9	33	19	0.17	3.6	27	81	1.1	0.54	-8	0.04
TC4-GE	1.9	0.5	18	0.80	3.2	16	76	1.7	0.43	-8	0.06
TC4-HE	2.3	3.0	25	0.06	2.5	1.5	81	0.09	0.13	-8	0.03
TC4-HW	0.66	45	14	0.14	4.3	9.6	186	8.0	0.71	-8	2.7
TC4-IE	1.2	54	19610	0.25	7.4	12	27	49	0.79	-8	0.86
TC4-JW	0.29	89	3530	0.14	7.9	2.5	19	78	1.1	-8	2.5
TC4-KE	19	86	7.5	0.16	4.0	549	66	31	9.4	-8	34
TC4-KW	1.8	16	93	0.31	1.1	4.5	26	56	0.47	-8	0.06
TC4-LE	1.5	11	502	0.15	9.7	8.3	24	30	0.31	-8	0.03

Table C.5 Continued.

Lysimeter	Aqueous Concentration (μg L^{-1})										
ID	Sb	As	Ba	Cd	Cu	Pb	Mn	Mo	Ni	Se	Tl
TC5-BW	41	28	56	2.9	9.1	8.4	2824	33	124	-8	1.3
TC5-CE	0.86	37	9.3	0.10	6.3	23	5519	17	122	-8	19
TC5-DE	1.3	151	5.1	0.43	8.2	4.4	287	21	4.3	-8	8.0
TC5-EW	0.65	146	4.0	0.71	9.0	2.8	480	28	11	-8	23
TC5-GE	1.0	36	3.9	0.27	1.3	7.0	177	16	1.9	-8	4.6
TC5-GW	0.76	113	5.6	0.12	11	13	239	19	14	-8	38
TC5-HE	3.4	39	3.9	0.23	3.1	7.5	211	17	10	-8	30
TC5-HW	0.55	24	3.3	0.24	0.93	6.6	157	16	15	-8	53
TC5-IE	0.94	101	7.1	0.14	1.6	3.0	231	18	13	-8	54
TC5-IW	1.1	69	3.5	0.23	0.84	3.5	159	18	14	-8	51
TC5-JW	2.0	21	2.0	0.61	7.8	5.6	17180	7.2	366	-8	92
TC5-LE	7.1	21	2.3	0.15	3.5	2.9	61	7.1	11	-8	51
TC6-AE	13	10	33	178	5.2	15	64220	11	1724	-8	1.7
TC6-BW	2.2	91	3.5	1.5	3.7	2.8	49530	10	1167	-8	41
TC6-CE	11	41	30	3.1	1.3	1.7	6698	17	153	-8	4.3
TC6-DW	2.1	36	5.8	0.63	2.0	38	21990	12	313	-8	9.2
TC6-EW	0.84	78	2.5	0.16	1.4	9.4	848	26	6.3	-8	8.8
TC6-FE	10	46	4.6	0.15	5.4	3.1	299	10	3.1	-8	10
TC6-GE	0.73	159	8.3	0.32	1.6	4.3	165	16	5.4	-8	4.7
TC6-HE	1.0	69	1.0	0.05	1.7	2.7	146	17	2.9	-8	9.1
TC6-HW	0.71	17	3.4	0.11	2.5	7.2	66	34	0.36	-8	0.99
TC6-IE	4.4	77	21	0.12	2.7	16	146	40	8.6	-8	10
TC6-JW	1.6	138	3.8	1.35	0.6	2.2	8781	16	166	-8	79
TC6-KE	1.3	178	6.9	0.21	7.6	9.2	100	25	3.7	-8	6.8
TC6-KW	7.8	16	4.8	0.14	0.62	4.2	44	41	0.21	-8	0.03
TC6-LE	21	43	9.2	0.26	7.6	5.2	57	25	4.1	-8	9.2
TC7-AE	9.1	6.4	50	778	8.4	3.7	82940	12	1567	-8	2.4
TC7-BW	28	165	47	0.15	1.3	1.6	908	106	19	-8	1.4
TC7-CE	2.2	162	5.7	1.3	2.4	5.7	39090	11	688	-8	55
TC7-CW	12	120	13	0.08	-0.2	1.2	20690	41	226	-8	7.1
TC7-DE	1.3	23	2.0	0.16	8.0	7.8	110	19	1.0	-8	0.85
TC7-EW	1.9	22	84	0.11	0.03	1.2	94	26	1.3	-8	4.4
TC7-FW	1.3	15	14.2	0.11	0.10	2.6	71	8.9	-0.19	-8	0.19
TC7-GE	0.95	51	10610	0.08	3.1	1.7	39	17	0.6	-8	0.95
TC7-GW	0.58	16	10	0.15	3.3	11	113	5.2	0.47	-8	0.04
TC7-IW	0.88	51	17	0.12	3.2	3.6	246	10	1.9	-8	2.4
TC7-JW	0.62	76	20	0.46	10	18	748	14	0.79	-8	0.86
TC7-KE	7.8	32	1693	0.26	2.5	40	20	64	0.69	-8	2.7
TC7-KW	7.9	40	49	0.03	1.8	2.0	69	54	0.37	-8	2.7
TC7-LE	0.76	57	3.8	0.25	6.6	3.9	145	14	2.5	-8	1.0

Table C.6 Saturation indices calculated for pore-water samples collected in 2008.

	Saturation Indices (SIs) Calculated by MINTEQA2														
Lysimeter ID	$Al(OH)_3$ (amorph)	Anhydrite [$CaSO_4$]	Aragonite [$CaCO_3$]	Barite [$BaSO_4$]	Calcite [$CaCO_3$]	Dolomite [$CaMg(CO_3)_2$]	Epsomite [$MgSO_4{\cdot}7H_2O$]	Ferrihydrite [$Fe(OH)_3$]	Lepidocrocite [γ-FeOOH]	$Fe_3(OH)_8$	FeS (ppt)	Hydroxylapatite [$Ca_5(PO_4)_3(OH)$]	Gibbsite [$Al(OH)_3$]	Goethite [α-FeOOH]	Greigite [Fe_3S_4]
TC2-BE	-0.4	-0.3	-0.2	-0.1	0.0	0.6	-1.8	2.0	5.5	2.6	-3.0	-3.8	2.4	7.5	3.9
TC2-CE	-0.2	-0.3	0.1	0.3	0.3	1.4	-1.6	1.4	5.0	1.6	-3.2	-3.3	2.6	6.9	2.0
TC2-DE	-0.1	-0.3	0.0	-0.1	0.2	0.9	-1.8	-1.5	2.0	-8.1	-6.9	-3.5	2.7	3.9	-7.3
TC2-EE	-0.4	-0.3	0.3	0.2	0.5	1.5	-1.7	1.9	5.4	2.9	-1.8	-1.9	2.4	7.3	7.0
TC2-GE	-0.4	-0.3	0.5	-0.2	0.7	1.5	-2.3	0.3	3.9	-1.9	-3.9	0.2	2.5	5.7	0.6
TC2-HE	-0.9	-0.3	0.4	-0.4	0.6	1.1	-2.4	2.1	5.7	3.6	-2.0	1.4	1.9	7.5	6.3
TC2-KE	-0.7	-0.3	-0.3	0.4	-0.1	0.2	-1.8	-2.1	1.5	-12.7	-7.4	-0.1	2.2	3.2	-0.2
TC2-AW	0.2	-0.2	0.1	1.3	0.3	1.4	-1.4	-1.4	2.1	-8.6	-8.0	-2.0	3.0	4.0	-10.0
TC2-DW	-0.2	-0.3	0.5	0.1	0.7	1.4	-2.3	-0.6	2.9	-5.7	-5.8	-0.9	2.6	4.9	-3.1
TC2-EW	-0.7	-0.3	0.4	0.1	0.6	1.5	-2.1	0.7	4.2	-2.2	-5.5	-1.0	2.1	6.1	-2.1
TC2-FW	-0.6	-0.2	0.3	0.2	0.5	0.9	-2.4	0.0	3.5	-3.2	-4.5	-1.0	2.2	5.4	-0.3
TC2-HW	-0.5	-0.3	0.3	0.3	0.5	1.4	-1.9	0.2	3.7	-2.0	-3.6	-0.7	2.3	5.6	1.1
TC2-JW	-0.7	-0.4	0.0	0.3	0.2	0.5	-2.2	-0.7	2.9	-7.3	-7.1	0.1	2.1	4.6	-4.1
TC3-AW	-0.5	-0.2	0.0	1.1	0.2	1.3	-1.3	-1.5	2.1	-7.6	-5.5	-4.9	2.3	4.0	-2.9
TC3-CE	-0.3	-0.3	0.4	0.9	0.5	1.5	-2.0	-1.4	2.1	-7.9	-6.0	-1.4	2.5	4.0	-4.1
TC3-DE	-0.4	-0.3	0.2	-0.2	0.4	1.5	-1.6	3.9	7.4	6.8	-2.1	-0.8	2.4	9.3	10.1
TC3-EE	-0.2	-0.4	0.2	-0.3	0.4	1.2	-1.9	1.9	5.4	2.7	-2.7	-0.2	2.6	7.3	3.9
TC3-GE	-0.4	-0.4	0.3	-0.4	0.5	1.4	-2.0	2.3	5.8	4.1	-2.1	-2.2	2.4	7.7	5.6
TC3-HE	-0.9	-0.4	0.2	-0.1	0.4	0.9	-2.3	3.5	7.0	5.4	-3.1	1.1	2.0	8.8	6.8
TC3-IE	-0.3	-0.4	0.4	-0.1	0.6	1.4	-2.1	0.0	3.5	-3.5	-5.2	2.1	2.6	5.3	-2.7
TC3-LE	-0.3	-0.4	0.3	-0.5	0.5	1.0	-2.2	-0.2	3.3	-5.3	-6.3	2.3	2.5	5.1	-3.2
TC3-BW	0.0	-0.3	0.1	0.4	0.2	1.0	-1.8	0.7	4.2	-0.9	-3.1	-3.4	2.8	6.2	3.9
TC3-EW	-0.7	-0.3	0.4	-0.6	0.6	1.9	-1.6	0.2	3.8	-1.7	-3.5	-2.0	2.1	5.7	0.8
TC3-FW	-0.6	-0.3	0.3	0.0	0.5	1.5	-1.8	0.3	3.8	-1.9	-3.8	-2.0	2.2	5.7	0.7
TC3-GW	-0.5	-0.4	0.3	-0.3	0.5	1.4	-2.0	-0.1	3.4	-2.6	-2.6	-1.0	2.3	5.3	4.3
TC3-JW	-0.6	-0.4	0.2	-0.2	0.4	1.2	-2.0	-0.3	3.3	-4.3	-5.6	-0.9	2.2	5.0	-3.9
TC3-KW	-0.3	-0.4	0.2	0.2	0.4	0.7	-2.4	-0.6	2.9	-5.5	-5.8	-0.3	2.5	4.7	-3.7
TC4-AE	-0.3	-0.2	0.1	1.2	0.3	1.4	-1.5	-1.7	1.8	-9.2	-6.6	-3.5	2.5	3.7	-5.1
TC4-CE	-0.3	-0.3	0.3	0.2	0.5	1.5	-1.9	0.5	4.0	-2.3	-5.1	-1.6	2.5	5.9	-2.3
TC4-GE	-0.5	-1.0	0.7	0.4	0.9	2.4	-2.4	-1.9	1.6	-9.5	-4.5	2.3	2.3	3.5	3.6
TC4-HE	-0.7	-1.1	0.7	0.6	0.9	2.8	-2.1	-3.1	0.4	-11.1	-1.9	2.6	2.1	2.3	8.8
TC4-IE	-0.8	-4.7	0.5	0.4	0.7	2.7	-5.3	-0.9	2.6	-6.7	-4.9	-2.4	2.1	4.4	1.1
TC4-KE	-0.6	-0.9	0.6	0.2	0.8	2.3	-2.1	-0.4	3.1	-4.3	-4.3	-2.5	2.2	4.9	0.3
TC4-LE	-0.8	-3.2	0.4	0.5	0.6	2.4	-3.8	-0.9	2.7	-7.2	-5.4	-5.0	2.0	4.4	1.0
TC4-DW	-0.7	-0.4	0.6	-0.3	0.8	2.4	-1.7	-1.2	2.4	-5.5	-4.1	0.5	2.1	4.3	-1.4
TC4-EW	-0.4	-0.5	0.6	0.4	0.8	2.3	-1.9	-2.3	1.2	-8.8	-1.8	0.7	2.4	3.1	8.3
TC4-FW	-0.4	-1.1	0.7	0.4	0.9	2.5	-2.3	-1.7	1.8	-7.2	-1.8	2.4	2.4	3.7	8.7
TC4-HW	-0.3	-0.7	0.6	0.6	0.8	2.3	-2.0	-1.0	2.5	-5.0	-4.1	0.7	2.5	4.4	-1.6

Table C.6. Continued.

Lysimeter ID	Saturation Indices (SIs) Calculated by MINTEQA2														
	$Al(OH)_3$ (amorph)	Anhydrite [$CaSO_4$]	Aragonite [$CaCO_3$]	Barite [$BaSO_4$]	Calcite [$CaCO_3$]	Dolomite [$CaMg(CO_3)_2$]	Epsomite [$MgSO_4{\cdot}7H_2O$]	Ferrihydrite [$Fe(OH)_3$]	Lepidocrocite [γ-FeOOH]	$Fe_3(OH)_8$	FeS (ppt)	Hydroxylapatite [$Ca_5(PO_4)_3(OH)$]	Gibbsite [$Al(OH)_3$]	Goethite [α-FeOOH]	Greigite [Fe_3S_4]
TC4-JW	-0.7	-2.1	0.5	2.3	0.7	2.6	-2.8	-0.4	3.1	-4.6	-3.9	-1.4	2.1	4.9	2.7
TC4-KW	-0.6	-2.8	0.5	0.0	0.7	2.7	-3.5	-1.0	2.5	-6.3	-4.2	-3.7	2.3	4.3	1.9
TC5-CE	-0.1	-0.3	0.4	0.4	0.5	1.8	-1.7	1.6	5.1	2.4	-2.4	-1.1	2.7	7.1	3.8
TC5-DE	0.0	-0.4	0.7	0.2	0.9	2.5	-1.8	-0.5	3.0	-4.1	-3.7	5.5	2.8	4.9	1.1
TC5-GE	-0.4	-0.3	0.6	0.1	0.8	2.1	-2.0	0.9	4.4	0.7	-2.3	1.0	2.4	6.3	3.9
TC5-HE	-0.4	-0.4	0.5	0.1	0.7	1.8	-2.0	-0.2	3.3	-3.1	-4.3	-0.6	2.4	5.2	-2.0
TC5-IE	-0.7	-0.4	0.5	0.4	0.7	1.9	-1.9	0.6	4.1	-1.1	-4.1	-0.9	2.2	6.0	-0.5
TC5-LE	-0.7	-0.5	0.3	-0.1	0.5	1.3	-2.2	1.7	5.2	2.5	-2.8	-0.2	2.1	6.9	2.3
TC5-BW	0.1	-0.3	0.2	1.2	0.4	1.5	-1.7	-1.2	2.3	-7.0	-5.2	-3.7	2.9	4.2	-1.6
TC5-EW	-0.6	-0.4	0.6	0.1	0.8	2.2	-1.7	1.1	4.6	1.3	-2.4	-1.7	2.2	6.5	2.6
TC5-GW	-0.5	-0.4	0.5	0.3	0.7	1.8	-2.0	2.0	5.5	3.2	-2.4	-1.5	2.4	7.4	4.4
TC5-HW	-0.8	-0.4	0.6	0.0	0.8	2.0	-1.9	0.0	3.6	-2.3	-4.2	-2.5	2.1	5.4	-2.0
TC5-IW	-0.7	-0.5	0.5	0.0	0.7	1.5	-2.3	0.0	3.5	-3.0	-4.7	-1.9	2.1	5.3	-2.2
TC5-JW	-0.5	-0.3	-0.1	-0.1	0.1	0.7	-1.6	2.0	5.6	3.3	-2.6	-4.1	2.4	7.4	3.9
TC6-AE	-0.5	-0.2	0.0	1.2	0.1	0.9	-1.7	-2.1	1.4	-12.3	-10.2	-1.4	2.3	3.4	-12.9
TC6-CE	-0.3	-0.3	0.3	0.9	0.5	1.6	-1.7	-0.2	3.3	-3.5	-4.4	0.3	2.5	5.2	-0.9
TC6-FE	-0.3	-0.5	0.6	0.1	0.7	2.0	-2.1	-0.7	2.8	-4.0	-3.8	2.0	2.5	4.7	-0.9
TC6-GE	-0.5	-0.4	0.5	0.4	0.7	1.9	-1.9	0.1	3.6	-1.3	-2.4	1.5	2.3	5.5	3.0
TC6-HE	-0.7	-0.7	0.4	-0.6	0.6	1.9	-2.1	-0.2	3.3	-2.4	-3.2	0.9	2.1	5.1	0.1
TC6-IE	-0.6	-0.7	0.6	0.8	0.8	2.4	-1.8	-0.9	2.6	-5.1	-4.8	1.1	2.3	4.4	-3.2
TC6-KE	-0.6	-0.6	0.5	0.4	0.7	2.2	-1.7	0.0	3.6	-1.7	-3.1	0.6	2.3	5.3	0.7
TC6-LE	-0.6	-1.0	0.3	0.5	0.5	2.1	-2.0	-0.4	3.1	-3.3	-3.5	-0.2	2.3	4.9	0.1
TC6-BW	-0.3	-0.2	-0.1	0.1	0.0	0.9	-1.5	0.8	4.4	0.6	-3.0	-4.0	2.5	6.3	0.9
TC6-DW	0.1	-0.3	0.1	0.3	0.3	1.3	-1.6	1.0	4.5	1.2	-2.5	-2.6	2.9	6.4	2.2
TC6-EW	-0.4	-0.4	0.5	-0.1	0.7	2.1	-1.7	0.1	3.6	-1.4	-2.7	-2.1	2.4	5.5	1.7
TC6-HW	-0.4	-1.3	0.6	-0.1	0.8	2.8	-2.0	-1.4	2.1	-6.5	-4.7	1.1	2.4	4.0	-2.8
TC6-JW	-0.5	-0.5	0.2	0.1	0.4	1.5	-1.8	-0.8	2.8	-4.5	-4.8	-0.9	2.4	4.5	-4.2
TC6-KW	-0.9	-1.3	0.5	0.1	0.7	2.6	-2.0	-0.2	3.4	-3.6	-4.5	-0.7	2.0	5.1	-0.6
TC7-AE	0.0	-0.3	-0.4	1.2	-0.3	0.1	-1.8	-5.0	-1.5	-21.0	-14.8	-2.7	2.8	0.5	-28.4
TC7-DE	0.0	-1.0	0.7	-0.4	0.9	2.9	-2.0	-1.5	2.0	-6.9	-5.1	3.7	2.9	3.9	-4.0
TC7-GE	-0.9	-5.1	0.6	-0.2	0.8	2.9	-5.7	-0.9	2.6	-4.7	-2.7	2.9	1.9	4.5	4.1
TC7-KE	-0.5	-3.6	0.5	0.7	0.7	2.6	-4.2	-2.5	1.0	-10.7	-6.7	-4.5	2.4	2.8	-7.2
TC7-LE	-0.1	-0.5	0.4	0.0	0.6	1.2	-2.3	1.1	4.7	1.5	-2.0	-1.2	2.7	6.4	4.3
TC7-BW	-0.9	-0.3	0.9	1.1	1.0	2.9	-1.7	-1.4	2.1	-6.3	-3.8	0.9	1.9	4.1	0.7
TC7-CW	-0.6	-0.3	0.4	0.6	0.5	1.8	-1.7	-0.3	3.2	-2.8	-4.0	-2.5	2.2	5.2	-2.1
TC7-EW	-0.9	-1.8	0.6	0.7	0.8	2.5	-2.8	-2.3	1.2	-10.0	-6.4	1.0	1.9	3.1	-6.2
TC7-FW	-0.8	-1.5	0.7	0.2	0.9	2.8	-2.5	-1.3	2.2	-6.2	-4.5	3.7	2.0	4.1	-1.8
TC7-GW	-0.5	-1.3	0.7	0.1	0.9	2.5	-2.5	-1.2	2.3	-5.5	-3.0	4.7	2.3	4.2	2.8
TC7-IW	-0.6	-0.4	0.7	0.6	0.9	1.9	-2.2	-0.4	3.1	-3.2	-3.6	1.1	2.2	4.9	-0.5
TC7-JW	-0.5	-1.0	0.7	0.5	0.9	2.6	-2.2	-1.2	2.4	-6.2	-5.3	3.8	2.3	4.2	-3.9
TC7-KW	-0.5	-1.6	0.5	0.8	0.7	2.5	-2.5	-1.2	2.3	-7.8	-6.4	-1.3	2.4	4.1	-3.7

Table C.6 Continued.

Lysimeter ID	Saturation Indices (SIs) Calculated by MINTEQA2														
	Gypsum [$CaSO_4 \cdot 2H_2O$]	Mackinawite [$Fe_{1+x}S$]	Pyrite [FeS_2]	Quartz [SiO_2]	Siderite [$FeCO_3$]	SiO_2 (amorph)	Rhodochrosite [$MnCO_3$]	MnS (green)	Chalcopyrite [$CuFeS_2$]	Smithsonite [$ZnCO_3$]	$Zn(OH)_2$	ZnS (amorph)	Sphalerite [ZnS]	Wurtzite [ZnS]	Cerrusite [$PbCO_3$]
TC2-BE	-0.1	-2.2	18.1	-2.9	0.5	-3.9	0.4	-10.5	18.4	0.4	-1.6	3.1	5.8	3.8	-1.5
TC2-CE	-0.1	-2.4	16.6	-2.0	0.4	-3.0	0.3	-10.7	18.8	0.3	-1.6	2.9	5.6	3.5	-1.3
TC2-DE	0.0	-6.1	14.7	0.4	-3.4	-0.6	0.1	-10.8	14.8	0.3	-1.5	3.1	5.8	3.7	-1.7
TC2-EE	0.0	-1.0	18.9	-2.3	0.8	-3.3	-0.2	-10.2	21.2	0.0	-1.7	3.7	6.4	4.3	-1.2
TC2-GE	-0.1	-3.2	16.7	-0.3	-1.2	-1.3	-1.2	-11.3	19.1	-0.3	-1.7	3.3	6.0	4.0	-0.9
TC2-HE	0.0	-1.2	18.6	-2.0	0.4	-3.0	-1.3	-11.1	20.7	-0.8	-2.0	3.1	5.8	3.7	-2.0
TC2-KE	-0.1	-6.7	23.3	0.4	-8.4	-0.6	-1.2	-7.7	11.7	-6.6	-6.8	0.7	3.4	1.4	-3.9
TC2-AW	0.1	-7.3	14.3	0.4	-3.8	-0.6	0.6	-11.0	13.6	0.3	-1.8	2.2	4.9	2.9	-1.5
TC2-DW	0.0	-5.1	16.8	0.2	-2.9	-0.8	-0.9	-11.3	16.5	0.0	-1.7	3.3	6.0	4.0	-0.6
TC2-EW	-0.1	-4.7	17.2	-0.8	-2.0	-1.8	-0.9	-11.7	15.1	0.1	-1.5	2.9	5.6	3.6	-2.0
TC2-FW	0.1	-3.7	17.0	-0.4	-1.7	-1.4	-1.0	-11.3	17.8	-0.1	-1.8	3.3	6.0	4.0	-0.9
TC2-HW	-0.1	-2.9	16.7	0.0	-1.4	-1.0	-0.5	-10.2	18.6	-0.7	-1.8	3.3	6.0	4.0	-1.2
TC2-JW	-0.1	-6.4	18.8	0.4	-5.5	-0.6	-0.9	-10.0	15.8	-1.7	-2.2	3.0	5.7	3.7	-1.6
TC3-AW	0.0	-4.7	16.3	0.4	-2.8	-0.6	0.4	-9.7	16.7	0.2	-1.8	3.7	6.4	4.4	-1.7
TC3-CE	0.0	-5.3	16.2	0.6	-3.4	-0.4	-0.4	-10.4	16.5	0.4	-1.4	3.9	6.6	4.6	-1.5
TC3-DE	-0.1	-1.4	22.7	-4.3	0.7	-5.3	0.3	-9.9	19.6	0.4	-1.4	3.8	6.5	4.4	-1.8
TC3-EE	-0.1	-1.9	17.6	-2.4	0.8	-3.4	-0.4	-11.2	18.9	0.1	-1.8	2.9	5.6	3.6	-2.1
TC3-GE	-0.1	-1.4	18.2	-2.5	1.0	-3.5	-0.8	-11.3	19.7	0.0	-1.7	3.1	5.8	3.7	-1.5
TC3-HE	-0.1	-2.4	21.4	-3.8	0.0	-4.8	-0.3	-10.8	18.2	0.2	-1.4	3.3	6.0	3.9	-2.0
TC3-IE	-0.1	-4.5	16.3	-0.1	-2.3	-1.1	-1.0	-11.4	16.6	-0.5	-1.7	2.8	5.6	3.5	-1.0
TC3-LE	-0.1	-5.6	18.1	0.1	-3.9	-1.0	-1.1	-11.1	15.7	-0.7	-1.8	3.1	5.9	3.8	-1.6
TC3-BW	0.0	-2.4	18.4	-1.5	-0.6	-2.5	0.3	-9.7	19.3	0.3	-1.6	4.0	6.6	4.6	-2.0
TC3-EW	-0.1	-2.8	16.2	-0.4	-0.7	-1.4	-0.1	-10.4	18.2	0.2	-1.4	3.6	6.3	4.3	-1.9
TC3-FW	-0.1	-3.1	16.8	-0.6	-1.0	-1.6	-0.9	-11.2	18.7	0.0	-1.6	3.4	6.1	4.1	-1.8
TC3-GW	-0.1	-1.9	17.9	0.0	-1.1	-1.0	-1.2	-10.1	18.0	-2.3	-3.7	2.4	5.1	3.1	-1.7
TC3-JW	-0.1	-4.9	15.9	0.1	-2.6	-0.9	-1.2	-11.6	16.7	-0.3	-1.5	2.9	5.7	3.6	-1.6
TC3-KW	-0.1	-5.0	16.5	0.2	-3.2	-0.9	-1.2	-11.2	17.3	-0.3	-1.4	3.4	6.1	4.1	-1.6
TC4-AE	0.0	-5.9	16.4	0.7	-3.8	-0.4	0.9	-9.4	15.5	0.4	-1.7	3.7	6.4	4.4	-1.2
TC4-CE	-0.1	-4.4	16.3	-0.7	-1.5	-1.7	0.7	-10.4	16.4	0.5	-1.3	3.0	5.7	3.7	-1.3
TC4-GE	-0.8	-3.7	20.9	1.1	-3.7	0.1	-1.1	-9.3	13.7	-4.1	-6.3	1.4	4.1	2.1	-2.2
TC4-HE	-0.9	-1.1	21.0	1.1	-2.7	0.1	-1.0	-7.6	12.7	-7.1	-9.4	0.0	2.7	0.6	-6.5
TC4-IE	-4.4	-4.1	19.3	0.8	-3.0	-0.2	-1.2	-10.6	16.1	-2.4	-4.3	2.0	4.7	2.7	-1.3
TC4-KE	-0.6	-3.6	17.5	0.5	-1.8	-0.6	-1.1	-11.1	18.2	-0.6	-2.3	3.2	5.9	3.9	0.4
TC4-LE	-2.9	-4.7	20.5	0.7	-3.9	-0.3	-1.3	-10.3	15.5	-2.1	-3.8	2.7	5.4	3.3	-1.5
TC4-DW	-0.2	-3.4	15.1	0.8	-1.3	-0.2	-0.9	-11.1	17.8	-2.1	-4.1	1.2	3.9	1.9	-2.0
TC4-EW	-0.3	-1.1	20.3	1.1	-2.2	0.1	-1.0	-8.1	14.6	-6.9	-9.0	-0.4	2.3	0.3	-4.7
TC4-FW	-0.8	-1.1	20.7	1.1	-1.8	0.1	-1.0	-8.4	14.9	-5.5	-7.6	0.7	3.5	1.4	-3.5
TC4-HW	-0.4	-3.4	15.1	0.9	-1.1	-0.2	-0.8	-11.2	18.3	-2.4	-4.4	0.8	3.5	1.5	-1.3

Table C.6 Continued.

Lysimeter ID	Saturation Indices (SIs) Calculated by MINTEQA2														
	Gypsum [$CaSO_4{:}2H_2O$]	Mackinawite [$Fe_{1+x}S$]	Pyrite [FeS_2]	Quartz [SiO_2]	Siderite [$FeCO_3$]	SiO_2 (amorph)	Rhodochrosite [$MnCO_3$]	MnS (green)	Chalcopyrite [$CuFeS_2$]	Smithsonite [$ZnCO_3$]	$Zn(OH)_2$	ZnS (amorph)	Sphalerite [ZnS]	Wurtzite [ZnS]	Cerrusite [$PbCO_3$]
TC4-JW	-1.9	-3.1	19.0	0.7	-2.0	-0.3	-1.4	-10.7	17.4	-3.4	-5.3	0.9	3.7	1.6	-2.0
TC4-KW	-2.5	-3.5	18.9	0.9	-2.6	-0.1	-1.2	-10.3	15.8	-2.4	-4.1	2.3	5.0	3.0	-1.7
TC5-CE	-0.1	-1.7	16.8	-1.9	1.0	-2.9	0.3	-10.4	19.7	0.0	-1.8	2.8	5.6	3.5	-1.0
TC5-DE	-0.1	-3.0	16.8	0.6	-1.6	-0.4	-0.6	-10.2	18.4	-1.3	-2.8	2.8	5.5	3.5	-1.7
TC5-GE	-0.1	-1.6	16.9	-0.8	0.5	-1.8	-0.9	-11.2	19.7	-2.6	-4.3	0.8	3.5	1.5	-1.5
TC5-HE	-0.1	-3.6	15.0	0.2	-1.1	-0.8	-0.9	-11.6	17.8	-0.6	-2.2	2.4	5.1	3.1	-1.4
TC5-IE	-0.1	-3.4	16.2	-0.5	-0.9	-1.5	-0.9	-11.6	17.7	-0.4	-1.9	2.6	5.3	3.3	-1.8
TC5-LE	-0.2	-2.1	16.6	-1.4	0.2	-2.5	-1.5	-12.0	19.6	-0.5	-1.6	2.8	5.5	3.5	-1.8
TC5-BW	0.0	-4.4	16.9	0.4	-2.7	-0.6	-0.1	-10.0	17.2	-0.2	-2.2	3.5	6.2	4.2	-1.5
TC5-EW	-0.1	-1.7	15.7	-1.0	0.8	-2.0	-0.5	-11.2	20.0	-0.8	-2.5	2.2	4.9	2.8	-1.9
TC5-GW	-0.1	-1.7	17.7	-1.9	0.7	-2.9	-0.9	-11.5	20.2	-0.8	-2.4	2.3	5.0	2.9	-1.2
TC5-HW	-0.1	-3.5	14.9	-0.1	-0.9	-1.1	-1.0	-11.9	17.1	-0.2	-1.8	2.6	5.4	3.3	-1.5
TC5-IW	-0.2	-4.0	15.6	0.1	-1.5	-0.9	-1.0	-11.7	16.9	-0.6	-2.1	2.5	5.2	3.2	-1.8
TC5-JW	0.0	-1.8	17.7	-2.6	0.6	-3.6	0.4	-10.3	20.0	0.1	-1.3	3.2	6.0	3.9	-1.6
TC6-AE	0.0	-9.5	15.8	0.5	-6.2	-0.5	1.0	-10.4	10.9	0.9	-1.1	3.1	5.8	3.7	-1.3
TC6-CE	0.0	-3.6	16.2	-0.2	-1.2	-1.2	0.3	-10.3	17.1	0.0	-2.0	3.0	5.7	3.6	-2.2
TC6-FE	-0.3	-3.0	15.0	0.6	-1.0	-0.4	-0.7	-10.9	18.8	-1.5	-3.3	1.9	4.6	2.6	-1.8
TC6-GE	-0.2	-1.7	16.3	0.0	0.0	-1.0	-1.0	-10.9	19.6	-2.0	-3.7	1.8	4.5	2.5	-1.7
TC6-HE	-0.4	-2.5	15.0	0.4	-0.4	-0.7	-1.0	-11.2	18.9	-1.1	-2.7	2.3	5.0	2.9	-1.9
TC6-IE	-0.4	-4.0	14.8	0.8	-1.8	-0.2	-0.8	-11.3	17.5	-0.8	-2.4	2.5	5.2	3.2	-1.1
TC6-KE	-0.3	-2.4	15.6	0.2	-0.3	-0.8	-1.1	-11.5	19.8	-1.8	-3.4	1.6	4.3	2.3	-1.3
TC6-LE	-0.7	-2.8	15.8	0.4	-1.0	-0.6	-1.2	-11.2	19.6	-1.5	-3.0	2.2	5.0	2.9	-1.6
TC6-BW	0.0	-2.2	15.1	-1.7	0.9	-2.7	0.8	-10.4	18.2	0.6	-1.5	2.9	5.6	3.6	-2.0
TC6-DW	0.0	-1.7	15.5	-1.6	1.2	-2.6	0.7	-10.4	18.8	0.2	-1.8	2.8	5.5	3.4	-0.8
TC6-EW	-0.1	-2.0	15.5	-0.1	0.3	-1.2	-0.3	-10.7	19.1	-1.2	-3.0	2.1	4.8	2.8	-1.4
TC6-HW	-1.0	-4.0	15.1	0.8	-2.1	-0.3	-0.9	-10.9	17.4	-2.2	-3.9	1.4	4.2	2.1	-1.5
TC6-JW	-0.3	-4.1	14.0	0.4	-1.3	-0.7	0.6	-10.5	16.3	0.5	-1.3	3.1	5.9	3.8	-2.0
TC6-KW	-1.0	-3.8	17.0	0.6	-1.9	-0.5	-1.1	-11.2	17.4	-1.8	-3.3	1.8	4.6	2.5	-1.7
TC7-AE	0.0	-14.0	9.3	0.6	-9.1	-0.4	0.8	-12.3	4.8	0.6	-1.3	1.1	3.8	1.8	-2.0
TC7-DE	-0.7	-4.4	14.6	0.9	-2.0	-0.1	-0.8	-11.4	17.2	-1.8	-3.9	1.2	3.9	1.8	-1.5
TC7-GE	-4.8	-1.9	17.8	0.8	-0.9	-0.2	-1.1	-10.3	17.3	-2.3	-4.4	2.2	4.9	2.9	-2.2
TC7-KE	-3.3	-6.0	14.9	0.7	-4.0	-0.3	-1.3	-11.5	15.6	-1.8	-3.5	1.8	4.5	2.4	-0.8
TC7-LE	-0.2	-1.3	17.1	-1.2	0.7	-2.2	-1.2	-11.5	20.9	-1.7	-3.3	1.8	4.5	2.5	-1.7
TC7-BW	-0.1	-3.0	16.5	1.0	-1.6	-0.1	-0.1	-9.7	16.8	-2.4	-4.5	1.6	4.3	2.2	-2.2
TC7-CW	-0.1	-3.3	14.1	-0.1	-0.2	-1.2	0.9	-10.3	15.8	0.4	-1.7	2.9	5.6	3.5	-2.3
TC7-EW	-1.5	-5.7	15.0	0.8	-3.5	-0.2	-0.8	-11.1	13.7	-1.4	-3.4	1.9	4.6	2.6	-2.3
TC7-FW	-1.2	-3.7	15.5	0.9	-1.8	-0.1	-0.9	-11.0	16.1	-2.1	-4.0	1.5	4.2	2.2	-2.0
TC7-GW	-1.0	-2.2	17.1	0.9	-1.3	-0.2	-0.8	-9.9	17.4	-2.3	-4.2	2.2	4.9	2.9	-1.3
TC7-IW	-0.2	-2.9	15.3	0.4	-0.6	-0.6	-0.8	-11.3	18.7	-1.0	-2.9	2.2	4.9	2.9	-1.7
TC7-JW	-0.7	-4.5	15.2	0.9	-2.3	-0.2	0.0	-10.4	17.7	-2.5	-4.1	0.8	3.5	1.5	-1.0
TC7-KW	-1.4	-5.6	17.7	0.7	-4.0	-0.4	-0.8	-10.7	15.7	-1.7	-3.2	2.2	5.0	2.9	-2.0

Table C.6 Continued.

Lysimeter ID	Saturation Indices (SIs) Calculated by MINTEQA2												
	Anglesite [$PbSO_4$]	Galena [PbS]	$Pb(OH)_2$	$NiCO_3$	$Ni(OH)_2$	Millerite [NiS]	Orpiment [As_2S_3]	Realgar [As_4S_4]	Stibnite [Sb_2S_3]	Sb_2O_4	$Sb(OH)_3$	Native S	Tl_2S
TC2-BE	-3.2	2.0	-3.9	-5.5	-2.6	-0.5	-14.4	-13.5	-2.3	1.7	-0.9	8.1	-7.8
TC2-CE	-3.3	2.1	-3.6	-5.6	-2.5	-0.7	-12.8	-12.1	-2.2	1.3	-0.6	6.9	-8.7
TC2-DE	-3.5	1.9	-4.0	-5.7	-2.6	-0.7	-16.4	-14.8	-2.0	2.8	-0.7	8.7	-8.0
TC2-EE	-3.3	3.2	-3.5	-6.5	-3.2	-0.6	-11.0	-11.6	2.3	2.8	0.2	7.7	-7.2
TC2-GE	-3.2	3.5	-2.8	-7.0	-3.3	-1.1	-11.6	-11.8	1.5	3.4	0.4	7.6	-6.7
TC2-HE	-4.2	2.7	-3.7	-7.1	-3.2	-0.9	-10.4	-11.2	0.5	2.1	-0.2	7.6	-7.2
TC2-KE	-5.4	4.3	-4.8	-7.8	-2.7	1.8	-5.3	-13.7	1.2	2.4	-3.7	17.6	-4.2
TC2-AW	-3.3	1.2	-4.0	-5.3	-2.5	-1.1	-15.7	-14.8	-1.4	6.6	0.5	9.4	-11.7
TC2-DW	-2.9	3.5	-2.8	-6.8	-3.5	-1.2	-12.1	-13.1	-0.6	3.4	-0.6	9.6	-7.5
TC2-EW	-4.3	1.6	-4.1	-6.7	-3.3	-1.6	-14.2	-14.2	-2.2	4.4	-0.5	9.7	-7.4
TC2-FW	-3.0	3.3	-3.2	-6.8	-3.4	-1.1	-12.1	-12.6	0.6	3.1	-0.2	8.5	-7.0
TC2-HW	-3.4	3.6	-2.9	-7.2	-3.2	-0.9	-11.7	-11.7	1.4	2.3	0.1	7.3	-6.2
TC2-JW	-3.5	3.9	-2.9	-7.6	-2.9	-0.6	-14.1	-15.7	1.7	7.6	0.0	12.8	-5.4
TC3-AW	-3.4	2.6	-4.2	-5.4	-2.5	0.4	-11.1	-12.2	3.1	4.4	0.5	8.8	-10.4
TC3-CE	-3.7	2.8	-3.8	-6.1	-2.9	-0.2	-12.3	-13.0	1.7	4.4	0.1	9.3	-11.7
TC3-DE	-3.8	2.3	-4.1	-5.9	-2.7	-0.2	-10.6	-13.5	-0.4	5.1	-0.8	11.9	-8.3
TC3-EE	-4.2	1.4	-4.6	-6.4	-3.3	-1.4	-12.5	-12.2	-2.0	1.1	-0.8	7.3	-8.2
TC3-GE	-3.7	2.4	-3.7	-6.7	-3.3	-1.3	-11.4	-11.6	-1.2	1.4	-0.6	7.4	-7.4
TC3-HE	-4.2	1.9	-4.2	-6.4	-2.9	-1.0	-13.1	-14.6	-1.8	5.1	-0.9	11.6	-7.5
TC3-IE	-3.3	3.1	-2.9	-7.1	-3.1	-1.4	-13.2	-13.1	-0.9	3.4	-0.2	8.5	-7.0
TC3-LE	-3.7	3.1	-3.5	-7.5	-3.2	-1.3	-12.7	-14.3	1.7	7.0	0.4	11.4	-6.7
TC3-BW	-3.8	2.5	-4.3	-5.7	-2.7	0.3	-10.1	-11.6	-0.7	0.3	-1.4	8.6	-7.8
TC3-EW	-4.1	2.3	-4.0	-6.4	-3.0	-0.7	-12.5	-11.9	-0.9	0.3	-0.8	6.8	-6.7
TC3-FW	-3.9	2.4	-4.0	-6.7	-3.3	-1.0	-12.1	-12.1	-0.4	1.4	-0.6	7.6	-6.9
TC3-GW	-3.9	3.9	-3.6	-7.9	-4.2	-0.9	-8.2	-10.1	1.4	-1.2	-1.3	7.5	-11.5
TC3-JW	-3.8	2.5	-3.5	-7.0	-2.9	-1.4	-15.7	-14.3	-1.9	2.4	-0.7	8.4	-7.2
TC3-KW	-3.7	3.0	-3.4	-7.1	-2.9	-1.1	-15.0	-14.3	-0.1	3.5	-0.3	9.2	-6.6
TC4-AE	-3.0	2.9	-3.6	-5.2	-2.3	0.4	-11.4	-13.0	2.1	5.4	0.3	10.1	-11.3
TC4-CE	-3.5	2.1	-3.5	-5.7	-2.6	-0.9	-13.5	-13.2	-3.4	2.3	-1.0	8.5	-7.9
TC4-GE	-5.5	4.1	-5.0	-8.6	-5.6	-0.8	-6.9	-11.9	0.8	-3.2	-4.0	12.4	-10.0
TC4-HE	-9.9	1.4	-9.4	-9.1	-6.3	0.3	-0.3	-7.3	-1.0	-14.4	-7.5	9.9	-9.2
TC4-IE	-8.0	3.9	-3.9	-8.4	-5.1	-1.7	-6.7	-11.2	1.1	0.9	-1.9	11.1	-8.2
TC4-KE	-2.6	5.1	-2.0	-7.3	-3.7	-1.2	-8.5	-10.9	2.9	3.2	0.1	8.7	-6.1
TC4-LE	-6.6	4.2	-3.9	-8.8	-5.2	-1.7	-7.5	-12.4	1.0	1.7	-2.2	12.8	-10.5
TC4-DW	-4.5	2.2	-4.5	-8.3	-5.3	-2.6	-10.8	-10.8	0.0	-0.8	-0.9	6.2	-9.1
TC4-EW	-7.3	2.7	-7.3	-8.4	-5.5	0.4	-2.0	-7.8	-0.5	-11.5	-6.0	9.2	-9.6
TC4-FW	-6.7	3.6	-6.1	-8.5	-5.5	0.1	-1.3	-7.6	-0.1	-9.8	-5.5	9.5	-9.5
TC4-HW	-4.2	2.7	-3.9	-8.3	-5.2	-2.8	-10.3	-10.5	-0.9	-1.4	-1.2	6.2	-9.1

Table C.6 Continued.

Saturation Indices (SIs) Calculated by MINTEQA2

Lysimeter ID	Anglesite [$PbSO_4$]	Galena [PbS]	$Pb(OH)_2$	$NiCO_3$	$Ni(OH)_2$	Millerite [NiS]	Orpiment [As_2S_3]	Realgar [As_4S_4]	Stibnite [Sb_2S_3]	Sb_2O_4	$Sb(OH)_3$	Native S	Tl_2S
TC4-JW	-6.1	3.3	-4.5	-8.3	-4.8	-1.5	-6.5	-10.4	0.4	-0.8	-2.1	9.8	-7.3
TC4-KW	-6.6	3.8	-4.2	-8.6	-5.0	-1.6	-7.3	-10.9	1.0	-0.9	-2.2	10.0	-10.1
TC5-CE	-3.2	2.6	-3.3	-6.1	-3.0	-0.9	-12.3	-11.5	-2.6	-0.5	-1.1	6.3	-8.4
TC5-DE	-4.3	3.2	-3.8	-7.5	-4.1	-1.2	-8.2	-10.2	0.7	0.1	-1.0	7.6	-7.5
TC5-GE	-4.0	2.8	-3.8	-7.9	-4.5	-2.2	-10.7	-10.7	-0.8	-1.1	-1.0	6.2	-8.7
TC5-HE	-3.9	2.4	-3.6	-7.2	-3.6	-1.8	-12.2	-11.5	-1.3	0.7	-0.5	6.4	-7.5
TC5-IE	-4.3	2.0	-4.0	-7.1	-3.4	-1.8	-11.6	-11.7	-2.6	0.7	-1.0	7.3	-7.1
TC5-LE	-4.1	2.3	-3.7	-7.2	-2.9	-1.6	-13.3	-12.0	-1.1	1.5	-0.1	6.3	-6.9
TC5-BW	-3.5	3.0	-3.9	-6.1	-3.2	-0.1	-9.6	-11.6	3.6	4.6	0.5	9.2	-10.0
TC5-EW	-4.3	1.9	-4.1	-7.1	-3.8	-1.8	-11.1	-10.4	-2.7	-1.8	-1.2	5.2	-7.8
TC5-GW	-3.6	2.7	-3.4	-7.0	-3.5	-1.7	-11.2	-11.4	-2.5	0.1	-1.1	7.1	-7.3
TC5-HW	-3.9	2.2	-3.7	-7.0	-3.5	-1.9	-13.2	-11.9	-3.4	-0.8	-1.3	6.2	-7.2
TC5-IW	-4.2	2.2	-3.9	-7.1	-3.4	-1.7	-11.8	-11.8	-2.3	0.7	-1.0	7.3	-7.0
TC5-JW	-3.3	2.3	-3.8	-5.8	-2.0	-0.4	-12.7	-12.2	-1.7	1.1	-0.7	7.2	-7.2
TC6-AE	-3.0	1.7	-3.8	-5.0	-2.1	-0.6	-15.0	-16.3	-1.8	9.2	0.1	13.2	-11.6
TC6-CE	-4.3	1.6	-4.6	-6.0	-3.1	-0.7	-11.2	-11.7	0.6	2.7	0.0	7.6	-9.6
TC6-FE	-4.4	2.4	-4.1	-7.7	-4.4	-2.0	-10.6	-10.4	1.1	0.6	0.0	5.8	-8.1
TC6-GE	-4.1	2.9	-3.9	-7.5	-4.0	-1.3	-8.5	-9.4	-0.2	-2.0	-1.2	5.8	-8.4
TC6-HE	-4.5	2.4	-4.0	-7.7	-4.2	-2.0	-10.6	-10.2	-1.3	-1.8	-1.0	5.3	-8.1
TC6-IE	-3.9	3.0	-3.4	-7.3	-3.7	-1.7	-10.8	-10.9	-0.3	0.9	-0.4	6.5	-7.9
TC6-KE	-3.9	2.9	-3.7	-7.7	-3.9	-2.0	-9.5	-9.8	-0.6	-1.2	-0.9	5.7	-8.2
TC6-LE	-4.5	3.0	-3.8	-7.6	-3.8	-1.6	-9.9	-10.3	2.5	1.4	0.3	6.2	-7.3
TC6-BW	-3.6	1.1	-4.6	-5.2	-2.4	-0.6	-12.4	-11.0	-2.6	-0.5	-0.7	5.2	-8.8
TC6-DW	-2.7	2.6	-3.3	-5.7	-2.8	-0.8	-12.5	-11.0	-2.0	-1.0	-0.7	5.0	-9.6
TC6-EW	-3.8	2.7	-3.8	-7.4	-4.2	-1.8	-10.2	-10.0	-1.1	-2.1	-1.1	5.2	-8.4
TC6-HW	-4.9	2.9	-3.8	-8.7	-5.2	-2.7	-10.9	-11.1	-0.6	-0.9	-1.2	6.8	-9.1
TC6-JW	-4.2	1.6	-4.4	-6.0	-2.5	-1.0	-11.4	-10.9	-2.2	-0.3	-0.8	5.8	-7.1
TC6-KW	-5.0	2.8	-3.9	-9.0	-5.1	-3.0	-11.1	-12.1	1.3	3.0	-0.1	8.5	-12.4
TC7-AE	-3.3	-0.7	-4.4	-5.2	-2.2	-2.3	-20.6	-18.1	-7.2	8.7	-0.1	11.2	-13.3
TC7-DE	-4.7	2.3	-4.0	-8.2	-5.3	-2.9	-11.5	-11.4	-0.9	-0.1	-0.9	6.8	-10.0
TC7-GE	-9.4	3.1	-4.9	-8.5	-5.5	-1.7	-6.2	-9.1	0.8	-3.8	-2.3	7.5	-8.0
TC7-KE	-6.3	3.6	-3.2	-8.5	-4.9	-2.6	-10.2	-11.6	1.6	2.9	-0.1	8.5	-7.9
TC7-LE	-4.1	2.6	-4.1	-7.9	-4.1	-2.1	-10.1	-10.3	-0.7	-1.4	-1.1	6.0	-10.1
TC7-BW	-4.9	2.6	-4.7	-6.9	-4.1	-0.6	-6.8	-9.3	3.2	0.7	-0.3	7.3	-9.0
TC7-CW	-4.5	0.9	-4.9	-5.8	-3.0	-1.1	-11.8	-10.7	-0.8	0.8	0.0	5.2	-9.7
TC7-EW	-6.2	1.8	-4.8	-8.1	-5.0	-2.5	-10.8	-11.9	0.1	1.6	-0.8	8.4	-8.1
TC7-FW	-5.6	2.4	-4.4	-9.2	-6.0	-3.4	-10.6	-11.1	0.3	-0.3	-0.9	7.0	-10.6
TC7-GW	-4.8	4.0	-3.8	-8.5	-5.4	-1.7	-7.6	-9.6	0.9	-3.5	-2.1	7.1	-11.1
TC7-IW	-4.4	2.3	-4.2	-7.9	-4.6	-2.4	-10.6	-10.5	-1.0	-1.4	-1.1	5.8	-9.4
TC7-JW	-4.3	3.1	-3.4	-8.3	-4.7	-2.7	-10.4	-11.2	-1.5	-0.1	-1.2	7.4	-9.7
TC7-KW	-5.7	2.8	-4.3	-8.7	-4.9	-2.5	-9.5	-12.5	2.0	5.0	-0.2	11.0	-7.8

Table C.7 Most-probable number (MPN) populations of acid-producing (fermentative) bacteria (APB), iron-reducing bacteria (IRB) and sulfate-reducing bacteria (SRB) for core samples collected in November 2004.

Test Cell	Depth (m)	MPN Population (cells g^{-1})		
		APB	IRB	SRB
TC2	0.50	<0.02	1.3E+02	1.4E+02
	2.00	<0.02	3.3E+01	1.1E+02
	3.50	4.5E+00	7.8E+00	1.3E+02
TC3	0.50	8.8E+00	7.9E+01	3.3E+01
	2.00	<0.02	2.3E+01	1.3E+01
	3.50	<0.02	7.9E+01	3.3E+01
TC4	0.50	1.4E+02	7.9E+01	2.7E+01
	2.00	7.9E+06	7.9E+02	7.9E+01
	3.50	<0.02	2.3E+01	2.7E+01
TC5	0.50	1.1E+05	2.2E+05	6.8E+00
	2.00	9.3E+06	7.9E+05	2.4E+07
TC6	0.50	2.6E+06	4.8E+05	1.3E+07
	2.00	1.4E+01	3.3E+05	4.5E+00
	3.50	<0.02	7.9E+01	7.9E+01
TC7	0.50	4.8E+06	1.4E+05	7.8E+00
	2.00	7.9E+07	7.9E+05	1.3E+01
	3.50	4.5E+00	2.3E+01	7.6E+00

Table C.8 Most-probable number (MPN) populations of acid-producing (fermentative) bacteria (APB), iron-reducing bacteria (IRB) and sulfate-reducing bacteria (SRB) for core samples collected in October 2006.

Test Cell	Depth (m)	MPN Population (cells g^{-1})		
		APB	IRB	SRB
TC2	0.50	<0.02	7.9E+01	4.9E+01
	1.00	<0.02	7.9E+01	2.7E+01
	1.75	<0.02	7.0E+01	7.9E+01
	2.50	<0.02	4.0E+01	7.9E+01
	3.50	2.0E+00	2.3E+01	7.9E+01
TC3	0.50	<0.02	7.0E+01	1.3E+02
	1.00	<0.02	2.0E+04	2.3E+04
	1.75	<0.02	2.1E+03	3.3E+02
	2.50	<0.02	1.4E+02	2.1E+01
	3.50	5.0E+00	8.0E+02	2.1E+01
TC4	0.50	2.4E+01	1.4E+05	3.4E+06
	1.00	9.3E+02	1.1E+06	1.3E+06
	1.75	5.4E+04	4.0E+04	1.7E+05
	2.50	1.7E+04	2.1E+06	2.2E+07
	3.50	<0.02	2.3E+01	9.0E+01
TC5	0.50	2.2E+01	1.2E+04	4.9E+05
	1.00	4.0E+01	1.1E+03	4.9E+01
	1.75	5.4E+02	1.4E+03	1.7E+03
	2.50	<0.02	3.3E+01	1.1E+02
	3.50	<0.02	4.0E+01	2.4E+03
TC6	0.50	8.0E+00	2.0E+04	3.3E+04
	1.00	7.0E+00	1.7E+03	3.3E+06
	1.50	6.0E+02	9.0E+02	7.9E+06
	2.50	1.3E+02	2.7E+04	4.9E+06
	3.50	<0.02	4.0E+01	1.7E+03
TC7	0.50	9.4E+05	1.5E+05	7.9E+06
	1.00	2.2E+04	3.5E+04	7.9E+06
	1.50	3.4E+03	1.7E+04	4.9E+06
	2.00	5.0E+00	1.1E+04	7.9E+06
	3.50	<0.02	2.3E+01	7.9E+03

Table C.9 Most-probable number (MPN) populations of acid-producing (fermentative) bacteria (APB), iron-reducing bacteria (IRB) and sulfate-reducing bacteria (SRB) for core samples collected in August 2008.

Test Cell	Depth (m)	MPN Population (cells g^{-1})		
		APB	IRB	SRB
TC2	0.50	< 0.02	2.3E+01	7.9E+01
	1.00	< 0.02	2.3E+01	7.9E+01
	1.75	< 0.02	2.3E+01	2.3E+01
	2.50	< 0.02	4.9E+01	3.3E+01
	3.50	< 0.02	2.3E+01	4.9E+01
TC3	0.50	< 0.02	2.3E+01	2.0E+03
	1.00	< 0.02	2.3E+01	4.9E+01
	1.75	< 0.02	2.3E+01	2.0E+02
	2.50	< 0.02	2.3E+01	2.2E+02
	3.50	< 0.02	3.3E+01	1.7E+02
TC4	0.50	4.9E+01	2.3E+01	3.9E+06
	1.00	2.3E+02	2.3E+01	3.3E+06
	1.75	2.3E+02	2.3E+01	2.4E+06
	2.50	2.6E+04	2.3E+01	2.7E+05
	3.50	2.3E+01	2.3E+01	4.0E+03
TC5	0.50	2.3E+01	9.2E+02	1.3E+05
	1.00	7.9E+01	5.2E+02	4.9E+06
	1.75	1.3E+02	3.5E+02	3.3E+06
	2.50	4.9E+01	1.1E+02	2.0E+02
	3.50	2.3E+01	2.3E+01	1.7E+02
TC6	0.50	2.3E+01	2.3E+01	4.9E+04
	1.00	4.9E+01	1.2E+03	7.9E+06
	1.50	3.3E+01	4.6E+03	1.3E+06
	2.50	7.9E+01	1.3E+02	1.3E+06
	3.50	2.3E+01	2.3E+01	4.9E+04
TC7	0.50	2.3E+01	1.4E+03	1.7E+07
	1.00	1.4E+03	2.4E+03	3.5E+05
	1.50	2.3E+02	6.0E+03	2.6E+06
	2.00	7.9E+02	6.3E+01	4.9E+06
	3.50	2.3E+01	2.3E+01	2.6E+02

Table C.10 Deionized water extraction data for core samples collected in August 2008.

Test	Depth	Solid-Phase Concentration (mg kg^{-1})											
Cell	(m)	SO_4	Al	As	Ca	Cr	Fe	Mg	Pb	Sb	Se	Tl	Zn
TC2	0.50	2581	0.00	0.00	978	0.25	0.00	4.0	2.82	0.28	0.00	0.00	5.91
	1.00	1025	0.00	0.00	875	0.28	0.00	6.6	2.67	0.22	0.00	0.00	0.00
	1.75	1468	0.00	0.00	754	0.24	2.04	55.2	2.60	0.31	0.00	0.00	0.02
	2.50	1258	0.00	0.00	662	0.58	0.80	52.5	2.89	0.29	0.00	0.00	0.42
	3.50	1528	0.00	0.00	889	0.19	1.16	28.6	2.44	0.41	0.00	0.00	1.65
TC3	0.50	290	0.02	0.00	600	0.83	0.00	120.7	3.43	0.26	0.00	0.64	0.00
	1.00	2588	0.00	0.00	1337	0.65	0.00	36.5	2.60	0.05	0.00	0.00	5.32
	1.75	3719	0.00	0.09	1728	0.51	0.00	98.4	2.52	0.28	0.00	0.00	3.17
	2.50	700	0.39	0.00	569	0.00	0.00	0.0	2.13	0.19	0.00	0.00	0.91
	3.50	2361	0.00	0.00	1088	0.81	0.80	74.5	1.58	0.35	0.00	4.39	2.72
TC4	0.50	0	2.59	1.01	345	0.20	0.00	62.7	0.72	0.77	0.00	4.93	0.00
	1.00	1050	4.97	0.28	491	0.60	0.47	0.0	2.18	0.29	0.00	1.17	0.02
	1.75	1316	3.28	0.03	479	0.27	1.30	32.7	2.20	0.29	0.00	0.00	2.38
	2.50	360	5.38	1.02	283	0.59	0.04	55.8	0.47	0.93	0.00	5.64	0.00
	3.50	837	0.84	0.01	398	0.21	0.02	85.8	2.56	0.53	0.00	0.16	2.28
TC5	0.50	731	2.76	0.16	467	0.08	0.00	77.2	1.55	0.15	0.00	7.81	0.00
	1.00	547	0.00	0.12	449	0.27	0.00	46.8	2.02	0.37	0.00	8.57	0.14
	1.75	4079	4.18	0.00	1855	0.42	0.00	35.8	1.54	0.04	0.00	0.00	37.05
	2.50	148	5.53	0.04	497	0.32	0.00	26.9	1.89	0.33	0.00	1.42	0.00
	3.50	0	6.56	0.06	707	0.47	0.00	0.0	2.13	0.22	0.00	6.89	0.00
TC6	0.50	153	2.57	0.00	465	0.19	0.00	132.6	1.79	0.18	0.00	1.43	0.00
	1.00	0	7.00	0.26	268	0.17	0.00	0.0	1.34	0.54	0.18	2.31	0.00
	1.75	254	3.31	0.00	410	0.58	0.00	40.9	2.13	0.20	0.04	0.92	0.00
	2.50	0	3.35	0.45	285	0.59	1.35	0.0	0.24	0.84	0.00	0.00	0.00
	3.50	271	3.04	0.23	487	0.15	0.00	0.0	1.95	0.12	0.00	1.80	2.91
TC7	0.50	0	4.66	0.10	255	0.05	0.00	0.0	0.83	0.53	0.06	0.00	0.00
	1.00	0	4.10	2.14	180	0.43	1.03	0.0	0.44	0.24	0.00	3.07	0.00
	1.75	79	0.74	0.13	414	0.69	0.00	65.1	1.51	0.75	0.00	8.42	0.91
	2.50	285	2.35	0.08	425	0.05	0.00	80.6	2.22	0.36	0.00	8.24	3.94
	3.50	32	2.30	0.00	352	0.33	2.00	36.1	1.81	0.27	0.00	2.69	3.22

Table C.11 Weak reductant (ascorbic acid) extraction data for core samples collected in August 2008.

Field	Depth	Solid-Phase Concentration (mg kg^{-1})										
Cell	(m)	Al	As	Ca	Cr	Fe	Mg	Pb	Sb	Se	Tl	Zn
TC2	0.50	86.43	68.90	1394	6.94	2062	62	414	29.3	4.98	0.00	1298
	1.00	78.26	50.39	1130	6.03	1664	95	487	25.8	4.95	0.00	1075
	1.75	82.57	38.32	994	6.41	1545	144	430	24.4	5.33	0.00	953
	2.50	82.32	43.22	1275	7.17	1736	163	422	28.4	5.36	0.00	1091
	3.50	85.55	37.83	993	7.33	1525	119	604	24.5	5.64	0.00	925
TC3	0.50	72.30	53.98	1396	7.39	1972	221	409	27.0	5.46	0.00	1271
	1.00	76.62	64.68	1348	8.11	2068	135	390	28.0	4.65	0.00	1400
	1.75	65.80	43.56	1403	7.17	1629	160	473	29.1	5.00	0.00	986
	2.50	76.04	43.60	1276	7.89	1674	125	426	26.3	1.58	0.00	1118
	3.50	70.21	49.98	1135	6.68	1682	170	598	25.2	5.01	0.00	1072
TC4	0.50	61.93	22.64	767	6.16	955	131	314	12.5	5.48	0.00	385
	1.00	64.74	47.54	821	5.44	1405	30	321	18.9	5.16	0.00	953
	1.75	61.23	63.80	914	5.95	1736	91	382	20.9	5.36	0.00	1210
	2.50	55.72	40.13	945	5.87	1466	127	203	20.3	3.92	0.00	849
	3.50	64.30	34.51	753	6.37	1298	171	285	19.4	4.63	0.00	1254
TC5	0.50	68.95	61.62	1005	5.56	1824	154	437	22.0	6.01	0.00	1113
	1.00	80.58	45.89	991	5.65	1475	168	277	21.7	1.57	0.00	1073
	1.75	66.92	70.19	1248	5.48	1961	109	372	25.1	5.13	0.00	1317
	2.50	61.47	32.88	846	6.40	1365	134	395	19.3	5.84	0.00	727
	3.50	53.22	44.15	901	5.58	1609	0	334	19.6	5.35	0.00	1058
TC6	0.50	66.27	45.10	907	6.21	1449	198	368	23.1	5.50	0.00	821
	1.00	73.07	21.04	786	5.14	917	55	297	13.6	5.26	0.00	389
	1.75	69.84	50.81	920	6.67	1787	134	400	23.9	4.62	0.00	1111
	2.50	58.67	27.05	863	5.74	1359	27	1	9.9	4.91	0.00	378
	3.50	57.30	56.95	861	6.13	1786	28	353	24.7	4.97	0.00	1216
TC7	0.50	67.12	46.42	838	6.04	1580	63	322	19.6	5.41	0.00	1032
	1.00	57.42	29.36	892	5.44	982	39	244	16.5	4.99	0.00	508
	1.75	57.37	36.23	1002	5.01	1437	128	286	19.2	5.29	0.00	1000
	2.50	61.37	49.26	791	5.67	1591	129	277	20.7	5.72	0.00	1217
	3.50	60.29	54.20	692	5.85	1431	135	320	22.7	4.88	0.00	1222

Table C.12 Weak acid (0.5 M HCl) extraction data for core samples collected in August 2008.

Field	Depth	Solid-Phase Concentration (mg kg^{-1})										
Cell	(m)	Al	As	Ca	Cr	Fe	Mg	Pb	Sb	Se	Tl	Zn
TC2	0.50	937	132.7	58317	11.8	6566	26318	6225	35.6	0.13	19.3	2902
	1.00	948	52.9	63132	11.7	4968	28023	6733	28.3	0.00	19.8	1791
	1.75	1027	38.6	55280	12.2	4711	24821	6240	27.3	0.03	16.3	1567
	2.50	956	59.2	55836	11.6	5324	25609	6872	34.0	0.00	18.9	1970
	3.50	1047	79.1	55792	12.2	5508	25166	6447	32.3	0.28	16.4	2108
TC3	0.50	1082	82.6	54533	11.5	5384	24869	5737	27.8	0.11	9.2	2308
	1.00	1103	119.0	55807	12.1	6242	25775	5601	33.9	0.00	18.3	2759
	1.75	833	52.8	54790	11.0	4989	25445	6787	32.1	0.20	13.9	1887
	2.50	1044	89.2	56766	11.5	5633	25607	6013	29.7	0.20	15.8	2524
	3.50	1077	74.5	55453	11.4	5444	25406	5634	26.2	0.00	14.6	2319
TC4	0.50	1118	7.8	56778	10.8	4185	26193	2389	3.7	0.00	10.7	948
	1.00	1273	69.5	55082	10.8	4895	25320	6021	18.7	0.14	9.7	2030
	1.75	1179	98.5	51912	11.0	5461	23793	5834	22.4	0.05	11.0	2523
	2.50	1332	70.9	57423	11.6	5620	25911	5698	20.1	0.07	13.3	2416
	3.50	1014	81.3	53942	11.2	5221	25701	6218	26.1	0.09	17.3	2683
TC5	0.50	1159	85.5	49009	10.3	4981	21978	4985	24.1	0.01	4.4	2238
	1.00	1239	66.8	50217	9.8	4675	22971	5003	17.8	0.02	10.9	2328
	1.75	958	81.4	50008	10.4	5113	22689	5687	23.3	0.00	9.9	2386
	2.50	775	31.2	48538	10.8	4315	22036	5826	17.2	0.25	7.1	1264
	3.50	880	69.7	52114	10.5	4741	22316	6139	25.3	0.49	9.1	2095
TC6	0.50	1236	55.7	46053	10.7	3908	20627	5427	22.1	0.42	4.9	1459
	1.00	1000	16.4	48207	10.2	3580	21600	3099	8.1	0.00	4.5	933
	1.75	963	65.5	49064	11.8	4831	21878	5472	23.1	0.24	15.9	2177
	2.50	1009	35.0	48690	10.0	4412	22187	5534	17.4	0.03	10.2	1649
	3.50	951	73.0	54948	10.8	5171	24424	5991	27.0	0.00	12.5	2533
TC7	0.50	1172	64.2	48168	10.7	4523	21333	5105	16.9	0.26	8.0	2022
	1.00	1004	42.0	48789	11.0	4011	22003	5619	16.2	0.07	13.2	1555
	1.75	954	59.7	48986	10.3	4648	21856	5504	18.7	0.24	12.2	2065
	2.50	1325	67.8	51830	10.8	4560	23721	5590	19.5	0.46	12.8	2226
	3.50	1149	96.5	50577	11.8	5523	23968	6699	26.7	0.00	10.6	2897

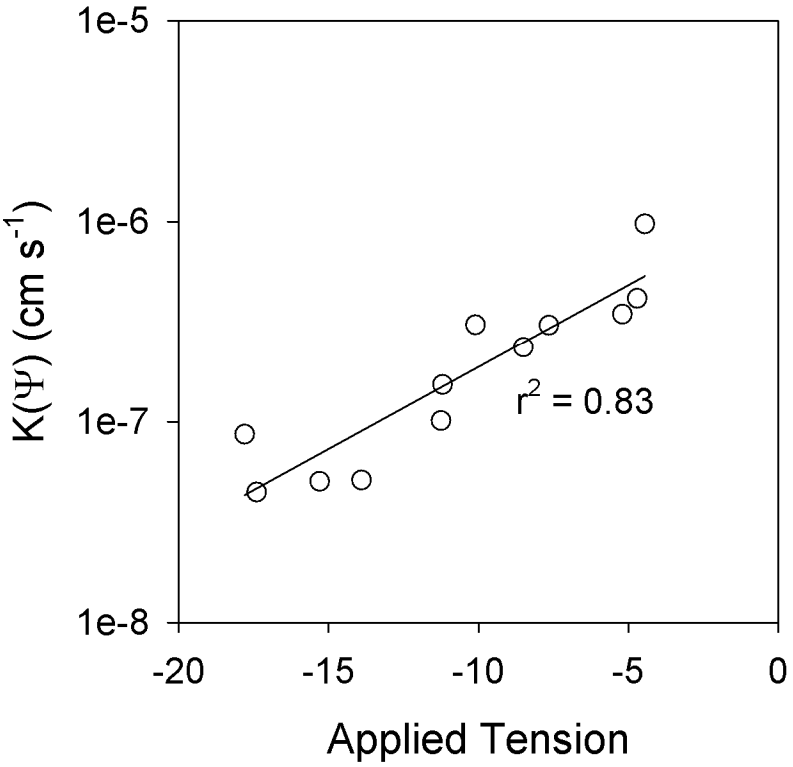

Figure C.1 Measured hydraulic conductivities as a function of applied tension.

Figure C.2 Temperatures monitored by thermisters installed at different depths from September 2006 through December 2008.

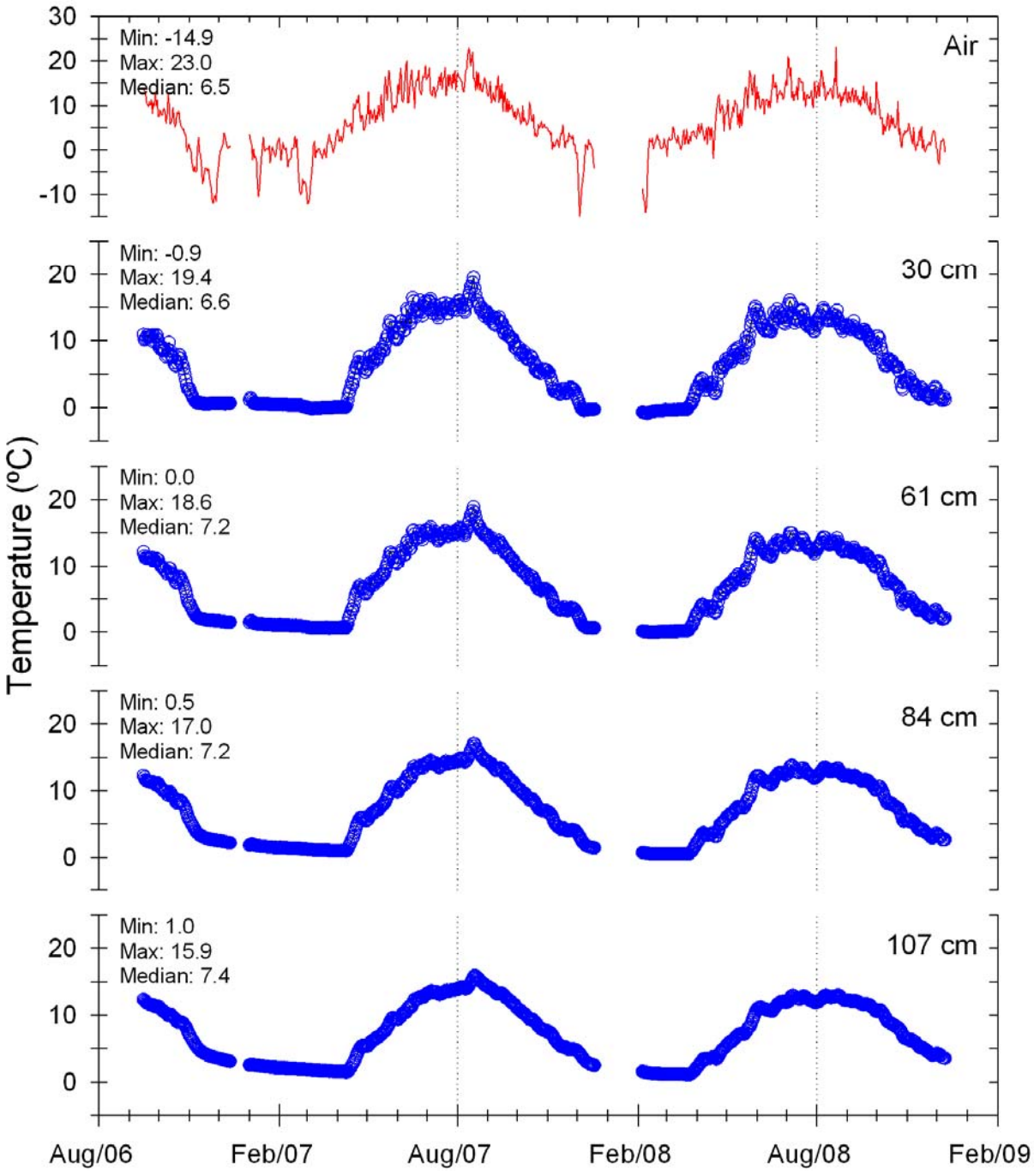

Figure C.2 Continued.